Quantum Dynamics in the Partial Wigner Picture

Author:
Geoffrey Martin Beck

Submitted in fulfilment of the academic requirements for the degree of Master of Science in the School of Chemistry and Physics, University of Kwazulu-Natal, Pietermaritzburg

February 11, 2013

Abstract

The Wigner formalism can be used to provide a representation of quantum dynamics in a classical-like phase space. However, there are many cases, such as when dealing with spin systems in a dissipative environment, in which one can more conveniently resort to a partial Wigner representation. The quantum propagator in the partial Wigner representation is, in general, a very complicated mathematical object. However, using a linear approximation, the propagator can be taken as a basis for describing the dynamics of hybrid quantum-classical systems. Such a hybrid system is composed of a quantum subsystem interacting with a coupled environment subsystem which evolves under classical-like dynamics represented in the Wigner phase space. In studying these hybrid dynamics it becomes apparent that, for a general environment system, there exists a series of quantum correction terms that restore the hybrid equation to exact quantum dynamics. Thus it is these correction terms that influence the existence of quantum effects in the dynamics of the environment subsystem and could therefore provide unique dynamical signatures indicating the existence of quantum effects. With the above motivation, we have derived an analytical expression for the quantum propagator, including correction terms, in the case of position-dependent couplings and polynomial-potential environment systems, and we have studied, numerically, the resulting quantum dynamics in a few relevant cases through comparison of quantum-classical and quantum-corrected evolutions. The type of system chosen for numerical study consisted of a two-level, or pseudo-spin, quantum system coupled to an environment represented by a quartic potential. It was found that the Rabi oscillations of the pseudo-spin are sensitive to the quantum corrections in a certain range of parameter values, either exhibiting stronger damping or stronger oscillations, depending on the tunnelling behaviour introduced by the corrections. If one were to interpret the pseudo-spin as a Cooper-pair box and the polynomial potential as representing the oscillatory behaviour of a buckled nano-rod, then this works suggests that one might be able to witness the transition of a non-linear nano-oscillator from the realm of classical dynamics to the quantum regime by observation of the pseudo-spin Rabi oscillations.

Contents

Preface and Declarations

The numerical and theoretical work described by this thesis was carried out at the University of Kwazulu-Natal, Department of Chemistry and Physics, Pietermaritzburg, from January 2011 until November 2012, under the supervision of Dr Alessandro Sergi. Some of this work was also carried out during a brief visiting period at the University of Messina, Italy.

This thesis is entirely, unless specifically contradicted in the text, the work of the candidate, Geoffrey Beck, and has not been previously submitted, in whole or in part, to any other tertiary institution. Where use has been made of the work of others, it is duly acknowledged in the text.

Declaration - Plagiarism

I, _____ declare that

1. The research reported in this thesis, except where otherwise indicated, is my original research.
2. This thesis has not been submitted for any degree or examination at any other university.
3. This thesis does not contain other persons' data, pictures, graphs or other information, unless specifically acknowledged as being sourced from other persons.
4. This thesis does not contain other persons' writing, unless specifically acknowledged as being sourced from other researchers. Where other written sources have been quoted, then:
    a. Their words have been rewritten but the general information attributed to them has been referenced.
    b. Where their exact words have been used, then their writing has been placed in italics and inside quotation marks, and referenced.
5. This thesis does not contain, text, graphics or tables copied and pasted from the Internet, unless specifically acknowledged, and the source being detailed in the thesis and in the References sections.

Signed: _____

Declaration - Publications

Details of publications that form part and/or include research presented in this thesis.

1.

Title: Quantum Dynamics of a Buckled Nano-rod.

Status: Submitted for publication.

Authors: Geoffrey M. Beck and Alessandro Sergi

Contributions: Numerical results obtained by G. Beck, paper initially composed by A. Sergi with editing and discussion text contributed by G. Beck.

Signed: _____

Acknowledgements

I would like to thank Dr Alessandro Sergi, my supervisor, for his guidance and patience, as well as all he has taught me through the production of this work, also for the education in ways of Sicily. I would also like to acknowledge the invaluable contribution of Professor Roger Raab, while his attention and effort were necessary to the readability and grammar of this work, his encouragement and support may have been more valuable. Additionally, thanks are due to Professor Paolo Giaquinta and other members of the physics department at the University of Messina, for their hospitality and for the opportunity to present a seminar about this work. The work presented in this thesis is based on research supported by the funding of the National Research Foundation of South Africa through their Scarce Skills scholarship programme.

Chapter 1

Introduction

The study of condensed matter systems with many interacting degrees of freedom is fraught with complexity. Strong interactions often prevent the use of perturbation-type treatments and the dynamical equations seldom admit analytical solutions. Moreover, the numerical solution of such problems can still prove intractable, as the computation time scales exponentially with the number of degrees of freedom [1]. As such, the efficient computational simulation of quantum dynamics in condensed matter systems remains an open problem with numerous approaches presented in the literature [2–8]. In this work we have focussed upon cases where one can identify a subset of the degrees of freedom, whose dynamics are of interest and whose mass is much smaller than the mass which characterises the remaining degrees of freedom. If the dynamics of the small mass degrees of freedom operate on a time scale more rapid than that of the large mass subset, one can make a Born-Oppenheimer type approximation. Such an approximation, however, tends to break down if strong non-adiabatic effects are present [9] . With this in mind, it might be more efficient, if one wishes to study systems that are strongly coupled, or exhibit significant non-adiabatic effects, to identify these 'light' degrees of freedom and to treat them as evolving under the laws of quantum mechanics, while the environmental degrees of freedom are replaced with an effective environment in the form of a classical or semi-classical bath. This singling-out of certain degrees of freedom allows for the examination of the essential dynamical properties of otherwise prohibitively large and complex systems [4]. A system, so treated, would then consist of a quantum subsystem interacting with a classical or semi-classical environmental subsystem that might then be represented in a classical-like phase space, such a system is known as a hybrid or quantum-classical system.

It would seem a plausible approach to obtain a formalism to address the dynamics of a hybrid system by starting with the fully quantum equations of motion and taking the classical limit of the environmental dynamics only, demanding that energy remains conserved. The result of this prescription is the quantum-classical dynamical equation proposed in [10]. Such a prescription is formulated in terms of a quantum-classical Liouville equation, a review of such formalisms can be found in the reference [11]. A system evolving in accordance with the quantum-classical Liouville equation is divided into a subsystem evolving under the laws of quantum mechanics, which interacts with an environmental system, whose evolution is semi-classical, similar in form to the classical Liouville equation [3, 10, 12]. The coupling between the quantum subsystem and the environment results in interactions that produce what is known as the quantum 'back-reaction' [12–14]. Whereby, the classical degrees of freedom experience induced quantum fluctuations, this is a result of directly coupling the state of the quantum subsystem to the state of the classical environment. However, these induced quantum fluctuations do not create uncertainty relations within the classical variables as this quantum-classical formulation violates the positivity of the density operator to preserve classical variable commutation [10, 12]. This means that a completely positive density operator will not remain so under time evolution in such a quantum-classical formalism [12], this is contrary to fully quantum evolution, in which case a positive density matrix remains positive [15–17]. This back-reaction is an essential element of similar hybrid dynamical theories [12–14] and is addressed by quantum-classical equation of [10] via the inclusion of the interaction effects in both the quantum and classical parts of the quantum-classical Liouville equation. The method used in this study to construct a formalism to address hybrid dynamics is found in the Wigner

picture of quantum mechanics, in which the dynamics appear to take place in a classical-like phase space [18], while the equations of motion take the form of a classical Liouville equation with the addition of an infinite series of correction terms [18, 19]. The similarity to classical dynamics is one of the chief advantages of the Wigner picture, providing explicit differentiation between quantum and classical terms and making it capable of offering convenient approaches to the classical limit of quantum dynamics.

If the Wigner transform of only the environmental degrees of freedom is taken, one would produce a dynamical picture, termed the partial Wigner picture, in which the quantum degrees of freedom interact with an environment that evolves under classical phase-space dynamics with the associated Wigner correction terms. The classical limit of this phase-space-represented environment might be naively taken by neglecting the correction terms through the assumption that $\hbar \to 0$, leaving the environmental system to evolve under classical dynamics. This partial Wigner prescription yields the exact same quantum-classical equation as found in [10, 20]. Given the methods used to obtain this quantum-classical equation, it is clear that for quantum-classical formulation to be valid, it must be some classical limit of the original fully quantum dynamics. In this regard, the naive manner of attaining this limit is not generally valid [21, 22], as is evinced by the contradictions which emerge by comparison of the Ehrenfest limit and Hamilton-Jacobi theory [23]. Both [20] and [14] present methods of taking a consistent quantum-classical limit of the fully quantum system. In the first reference, the authors show that in this partial Wigner picture, neglect of the correction terms, is equivalent to making a separation of the dynamics based on the two mass-scales of the system. This approach is analogous to the approximations made in the treatment of Brownian motion [20] and therefore coincides nicely with objective of hybrid dynamics, namely: to single out a few degrees of freedom of interest and treat the remainder of the system as a bath. In the second reference, the authors employ a group theory based approach and demonstrate that, if the quantum effects in the environmental system are insignificant in comparison to those of the quantum subsystem, then a linear approximation can be taken to obtain the quantum-classical equation of [10] as the natural evolution equation for the hybrid system. These two examples give some credence to defining the quantum-classical dynamics as the classical limit of the quantum dynamics for the full system and allow one to justify the neglect of the partial Wigner quantum-corrections when taking the classical limit of the environmental system. However, despite the existence of a consistent quantum-classical limit, this hybrid formalism conditionally violates the Jacobi identity [8, 12, 14]. In general, this violation means that time evolution under the hybrid formalism will not preserve either total system or individual subsystem Hamiltonian symmetries [12, 14, 24, 25]. This flaw does not diminish the usefulness of the quantum-classical hybrid methodology as a means of approximately treating the dynamics of complex condensed matter systems, as there exist systems where the Jacobi violations are insignificant or non-existent, it merely encourages the use of caution when applying this formalism. As such, a part of the work displayed in this study addresses the links between the quantum corrections and the preservation of Hamiltonian symmetries within hybrid systems, including a derivation, following a method similar to that in [12], of the limits in which the quantum-classical dynamical bracket constitutes a Lie bracket.

Application of a quantum-classical approach to the study of quantum events in a curved space-time, in the interest of determining the quantum back-reaction on the form of space-time [14], was a motivation for the study in [13] but the considerations mentioned previously suggest that this approach might lack consistency in such an application. This is because the quantum-classical equation suggested in [10] is an approximate limit of the fully quantum dynamical theory which therefore conflicts with the inability to quantise gravity in any straightforward manner.

Hybrid quantum-classical theories in quantum mechanics still merit further investigation. Not only do they offer computationally attractive formalisms for analysing the dynamics of many physically relevant systems [2, 4], but might also provide routes to investigate open quantum systems [26, 27]. Examples of systems that merit hybrid treatment would be proton or electron transport in solvents or other chemical environments composed of heavy atoms [28], diffusion processes in condensed-phase systems, vibrational motion of molecules in a liquid [20], excited state relaxation processes [29] and the calculation of chemical reaction rates[14, 30]. This means that such a hybrid dynamical methodology has broad application to the field of chemical and condensed matter physics and might facilitate the efficient calculation of transport coefficients

or rate constants. Continuing in this line of reasoning, the usefulness of the hybrid approach to transport problems suggests that it might have applications in the burgeoning field of quantum biology, where evidence of possible coherent energy transport has been found in otherwise classical systems [31]. In all these cases, one's ability to solve the problem benefits greatly from the hybrid approach, in that, singling out quantum degrees of freedom greatly reduces the complexity of the problem without significantly affecting the physics being treated, provided the quantum-classical limit is valid. Moreover, the Jacobi identity violations are unlikely to affect the formalism in such applications, since systems that require the hybrid treatment seldom exhibit high degrees of symmetry, this being among the principle difficulties in analysing such systems.

Importantly, due to the fact that quantum-classical dynamics can exist as the classical limit of the fully quantum formalism, it might be possible to make use of the hybrid formalism in studying the transition between quantum and classical behaviours. This is because the quantum correction terms can be viewed as the dynamical source of quantum effects in the environmental degrees of freedom [18] and, while this system is in the classical regime, these effects would be negligible. If the environment system were to then transition into the realm of quantum dynamics, the correction terms would likely have greater influence on the dynamical behaviour. Thus, by comparing an uncorrected quantum-classical evolution to an evolution with full quantum corrections, differences in the dynamical properties could be used to identify unique quantum signatures, making possible a differentiation between systems exhibiting quantum dynamical features and those which do not. Therefore, if a system were then set up consisting of a nano-mechanical oscillator coupled to some fully quantum subsystem, the study of the effects of these correction terms might offer the possibility of witnessing the transition of the nano-mechanical system from the regime of classical dynamics into the realm of greater quantum influence. It is this aspect of the partially Wigner-represented quantum-classical formalism which is examined in this study and, for this reason, the quantum-corrections form the focus of this work.

The study of witnessing quantum effects in nano-mechanical systems has recently been one which has received great interest [32]. This is in part due to the fact that several experiments in cooling nano-mechanical systems have approached the limit of quantum behaviour [33–36] and that theoretical progress has been made in the cooling of nano-mechanical systems [37–39]. Other interest in these systems is due to the fact that they represent the possibility to produce devices for the measurement of displacement and forces with unprecedented levels of precision [32, 33]. Such systems might also have applications in the detection of gravitational waves and in nano-scale quantum information processing [33, 40], both recently topics of particular interest in the scientific community. The witnessing of quantum effects in such systems would prove an important test of quantum mechanics at the nano-scale [32, 33, 41–43], which exists at the boundary of the quantum and the classical worlds. However, many quantum properties, including the zero-point motion of a nano-oscillator, are extremely difficult to detect [33]. Despite these difficulties, nano-mechanical resonator systems are believed to be capable of exhibiting quantum effects in laboratory realisable conditions [44–46], due to their high frequency of oscillation (≈ 1 GHz) and their tiny mass [44]. Therefore, devising new means of testing the quantum properties of nano systems is a problem of particular importance, not only in the confirmation of the predictions of quantum mechanics at the nano-scale but also because of the great potential of nano-scale devices in future technology and instrumentation. Previous studies have been performed on both harmonic oscillators [47–51] and also on some non-linear oscillators [44, 52–54]. The fact that this study particularly focusses upon utilisation of non-linear oscillatory behaviour is vital, simply due to the fact that a coherent state formed in a system using harmonic nano-oscillators can be difficult to distinguish from the behaviour of the classical harmonic oscillator [44]; it is also a hypothesis of this work that non-linear oscillatory behaviour can be exploited to reveal uniquely quantum dynamical effects.

The results of the calculations using the pseudo-spin and polynomial potential system were then further used to study the possibilities of witnessing quantum behaviour in a mechanical nano-oscillator, possibly in the form of a buckled nano-rod, by coupling it capacitively to a super-conducting circuit or a Cooper-pair box, in a manner similar to that discussed in [44]. A Cooper-pair box consists of a small Josephson junction that is voltage biased to ensure that only two energy levels are accessible [44], allowing it to be modelled effectively by a pseudo-spin system. The Cooper-pair box is chosen because it has been shown that it is possible for such a system to exhibit long decoherence times when coupled to nano-mechanical systems [55], certainly on

time scales much longer than the period of the nano-mechanical oscillations. This application involves modelling the nano-rod oscillations with a polynomial potential and the Cooper-Pair box is then modelled by a two-level, or pseudo-spin, system, meaning that such a system falls neatly into the category of those under examination in this study. If the rod is subject to a stress below the critical value its oscillatory potential is quadratic in nature and thus quantum-classical dynamics would yield an exact description. However, if subject to a stress beyond the critical value, which is feasible while the ends of the rod are fixed [56], the nano-rod begins to exhibit non-linear oscillatory behaviour and can then be modelled by a double-well potential [56, 57]. It is hypothesised that a transition of such an oscillator system from classical, or insignificantly quantum-influenced, dynamics to quantum dynamics can be witnessed by observing the damping experienced by the Cooper-pair population of the Josephson junction, based on the main result of this study and the tuning of the system parameters.

Therefore, the motivation behind this study is to analyse the effects of the quantum correction terms on quantum-classical dynamics as well as demonstrating the effectiveness of the partial Wigner formalism as a tool for the study of hybrid dynamical systems. This work is also motivated by the notion that the analysis of the quantum-correction terms might yield ways to identify uniquely quantum dynamical behaviour within lab-realisable systems, which could have great application in the witnessing of the classical-to-quantum transition of nano-mechanical systems, particularly those that exhibit non-linear oscillatory behaviour. The non-linearity of the oscillators is vital, due to the fact that this form of potential introduces quantum-correction effects to the dynamics, unlike the harmonic case, where all corrections are identically zero. Therefore, study of the effects of these corrections might allow for the identification of dynamical properties that indicate that the quantum corrections are significantly influencing the behaviour of the system, which in turn suggests the system must be in the regime of strong quantum dynamical effects.

As part of this work an analytical form for the complete quantum propagator, in the partial Wigner picture, was derived for a quantum subsystem with position-dependent coupling to an environmental system represented by an arbitrary polynomial potential. This was then used to study the effects of neglecting the correction terms in the quantum-classical approximation. The test system used for this consisted of a tunnelling pseudo-spin coupled to an environmental system in the form of a quartic polynomial potential. The coupling between these systems was chosen to match that used by Leggett in [28]. This particular class of systems was selected because both subsystem types are applicable in a broad range of physical problems. The two-level, or pseudo-spin, system is widely applicable in the modelling of simple quantum systems [28]; such a system may be employed to model the strangeness of the neutral K meson, the spin projection in spin $\frac{1}{2}$ systems, the polarisation of a photon [28] or tunnelling of Cooper-pairs in a Josephson junction [44]. Similarly, polynomial potentials have a wide range of physical applications, including the ubiquitous harmonic oscillator, with its role in the study of fields [58], the famous double well potential, which can be used in the modelling of chemical reactions, the motion of defects in crystalline solids [28, 30] or in modelling the oscillations of a buckled nano rod [56, 57]. Moreover, the chosen class of coupled systems can also be used for the analysis of decoherence in open qubit systems [59] or the modelling of spin-half ions in an optical cavity, as modes of the electromagnetic field admitted by the cavity can be represented by harmonic oscillators and thus polynomial potentials [58].

To facilitate this study, a computational technique for the numerical solution of partial Wigner dynamics was developed and tested by comparison to the established 'surface-hopping' approximation [3, 60, 61]. The developed technique is a method of lines approach to partial differential equations on a phase-space grid and is built on the Runge-Kutta 5 Cash-Karp method [62]. This method of lines technique is shown to be particularly suited to addressing strongly interacting degrees of freedom in low dimensional systems and it was further used to numerically test the dynamical effects of the partial Wigner correction terms. Where it was demonstrated that, in a particular range of coupling parameters, the partial Wigner correction terms had a significant influence on both the behaviour of the environmental subsystem and the behaviour of observables in the quantum subsystem.

In fact, the Rabi oscillations which occur in the pseudo-spin system were found to be sensitive to the effects of the quantum corrections in the limit of certain parameter values that encompass a regime here characterised as that of medium strength coupling between the quantum subsystem and its environment. This work suggests that quantum mechanical effects, or a transition from

classical to quantum regimes, within the oscillator degrees of freedom, might be witnessed by the measurement of the Rabi oscillation damping in the pseudo-spin system. As the Rabi oscillations demonstrate differing behaviours when the effects of the corrections becomes significant, such quantum dynamical behaviour might then be used to identify quantum effects in systems where the unambiguous detection of such phenomena otherwise proves difficult. In particular the results presented here demonstrate that the principle contribution of the quantum-corrections, for the studied model, is the introduction of additional quantum-tunnelling effects to the dynamics of the oscillator degrees of freedom. The tunnelling behaviour thus introduced is found to be the cause of the alterations to the Rabi oscillations. This means that the study of the Rabi oscillation behaviour offers the opportunity to indirectly witness the quantum tunnelling of the oscillator system in particular, in addition to the general possibility witnessing of the quantum or classical features of the coupled system dynamics.

The structure of this thesis is as follows: Chapter 2 reviews the Wigner and partial Wigner pictures including the derivation of the partial Wigner correction terms and equations of motion. Chapter 3 makes a review of the numerical solution of partial differential equations by the method of lines approach; it also lays out the numerical methods used in the computational simulations. Chapter 4 is focussed on the nature of the computational simulations, detailing the equations of motion in the diabatic basis, the models used in the simulations and the parameters chosen. Chapter 5 displays the results and details the application of these results to the study of witnessing quantum effects in nano oscillators. Chapter 6 is devoted to concluding remarks and the Appendices contain a review of quantum statistical mechanics and assorted derivations not included in the main matter.

Chapter 2

Wigner and Partial Wigner pictures

2.1 The Wigner Picture

The Wigner picture of quantum mechanics is one which allows a quantum system to be represented in phase space, in a manner similar to a system in classical mechanics [18]. As one would expect, this picture requires the degrees of freedom of the system to be representable in some form of phase space but, despite appearances, the behaviour of the system remains fully quantum [18, 21].

The Wigner picture is obtained from the abstract Dirac representation through the Wigner/Weyl transformation of Hilbert space operators [21]. These transformed operators take the form of phase-space functions and allow for the calculation of averages in a manner similar to that employed for their counterparts in classical statistical mechanics.

2.1.1 Operators in the Wigner Picture

Consider a quantum system with canonical conjugate degrees of freedom $(\hat{r}_1, \hat{p}_1, \ldots, \hat{r}_N, \hat{p}_N)$, having states of definite position given by

$$\hat{\mathbf{r}} \left|\mathbf{R}\right\rangle = \mathbf{R} \left|\mathbf{R}\right\rangle \ .$$

In the Wigner picture, operators are mapped onto phase-space functions by means of the Wigner/Weyl transform $\mathcal{W}$, defined for an arbitrary Hilbert space operator $\hat{A}$ by [18, 21]

$$\begin{aligned}\mathcal{W}(\hat{A}) &= \int_{-\infty}^{\infty} d\mathbf{q}\, \mathrm{e}^{\frac{i}{\hbar}\mathbf{P}\cdot\mathbf{q}} \left\langle \mathbf{R} - \frac{\mathbf{q}}{2}\right| \hat{A} \left|\mathbf{R} + \frac{\mathbf{q}}{2}\right\rangle \ , \\ &= \int_{-\infty}^{\infty} d\mathbf{q}\, \mathrm{e}^{\frac{i}{\hbar}\mathbf{P}\cdot\mathbf{q}} A\left(\mathbf{R} - \frac{\mathbf{q}}{2}, \mathbf{R} + \frac{\mathbf{q}}{2}\right) \ ,\end{aligned}$$

here $\mathbf{R}$ and $\mathbf{P}$ form a pair of canonically conjugate variables defining a phase space [18]. To obtain an idea of the nature of the transformed operators it is instructive to consider the Wigner transform of the position and momentum operators $\hat{\mathbf{r}} = (r_1, \ldots, r_N)$ and $\hat{\mathbf{p}} = (p_1, \ldots, p_N)$.

$$\mathcal{W}(\hat{\mathbf{r}}) = \int_{-\infty}^{\infty} d\mathbf{q}\, \mathrm{e}^{\frac{i}{\hbar}\mathbf{P}\cdot\mathbf{q}} \left\langle \mathbf{R} - \frac{\mathbf{q}}{2}\right| \hat{\mathbf{r}} \left|\mathbf{R} + \frac{\mathbf{q}}{2}\right\rangle \ .$$

This can be evaluated by simply noting that the states $\left|\mathbf{R} + \frac{\mathbf{q}}{2}\right\rangle$ are still states of definite position:

$$\begin{aligned}\mathcal{W}(\hat{\mathbf{r}}) &= \int_{-\infty}^{\infty} d\mathbf{q}\, \mathrm{e}^{\frac{i}{\hbar}\mathbf{P}\cdot\mathbf{q}} \left\langle \mathbf{R} - \frac{\mathbf{q}}{2}\right| \left(\mathbf{R} + \frac{\mathbf{q}}{2}\right) \left|\mathbf{R} + \frac{\mathbf{q}}{2}\right\rangle \\ &= \int_{-\infty}^{\infty} d\mathbf{q}\, \mathrm{e}^{\frac{i}{\hbar}\mathbf{P}\cdot\mathbf{q}} \left(\mathbf{R} + \frac{\mathbf{q}}{2}\right) \left\langle \mathbf{R} - \frac{\mathbf{q}}{2}\right| \mathbf{R} + \frac{\mathbf{q}}{2}\right\rangle \ .\end{aligned}$$

Since $\left\langle \mathbf{R} - \frac{\mathbf{q}}{2} \middle| \, \mathbf{R} + \frac{\mathbf{q}}{2} \right\rangle = \delta(\mathbf{q})$ by orthonormality requirements,

$$\mathcal{W}(\hat{\mathbf{r}}) = \mathbf{R} \, .$$

Similarly

$$\begin{aligned}
\mathcal{W}(\hat{\mathbf{r}}^2) &= \int_{-\infty}^{\infty} d\mathbf{q} \, \mathrm{e}^{\frac{i}{\hbar}\mathbf{P}\cdot\mathbf{q}} \left\langle \mathbf{R} - \frac{\mathbf{q}}{2} \middle| \left(\mathbf{R} + \frac{\mathbf{q}}{2}\right) \cdot \left(\mathbf{R} + \frac{\mathbf{q}}{2}\right) \middle| \mathbf{R} + \frac{\mathbf{q}}{2} \right\rangle \\
&= \int_{-\infty}^{\infty} d\mathbf{q} \, \mathrm{e}^{\frac{i}{\hbar}\mathbf{P}\cdot\mathbf{q}} \left(\mathbf{R} + \frac{\mathbf{q}}{2}\right) \cdot \left(\mathbf{R} + \frac{\mathbf{q}}{2}\right) \delta(\mathbf{q}) \\
&= \mathbf{R}^2 \, .
\end{aligned}$$

Turning to the Wigner transform of $\hat{\mathbf{p}}$ and using the definition $\langle \mathbf{r} | \, \hat{\mathbf{p}} \, | \mathbf{r} \rangle = -i\hbar \frac{\partial}{\partial \mathbf{r}}$ [63, 64] which implies the more general relation

$$\langle \mathbf{r}' | \, \hat{\mathbf{p}} \, | \mathbf{r} \rangle = -i\hbar \frac{\partial}{\partial \mathbf{r}} \delta(\mathbf{r} - \mathbf{r}') \, .$$

This, combined with the change of coordinates

$$\begin{aligned}
\mathbf{r} &= \mathbf{R} - \frac{\mathbf{q}}{2} \, , \\
\mathbf{r}' &= \mathbf{R} + \frac{\mathbf{q}}{2} \, ,
\end{aligned}$$

yields a new representation for the offset matrix element of the momentum operator, which can be employed in its Wigner transform

$$\mathcal{W}(\hat{\mathbf{p}}) = -i\hbar \int_{-\infty}^{\infty} d\mathbf{q} \, \mathrm{e}^{\frac{i}{\hbar}\mathbf{P}\cdot\mathbf{q}} \left(-\frac{\partial}{\partial \mathbf{q}} + \frac{1}{2} \frac{\partial}{\partial \mathbf{R}} \right) \delta(\mathbf{q}) \, .$$

Integrating this expression by parts gives

$$\begin{aligned}
\mathcal{W}(\hat{\mathbf{p}}) &= i\hbar \int_{-\infty}^{\infty} d\mathbf{q} \, \delta(\mathbf{q}) \left(-\frac{\partial}{\partial \mathbf{q}} + \frac{1}{2} \frac{\partial}{\partial \mathbf{R}} \right) \mathrm{e}^{\frac{i}{\hbar}\mathbf{P}\cdot\mathbf{q}} \\
&= i\hbar \left(-\frac{i}{\hbar} \mathbf{P} \right) \\
&= \mathbf{P} \, .
\end{aligned}$$

Similarly, one can consider the square of the momentum operator

$$\begin{aligned}
\mathcal{W}(\hat{\mathbf{p}}^2) &= -\hbar^2 \int_{-\infty}^{\infty} d\mathbf{q} \, \mathrm{e}^{\frac{i}{\hbar}\mathbf{P}\cdot\mathbf{q}} \left(\frac{\partial^2}{\partial \mathbf{q}^2} - \frac{\partial^2}{\partial \mathbf{R} \partial \mathbf{q}} + \frac{1}{4} \frac{\partial^2}{\partial \mathbf{R}^2} \right) \delta(\mathbf{q}) \\
&= -\hbar^2 \int_{-\infty}^{\infty} d\mathbf{q} \, \delta(\mathbf{q}) \left(\frac{\partial^2}{\partial \mathbf{q}^2} - \frac{\partial^2}{\partial \mathbf{R} \partial \mathbf{q}} + \frac{1}{4} \frac{\partial^2}{\partial \mathbf{R}^2} \right) \mathrm{e}^{\frac{i}{\hbar}\mathbf{P}\cdot\mathbf{q}} \\
&= -\hbar^2 (\frac{i}{\hbar}\mathbf{P}) \cdot (\frac{i}{\hbar}\mathbf{P}) \\
&= \mathbf{P}^2 \, .
\end{aligned}$$

Thus, in more general terms

$$\mathcal{W}(\hat{A}) = A_W(\mathbf{R}, \mathbf{P}) \, ,$$

where the W subscript denotes a Wigner-transformed operator. Therefore, if the action of the operator $\hat{A}$ can be represented in terms of position and momentum operators, then a simple replacement prescription can be followed to implement this transformation

$$\begin{aligned}
\hat{\mathbf{p}} &\to \mathbf{P} \, , \\
\hat{\mathbf{r}} &\to \mathbf{R} \, ,
\end{aligned}$$

which demonstrates that quantum operators are changed into phase-space functions by a Wigner transform.

Clearly the Wigner transform, which is unitary by virtue of the fact that it is, in essence, a Fourier transform, can be used to define a picture of quantum mechanics in which the dynamics take place in a classical-like phase space where each observable operator is represented by some phase-space function. To have a complete picture of dynamics in this Wigner phase space, it remains to determine how dynamical averages are calculated and how the commutator of quantum operators are represented.

2.1.2 The Wigner Function

Consider a Wigner-transformed system with position and momentum degrees of freedom $\mathbf{X} = (R_1, P_1, \ldots, R_N, P_N)$. In classical statistical mechanics, represented in the phase space $(\mathbf{R}, \mathbf{P})$, the system is described by the $f(\mathbf{R}, \mathbf{P})$, which assigns a probability to system occupying the state $(\mathbf{R}, \mathbf{P})$ [15, 65]. This function is vital to the calculation of averages of phase-space properties, which take the form [15, 65]

$$\langle A \rangle = \int d\mathbf{R}\, d\mathbf{P}\, A(\mathbf{R}, \mathbf{P}) f(\mathbf{R}, \mathbf{P}) \,,$$

where $A(\mathbf{R}, \mathbf{P})$ is an arbitrary phase-space function and $\langle A \rangle$ is its phase-space average. In quantum statistical mechanics, the system is described by a density operator $\hat{\rho}$ which fulfils an analogous role with regards to the calculation of averages, for more details see Appendix A. Therefore, if one were to represent quantum mechanics in phase space then the one might expect the transformed density operator to represent the phase space system in a similar manner as the classical distribution function. This makes finding the phase-space represented density operator the first priority for one wishing to formulate quantum statistical mechanics in the Wigner picture. The transformed density operator is known as the Wigner function and is defined [18, 21]

$$W(\mathbf{X}, t) = \frac{1}{h^N} \mathcal{W}(\hat{\rho}(t)) = \frac{1}{h^N} \int_{-\infty}^{\infty} d\mathbf{q}\, \mathrm{e}^{\frac{i}{\hbar}\mathbf{P}\cdot\mathbf{q}} \left\langle \mathbf{R} - \frac{\mathbf{q}}{2} \right| \hat{\rho}(t) \left| \mathbf{R} + \frac{\mathbf{q}}{2} \right\rangle \,, \tag{2.1}$$

It will be seen in the following sections that the Wigner function plays an analogous role to the classical distribution function with regards to the calculation of the dynamical properties of the system. However, first it is worth noting a simple, yet important, property of the Wigner function, it is not positive definite. This can be illustrated by considering the definition of density operator on some pure state $|\psi\rangle$ [15–17, 63, 65], or

$$\hat{\rho} = |\psi\rangle \langle\psi| \,.$$

Then the wavefunctions $\psi_1(\mathbf{q}, \mathbf{R}, \mathbf{P}) = \mathrm{e}^{\frac{i}{\hbar}\mathbf{P}\cdot\mathbf{q}} \psi\left(\mathbf{R} + \frac{\mathbf{q}}{2}\right)$ and $\psi_2(\mathbf{q}, \mathbf{R}) = \psi\left(\mathbf{R} - \frac{\mathbf{q}}{2}\right)$ can be defined, with $\psi(\mathbf{R}) = \langle\psi|\, \mathbf{R}\rangle$. In order that these be normalised, a factor of $\left(\frac{1}{\sqrt{2}}\right)^N$, or one factor of $\frac{1}{\sqrt{2}}$ for each of the N position degrees of freedom, must be introduced to each wavefunction. These wavefunctions can be used, along with the definition of the density operator to express the Wigner function, as defined in Eq. (2.1), as [21]

$$W(\mathbf{R}, \mathbf{P}) = \left(\frac{2}{h}\right)^N \int d\mathbf{q}\, \psi_1(\mathbf{q}, \mathbf{R}, \mathbf{P}) \psi_2^*(\mathbf{q}, \mathbf{R}) \,.$$

Therefore the Wigner function is bounded in magnitude according to [19, 21]

$$\left|W(\mathbf{R}, \mathbf{P})\right| \leq \left(\frac{2}{h}\right)^N$$

Therefore, unlike the classical distribution, which must be positive definite [66], the Wigner function can take on negative values and is bounded from above [19]. It is worth noting that several authors have linked Wigner function negativity to the existence of non-classical effects [17, 19, 21, 67]. It is no surprise then that this particular property will be the first means of differentiating between the Wigner function and the analogous classical distribution.

2.1.3 Wigner Picture Averages

As stated in the review of quantum statistical mechanics found in the Appendix A, the quantum average of some observable $\hat{A}$ is found, in the Schrödinger picture, by taking the following trace [15–17, 65]

$$\langle \hat{A}(t) \rangle = \mathrm{Tr}(\hat{\rho}(t)\hat{A}) \ .$$

In order to find the Wigner transform of this equation, consider first the more general result

$$\mathrm{Tr}(\hat{A}\hat{B}) = \frac{1}{h^N} \int d\mathbf{X} \ A_W(\mathbf{X}) B_W(\mathbf{X}) \ , \tag{2.2}$$

where there are N pairs of conjugate coordinates (R_i, P_i), this result is proved in Appendix. B.1. Applying this to the calculation of the quantum average yields

$$\langle \hat{A}(t) \rangle = \frac{1}{h^N} \int d\mathbf{X} \ A_W(\mathbf{X}) W(\mathbf{X}, t) \ ,$$

which, apart from the factor $\frac{1}{h^N}$, looks remarkably like an average in classical phase space.

It must be noted, at this point, that the Wigner function appears to be analogous to a classical distribution function; however, the completeness of this analogy is scuppered by the fact that, as has been shown in previous sections, the Wigner function is not in general positive definite [66]. This might be intuitively expected as the density operator itself is not in general composed of strict probability components, as demonstrated in the review of quantum statistical mechanics found in Appendix A, and so it is intuitively reasonable that the Wigner-transformed density operator only corresponds to a quasi-probability distribution [66].

So far, the Wigner transform appears to yield a picture of quantum dynamics that looks very much like classical dynamics in phase space. However, despite this appearance, no 'quantumness' has been lost. The reason for this is that, in addition to the fact that the Wigner function is not strictly a probability distribution, the equations of motion still contain dynamical sources of 'quantumness'. This can be more readily appreciated after a study of the Wigner-Liouville equation, which will be conducted in the following sections.

2.1.4 The Wigner-Liouville Equation

In quantum statistical mechanics a quantum system is represented by a density operator which evolves according to the Liouville equation [15–17, 65]

$$\frac{\partial}{\partial t}\hat{\rho} = \frac{i}{\hbar}[\hat{\rho}, \hat{H}] \ ,$$

where

$$\hat{H} = \frac{\hat{\mathbf{p}}^2}{2m} + V(\hat{\mathbf{r}}) \ . \tag{2.3}$$

In the Wigner picture, the corresponding time evolution equation is known as the Wigner-Liouville equation and is given by

$$\frac{\partial}{\partial t} W(\mathbf{X}, t) = -\frac{\mathbf{P}}{m} \cdot \frac{\partial}{\partial \mathbf{R}} W(\mathbf{X}, t) + \sum_{n=1,3,5,\cdots} \frac{1}{n!} \left(\frac{\hbar}{2i} \right)^{n-1} \frac{\partial^n V(\mathbf{R})}{\partial \mathbf{R}^n} \cdot \frac{\partial^n W(\mathbf{X}, t)}{\partial \mathbf{P}^n} \ . \tag{2.4}$$

This result applies only if the potential $V(\mathbf{R})$ is continuous. For a complete derivation of this result the reader is invited to refer to Appendix B.2.

2.1.5 Analysis of the Dynamics in the Wigner Picture

For the given Hamiltonian form, the Wigner-Liouville equation can be reformulated in such a way that its divergence from purely classical phase-space dynamics becomes obvious. This will be done by first making the identification

$$-\frac{\mathbf{P}}{m} \cdot \frac{\partial}{\partial \mathbf{R}} W(\mathbf{X}, t) = -\frac{\partial H_W(\mathbf{X})}{\partial \mathbf{P}} \cdot \frac{\partial W(\mathbf{X}, t)}{\partial \mathbf{R}} \ .$$

Here the Wigner-transformed Hamiltonian is defined by

$$H_W(\mathbf{X}) = \mathcal{W}(\hat{H}) \ ,$$

and $\hat{H}$ has the form of the Hamiltonian in Eq. (2.3). So the Wigner-Liouville equation might be rewritten

$$\frac{\partial}{\partial t}W(\mathbf{X},,t) = -\frac{\partial H_W(\mathbf{X})}{\partial \mathbf{P}} \cdot \frac{\partial W(\mathbf{X},t)}{\partial \mathbf{R}} + \sum_{n=1,3,5,\cdots} \frac{1}{n!}\left(\frac{\hbar}{2i}\right)^{n-1} \frac{\partial^n V(\mathbf{R})}{\partial \mathbf{R}^n} \cdot \frac{\partial^n W(\mathbf{X},t)}{\partial \mathbf{P}^n} \ .$$

Then the summation term can be rewritten so that it is given by

$$\sum_{n=1,3,5,\cdots} \frac{1}{n!}\left(\frac{\hbar}{2i}\right)^{n-1} \frac{\partial^n V(\mathbf{R})}{\partial \mathbf{R}^n} \cdot \frac{\partial^n W(\mathbf{R},\mathbf{P},t)}{\partial \mathbf{P}^n} = \frac{\partial V(\mathbf{R})}{\partial \mathbf{R}} \cdot \frac{\partial W(\mathbf{X},t)}{\partial \mathbf{P}} + \sum_{n=3,5,7,\cdots} \frac{1}{n!}\left(\frac{\hbar}{2i}\right)^{n-1} \frac{\partial^n V(\mathbf{R})}{\partial \mathbf{R}^n} \cdot \frac{\partial^n W(\mathbf{X},t)}{\partial \mathbf{P}^n} \ .$$

At this point it is important to note that

$$\frac{\partial V(\mathbf{R})}{\partial \mathbf{R}} = \frac{\partial H_W(\mathbf{X})}{\partial \mathbf{R}} \ ,$$

so that

$$\frac{\partial}{\partial t}W(\mathbf{X},t) = \frac{\partial H_W(\mathbf{X})}{\partial \mathbf{R}} \cdot \frac{\partial W(\mathbf{X},t)}{\partial \mathbf{P}} - \frac{\partial H_W(\mathbf{X})}{\partial \mathbf{P}} \cdot \frac{\partial W(\mathbf{X},t)}{\partial \mathbf{R}} + \sum_{n=3,5,\cdots} \frac{1}{n!}\left(\frac{\hbar}{2i}\right)^{n-1} \frac{\partial^n V(\mathbf{R})}{\partial \mathbf{R}^n} \cdot \frac{\partial^n W(\mathbf{X},t)}{\partial \mathbf{P}^n} \ .$$

This can be simplified by introducing the phase-space Poisson bracket $\{\cdot,\cdot\}$:

$$\frac{\partial}{\partial t}W(\mathbf{X},t) = \{H_W(\mathbf{X}), W(\mathbf{X},t)\} + \sum_{n=3,5,\cdots} \frac{1}{n!}\left(\frac{\hbar}{2i}\right)^{n-1} \frac{\partial^n V(\mathbf{R})}{\partial \mathbf{R}^n} \cdot \frac{\partial^n W(\mathbf{X},t)}{\partial \mathbf{P}^n} \ , \tag{2.5}$$

where

$$\{H_W(\mathbf{X}), W(\mathbf{X},t)\} = \frac{\partial H_W(\mathbf{X})}{\partial \mathbf{R}} \cdot \frac{\partial W(\mathbf{X},t)}{\partial \mathbf{P}} - \frac{\partial H_W(\mathbf{X})}{\partial \mathbf{P}} \cdot \frac{\partial W(\mathbf{X},t)}{\partial \mathbf{R}} \ .$$

Hence the evolution equation for an operator in the Wigner picture can be expressed in terms of the classical Poisson bracket and an infinite series of terms, each of a successively higher power in $\hbar$. These $\hbar$ terms then provide 'quantum corrections' to the classical dynamics given by the Poisson bracket. It is evident that the inclusion of these 'correction' terms incorporates successively more non-locality into the phase-space dynamics, as each term contains higher order phase-space derivatives. Inclusion of these higher-order non-local terms into the equations of motion is what prevents the dynamics from remaining purely classical, and so it might be concluded that this infinite series of terms contains the 'quantumness' which is still present in the dynamics.

2.1.6 Bracket formulation of the Wigner-Liouville Equation

The fact that the Wigner-transformed commutator in the Wigner-Liouville equation is not identically zero suggests that, despite quantum operators being represented in phase space, their commutator relations are preserved. This can be expressed more explicitly by rewriting the Wigner-Liouville equation in a bracket formulation, known as the Moyal bracket [68]. To this end one introduces the notation

$$\overleftarrow{\boldsymbol{\partial}} = \begin{pmatrix} \frac{\overleftarrow{\partial}}{\partial \mathbf{R}} \\ \frac{\overleftarrow{\partial}}{\partial \mathbf{P}} \end{pmatrix} \ ,$$

$$\boldsymbol{\epsilon} = \begin{pmatrix} 0 & 1 \\ -1 & 0 \end{pmatrix} \ ,$$

$$\mathbf{B} = \begin{pmatrix} \mathbf{0} & \mathbf{1} \\ -\mathbf{1} & \mathbf{0} \end{pmatrix} \ ,$$

$$\Lambda = \overleftarrow{\boldsymbol{\partial}} \cdot \mathbf{B} \cdot \overrightarrow{\boldsymbol{\partial}} = \frac{\overleftarrow{\partial}}{\partial \mathbf{R}} \cdot \frac{\overrightarrow{\partial}}{\partial \mathbf{P}} - \frac{\overleftarrow{\partial}}{\partial \mathbf{P}} \cdot \frac{\overrightarrow{\partial}}{\partial \mathbf{R}} \ ,$$

here the arrows indicate the direction in which a derivative acts. This allows for the expression of the Liouville equation as

$$\frac{\partial}{\partial t}\hat{\rho} = -\frac{i}{\hbar}\begin{pmatrix} \hat{H} & \hat{\rho} \end{pmatrix} \cdot \boldsymbol{\epsilon} \cdot \begin{pmatrix} \hat{H} \\ \hat{\rho} \end{pmatrix} = -\frac{i}{\hbar}\begin{pmatrix} \hat{H} & \hat{\rho} \end{pmatrix} \cdot \begin{pmatrix} \hat{\rho} \\ -\hat{H} \end{pmatrix} = -\frac{i}{\hbar}\left(\hat{H}\hat{\rho} - \hat{\rho}\hat{H}\right) . \tag{2.6}$$

Using the introduced operator Λ, it is shown in Appendix B.3 that the Wigner-Liouville equation can also be expressed in the form

$$\frac{\partial}{\partial t}W(\mathbf{X},t) = -\frac{i}{\hbar}\left(H_W(\mathbf{X})\mathrm{e}^{\frac{i\hbar}{2}\Lambda}W(\mathbf{X},t) - W(\mathbf{X},t)\mathrm{e}^{\frac{i\hbar}{2}\Lambda}H_W(\mathbf{X})\right) = (H_W(\mathbf{X}), W(\mathbf{X},t))_M , \tag{2.7}$$

where $(\cdot,\cdot)_M$ is the Moyal bracket. This result is sufficient to reveal how the quantum-commutator is preserved in the Wigner phase-space representation, as it is clear that if one were to define a product of two phase-space observables through the Moyal star product [68] or

$$A_W * B_W = A_W \mathrm{e}^{\frac{i\hbar}{2}\Lambda} B_W ,$$

then the Wigner-Liouville equation has the simple form

$$\frac{\partial}{\partial t}W(\mathbf{X},t) = -\frac{i}{\hbar}\left[H_W(\mathbf{X}), W(\mathbf{X},t)\right]_* ,$$

where $[\cdot,\cdot]_*$ is the Moyal star-product form of the quantum commutator. Clearly then, with this definition of the product in the quantum commutator, it is possible for the commutation relations between observables to be preserved even when quantum mechanics is represented in the Wigner phase space. This result ensures that the Heisenberg uncertainty principle, which is formulated in terms of commutator relations [63, 64, 69, 70], is preserved even in this phase-space representation.

The Wigner-Liouville equation can then be written in an anti-symmetric bracket form, analogous to Eq. (2.6), by first expressing it as follows

$$\frac{\partial}{\partial t}W(\mathbf{X},t) = -\frac{i}{\hbar}\left(H_W(\mathbf{X})\left(\mathrm{e}^{\frac{i\hbar}{2}\Lambda}\right)W(\mathbf{X},t) + W(\mathbf{X},t)\left(-\mathrm{e}^{\frac{i\hbar}{2}\Lambda}\right)H_W(\mathbf{X})\right) ,$$

to which the $\boldsymbol{\epsilon}$ notation is introduced, yielding

$$\frac{\partial}{\partial t}W(\mathbf{X},t) = -\frac{i}{\hbar}\begin{pmatrix} H_W(\mathbf{X}) & W(\mathbf{X},t) \end{pmatrix} \cdot \boldsymbol{\epsilon}\mathrm{e}^{\frac{i\hbar}{2}\Lambda} \cdot \begin{pmatrix} H_W(\mathbf{X}) \\ W(\mathbf{X},t) \end{pmatrix} . \tag{2.8}$$

This abstract bracket formulation of the Wigner-Liouville equation expresses Moyal's phase-space representation of the quantum commutator between observables [68] and its notation becomes useful when one wishes to extend the Wigner picture treatment to systems in which only a subset of the degrees of freedom are Wigner transformed. By comparing Eq. (2.8) or Eq. (2.7) and Eq. (2.6), this formulation provides an explicit confirmation that the commutator of operators is preserved in the Wigner picture, despite the fact that the operators would now commute under the rules of the abstract algebra for Hilbert space operators. Therefore, it is the algebraic modification embodied by the Moyal star product, evident in Eq. (2.7), that allows the nature of the commutator, and thus the uncertainty principle, to be preserved in the phase-space representation.

2.1.7 The Wigner Picture and the Classical Limit

It is tempting, upon viewing Eq. (2.5), to attempt to take the classical limit simply by discarding the quantum correction terms; it becomes doubly tempting when one realises that this could seemingly be accomplished by letting $\hbar \to 0$. However, this naive approach to classical limit is not generally valid in the Wigner picture [21, 22], for the simple reason that the n-th order quantum correction term is only superficially proportional to $\hbar^{n-1}$. If one were to examine the definition of the Wigner function in Eq. (2.1) then one would see that the derivative $\frac{\partial^n W}{\partial \mathbf{P}^n}$ would introduce a factor of $\frac{1}{\hbar^n}$, meaning that the correction terms cannot be neglected as $\hbar \to 0$.

Therefore, without some fortuitous contribution from the density operator itself, the classical limit cannot be generally reached by letting $\hbar \to 0$ and using this to justify the neglect of the quantum correction terms. There are, however, other means of achieving this same goal that will be discussed further, in the case of the quantum-classical hybrid system, in Section 2.2.4.

2.2 Partial Wigner Picture

It is evident from the construction of the Wigner transform that the Wigner picture can only be employed when considering a system which possesses some phase-space representation. Importantly the Wigner transform depends on the position eigenstates of the transformed system. This means that if one were to consider a system which consists of two interacting subsystems, wishing to express only one of them in phase space, then Wigner transform for this system must be carefully defined. In such a case, it is possible to apply the Wigner transform to only one set of position eigenstates, resulting in only one of the interacting systems being represented in phase space. The remaining degrees of freedom are left represented in a Hilbert space which is parameterised by the new phase-space variables. For such systems, the Wigner transform is referred to as a *partial* Wigner transform and the corresponding picture of quantum mechanics is the partial Wigner picture.

The partial Wigner picture, as will be seen, lends itself well to approximation techniques, as its Liouville equation can be written in terms of some hybrid quantum-classical dynamics with a series of correction terms. It is these correction terms that form the focus of this study; not only are they derived for arbitrary polynomial potentials and couplings but their impact on the dynamics of a quantum system forms the core focus of this study.

2.2.1 Partial Wigner Transformations

Consider a Hamiltonian of the form $\hat{H} = \hat{H}_s(\hat{s}) + \hat{H}_c(\hat{s}, \hat{\mathbf{X}}) + \hat{H}_x(\hat{\mathbf{X}})$, where $\hat{H}_s(\hat{s})$ is the Hamiltonian of a subsystem with degrees of freedom $\hat{s}$, that will not be Wigner transformed; $\hat{H}_x(\hat{\mathbf{X}})$ is the Hamiltonian of another subsystem x, whose degrees of freedom are the operators $\hat{\mathbf{X}}$, that act only on the x-subsystem and have phase-space analogues; and $\hat{H}_c(\hat{s}, \hat{\mathbf{X}})$ is the coupling Hamiltonian. The partial Wigner form $\hat{H}_w(\mathbf{X})$ of the Hamiltonian $\hat{H}$ is defined by taking the Wigner transform as before:

$$\hat{H}_w(\mathbf{X}) = \hat{H}_s(\hat{s}) + \int_{-\infty}^{\infty} d\mathbf{q}\, \mathrm{e}^{i\frac{\mathbf{P}}{\hbar}\cdot\mathbf{q}} \left\langle \mathbf{R} - \frac{\mathbf{q}}{2} \right| \hat{H}_c + \hat{H}_x \left| \mathbf{R} + \frac{\mathbf{q}}{2} \right\rangle \ .$$

Since the operator $\hat{H}_s(\hat{s})$ does not act upon the position states of the x-subsystem, the Wigner transform reduces to a multiplication by the identity operator. The partial Wigner Hamiltonian is, in this way, not simply a phase-space function, as it still contains Hilbert space operators that act upon the s-subsystem.

It is clear that this treatment might be extended to any arbitrary operator on the system. Such an operator remains a pure operator only if it acts strictly on the s-subsystem; or the operator becomes a pure phase-space function if it acts on the x-subsystem only; otherwise it is an operator dependent on, or parameterised by, the phase-space variables. I is important to note that such partial Wigner operators possess two forms of commutator, pure operators commutation is defined by ordinary operator multiplication, while phase-space operator commutation is defined in terms of the Moyal star product [68]. General hybrid observables commutators are composed of both the Moyal star commutator and the standard quantum commutator. In this way the observables related only to subsystem s are assumed to commute with those which act only on system x.

2.2.2 Partial Wigner Density Operator

The density operator, when cast in this partial Wigner form, is not simply the Wigner function of the system. For example, let $|s\rangle$ be the s-subsystem state vector and $|x\rangle$ be the state vector of the x-subsystem. Now assume that the state $|\Phi\rangle$ of the whole system is separable, given by,

$$|\Phi\rangle = |x\rangle \otimes |s\rangle \ .$$

In this case, the density operator has the form

$$\hat{\rho} = |x\rangle \otimes |s\rangle \langle s| \otimes \langle x| \ .$$

The Wigner function, then, would be given by

$$W(\mathbf{X}) = \int_{-\infty}^{\infty} d\mathbf{q}\, \mathrm{e}^{i\frac{\mathbf{P}}{\hbar}\cdot\mathbf{q}} \left\langle \mathbf{R} - \frac{\mathbf{q}}{2} \right| \hat{\rho} \left| \mathbf{R} + \frac{\mathbf{q}}{2} \right\rangle \ .$$

However, since the state $|s\rangle$ has no intersection with the eigenstates of $\hat{\mathbf{X}}$, the Wigner function here is not solely a phase-space function. Rather, the transformed density operator $\hat{\rho}_w(\mathbf{X})$ is the product of the Wigner function, for the x-subsystem degrees of freedom, and the density operator for the s-subsystem.

$$\begin{aligned}\hat{\rho}_w(\mathbf{X}) &= |s\rangle\langle s| \otimes \int_{-\infty}^{\infty} d\mathbf{q}\, \mathrm{e}^{i\frac{\mathbf{P}}{\hbar}\cdot\mathbf{q}} \left\langle \mathbf{R} - \frac{\mathbf{q}}{2}\right| x\right\rangle \left\langle x\right| \mathbf{R} + \frac{\mathbf{q}}{2}\right\rangle \ , \\ &= \hat{\rho}_s \otimes W_x(\mathbf{X}) \ .\end{aligned}$$

Considering a general case, the partial Wigner density operator $\hat{\rho}_w(\mathbf{X})$ is the familiar density operator on the s-subsystem but is parameterised by the phase-space degrees of freedom $\mathbf{X}$.

2.2.3 Partial Wigner Picture Averages

The problems under consideration for this picture possess two distinct sets of degrees of freedom. Thus the representation of averages in this picture needs to be examined with this in mind. The trace over the operator product may be expressed in this picture by the result:

$$\mathrm{Tr}(\hat{A}\hat{B}) = \mathrm{Tr}_s \left(\frac{1}{h^N} \int d\mathbf{X}\ \hat{A}_w(\mathbf{X})\hat{B}_w(\mathbf{X}) \right) \ , \tag{2.9}$$

where Tr_s is the trace over the s-subsystem degrees of freedom $\hat{s}$. This is intuitively reasonable, in that the average consists of a trace over the Hilbert space degrees of freedom and an integral over the Wigner phase space. The mathematical reasons for the average taking the form of Eq. (2.9) are considered in Appendix B.4.

2.2.4 Equations of Motion in the Partial Wigner Picture

The Quantum Classical Equation

Consider a system defined by the total Hamiltonian operator

$$\hat{H} = \hat{H}_s(\hat{s}) + \hat{H}_c(\hat{s}, \hat{\mathbf{X}}) + \hat{H}_x(\hat{\mathbf{X}}) \ . \tag{2.10}$$

In Eq. (2.10), $\hat{H}_s$ is the Hamiltonian operator of a system with coordinates $\hat{s}$, which will be unaffected by the partial Wigner transform. $\hat{H}_x$ is the Hamiltonian of the x-subsystem, described by pairs of canonically conjugate operators $\hat{\mathbf{X}} = (\hat{\mathbf{R}}, \hat{\mathbf{P}})$, in keeping with previous notation. These operators are taken to be the generalised position and momentum coordinates of the system and therefore may be Wigner transformed as previously established. Also, $\hat{H}_c$ describes the coupling between the coordinates $\hat{s}$ and $\hat{\mathbf{R}}$ and is assumed to be capable of representation by the tensor product: $\hat{H}_c = V'(\hat{s}) \otimes V_c(\hat{\mathbf{X}})$.

We now recall the previously used definition of the completely antisymmetric matrix $\boldsymbol{\epsilon} = -\boldsymbol{\epsilon}^T$, given in block form by

$$\boldsymbol{\epsilon} = \begin{pmatrix} 0 & 1 \\ -1 & 0 \end{pmatrix} \ .$$

Consider then the von Neumann, or quantum Liouville, equation for the chosen system, written in terms of $\boldsymbol{\epsilon}$ as [26]

$$\frac{\partial}{\partial t}\hat{\rho} = -\frac{i}{\hbar} \begin{pmatrix} \hat{H} & \hat{\rho} \end{pmatrix} \cdot \boldsymbol{\epsilon} \cdot \begin{pmatrix} \hat{H} \\ \hat{\rho} \end{pmatrix} \ , \tag{2.11}$$

In order to take a partial Wigner transformation of Eq. (2.11), the result in Eq. (2.8) is used, yielding:

$$\frac{\partial}{\partial t}\hat{\rho}_w = -\frac{i}{\hbar} \left(\hat{H}_w \mathrm{e}^{\frac{i\hbar}{2}\Lambda} \hat{\rho}_w - \hat{\rho}_w \mathrm{e}^{\frac{i\hbar}{2}\Lambda} \hat{H}_w \right) \ ,$$

where the subscript w denotes a partial Wigner-transformed operator. The use of Eq. (2.8) seems to place limitations on the nature of the Hamiltonian, however, it is generally true that the partial Wigner transform of an operator product $\hat{A}\hat{B}$ is given by [71]:

$$\mathcal{W}\left(\hat{A}\hat{B}\right) = \hat{A}_w(\mathbf{X}) \mathrm{e}^{\frac{i\hbar\Lambda}{2}} \hat{B}_w(\mathbf{X}) \ , \tag{2.12}$$

where Λ is a differential operator given by

$$\Lambda = \frac{\overleftarrow{\partial}}{\partial \mathbf{R}} \cdot \frac{\overrightarrow{\partial}}{\partial \mathbf{P}} - \frac{\overleftarrow{\partial}}{\partial \mathbf{P}} \cdot \frac{\overrightarrow{\partial}}{\partial \mathbf{R}} = \overleftarrow{\boldsymbol{\partial}} \cdot \boldsymbol{B} \cdot \overrightarrow{\boldsymbol{\partial}} \, .$$

Once again the arrows indicate the direction in which the derivative acts. This Wigner-transformed operator product naturally yields the Moyal star product, giving credence to defining the Moyal bracket, as seen in Section 2.1.6, as the general dynamical bracket for quantum mechanics expressed in the Wigner phase space.

We now introduce an antisymmetric matrix operator $\mathbf{D}$, defined by

$$\mathbf{D} = \boldsymbol{\epsilon} \mathrm{e}^{\frac{i\hbar}{2}\Lambda} \, , \tag{2.13}$$

with this definition, the partial Wigner transform of Eq. (2.11) now reads

$$\frac{\partial}{\partial t}\hat{\rho}_w(\mathbf{X},t) = -\frac{i}{\hbar} \begin{pmatrix} \hat{H}_w(\mathbf{X}) & \hat{\rho}_w(\mathbf{X},t) \end{pmatrix} \cdot \mathbf{D} \cdot \begin{pmatrix} \hat{H}_w(\mathbf{X}) \\ \hat{\rho}_w(\mathbf{X},t) \end{pmatrix} \, . \tag{2.14}$$

The operator $\mathbf{D}$ can now be expanded as a Taylor series in the argument $\frac{i\hbar}{2}\Lambda$:

$$\mathbf{D} = \boldsymbol{\epsilon} \left(1 + \frac{i\hbar}{2}\Lambda + \left(\frac{i\hbar}{2}\Lambda\right)^2 /2! + \ldots \right) \, ,$$

or

$$\mathbf{D} = \boldsymbol{\epsilon} \lim_{N\to\infty} \sum_{n=0}^{N} \left(\frac{i\hbar}{2}\Lambda\right)^n /n! \, . \tag{2.15}$$

If terms given only by $n = 0$ and $n = 1$ are considered [26]:

$$\frac{\partial \hat{\rho}_w}{\partial t} = -\frac{i}{\hbar} \begin{pmatrix} \hat{H}_w(\mathbf{X}) & \hat{\rho}_w \end{pmatrix} \cdot \boldsymbol{\epsilon} \cdot \begin{pmatrix} \hat{H}_w(\mathbf{X}) \\ \hat{\rho}_w \end{pmatrix} - \frac{i}{\hbar}\frac{i\hbar}{2} \begin{pmatrix} \hat{H}_w(\mathbf{X}) & \hat{\rho}_w \end{pmatrix} \cdot \boldsymbol{\epsilon}\Lambda \cdot \begin{pmatrix} \hat{H}_w(\mathbf{X}) \\ \hat{\rho}_w \end{pmatrix} \, , \tag{2.16}$$

which can be expanded

$$\frac{\partial \hat{\rho}_w}{\partial t} = -\frac{i}{\hbar}\left(\hat{H}_w\hat{\rho}_w - \hat{\rho}_w\hat{H}_w\right) + \frac{1}{2}\left(\hat{H}_w \left(\frac{\overleftarrow{\partial}}{\partial \mathbf{R}} \cdot \frac{\overrightarrow{\partial}}{\partial \mathbf{P}} - \frac{\overleftarrow{\partial}}{\partial \mathbf{P}} \cdot \frac{\overrightarrow{\partial}}{\partial \mathbf{R}} \right) \hat{\rho}_w - \hat{\rho}_w \left(\frac{\overleftarrow{\partial}}{\partial \mathbf{R}} \cdot \frac{\overrightarrow{\partial}}{\partial \mathbf{P}} - \frac{\overleftarrow{\partial}}{\partial \mathbf{P}} \cdot \frac{\overrightarrow{\partial}}{\partial \mathbf{R}} \right) \hat{H}_w \right) \, .$$

This can be simplified by invoking the definition of the Poisson bracket for $\mathbf{X}$ and quantum commutator for $\hat{s}$

$$\begin{aligned} \frac{\partial \hat{\rho}_w}{\partial t} &= -\frac{i}{\hbar}[\hat{H}_w, \hat{\rho}_w] + \frac{1}{2}\left(\{\hat{H}_w, \hat{\rho}_w\} - \{\hat{\rho}_w, \hat{H}_w\} \right) \, , \\ &= (\hat{H}_w, \hat{\rho}_w)_{qc} \end{aligned} \tag{2.17}$$

This final form of the equation is the quantum-classical approximation, in which the dynamics are composed of a quantum commutator, representing quantum dynamics of the s-subsystem, and the classical-like dynamics of the Poisson bracket for the x-subsystem. It is evident that the coupling features in both the classical-like dynamics and quantum dynamics, as it depends on both an s-subsystem operator and on the phase-space coordinates $\mathbf{X}$. It is this feature of the coupling between subsystems that produces the 'back-reaction' of the quantum variables onto their classical counterparts, resulting in induced quantum fluctuations in the classical variables [12, 13]. Such quantum fluctuations do not spoil the commutation of the phase-space variables, as this approximation violates the positivity of the density operator [10, 12]. In the formulation of this approximation, terms of higher order in $\hbar$ have been neglected, so far without justification. However, the determination of the consequences of this omission of higher-order expansion terms is the objective of this study and therefore such terms, as well as conditions that might justify their neglect, must still be considered.

Conservation of Energy by the Quantum-Classical Equation

In some of the literature on quantum-classical hybrid brackets, the proposed non-Hamiltonian quantum-classical brackets, such as that proposed in [13], failed to conserve energy. It is therefore vital to demonstrate that the formulation of the quantum-classical bracket given by Eq. (2.17), which is essentially an anti-symmetric analogue of the bracket in [13], is completely consistent with conservation of energy.

As has been previously stated, the average of an observable operator $\hat{A}$ in the Schrödinger picture of quantum mechanics is given by the trace of the product of the operator with the density operator

$$\langle \hat{A}(t) \rangle = \mathrm{Tr}(\hat{A}\hat{\rho}(t)) \; ,$$

where $\hat{\rho}(t)$ is time-dependent density operator. Therefore, in the partial Wigner formalism

$$\langle \hat{A}_w \rangle = \mathrm{Tr}(\hat{A}_w \hat{\rho}_w(t)) \; ,$$

where $\hat{A}_w$ and $\hat{\rho}_w(t)$ are the partial Wigner-transformed operators $\hat{A}$ and $\hat{\rho}(t)$ and the trace over the Wigner phase-space degrees of freedom will take the form of an integral as previously outlined in Section 2.1.3.

The quantum-classical equation conserves energy, if

$$\frac{d}{dt}\langle \hat{H}_w \rangle = 0 \; ,$$

or

$$\frac{d}{dt}\mathrm{Tr}(\hat{H}_w \hat{\rho}_w(t)) = 0 \; .$$

Applying the time derivative leads to the result

$$\mathrm{Tr}\left(\hat{H}_w \frac{\partial \hat{\rho}_w(t)}{\partial t}\right) = 0 \; ,$$

which must be satisfied when the equation of motion is substituted for $\frac{\partial \hat{\rho}_w(t)}{\partial t}$, otherwise the equation of motion will not be consistent with the principle of energy conservation. In order that this quantum-classical equation be subjected to this test, it will be considered in two parts: thus the linearity of the trace [15, 72] will be used to perform the following separation

$$\mathrm{Tr}\left(\hat{H}_w \frac{\partial \hat{\rho}_w(t)}{\partial t}\right) = -\frac{i}{\hbar}\mathrm{Tr}\left(\hat{H}_w[\hat{H}_w, \hat{\rho}_w]\right) + \frac{1}{2}\mathrm{Tr}\left(\hat{H}_w\{\hat{H}_w, \hat{\rho}_w\} - \hat{H}_w\{\hat{\rho}_w, \hat{H}_w\}\right) \; .$$

First, consider the quantum-commutator component of the trace

$$\mathrm{Tr}\left(\hat{H}_w[\hat{H}_w, \hat{\rho}_w]\right) = \mathrm{Tr}\left(\hat{H}_w^2\hat{\rho}_w - \hat{H}_w\hat{\rho}_w\hat{H}_w\right) \; .$$

This can be further subdivided

$$\mathrm{Tr}\left(\hat{H}_w[\hat{H}_w, \hat{\rho}_w]\right) = \mathrm{Tr}\left(\hat{H}_w^2\hat{\rho}_w\right) - \mathrm{Tr}\left(\hat{H}_w\hat{\rho}_w\hat{H}_w\right) \; .$$

Applying the cyclic invariance of the trace yields

$$\mathrm{Tr}\left(\hat{H}_w[\hat{H}_w, \hat{\rho}_w]\right) = \mathrm{Tr}\left(\hat{H}_w^2\hat{\rho}_w\right) - \mathrm{Tr}\left(\hat{H}_w^2\hat{\rho}_w\right) \; ,$$

so that there is complete cancellation

$$\mathrm{Tr}\left(\hat{H}_w[\hat{H}_w, \hat{\rho}_w]\right) = 0 \; .$$

Consider the Poisson bracket component of the trace:

$$\mathrm{Tr}\left(\hat{H}_w\{\hat{H}_w, \hat{\rho}_w\} - \hat{H}_w\{\hat{\rho}_w, \hat{H}_w\}\right) = \mathrm{Tr}'\left(\int_{-\infty}^{\infty}\int_{-\infty}^{\infty} d\mathbf{R}\, d\mathbf{P}\; \hat{H}_w\{\hat{H}_w, \hat{\rho}_w\} - \hat{H}_w\{\hat{\rho}_w, \hat{H}_w\}\right) \; ,$$

where Tr' is the trace over the s-subsystem's degrees of freedom. Expanding the Poisson bracket combination gives

$$\begin{aligned}&\mathrm{Tr}\left(\hat{H}_w\{\hat{H}_w,\hat{\rho}_w\}-\hat{H}_w\{\hat{\rho}_w,\hat{H}_w\}\right)\\&=\mathrm{Tr}'\left(\int_{-\infty}^{\infty}\int_{-\infty}^{\infty}d\mathbf{R}\,d\mathbf{P}\;\hat{H}_w\frac{\partial\hat{H}_w}{\partial\mathbf{R}}\cdot\frac{\partial\hat{\rho}_w}{\partial\mathbf{P}}-\hat{H}_w\frac{\partial\hat{H}_w}{\partial\mathbf{P}}\cdot\frac{\partial\hat{\rho}_w}{\partial\mathbf{R}}-\hat{H}_w\frac{\partial\hat{\rho}_w}{\partial\mathbf{R}}\frac{\partial\hat{H}_w}{\partial\mathbf{P}}+\hat{H}_w\frac{\partial\hat{\rho}_w}{\partial\mathbf{P}}\cdot\frac{\partial\hat{H}_w}{\partial\mathbf{R}}\right)\,.\end{aligned}$$

Considering each term individually, using the cyclic invariance of the trace and integrating by parts, assuming that $\hat{\rho}_w$ vanishes at the bounds of the integration, yields

$$\begin{aligned}\mathrm{Tr}'\left(\int_{-\infty}^{\infty}\int_{-\infty}^{\infty}d\mathbf{R}\,d\mathbf{P}\;\hat{H}_w\frac{\partial\hat{H}_w}{\partial\mathbf{R}}\cdot\frac{\partial\hat{\rho}_w}{\partial\mathbf{P}}\right)&=-\mathrm{Tr}'\left(\int_{-\infty}^{\infty}\int_{-\infty}^{\infty}d\mathbf{R}\,d\mathbf{P}\;\left(\frac{\partial\hat{H}_w}{\partial\mathbf{P}}\cdot\frac{\partial\hat{H}_w}{\partial\mathbf{R}}+\hat{H}_w\frac{\partial^2\hat{H}_w}{\partial\mathbf{P}\partial\mathbf{R}}\right)\hat{\rho}_w\right)\,,\\\mathrm{Tr}'\left(\int_{-\infty}^{\infty}\int_{-\infty}^{\infty}d\mathbf{R}\,d\mathbf{P}\;\hat{H}_w\frac{\partial\hat{H}_w}{\partial P}\cdot\frac{\partial\hat{\rho}_w}{\partial R}\right)&=-\mathrm{Tr}'\left(\int_{-\infty}^{\infty}\int_{-\infty}^{\infty}d\mathbf{R}\,d\mathbf{P}\;\left(\frac{\partial\hat{H}_w}{\partial\mathbf{R}}\cdot\frac{\partial\hat{H}_w}{\partial\mathbf{P}}+\hat{H}_w\frac{\partial^2\hat{H}_w}{\partial\mathbf{P}\partial\mathbf{R}}\right)\hat{\rho}_w\right)\,,\\\mathrm{Tr}'\left(\int_{-\infty}^{\infty}\int_{-\infty}^{\infty}d\mathbf{R}\,d\mathbf{P}\;\hat{H}_w\frac{\partial\hat{\rho}_w}{\partial\mathbf{R}}\cdot\frac{\partial\hat{H}_w}{\partial\mathbf{P}}\right)&=-\mathrm{Tr}'\left(\int_{-\infty}^{\infty}\int_{-\infty}^{\infty}d\mathbf{R}\,d\mathbf{P}\;\left(\frac{\partial\hat{H}_w}{\partial\mathbf{P}}\cdot\frac{\partial\hat{H}_w}{\partial\mathbf{R}}+\frac{\partial^2\hat{H}_w}{\partial\mathbf{P}\partial\mathbf{R}}\hat{H}_w\right)\hat{\rho}_w\right)\,,\\\mathrm{Tr}'\left(\int_{-\infty}^{\infty}\int_{-\infty}^{\infty}d\mathbf{R}\,d\mathbf{P}\;\hat{H}_w\frac{\partial\hat{\rho}_w}{\partial\mathbf{P}}\cdot\frac{\partial\hat{H}_w}{\partial\mathbf{R}}\right)&=-\mathrm{Tr}'\left(\int_{-\infty}^{\infty}\int_{-\infty}^{\infty}d\mathbf{R}\,d\mathbf{P}\;\left(\frac{\partial\hat{H}_w}{\partial\mathbf{R}}\frac{\partial\hat{H}_w}{\partial\mathbf{P}}+\frac{\partial^2\hat{H}_w}{\partial\mathbf{P}\partial\mathbf{R}}\hat{H}_w\right)\hat{\rho}_w\right)\,.\end{aligned}$$

Reassembling these terms results in

$$\mathrm{Tr}\left(\hat{H}_w\{\hat{H}_w,\hat{\rho}_w\}-\hat{H}_w\{\hat{\rho}_w,\hat{H}_w\}\right)=\mathrm{Tr}'\left(\int_{-\infty}^{\infty}\int_{-\infty}^{\infty}d\mathbf{R}\,d\mathbf{P}\;-\{\hat{H}_w,\hat{H}_w\}\hat{\rho}_w+\{\hat{H}_w,\hat{H}_w\}\hat{\rho}_w\right)\,,$$

so that, once again, there is complete cancellation of all terms

$$\mathrm{Tr}\left(\hat{H}_w\{\hat{H}_w,\hat{\rho}_w\}-\hat{H}_w\{\hat{\rho}_w,\hat{H}_w\}\right)=0\,.$$

Finally, combining the two component results yields

$$\mathrm{Tr}\left(\hat{H}_w\frac{\partial\hat{\rho}_w(t)}{\partial t}\right)=0\,,$$

as required by conservation of energy. The preceding results would also suggest that both the Poisson bracket combination and quantum commutator conserve energy independently. However, this does not preclude energy transfer between the quantum subsystem and the phase-space system, as the coupling operators feature in both sets of brackets. This independent energy conservation becomes important when the coupling is removed and each of the brackets must conserve energy in isolation.

The Quantum-Classical Limit

So far the quantum-classical equation has appeared only as an arbitrary prescription. That is, there was no physical motivation for the cut-off of the $\mathcal{O}(\hbar^2)$ terms in the expansion given in Eq. (2.25). If the quantum-classical equation is produced via this cut-off it is indeed merely an arbitrary prescription as it does not qualify as a consistent limit of the original quantum-quantum system [12]. This problem can be obviated by making a mass-scale separation of the two subsystems. Assume a Hamiltonian of the form:

$$\hat{H}=\hat{H}_s(\hat{r},\hat{p})+\hat{H}_x(\hat{R},\hat{P})+\hat{H}_c(\hat{r},\hat{R})\,.$$

Where the degrees of freedom for the s-subsystem are associated with a mass m and the x-subsystem has a mass M. Then the Hamiltonian can be rescaled by the energy parameter ω,

defining some arbitrary energy unit. The corresponding time and length scales t_ω and λ_ω are then given by [20]

$$t_\omega = \frac{\hbar}{\omega} ,$$
$$\lambda_\omega = \sqrt{\frac{\hbar^2}{m\omega}} .$$

In particular this length rescaling parameter corresponds to the ω-unit de Broglie wavelength of the x-subsystem [20]. Then the rescaling factors for the momenta of the x and s subsystem, p_m and P_M respectively, are found to be

$$p_m = \frac{m\lambda_\omega}{t_\omega} = \sqrt{m\omega} ,$$
$$P_M = \sqrt{M\omega} .$$

Unlike the momenta, the position operators $\hat{R}$ and $\hat{r}$ are rescaled by the same factor, this being the wavelength λ_ω. This rescaling is then analogous to that used in describing the Brownian motion of a heavy particle in a bath of light particles [20]. The rules for this rescaling can therefore be written as

$$\hat{r}' = \frac{\hat{r}}{\lambda_\omega} \text{ and } \hat{p}' = \frac{\hat{p}}{p_m} ,$$
$$\hat{R}' = \frac{\hat{R}}{\lambda_\omega} \text{ and } \hat{P}' = \frac{\hat{P}}{P_M} ,$$
$$\hat{H}' = \frac{\hat{H}}{\omega} \text{ and } t' = \frac{t\omega}{\hbar} .$$

If one were then to consider the rescaling of Eq. (2.14)

$$\frac{\omega}{\hbar}\frac{\partial}{\partial t'}\hat{\rho}'_w = -\frac{i}{\hbar}\begin{pmatrix} \omega\hat{H}'_w & \hat{\rho}'_w \end{pmatrix} \cdot \boldsymbol{\epsilon} \mathrm{e}^{\frac{i\mu}{2}\Lambda'} \cdot \begin{pmatrix} \omega\hat{H}'_w \\ \hat{\rho}'_w \end{pmatrix} . \tag{2.18}$$

Where $\mu = \sqrt{\frac{m}{M}}$ and

$$\Lambda = \frac{\overleftarrow{\partial}}{\partial R}\cdot\frac{\overrightarrow{\partial}}{\partial P} - \frac{\overleftarrow{\partial}}{\partial P}\cdot\frac{\overrightarrow{\partial}}{\partial R} = \frac{1}{\sqrt{M\omega}}\frac{\sqrt{m\omega}}{\hbar}\left(\frac{\overleftarrow{\partial}}{\partial R'}\cdot\frac{\overrightarrow{\partial}}{\partial P'} - \frac{\overleftarrow{\partial}}{\partial P'}\cdot\frac{\overrightarrow{\partial}}{\partial R'}\right) .$$

The quantum-classical equation can then be found if one takes the limit where $M \gg m$, in particular [20]

$$\lim_{\mu\ll 1} \mathrm{e}^{\frac{i\mu}{2}\Lambda'} = 1 + \frac{i\mu}{2}\Lambda' = 1 + \frac{i\hbar}{2}\Lambda , \tag{2.19}$$

which yields the truncated equation Eq. (2.16) when substituted into Eq. (2.18). Taking the truncation in the limit $M \gg m$ is equivalent to averaging out the short wavelength de Broglie oscillations related to P_M on the scale of the long de Broglie wavelengths associated to p_m [20].

This mass separation might also be compared to the method shown in [14] where the Heisenberg group which describes the two interacting quantum systems is taken to be a nilpotent Lie group with a two dimensional centre [14]. Such a Lie group is assumed to possess separate Planck constants for each of the two subsystems, as the observables of each subsystem as assumed to commute, one corresponding to the character of each element of the centre. When the character value of $\hbar$ for one of the subsystems becomes insignificant compared to that of the other subsystem, the quantum-classical bracket is found to be the approximate Lie bracket for the system [14]. This more involved process bears strong analogy with interpretation given for the simple rescaling procedure presented above and is far more general, since it makes reference only to the algebraic structure of the theory and not to the properties of any system.

In systems where one of these scale-separation procedures is possible, the quantum-classical approximation constitutes a clearly consistent classical limit of the original fully quantum system. Moreover, the derivation discussed in [14] suggests that the quantum-classical equation naturally arises as a dynamical approximation when the quantum effects in the dynamics of one of the

component systems become insignificant. The idea of the mass-scale separation presented here notably does not cover pseudo-spin systems, which feature no mass. However, such cases can be treated in the same manner, the pseudo-spin system, with its two energy levels, is simply considered an approximation for a system with more energy levels, but one that is largely unable to realise any level higher than the first excited state. In such a system there is a definite mass, that might be used to justify the kind of scale-separation procedure detailed above, but does not appear explicitly in the approximate two-level Hamiltonian.

Quantum Corrections to the Quantum-Classical Equation

It might be assumed, if one were attempting to view the quantum-classical equation from a perturbative standpoint, that the non-linear terms, neglected when making the quantum-classical approximation, are small enough to have little effect on the dynamics. However, outside of the perturbative limit that might justify the quantum-classical approximation, the non-locality of these terms makes it difficult to estimate the magnitude of their effect on the dynamics of a given system. Therefore, the purpose of this study is to investigate fully the role that these corrections play in the dynamics of a coupled subsystem and environment. In this section, these non-linear terms will be examined, for a given class of Hamiltonians, with a view to testing their effects on the dynamics of chosen model systems that feature couplings dependent on position coordinates $\mathbf{R}$ and polynomial potentials for the x-subsystem. As has been seen in Eq. (2.15), general terms in the partial Wigner-Liouville equation are characterised by the operators

$$D_n = \left(\frac{i\hbar}{2}\Lambda\right)^n /n! \, .$$

Recall that, as detailed above, the Hamiltonian will be of the of the form

$$\hat{H}_w = H_{x,w}(\mathbf{X}) + H(\hat{s}) + V'(\hat{s}) \times V_{c,w}(\mathbf{R}) \, ,$$

where all the symbols retain their previous meanings and $H_{x,w} = \frac{\mathbf{P}^2}{2} + \sum_{k=1}^{n_k} \frac{b_k}{k!}\mathbf{R}^k$. In order to reformulate the operator D_n, an examination of the properties of the operator Λ^n is required. To this end, refer to Eq. (B.6), which, for the given class of Hamiltonians, allows one to write

$$\Lambda^n = \frac{\overleftarrow{\partial^n}}{\partial \mathbf{R}^n} \cdot \frac{\overrightarrow{\partial^n}}{\partial \mathbf{P}^n} + (-1)^n \frac{\overleftarrow{\partial^n}}{\partial \mathbf{P}^n} \cdot \frac{\overrightarrow{\partial^n}}{\partial \mathbf{R}^n} \, ,$$

which can be further applied to generate the form of the operators D_n:

$$D_n = \left(\frac{i\hbar}{2}\right)^n \left(\frac{\overleftarrow{\partial^n}}{\partial \mathbf{R}^n} \cdot \frac{\overrightarrow{\partial^n}}{\partial \mathbf{P}^n} + (-1)^n \frac{\overleftarrow{\partial^n}}{\partial \mathbf{P}^n} \cdot \frac{\overrightarrow{\partial^n}}{\partial \mathbf{R}^n} \right) /n! \, .$$

In terms of this notation the operator $\mathbf{D}$ is defined by

$$\mathbf{D} = \boldsymbol{\epsilon} \left(\lim_{N\to\infty} \sum_{n=0}^{N} D_n \right) \, . \tag{2.20}$$

Additionally, this form of the bracket operator encompasses coupling potentials to any arbitrary polynomial order in $\mathbf{R}$, as no assumptions about the coupling were made beyond its $\mathbf{R}$ dependence. With the Wigner-Liouville equation expressed in terms of the operator $\boldsymbol{D}$, with $\mathbf{D}$ given by Eq. (2.20), one still obtains exact equations of motion for the given class of Hamiltonians. In a more explicit form, the exact equations of motion can now be written as

$$\begin{aligned} \frac{\partial}{\partial t}\hat{\rho}_w = &- \frac{i}{\hbar}\left[\hat{H}_s + V'(\hat{s}) \otimes V_{c,w}, \hat{\rho}_w\right] - \frac{i}{\hbar} \lim_{N\to\infty} \sum_{n=1}^{N} \left(V'(\hat{s}) \otimes V_{c,w} D_n \hat{\rho}_w - \hat{\rho}_w D_n V'(\hat{s}) \otimes V_{c,w}\right) \\ &- \frac{i}{\hbar} \lim_{N\to\infty} \sum_{n=1}^{N} \left(H_{x,w} D_n \hat{\rho}_w - \hat{\rho}_w D_n H_{x,w}\right) \, . \end{aligned} \tag{2.21}$$

In order to obtain a general feel for the nature of the quantum correction terms, consider the contribution of the term

$$-\frac{i}{\hbar}\lim_{N\to\infty}\sum_{n=1}^{N}\left(H_{x,w}D_n\hat{\rho}_w-\hat{\rho}_wD_nH_{x,w}\right)\ .$$

For $n=1$, the definition of D_n yields

$$D_1=\left(\frac{i\hbar}{2}\right)\left(\Lambda^1\right)=\left(\frac{i\hbar}{2}\right)\left(\frac{\overleftarrow{\partial}}{\partial\mathbf{R}}\cdot\frac{\overrightarrow{\partial}}{\partial\mathbf{P}}-\frac{\overleftarrow{\partial}}{\partial\mathbf{P}}\cdot\frac{\overrightarrow{\partial}}{\partial\mathbf{R}}\right)\ ,$$

so that

$$\frac{1}{2}\left(H_{x,w}D_1\hat{\rho}_w-\hat{\rho}_wD_1H_{x,w}\right)=\frac{1}{2}\left(\{H_{x,w},\hat{\rho}_w\}-\{\hat{\rho}_w,H_{x,w}\}\right)\ .$$

This means that this particular term in the corrections is just part of an anti-symmetric Poisson bracket combination, which agrees with the earlier derivation of the quantum-classical equation. It similarly evident that

$$-\frac{i}{\hbar}\left(V'(\hat{s})\otimes V_{c,w}D_1\hat{\rho}_w-\hat{\rho}_wD_1V'(\hat{s})\otimes V_{c,w}\right)=\frac{1}{2}\left(\{V'(\hat{s})\otimes V_{c,w},\hat{\rho}_w\}-\{\hat{\rho}_w,V'(\hat{s})\otimes V_{c,w}\}\right)\ .$$

It is clear, then, that only terms with $n>1$ will be of interest as quantum corrections, since the $n=1$ Poisson bracket terms describe classical-like phase-space dynamics.

For the remaining terms in the series, namely

$$-\frac{i}{\hbar}\lim_{N\to\infty}\sum_{n=2}^{N}\left(H_{x,w}D_n\hat{\rho}_w-\hat{\rho}_wD_nH_{x,w}\right)\ ,$$

it is instructive to expand the expression for a general term of order k

$$\begin{aligned}-\frac{i}{\hbar}\left(H_{x,w}D_k\hat{\rho}_w-\hat{\rho}_wD_kH_{x,w}\right)=&\frac{1}{2}\left(\frac{i\hbar}{2}\right)^{k-1}H_{x,w}\left(\frac{\overleftarrow{\partial^k}}{\partial\mathbf{R}^k}\cdot\frac{\overrightarrow{\partial^k}}{\partial\mathbf{P}^k}+(-1)^k\frac{\overleftarrow{\partial^k}}{\partial\mathbf{P}^k}\cdot\frac{\overrightarrow{\partial^k}}{\partial\mathbf{R}^k}\right)\hat{\rho}_w\\&-\frac{1}{2}\left(\frac{i\hbar}{2}\right)^{k-1}\hat{\rho}_w\left(\frac{\overleftarrow{\partial^k}}{\partial\mathbf{R}^k}\cdot\frac{\overrightarrow{\partial^k}}{\partial\mathbf{P}^k}+(-1)^k\frac{\overleftarrow{\partial^k}}{\partial\mathbf{P}^k}\cdot\frac{\overrightarrow{\partial^k}}{\partial\mathbf{R}^k}\right)H_{x,w}\ .\end{aligned}$$

Since $H_{x,w}$ is a phase-space function it therefore commutes with operators on the s-subsystem, which means that terms with similar derivative order to can be conveniently grouped through commuting $H_{x,w}$ and $\hat{\rho}_w$ as follows:

$$\begin{aligned}-\frac{i}{\hbar}\left(H_{x,w}D_k\hat{\rho}_w-\hat{\rho}_wD_kH_{x,w}\right)=&\frac{1}{2}\left(\frac{i\hbar}{2}\right)^{k-1}H_{x,w}\left(\frac{\overleftarrow{\partial^k}}{\partial\mathbf{R}^k}\cdot\frac{\overrightarrow{\partial^k}}{\partial\mathbf{P}^k}+(-1)^{k+1}\frac{\overleftarrow{\partial^k}}{\partial\mathbf{R}^k}\cdot\frac{\overrightarrow{\partial^k}}{\partial\mathbf{P}^k}\right)\hat{\rho}_w\\&-\frac{1}{2}\left(\frac{i\hbar}{2}\right)^{k-1}\hat{\rho}_w\left(\frac{\overleftarrow{\partial^k}}{\partial\mathbf{R}^k}\cdot\frac{\overrightarrow{\partial^k}}{\partial\mathbf{P}^k}+(-1)^{k+1}\frac{\overleftarrow{\partial^k}}{\partial\mathbf{R}^k}\cdot\frac{\overrightarrow{\partial^k}}{\partial\mathbf{P}^k}\right)H_{x,w}\ .\end{aligned}$$

Therefore, only terms of this type with k odd will be non-zero, so that these corrections can be simplified to a form familiar from the earlier discussion of the Wigner picture

$$-\frac{i}{\hbar}\lim_{N\to\infty}\sum_{n=2}^{N}\left(H_{x,w}D_n\hat{\rho}_w-\hat{\rho}_wD_nH_{x,w}\right)=\sum_{n=3,5,\cdots}^{N}\frac{1}{n!}\left(\frac{\hbar}{2i}\right)^{n-1}\frac{\partial^nH_{x,w}}{\partial\mathbf{R}^n}\cdot\frac{\partial^n\hat{\rho}_w}{\partial\mathbf{P}^n}\ ,$$

since $\frac{\partial^nH_{x,w}}{\partial\mathbf{P}^n}=0$ if $n>2$. However, in the case of the correction series due to the coupling potential, there is a more limited simplification possible as the potential $V'(\hat{s})\otimes V_{c,w}$ still contains an operator on the s-subsystem. This simplification relies on the assumption that the coupling

is dependent only on phase-space position $\mathbf{R}$. Consider, then, the series of correction terms that stem from the coupling potential:

$$-\frac{i}{\hbar}\lim_{N\to\infty}\sum_{n=2}^{N}\left(V'(\hat{s})\otimes V_{c,w}D_n\hat{\rho}_w-\hat{\rho}_wD_nV'(\hat{s})\otimes V_{c,w}\right)\ .$$

The first part of the general summation term may be expressed, by expanding D_n, as

$$V'(\hat{s})\otimes V_{c,w}D_n\hat{\rho}_w=\left(\frac{i\hbar}{2}\right)^n\frac{1}{n!}V'(\hat{s})\otimes V_{c,w}\left(\frac{\overleftarrow{\partial^n}}{\partial\mathbf{R}^n}\cdot\frac{\overrightarrow{\partial^n}}{\partial\mathbf{P}^n}+(-1)^n\frac{\overleftarrow{\partial^n}}{\partial\mathbf{P}^n}\cdot\frac{\overrightarrow{\partial^n}}{\partial\mathbf{R}^n}\right)\hat{\rho}_w\ .$$

Under the assumption that $V_{c,w}\equiv V_{c,w}(\mathbf{R})$ this reduces to

$$V'(\hat{s})\otimes V_{c,w}D_n\hat{\rho}_w=\left(\frac{i\hbar}{2}\right)^n\frac{1}{n!}V'(\hat{s})\otimes V_{c,w}\left(\frac{\overleftarrow{\partial^n}}{\partial\mathbf{R}^n}\cdot\frac{\overrightarrow{\partial^n}}{\partial\mathbf{P}^n}\right)\hat{\rho}_w\ .$$

Similarly, the second part of the term may, after following the same procedure, be expressed as

$$\hat{\rho}_wD_nV'(\hat{s})\otimes V_{c,w}=\left(\frac{i\hbar}{2}\right)^n\frac{1}{n!}(-1)^n\hat{\rho}_w\left(\frac{\overleftarrow{\partial^n}}{\partial\mathbf{P}^n}\cdot\frac{\overrightarrow{\partial^n}}{\partial\mathbf{R}^n}\right)V'(\hat{s})\otimes V_{c,w}\ .$$

Thus the correction terms due to the coupling potential may be written explicitly in terms of the phase-space derivatives of the coupling potential

$$\begin{aligned}&-\frac{i}{\hbar}\lim_{N\to\infty}\sum_{n=2}^{N}\left(V'(\hat{s})\otimes V_{c,w}D_n\hat{\rho}_w-\hat{\rho}_wD_nV'(\hat{s})\otimes V_{c,w}\right)\\&=\lim_{N\to\infty}\sum_{n=2}^{N}\frac{1}{2^nn!}\left(\frac{i}{\hbar}\right)^{n-1}\left(V'(\hat{s})\otimes\frac{\partial^nV_{c,w}}{\partial\mathbf{R}^n}\cdot\frac{\partial^n\hat{\rho}_w}{\partial\mathbf{P}^n}+(-1)^{n-1}\frac{\partial^n\hat{\rho}_w}{\partial\mathbf{P}^n}\cdot\frac{\partial^nV_{c,w}}{\partial\mathbf{R}^n}\otimes V'(\hat{s})\right)\ .\end{aligned}$$

This allows the equation of motion to be expressed in an explicit form, free of the D operators:

$$\begin{aligned}\frac{\partial\hat{\rho}_w}{\partial t}=&-\frac{i}{\hbar}[\hat{H}_w,\hat{\rho}_w]+\frac{1}{2}\left(\{\hat{H}_w,\hat{\rho}_w\}-\{\hat{\rho}_w,\hat{H}_w\}\right)\\&+\sum_{n=3,5,\ldots}\left(\frac{\hbar}{2i}\right)^{n-1}\frac{1}{n!}\frac{\partial^nH_{x,w}}{\partial\mathbf{R}^n}\cdot\frac{\partial^n\hat{\rho}_w}{\partial\mathbf{P}^n}\\&+\sum_{n=2,3,\ldots}\frac{1}{2^nn!}\left(\frac{i}{\hbar}\right)^{n-1}\left(V'(\hat{s})\otimes\frac{\partial^nV_{c,w}}{\partial\mathbf{R}^n}\cdot\frac{\partial^n\hat{\rho}_w}{\partial\mathbf{P}^n}+(-1)^{n-1}\frac{\partial^n\hat{\rho}_w}{\partial\mathbf{P}^n}\cdot\frac{\partial^nV_{c,w}}{\partial\mathbf{R}^n}\otimes V'(\hat{s})\right)\ .\end{aligned}$$

Clearly, the lowest order phase-space derivative in the coupling correction series is of order 2. With this in mind, it is now possible to obtain a more extensive simplification if the coupling is linear in $\mathbf{R}$. The linear dependence of $V_{c,w}$ on $\mathbf{R}$ means that all higher order corrections vanish, mathematically stated, one has:

$$\frac{\partial^n}{\partial\mathbf{R}^n}V'(\hat{s})\otimes V_{c,w}=\frac{\partial^n}{\partial\mathbf{P}^n}V'(\hat{s})\otimes V_{c,w}=0\ \ \forall\ n>1\ .$$

Therefore, for systems where the coupling potential is linear in $\mathbf{R}$, the corrections stem only from the phase-space potential and have a form strongly analogous to the quantum corrections in the full Wigner picture for an isolated system. This allows the partial Wigner-Liouville equation for linearly coupled systems to be written as

$$\frac{\partial\hat{\rho}_w}{\partial t}=-\frac{i}{\hbar}[\hat{H}_w,\hat{\rho}_w]+\frac{1}{2}\left(\{\hat{H}_w,\hat{\rho}_w\}-\{\hat{\rho}_w,\hat{H}_w\}\right)+\sum_{n=3,5,\cdots}^{N}\left(\frac{\hbar}{2i}\right)^{n-1}\frac{1}{n!}\frac{\partial^nH_{x,w}}{\partial\mathbf{R}^n}\cdot\frac{\partial^n\hat{\rho}_w}{\partial\mathbf{P}^n}\ .\quad(2.22)$$

The dynamics in the case of an arbitrary coupling and phase-space potential are then just the same hybrid dynamics of the quantum-classical equation but with the addition of some non-local phase-space correction terms. The correction terms stemming from the phase-space potential $V_{c,w}$ are

identical in form to the phase-space corrections that appeared in the Wigner-Liouville equation. For a system that exhibits such correction terms, one might then expect that the higher the order of existing, significant corrections, the greater the prevalence of non-local dynamical effects. The clear expression of the evolution equation in terms of a classical Poisson bracket and some additional non-local terms suggests that the dynamical differences between a quantum phase-space evolution and a classical evolution lie in these non-local correction terms. Moreover, if the coupling is removed, the anti-symmetric Poisson bracket combination can be resolved using the fact that the purely quantum components of the Hamiltonian have no phase-space derivatives

$$\frac{1}{2}\Big(\{\hat{H}_w,\hat{\rho}_w\}-\{\hat{\rho}_w,\hat{H}_w\}\Big)=\frac{1}{2}\Big(\{H_{x,w},\hat{\rho}_w\}-\{\hat{\rho}_w,H_{x,w}\}\Big)\ ,$$

which, since $H_{x,w}$ is a phase-space function, can be rewritten as a simple Poisson bracket

$$\frac{1}{2}\Big(\{\hat{H}_w,\hat{\rho}_w\}-\{\hat{\rho}_w,\hat{H}_w\}\Big)=\{H_{x,w},\hat{\rho}_w\}\ .$$

Thus the partial Wigner-Liouville equation for uncoupled subsystems has the form

$$\frac{\partial\hat{\rho}_w}{\partial t}=-\frac{i}{\hbar}[\hat{H}_s,\hat{\rho}_w]+\{H_{x,w},\hat{\rho}_w\}+\sum_{n=3,5,\cdots}^{N}\left(\frac{\hbar}{2i}\right)^{n-1}\frac{1}{n!}\frac{\partial^n H_{x,w}}{\partial\mathbf{R}^n}\cdot\frac{\partial^n\hat{\rho}_w}{\partial\mathbf{P}^n}\ .$$

It follows, then, that in the limit of zero coupling, the dynamics consist of isolated quantum dynamics for the s-subsystem and Wigner classical-like dynamics for the x-subsystem. Therefore, the dynamics obey the requirement that, when uncoupled, both subsystems evolve in isolation under exact quantum dynamics. If the case where the corrections are neglected is then considered, the x-subsystem evolves under purely classical dynamics when the coupling is removed. It has already been demonstrated that the Poisson bracket combination and quantum commutator conserve energy independently when the subsystems evolve in isolation; so the zero coupling limit satisfies both the requirements of dynamical separation and energy conservation for isolated systems.

Examining the complete equation Eq. (2.21), or any of the simplifications presented above, it is evident that the dynamics of a partially Wigner-transformed system can be viewed from a Eulerian perspective. That is, the equations of motion can be taken to represent Hilbert space dynamics for the s-subsystem at any point $\mathbf{X}$ in the phase space, therefore evaluating the dynamics of the system amounts to evaluating phase-space dynamics and the dynamics of a set of Hilbert spaces, each parameterised by a set of phase-space coordinates. This Eulerian viewpoint is especially evident in the calculation of the averages Eq. (2.9), in which one sees that taking the average of an observable is equivalent to taking the observable average in each individual Hilbert space parameterised by the point $\mathbf{X}$ and then averaging over the entire phase space.

Therefore, with all the preceding discussion in mind, a system which possesses a finite number of non-zero correction terms should allow for a comparison between its evolution under classical dynamics, by means of discarding the correction terms, and its evolution under fully quantum dynamics. This comparison would allow for the identification of purely quantum dynamical effects, as the only difference in the evolution are the non-local quantum-corrections. Thus, study of the effects of these correction terms could lead to indirect methods of observing quantum behaviour and testing the principles of quantum mechanics in man-made systems, such as nano-mechanical oscillators, which straddle the divide between the quantum and classical worlds. Moreover, such studies highlight the fundamental differences between quantum dynamics and classical dynamics, offering an opportunity to visualise, through the Wigner phase space, what it is that separates the evolution of quantum systems from those classical systems we are more directly familiar with. For these reasons, the numerical work in this study is devoted to determining how the quantum corrections affect the evolution of a model quantum system, a non-linear oscillator coupled to a two-level pseudo-spin system, with the aim to highlight particular quantum dynamical effects that result from the quantum-correction terms.

Analysis of the Algebraic Structure in Quantum-Classical Dynamics

Both Classical and Quantum mechanics feature canonical commutation relations between the generalised momentum and the generalised position quantities. In fact, commutation relations play

an additional important role in quantum mechanics due to the fact that operator families like the Pauli spin operators, which possess a cyclic commutation relation, form the generators of additional Lie algebras [24]. If the Lie algebra corresponds to a Lie group, then the operators in question are the generators of infinitesimal symmetry transformations [24, 73]. In addition to this consideration, quantities which commute with the Hamiltonian are found to represent the symmetries of the system [63] in both the quantum and classical regimes. It is therefore vital that the dynamical equations for the evolution of physical systems, which can also be expressed in terms of commutators, preserve such canonical or symmetry-related commutation relations, to do otherwise means the loss of some symmetry associated with the physical system.

To ensure that such symmetries are preserved, a dynamical bracket $(\cdot,\cdot)$ must meet certain requirements, the first being anti-symmetry:

$$(A,B) = -(B,A)\ .$$

This is required to ensure that all quantities, without explicit time dependence, self-commute:

$$(A,A) = -(A,A) = 0\ .$$

In particular this means that time-independent Hamiltonians are conserved. The second requirement is the Jacobi identity [24, 73]

$$((A,B),C) + ((B,C),A) + ((C,A),B) = 0\ .$$

Here the quantities A, B and C can be commuting phase-space functions or non-commuting operators. It is a simple matter to demonstrate that both these requirements are obeyed by the quantum and classical brackets, $[\cdot,\cdot]$ and $\{\cdot,\cdot\}$ respectively. These brackets are defined by [63, 74]

$$\begin{aligned}\left[\hat{A},\hat{B}\right] &= \hat{A}\hat{B} - \hat{B}\hat{A}\ ,\\ \{A,B\} &= \frac{\partial A}{\partial \mathbf{r}}\cdot\frac{\partial B}{\partial \mathbf{p}} - \frac{\partial A}{\partial \mathbf{p}}\cdot\frac{\partial B}{\partial \mathbf{r}}\ .\end{aligned}$$

The Poisson bracket $\{\cdot,\cdot\}$ is defined here on the phase space $(\mathbf{r},\mathbf{p})$.

There is one further requirement for a dynamical bracket and that is that the bracket forms a derivation. This means that the bracket corresponds to the generalisation of a derivative on some algebra. In the case of quantum mechanics this algebra is formed from the linear operators acting the Hilbert space of the system [65], while in classical mechanics the algebra is composed of smooth phase-space functions [74]. The defining property of a derivation D is known as the Leibniz condition and is given by

$$D(AB) = D(A)\cdot B + A\cdot D(B)\ .$$

In quantum mechanics the dynamical bracket $[\cdot,\hat{H}]$ forms a derivation

$$[\hat{A}\hat{B},\hat{H}] = \hat{A}\hat{B}\hat{H} - \hat{H}\hat{A}\hat{B} = \hat{A}\hat{B}\hat{H} - \hat{H}\hat{A}\hat{B} + \hat{A}\hat{H}\hat{B} - \hat{A}\hat{H}\hat{B} = [\hat{A},\hat{H}]\hat{B} + \hat{A}[\hat{B},\hat{H}]\ .$$

The classical bracket $\{\cdot,H\}$ is also a derivation

$$\{AB,H\} = \{A,H\}B + \{B,H\}A\ ,$$

which emerges simply by invoking the product rule for derivatives. The fact that these dynamical brackets form derivations validates their use in the equations of motion

$$\begin{aligned}\frac{d}{dt}\hat{A} &= \frac{1}{i\hbar}[\hat{A},\hat{H}]\ ,\\ \frac{d}{dt}A &= \{A,H\}\ .\end{aligned}$$

If the quantum-classical bracket of Eq. (2.17) is to provide a consistent description of the dynamics of interacting quantum and classical systems it is vital to ensure that it preserves the

symmetries associated with the system. To determine this, the quantum-classical bracket will be analysed to see whether or not is anti-symmetric, a derivation and whether it satisfies the Jacobi identity.

Before beginning a discussion of the quantum-classical equation it is important to establish some terminology: A quantum-classical system consists of a quantum sector, or subsystem, coupled to a classical, or phase-space, subsystem. A hybrid operator is one that acts upon both the quantum subsystem and the phase-space subsystem, being the product of a phase-space function and an operator that acts on the quantum subsystem. It is additionally important to establish what is meant by the notion of dynamical consistency, in the context of the hybrid dynamics, consistency is defined here to mean that the dynamical formalism inherits all the mathematical advantages of quantum and classical mechanics, namely that it conserves the intrinsic symmetries of a physical system and defines some notion of a derivative on the manifold associated to some Lie algebra.

It should be noted, at this point, that the Lie group in question is the nilpotent Lie group with a two-dimensional centre mentioned in Section 2.2.4.

It is clear that the quantum-classical equation is anti-symmetric, even when acting on non-commuting operators. This is because the commutator $[\cdot,\cdot]$ is anti-symmetric by definition and the Poisson bracket combination can be seen to be anti-symmetric by examining

$$\{\hat{A},\hat{B}\} - \{\hat{B},\hat{A}\} = -\left(\{\hat{B},\hat{A}\} - \{\hat{A},\hat{B}\}\right) \ .$$

In order to determine whether the quantum-classical bracket is a derivation, consider the Wigner transform of the Leibniz condition:

$$\mathcal{W}\left([AB,H]\right) = \mathcal{W}\left(A[B,H] + [A,H]B\right) \ ,$$

this can be expanded using Eq. (2.12) with the result:

$$\begin{aligned}\mathcal{W}\left([AB,H]\right) &= \mathcal{W}(AB)\mathrm{e}^{\frac{i\hbar}{2}\Lambda}H_w - H_w\mathrm{e}^{\frac{i\hbar}{2}\Lambda}\mathcal{W}(AB) \ , \\ &= A_w\mathrm{e}^{\frac{i\hbar}{2}\Lambda}\left(B_w\mathrm{e}^{\frac{i\hbar}{2}\Lambda}H_w - H_w\mathrm{e}^{\frac{i\hbar}{2}\Lambda}B_w\right) - \left(A_w\mathrm{e}^{\frac{i\hbar}{2}\Lambda}H_w - H_w\mathrm{e}^{\frac{i\hbar}{2}\Lambda}A_w\right)\mathrm{e}^{\frac{i\hbar}{2}\Lambda}B_w \ .\end{aligned}$$

Here the w subscript denotes the partial Wigner-transformed operator and, in subsequent notation, the constants $\frac{i\hbar}{2}$ will be absorbed into the Λ operator, meaning that $\mathcal{O}(\hbar^n) \equiv \mathcal{O}(\Lambda^n)$. Expanding the correction series about the operator Λ results in the exact, but complicated, expression

$$\begin{aligned}\mathcal{W}\left([AB,H]\right) &= A_w(1+\Lambda+\frac{1}{2}\Lambda^2+\ldots)\left(B_w(1+\Lambda+\frac{1}{2}\Lambda^2+\ldots)H_w - H_w(1+\Lambda+\frac{1}{2}\Lambda^2+\ldots)B_w\right) \\ &\quad - \left(A_w(1+\Lambda+\frac{1}{2}\Lambda^2+\ldots)H_w - H_w(1+\Lambda+\frac{1}{2}\Lambda^2+\ldots)A_w\right)(1+\Lambda+\frac{1}{2}\Lambda^2+\ldots)B_w \ , \\ &= A_wB_wH_w - A_wH_wB_w + A_wH_wB_w - H_wA_wB_w \\ &\quad + A_w\Lambda(B_wH_w) - A_w\Lambda(H_wB_w) + A_w(B_w\Lambda H_w) - A_w(H_w\Lambda B_w) \\ &\quad + (A_wH_w)\Lambda B_w - (H_wA_w)\Lambda B_w + (A_w\Lambda H_w)B_w - (H_w\Lambda A_w)B_w \\ &\quad + A_w\Lambda(B_w\Lambda H_w) - A_w\Lambda(H_w\Lambda B_w) + (A_w\Lambda H_w)\Lambda B_w - (H_w\Lambda A_w)\Lambda B_w \\ &\quad + A_w(B_w\frac{1}{2}\Lambda^2H_w - H_w\frac{1}{2}\Lambda^2B_w) - (A_w\frac{1}{2}\Lambda^2H_w - H_w\frac{1}{2}\Lambda^2A_w)B_w \\ &\quad + A_w\frac{1}{2}\Lambda^2(B_wH_w - H_wB_w) - (A_wH_w - H_wA_w)\frac{1}{2}\Lambda^2B_w + \mathcal{O}(\Lambda^3) \ .\end{aligned} \tag{2.23}$$

The previous result must then be compared to the quantum-classical bracket for the product A_wB_w in order to locate the limits in which the bracket forms a derivation. To this end, consider the bracket evaluation

$$-\frac{\hbar}{i}(A_wB_w,H_w)_{qc} = A_wB_wH_w - H_wA_wB_w + (A_wB_w)\Lambda H_w - H_w\Lambda(A_wB_w) \ .$$

This expression can be expanded via the definition of Λ and the product rule of differential oper-

ators, with the result

$$
\begin{aligned}
-\frac{\hbar}{i}(A_wB_w,H_w)_{qc} &= A_wB_wH_w - H_wA_wB_w - A_wH_wB_w + A_wH_wB_w + A_w\left(B_w\Lambda H_w\right) - A_w\left(H_w\Lambda B_w\right) \\
&\quad + \frac{i\hbar}{2}\left(\frac{\partial A_w}{\partial \mathbf{R}}B_w\cdot\frac{\partial H_w}{\partial \mathbf{P}} - \frac{\partial A_w}{\partial \mathbf{P}}B_w\cdot\frac{\partial H_w}{\partial \mathbf{R}} - \frac{\partial H_w}{\partial \mathbf{R}}A_w\cdot\frac{\partial B_w}{\partial \mathbf{P}} + \frac{\partial H_w}{\partial \mathbf{P}}A_w\cdot\frac{\partial B_w}{\partial \mathbf{R}}\right) , \\
&= A_w[B_w,H_w] + [A_w,H_w]B_w + A_w\left(B_w\Lambda H_w\right) - A_w\left(H_w\Lambda B_w\right) \\
&\quad + \left(A_w\Lambda H_w\right)B_w - \left(H_w\Lambda A_w\right)B_w + \frac{i\hbar}{2}\left(\frac{\partial A_w}{\partial \mathbf{R}}\cdot\left[B_w,\frac{\partial H_w}{\partial \mathbf{P}}\right] - \frac{\partial A_w}{\partial \mathbf{P}}\cdot\left[B_w,\frac{\partial H_w}{\partial \mathbf{R}}\right]\right) \\
&\quad + \frac{i\hbar}{2}\left(\left[\frac{\partial H_w}{\partial \mathbf{P}},A_w\right]\cdot\frac{\partial B_w}{\partial \mathbf{R}} - \left[\frac{\partial H_w}{\partial \mathbf{R}},A_w\right]\cdot\frac{\partial B_w}{\partial \mathbf{P}}\right) .
\end{aligned}
$$

In order to demonstrate the equivalence of the terms linear in Λ with those in Eq. (2.23), consider the expansion

$$
\begin{aligned}
&\frac{2}{i\hbar}\left(A_w\Lambda(B_wH_w) - A_w\Lambda(H_wB_w) + (A_wH_w)\Lambda B_w - (H_wA_w)\Lambda B_w\right) \\
&= \frac{\partial A_w}{\partial \mathbf{R}}\cdot\frac{\partial B_w}{\partial \mathbf{P}}H_w + \frac{\partial A_w}{\partial \mathbf{R}}B_w\cdot\frac{\partial H_w}{\partial \mathbf{P}} - \frac{\partial A_w}{\partial \mathbf{R}}\cdot\frac{\partial H_w}{\partial \mathbf{P}}B_w - \frac{\partial A_w}{\partial \mathbf{R}}H_w\frac{\partial B_w}{\partial \mathbf{P}} - \frac{\partial A_w}{\partial \mathbf{P}}\cdot\frac{\partial B_w}{\partial \mathbf{R}}H_w - \frac{\partial A_w}{\partial \mathbf{P}}B_w\cdot\frac{\partial H_w}{\partial \mathbf{R}} \\
&+ \frac{\partial A_w}{\partial \mathbf{P}}\cdot\frac{\partial H_w}{\partial \mathbf{R}}B_w + \frac{\partial A_w}{\partial \mathbf{P}}H_w\cdot\frac{\partial B_w}{\partial \mathbf{R}} + \frac{\partial A_w}{\partial \mathbf{R}}H_w\cdot\frac{\partial B_w}{\partial \mathbf{P}} + A_w\frac{\partial H_w}{\partial \mathbf{R}}\cdot\frac{\partial B_w}{\partial \mathbf{P}} - \frac{\partial H_w}{\partial \mathbf{R}}A_w\cdot\frac{\partial B_w}{\partial \mathbf{P}} - H_w\frac{\partial A_w}{\partial \mathbf{R}}\cdot\frac{\partial B_w}{\partial \mathbf{P}} \\
&- \frac{\partial A_w}{\partial \mathbf{P}}H_w\cdot\frac{\partial B_w}{\partial \mathbf{R}} - A_w\frac{\partial H_w}{\partial \mathbf{P}}\cdot\frac{\partial B_w}{\partial \mathbf{R}} + \frac{\partial H_w}{\partial \mathbf{P}}A_w\cdot\frac{\partial B_w}{\partial \mathbf{R}} + H_w\frac{\partial A_w}{\partial \mathbf{P}}\cdot\frac{\partial B_w}{\partial \mathbf{R}} \\
&= \frac{\partial A_w}{\partial \mathbf{R}}\cdot\left[B_w,\frac{\partial H_w}{\partial \mathbf{P}}\right] - \frac{\partial A_w}{\partial \mathbf{P}}\cdot\left[B_w,\frac{\partial H_w}{\partial \mathbf{R}}\right] + \left[\frac{\partial H_w}{\partial \mathbf{P}},A_w\right]\cdot\frac{\partial B_w}{\partial \mathbf{R}} - \left[\frac{\partial H_w}{\partial \mathbf{R}},A_w\right]\cdot\frac{\partial B_w}{\partial \mathbf{P}} + [\{A_w,B_w\},H_w] .
\end{aligned}
$$

The term $[\{A_w,B_w\},H_w]$ vanishes if A and B are either both phase-space functions or both quantum operators, additionally, it will also vanish if either A or B is a quantum operator. This means that this term will vanish for any hybrid operator product that can be expressed as the product of a phase-space function and a quantum subsystem operator. Moreover, any higher-order term in the expansion that features phase-space derivatives acting on both A_w and B_w will vanish for similar reasons. Therefore, the quantum-classical bracket is a derivation up to first order in the differential operator.

$$
-\frac{\hbar}{i}(A_wB_w,H_w)_{qc} + \mathcal{O}(\Lambda^2) = \mathcal{W}\left(A[B,H] + [A,H]B\right) .
$$

This agrees with the general form of the correction terms, found in Eq. (2.21), which demonstrates that the lowest-order quantum correction terms contain phase-space derivatives of second order. Therefore, if the hybrid operator components of the Hamiltonian depend, at most, linearly on either of the phase-space variables, the quantum-classical equation is a derivation. The general non-commutativity of the operators $\hat{A}$ and $\hat{B}$ lies at the heart of this failure to satisfy the Leibniz condition. It might be noted that if this bracket is used merely as an approximation, this failure does not present one with any trouble. It may noted that if A and B are either purely quantum operators or purely phase-space functions then the bracket does form a derivation, as it reduces to a quantum or classical bracket respectively.

One can now turn to examination of the Jacobi identity for quantum-classical systems. Since both the Poisson bracket and the quantum commutator satisfy the Jacobi identity individually, the identity is preserved for the subsets of operators that act only only on one of the subsystems. However, for general hybrid operators, it will turn out that the Jacobi identity only holds conditionally and the previously demonstrated derivation of the correction terms will allow for the identification of the explicit conditions that determine whether or not the symmetries associated with a chosen operator will be preserved by the quantum-classical equation. First, consider the exact equation partial Wigner bracket

$$
(\hat{A},\hat{B})_{pw} = \left[\hat{A}_w,\hat{B}_w\right] + \lim_{N\to\infty}\sum_{n=1}^{N}\left(\hat{A}_wD_n\hat{B}_w - \hat{B}_wD_n\hat{A}_w\right) . \tag{2.24}
$$

With

$$D_n = \left(\frac{i\hbar}{2}\right)^n \Lambda^n/n! \,,$$

as previously defined. This equation may be expanded [12]

$$(\hat{A},\hat{B})_{pw} = F_0(\hat{A}_w,\hat{B}_w) + \hbar F_1(\hat{A}_w,\hat{B}_w) + \hbar^2 F_2(\hat{A}_w,\hat{B}_w) + \dots \,, \tag{2.25}$$

where the functions F_n are independent of $\hbar$ and defined by

$$F_n(\hat{Q}_w,\hat{S}_w) = \frac{1}{n!}\left(\frac{i}{2}\right)^n \left(\hat{Q}_w\Lambda^n\hat{S}_w - \hat{S}_w\Lambda^n\hat{Q}_w\right) \,.$$

Having established this expansion representation of the partial Wigner bracket, the quantum-classical Jacobi identity takes the form

$$((A,B)_{qc},C)_{qc} + \text{c.p} = 0 \,.$$

Here A, B and C are assumed to represent partial Wigner-transformed operators and c.p stands for cyclic permutations. Each of the terms in this identity can be expanded in a manner similar to Eq. (2.25), yielding

$$\begin{aligned}(A,(B,C)_{pw})_{pw} &= F_0(A,F_0(B,C)) + \hbar F_0(A,F_1(B,C)) + \hbar F_1(A,F_0(B,C)) \\ &\quad + \hbar^2 F_0(A,F_2(B,C)) + \hbar^2 F_2(A,F_0(B,C)) + \hbar^2 F_1(A,F_1(B,C)) + \dots \\ &= \sum_{n=0}\sum_{k=0}^{n} \hbar^n F_k(F_{n-k}(A,B),C) \,.\end{aligned}$$

The complete partial Wigner Jacobi identity can then be divided into one Jacobi identity for each order of $\hbar$ [12]

$$F_0(F_0(A,B),C) + \text{c.p} = 0 \,, \tag{2.26}$$

$$\hbar F_0(F_1(A,B),C) + \hbar F_1(F_0(A,B),C) + \text{c.p} = 0 \,, \tag{2.27}$$

$$\hbar^2 F_0(F_2(A,B),C) + \hbar^2 F_2(F_0(A,B),C) + \hbar^2 F_1(F_1(A,B),C) + \text{c.p} = 0 \,, \tag{2.28}$$

$$\vdots$$

In order to determine whether the quantum-classical bracket will violate the Jacobi identity the same single term of the identity is evaluated for this choice of bracket

$$\begin{aligned}(A_w,(B_w,C_w)_{qc})_{qc} &= A_wB_wC_w - A_wC_wB_w + C_wB_wA_w - B_wC_wA_w + A_w(B_w\Lambda C_w - C_w\Lambda B_w) \\ &\quad - (B_w\Lambda C_w - C_w\Lambda B_w)A_w + A_w\Lambda(B_wC_w - C_wB_w) - (B_wC_w - C_wB_w)\Lambda A_w \\ &\quad + A_w\Lambda(B_w\Lambda C_w - C_w\Lambda B_w) - (B_w\Lambda C_w - C_w\Lambda B_w)\Lambda A_w \\ &= F_0(A_w,F_0(B_w,C_w)) + \hbar F_1(A_w,F_0(B_w,C_w)) \\ &\quad + \hbar F_0(A_w,F_1(B_w,C_w)) + \hbar^2 F_1(A_w,F_1(B_w,C_w)) \,.\end{aligned}$$

The F_n notation allows one to see that the terms $F_2(A_w,F_0(B_w,C_w))$, $F_0(A_w,F_2(B_w,C_w))$ and all terms of $\mathcal{O}(\hbar^3)$, or higher, do not appear in the quantum-classical evaluation. This means that for the quantum-classical bracket to satisfy the Jacobi identity, these extra terms must vanish:

$$F_2(A_w,F_0(B_w,C_w)) + F_0(A_w,F_2(B_w,C_w)) + \text{c.p} = 0 \,,$$

$$F_3(A_w,F_0(B_w,C_w)) + F_0(A_w,F_3(B_w,C_w)) + F_2(A_w,F_1(B_w,C_w)) + F_1(A_w,F_2(B_w,C_w)) + \text{c.p} = 0 \,,$$

$$\vdots$$

$$\sum_{k=0}^{n} F_k(A_w,F_{n-k}(B_w,C_w)) + \text{c.p} = 0 \,,$$

This will clearly be satisfied if we deal with hybrid observables that are, at most, linearly dependent on the phase-space degrees of freedom. This means, with the appropriate choice of Hamiltonian, and for a restricted class of observables one might find the quantum-classical bracket to be a Lie bracket. The choice of Hamiltonian only directly guarantees that the bracket constitutes a derivation; the Jacobi identity will still hold only for a restricted class of observables and thus any symmetries related to hybrid operators that are at least quadratic in the phase-space degrees of freedom may be violated by time evolution under the quantum-classical bracket. Importantly, one can see that for the terms $F_0(A_w, F_2(B_w, C_w))$ to be non-zero, at least two of the observables must be both hybrid observables and quadratic in the phase-space degrees of freedom [12]. The existence of generally non-vanishing non-linear terms in the Jacobi identity suggests that, even if a consistent quantum-classical limit exists, the Jacobi identity is not preserved.

The quantum corrections, as shown in equation Eq. (2.21), are clearly also given by F_n functions, this means if the F_2 term is added to the quantum-classical equation one finds the first Jacobi identity term to appear as

$$\begin{aligned}(A_w, (B_w, C_w)_{qc})_{qc} = {} & F_0(A_w, F_0(B_w, C_w)) + \hbar F_1(A_w, F_0(B_w, C_w)) + \hbar F_0(A_w, F_1(B_w, C_w)) \\ & + \hbar^2 F_1(A_w, F_1(B_w, C_w)) + \hbar^2 F_2(A_w, F_0(B_w, C_w)) + \hbar^2 F_0(A_w, F_2(B_w, C_w)) \\ & + \hbar^3 F_2(A_w, F_1(B_w, C_w)) + \hbar^3 F_1(A_w, F_2(B_w, C_w)) \, .\end{aligned}$$

The Jacobi identity now holds up to $\mathcal{O}(\hbar^2)$. The introduction of the correction term shifts the violation of the identity into the third order. Similarly, for each order of correction term added to the quantum-classical bracket the Jacobi identity is preserved to a correspondingly higher order. Since the structure of the Hamiltonian is the source of the correction terms, it is evident that the Jacobi and Leibniz violations will depend upon the Hamiltonian that governs the time evolution of the system. If one of the operators in the Jacobi identity is chosen to be the Hamiltonian and the other two are arbitrary hybrid operators, then it is evident that the Hamiltonian commutator with arbitrary observables will not be preserved under time evolution. Additionally, if only one arbitrary hybrid operator is chosen, accompanying the Hamiltonian and either a purely quantum operator or phase-space function, then the violation of the Jacobi identity depends only on the nature of the coupling function. This is because the coupling function is the only hybrid operator within the Hamiltonian, therefore it dictates whether the Hamiltonian will constitute a quadratic hybrid operator or not, as two such operators are required for violation of the Jacobi identity. This means that, if the coupling is at most a quadratic in the hybrid degrees of freedom, then the Jacobi identity will be satisfied, independent of the choice of the arbitrary hybrid observable. This means that the Hamiltonian symmetries associated with purely quantum operators and pure phase-space functions will be preserved by the quantum-classical equation under time evolution. However, it is evident that even these symmetries are not generally preserved for arbitrary coupling functions.

Consideration of operator non-commutativity means that the higher-order terms of the Jacobi identity will clearly only vanish for a limited class of observables. Therefore, for general observables this means that the Jacobi identity is always violated by time evolution under the quantum-classical bracket, regardless of the existence of a valid quantum-classical limit for the system. It is also noteworthy that all the $\mathcal{O}(\hbar^2)$ and higher-order terms vanish if at least two of the operators are restricted to being purely quantum operators or purely phase-space variables. This means that any commutation relations between pure quantum operators or phase-space functions are preserved by dynamical evolution under the quantum-classical bracket. This ensures that canonical commutation relations, and other quantum operator commutation relations, are preserved for both subsystems. It would seem then that the quantum-classical approximation is best suited either to the study of systems where the only hybrid observables of interest meet the restriction of being, at most, quadratic in the hybrid degrees of freedom, or possess few critical symmetries, as highly symmetric systems risk the loss of Hamiltonian symmetries under quantum-classical evolution. However, highly symmetric systems are likely to be able to be treated through some other method; hybrid dynamical methods are truly convenient in the case that there are no providential symmetries to simplify the solution of the dynamics, an example of such a symmetry-lacking system would be the type of many body condensed matter system that hybrid methods are designed to address. The link between the quantum corrections and the Jacobi identity is now obvious, if corrections are introduced up $\mathcal{O}(\hbar^n)$ then the Jacobi identity will be preserved up to this same order.

This suggests that the quantum-classical equation can be made use of, as an approximation, by always introducing a finite number of correction terms in order to preserve the relevant symmetries. However, it must be noted that if corrections are included to all orders, then the phase-space subsystem is no longer classical at all, this is problematic if one wishes for a formalism to universally address interacting quantum and classical systems. This being said, the fully corrected quantum-classical equation can still be made use of because it benefits from a significant reduction in computational complexity [2] and the corrected equation largely retains this advantage, provided that the added correction series is finite. It should be noted that for longer corrections series this advantage is lost, due to the computational cost of the higher-order derivatives.

The literature [10, 12–14, 75] is contentious as to whether the quantum-classical equation provides a consistent formalism for the treatment of interacting quantum and classical sectors and failure of the Leibniz condition and conditional Jacobi violation throws into doubt whether or not the quantum-classical equation represents a consistent coupling between quantum and classical sectors [12]. While it is true that the failings demonstrated here do not diminish the usefulness of the quantum-classical equation as an approximation, it means that it is less than certain that this bracket constitutes universally valid hybrid dynamics. Moreover, one notes that to restore the bracket to the status of a Lie bracket, one must include all orders of quantum corrections, effectively restoring the system to a pair of interacting quantum systems. It is the view of this author then, that despite the availability of consistent methods of achieving the quantum-classical limit, the coupled dynamics of quantum and classical subsystems, of the type presented in [10], do not appear to result in a consistent formalism capable of universally treating interacting quantum and classical sectors. This is because despite a consistent quantum-classical limit existing, the Jacobi identity is violated and the Leibniz condition is only preserved based on the structure of the Hamiltonian. There is some room for doubt in this conclusion, as it is not clear that any hybrid symmetries would be relevant to the dynamics of the total system; were this the case, then the violation of the Jacobi identity for hybrid observables becomes irrelevant. However, despite this, for general coupling functions, the Hamiltonian symmetries related to the individual quantum or classical subsystems are still violated by quantum-classical evolution; although one cannot discount the possibility that these violations might turn out to be a physical aspect of hybrid systems.

This conclusion, with its uncertainties, does not seriously diminish the usefulness of the quantum-classical formalism. Moreover, such non-Hamiltonian integration schemes demonstrate the potential to address open quantum systems [27, 76] and allow for combining thermostat or barostat types systems while maintaining other thermodynamic constraints [26]. It is also clear that such hybrid methods have value in cases that exhibit few symmetries pertaining to the total system, as the isolation of the quantum degrees of freedom reduces the computational complexity and, without many Hamiltonian symmetries, the disadvantages of the formalism do not manifest. It is also important to note that canonical commutations relations and commutation relations between quantum operator families, which define internal symmetries of the quantum system, are not compromised by the violation of the Jacobi identity. Finally, the algebraic structure of the theory can still be exploited to examine the dynamical differences between quantum and classical evolutions, through comparison of quantum-classical and quantum corrected dynamics. The failings of this quantum-classical treatment does not dismiss it, but merely suggests that caution must be exercised in its application and that there are still important questions to be answered about such formalisms.

Chapter 3

Numerical Methods

This chapter details the methods used in this work for the numerical solution of partial differential equations and for the numerical evaluation of phase-space averages. In the course of this chapter the method of lines technique for solving partial differential equations will be discussed, along with the attendant method of finite differences used to approximate phase-space derivatives in the equations if motion. Ordinary differential equation integrators will also be discussed, with particular emphasis on the Runge-Kutta 5 Cash-Karp method used in obtaining the numerical results presented in this work. Finally the method of calculating phase-space averages via the Simpson's rule technique of numerical integration will be presented.

3.1 Partial Differential Equations

A partial differential equation is one which features derivatives with respect to two, or more, independent variables. In particular, wave equations are generally presented as a relationship between the spatial derivatives and the temporal derivative of a wave function. This means that, due to the strong association between quantum dynamics and the dynamics of waves, the study of partial differential equations has a bearing on the solution of problems in quantum dynamics. Indeed, partial differential equations are a prominent aspect of many fields of physics, some examples being: statistical mechanics, fluid dynamics, thermodynamics, general relativity and electromagnetism. The discussion of this rich field of study is limited here to a basic over-view and the exposition of the numerical solution methods used in this particular research endeavour.

Let $y(x,t)$ be a function of the independent variables x and t. Then a partial differential equation, to which y is a solution, might be generally expressed as

$$\sum_n \left(\alpha_n(x,y,t) \frac{\partial^n}{\partial x^n} y + \beta_n(x,y,t) \frac{\partial^n}{\partial t^n} y \right) + \gamma(x,y,t) y = \kappa(x,t) \; . \tag{3.1}$$

3.1.1 Examples and Terminology

The *order* of a differential equation is determined by the highest-order derivative in that equation. A differential equation is linear if, when written in the form of Eq. (3.1), the coefficients α, β and γ are independent of y. The linearity of a partial differential equation can play a significant role in whether or not an analytical solution exists for the equation [77].

An example of a partial differential equation of physical relevance would be Schrödinger's equation [63]:

$$i\hbar \frac{\partial}{\partial t} \psi(\mathbf{r},t) = \left(-\frac{\hbar^2}{2m} \nabla^2 + V(\mathbf{r},t) \right) \psi(\mathbf{r},t) \; ,$$

where in three dimensions

$$\nabla^2 = \frac{\partial^2}{\partial x^2} + \frac{\partial^2}{\partial y^2} + \frac{\partial^2}{\partial z^2} \; .$$

Schrödinger's equation clearly features derivatives with respect to both time and space, making it a partial differential equation. Moreover, because it features second-order spatial derivatives, it is

a partial differential equation of second order. Finally, Schrödinger's equation is also linear as ψ appears only to the first power throughout the equation.

A second example is the Laplace equation

$$\nabla^2 \xi = 0 \,,$$

where ∇^2 is the Laplace operator. This equation is second order and linear.

3.1.2 General Solution

In general, a partial differential cannot be solved using simple ordinary differential equation solution methods, as it features derivatives with respect to more than one independent variable and cannot always be separated into a system of ordinary differential equations. However, despite this difficulty, many of the numerical techniques used in the approximate solution of ordinary differential equations are still useful in the case of the partial differential equation.

It is also not possible to solve analytically either non-linear partial differential equations or large systems of partial differential equations [77]. This makes numerical analysis approximation methods extremely important in the solution of these problems, as exact methods often do not exist. The method of particular interest in this study is the Method of Lines. However, before moving on to an explanation of this method, it is appropriate to examine first a technique from the approximate solution of ordinary differential equations: the Method of Finite Differences.

3.2 Method of Finite Differences

The method of finite differences is a simple approach to the approximation of derivatives, which has its origin in the definition of the derivative

$$\frac{dy}{dt} = \lim_{dt \to 0} \frac{y(t+dt) - y(t)}{dt} \,. \tag{3.2}$$

If the quantity dt is allowed to retain a finite size, rather than being reduced to 0, a simple approximation is obtained for the derivative with respect to t. This approximation must evidently be highly sensitive to the magnitude of the quantity dt. Requiring that dt is small, while desirable for ensuring the accuracy of a computation, may be an impractical or inefficient use of computational resources if derivatives of y must be evaluated over some large interval. However, it is possible to generalise this simple approximation to obtain formulae that are not linearly dependent on the magnitude of dt. These approximate formulae are derived by considering the truncation of a Taylor-series expansion of the function $y(t + \beta dt)$, where β is some real constant. Through this method it is also possible to extend this treatment to derivatives of higher order.

3.2.1 First Derivatives

The formula obtained by approximating the derivative definition can also be obtained by the method of Taylor series truncation. In order to approximate the first derivative of the function $y(t)$, consider the Taylor expansion:

$$y(t+dt) = y(t) + \frac{dy}{dt} dt + \mathcal{O}(dt^2) \,.$$

Where $\mathcal{O}(dt^2)$ represents the remainder of the series, where the leading order term is proportional to dt^2. A simple rearrangement of the previous formula yields

$$\frac{dy}{dt} = \frac{y(t+dt) - y(t)}{dt} + \mathcal{O}(dt) \,,$$

which allows for the approximation:

$$\frac{dy}{dt} \approx \frac{y(t+dt) - y(t)}{dt} \,.$$

This approximation is accurate only up to $\mathcal{O}(dt)$.

The determination of a more accurate approximation might be possible if one were to cancel out the $\mathcal{O}(dt^2)$ term in the Taylor expansion of $y(t+dt)$. In order to achieve this, consider the Taylor expansions:

$$y(t+dt) = y(t) + \frac{dy(t)}{dt}dt + \frac{1}{2!}\frac{d^2y(t)}{dt^2}dt^2 + \frac{1}{3!}\frac{d^3y(t)}{dt^3}dt^3 + \mathcal{O}(dt^4)\ , \tag{3.3}$$

$$y(t-dt) = y(t) - \frac{dy(t)}{dt}dt + \frac{1}{2!}\frac{d^2y(t)}{dt^2}dt^2 - \frac{1}{3!}\frac{d^3y(t)}{dt^3}dt^3 + \mathcal{O}(dt^4)\ . \tag{3.4}$$

Clearly, if one were to compute $y(t+dt) - y(t-dt)$ the terms of order dt^2 would be cancelled out, leaving the dt^3 terms as the leading order contributions to the error. Thus the approximation is found by evaluation of $y(t+dt) - y(t-dt)$:

$$y(t+dt) - y(t-dt) = 2\frac{dy(t)}{dt}dt + \frac{2}{3!}\frac{d^3y(t)}{dt^3}dt^3 + \mathcal{O}(dt^5)\ ,$$

this expression can be truncated, with an error of order dt^2, to provide an approximation to the first derivative, $\frac{dy}{dt}$,

$$\frac{dy}{dt} \approx \frac{y(t+dt) - y(t-dt)}{2dt}\ .$$

By considering more complicated combinations of Taylor expansions it is possible, in principle, to determine such an approximation to any desired order. In this study, the highest-order finite-difference approximation employed is of the fourth order and is given by [77]:

$$\frac{dy}{dt} \approx \left(\frac{y(t-2dt) - 8y(t-dt) + 8y(t+dt) - y(t+2dt)}{12dt}\right)\ .$$

3.2.2 Higher-Order Derivatives

An approximation to the second derivative of the function $y(t)$ can be immediately determined by adding Eq. (3.3) and Eq. (3.4):

$$y(t+dt) + y(t-dt) = 2y(t) + \frac{d^2y(t)}{dt^2}dt^2 + \frac{2}{4!}\frac{d^4y(t)}{dt^4}dt^4 + \mathcal{O}(dt^6)\ .$$

This can be rearranged to yield the approximation

$$\frac{d^2y(t)}{dt^2} \approx \frac{y(t+dt) - 2y(t) + y(t-dt)}{dt^2}\ ,$$

which is accurate to $\mathcal{O}(dt^2)$.

If a more complicated combination of Taylor expansions is chosen, for instance:

$$\begin{aligned} y(t+2dt) + y(t-2dt) - 16(y(t+dt) + y(t-dt)) = 2y(t) + 4\frac{d^2y(t)}{dt^2}dt^2 + \frac{32}{4!}\frac{d^4y(t)}{dt^4}dt^4 \\ - 16\left(2y(t) + \frac{d^2y(t)}{dt^2}dt^2 + \frac{2}{4!}\frac{d^4y(t)}{dt^4}dt^4\right) + \mathcal{O}(dt^6)\ , \end{aligned}$$

the approximation is found to be

$$\frac{d^2y(t)}{dt^2} \approx \frac{16y(t+dt) + 16y(t-dt) - 30y(t) - y(t+2dt) - y(t-2dt)}{12dt^2}\ ,$$

which has leading order uncancelled terms proportional to $\mathcal{O}(dt^4)$.

The last finite difference formula that is important for use in this study is a third-order derivative formula. The derivations previously seen suggest considering a difference of terms with the form

$$y(t+\beta dt) - y(t-\beta dt)\ .$$

To this end, consider the expansions

$$\begin{aligned} y(t+dt)-y(t-dt) &= 2\frac{dy(t)}{dt}dt+\frac{2}{3!}\frac{d^3y(t)}{dt^3}dt^3+\frac{2}{5!}\frac{d^5y(t)}{dt^5}dt^5+\mathcal{O}(dt^7)\ , \\ y(t+2dt)-y(t-2dt) &= 4\frac{dy(t)}{dt}dt+\frac{16}{3!}\frac{d^3y(t)}{dt^3}dt^3+\frac{64}{5!}\frac{d^5y(t)}{dt^5}dt^5+\mathcal{O}(dt^7)\ , \\ y(t+3dt)-y(t-3dt) &= 6\frac{dy(t)}{dt}dt+\frac{54}{3!}\frac{d^3y(t)}{dt^3}dt^3+\frac{162}{5!}\frac{d^5y(t)}{dt^5}dt^5+\mathcal{O}(dt^7)\ . \end{aligned} \tag{3.5}$$

To obtain a higher order of accuracy one might consider a linear combination of these three equations:

$$a\left(y(t+dt)-y(t-dt)\right)+b\left(y(t+2dt)-y(t-2dt)\right)+c\left(y(t+3dt)-y(t-3dt)\right)\ , \tag{3.6}$$

where a, b and c are real-number coefficients. By requiring that terms of order dt and dt^5 vanish, resulting in the leading-order terms being dt^7, a set of simultaneous equations in a, b and c is constructed:

$$\begin{aligned} a+2b+3c &= 0\ , \\ a+32b+81c &= 0\ . \end{aligned}$$

These equations provide two restrictions for the three variables, it transpires, from the examination of Eq. (3.5) and Eq. (3.6) that one must require that

$$2a+16b+54c\neq 0\ .$$

This restriction must be applied in order to prevent the coefficient of the third derivative being zero. Therefore, let the set of equations be

$$\begin{aligned} a+2b+3c &= 0\ , \\ a+32b+81c &= 0\ , \\ a+8b+27c &= 3\ . \end{aligned}$$

The constant 3 in the last line is chosen for numerical convenience.

This has the solution

$$\begin{aligned} a &= -\frac{13}{8}\ , \\ b &= 1\ , \\ c &= -\frac{1}{8}\ . \end{aligned}$$

Therefore, the approximation for the third derivative can be formulated as follows

$$\frac{d^3y(t)}{dt^3}\approx\frac{1}{dt^3}\left(\frac{1}{8}y(t-3dt)+y(t+2dt)+\frac{13}{8}y(t-dt)-\frac{13}{8}y(t+dt)-y(t-2dt)-\frac{1}{8}y(t+3dt)\right)\ , \tag{3.7}$$

where the error is given by leading-order uncancelled terms proportional to $\mathcal{O}(dt^4)$.

3.3 Method of Lines

The method of lines is a technique designed to solve partial differential equations numerically by converting them into approximate ordinary differential equations. As previously stated, there is no general analytical way to decompose partial differential equations into ordinary differential equations. Instead, the method accomplishes this transformation by replacing the partial derivatives, with respect to all but one variable, with finite difference approximations of some suitably chosen order. The critical point is that derivatives with respect to a single variable are left unapproximated. The reason for this is that, with only one type of derivative remaining, the equation

is now an ordinary differential equation and can be solved numerically with an appropriate numerical integration method.

The numerical error incurred by the method of lines depends upon both the error of the finite-difference approximations and the ordinary differential integrator that was used [78]. This means the error cannot be generally determined and must be considered for the particular combination of finite difference order and integrator in use, this means that for more complicated ordinary differential equation solvers there is often no analytical form for the total error [77].

In this study, the method of lines is employed to replace derivatives in phase-space variables R and P with fourth-order finite-difference approximations. The ordinary differential equation integrator used is the Runge-Kutta 5 Cash-Karp method. A detailed discussion of ordinary differential equation integrators follows in the next section.

3.4 Ordinary Differential Equation Integrators

There exists a profusion of ordinary differential equation integrators, each with its own properties to recommend it. This section begins by examining two of the more basic integration methods: the Explicit and Implicit Euler methods. These basic methods proved too inaccurate for the purposes of this study and so the commonly used Runge-Kutta 4 and Runge-Kutta 5 Cash-Karp methods are presented afterwards, as these were used to complete the numerical analysis that is presented in the following chapter.

3.4.1 The Explicit Euler Method

Euler's explicit method is the simplest one-step numerical integrator that can be employed to solve an ordinary differential equation. Its simplicity, however, comes at the cost of accuracy, as the method incurs an error of $\mathcal{O}(dt)$.

Consider the problem $\frac{dy}{dt} = F(y,t)$. A Taylor expansion of $y(t+dt)$ about t results in:

$$y(t+dt) = y(t) + dt\frac{dy}{dt}\bigg|_t + \mathcal{O}(dt^2) \ .$$

In the case of the given differential equation, this Taylor expansion offers a simple truncation approximation

$$y(t+dt) \approx y(t) + dtF(y,t) \ ,$$

which is valid up to first order in dt. This result can be immediately generalised to a system of equations $\frac{d}{dt}\mathbf{y} = \mathbf{F}(\mathbf{y},t)$, yielding

$$\mathbf{y}(t+dt) = \mathbf{y}(t) + dt\mathbf{F}(\mathbf{y},t) \ .$$

Due to its lack of accuracy, the explicit Euler method can be employed only with a small dt interval. In computationally intensive processes this necessitates having to perform many additional calculations, as having dt very small means many more calculations must be performed over the same interval in t. Therefore, in order to achieve sufficient accuracy the explicit Euler method must sacrifice a large degree of computational efficiency.

3.4.2 The Implicit Euler Method

The implicit Euler method closely resembles the explicit method; however, this method is stable for any ordinary differential equation and for many partial differential equations [78]. The implicit Euler method has the same order of accuracy as the explicit version.

Euler's implicit method, in the simplest one-dimensional case, can be derived by considering the smooth, continuous function $y(t)$. By invoking the definition of the derivative of y at $t+dt$, one finds

$$y'(t+dt) = \lim_{dt\to 0} \frac{y(t+dt) - y(t)}{dt} \ ,$$

where $y'(t) = \frac{dy(t)}{dt}$. This means that the Taylor expansion of $y(t+dt)$ around t might be rewritten as

$$y(t+dt) = y(t) + dty'(t+dt) + \mathcal{O}(dt^2) \ .$$

This expansion can then be truncated to produce the approximation:

$$y(t+dt) \approx y(t) + dtF(y(t+dt), t+dt) \ ,$$

with an error per step of $\mathcal{O}(dt^2)$, making the global error $\mathcal{O}(dt)$.

For the simple problem $y' = -cy$, with c being a positive constant, the approximate solution is given by

$$y(t+dt) = \frac{y(t)}{1+cdt} \ .$$

This can be immediately generalised to a system of equations $\mathbf{y}' = -\mathbf{C} \cdot \mathbf{y}$, where $\mathbf{C}$ is a positive-definite matrix [78],

$$\mathbf{y}(t+dt) = (\mathbf{1} + dt\mathbf{C})^{-1} \mathbf{y}(t) \ ,$$

which is A-stable [78]. However, if the problem is somewhat more complicated, being of the form

$$\mathbf{y}' = \mathbf{F}(\mathbf{y}, t) \ ,$$

where $\mathbf{F}$ is some function of $\mathbf{y}$, possibly non-linear, the problem cannot be immediately inverted as before. Consequently, iterative methods may become necessary.

The implicit-difference problem, in the general non-invertible case, is then

$$\mathbf{y}(t+dt) = \mathbf{y}(t) + dt\mathbf{F}(\mathbf{y}(t+dt), t+dt) \ .$$

However, this method seems to require knowledge of $\mathbf{y}(t+dt)$ in order to calculate $\mathbf{y}(t+dt)$. The problem can be circumvented in numerous ways, the first and most simple being iteration:

$$\mathbf{y}^{(k+1)}(t+dt) = \mathbf{y}(t) + dt\mathbf{F}(\mathbf{y}^{(k)}(t+dt), t+dt) \ ,$$

where the superscript (k) is an iteration number. The previous value $\mathbf{y}(t)$ can be used as an estimate to begin iteration, or $\mathbf{y}^{(0)}(t+dt) = \mathbf{y}(t)$. Then the iteration scheme can be repeated until the results converge to within some desired accuracy. In practice, this convergence requirement might be represented by the inequality:

$$\left| \frac{\mathbf{y}^{(k+1)}(t+dt)}{\mathbf{y}^{(k)}(t+dt)} \right| \leq \epsilon \ ,$$

where ϵ is some small numerical tolerance factor.

Since it suffers from the same accuracy-based weakness as the explicit method and requires an additional computational step, without providing additional accuracy, the usefulness of the implicit Euler method is somewhat limited in intensive computations. However, it can still be of use when stability, rather than accuracy, is the numerical priority.

3.4.3 The Runge-Kutta 4 Method

The Runge-Kutta family of numerical integrators is a famous and widely used set of differential equation solvers. The Runge-Kutta 4 method, in particular, provides a good ratio of fourth-order accuracy to five computational operations per step. The chief downsides of this algorithm is that it lacks an inherent means of error estimation [78] and it does not offer any guarantee of numerical stability. The lack of a means of error estimation and an inability to dynamically adjust the step size mean that the Runge-Kutta 4 method is largely unsuitable for Method of Lines calculations.

Definition

For an equation $\frac{dy}{dt} = f(y,t)$ the widely used Runge-Kutta 4 algorithm is formulated as [78]

$$\begin{aligned} k_1 &= dtF(y,t) \ , \\ k_2 &= dtF\left(y + \frac{1}{2}k_1, t + \frac{1}{2}dt\right) \ , \\ k_3 &= dtF\left(y + \frac{1}{2}k_2, t + \frac{1}{2}dt\right) \ , \\ k_4 &= dtF(y + k_3, t + dt) \ , \\ y(t+dt) &\approx y(t) + \frac{1}{6}\left(k_1 + 2k_2 + 2k_3 + k_4\right) \ . \end{aligned}$$

This method has a global error of the order dt^4..

For use in this study the method must first be extended to the system of equations $\frac{d\mathbf{y}}{dt} = \mathbf{F}(\mathbf{y},t)$. This extension simply means redefining the k variables in vector form

$$\begin{aligned} \mathbf{k}_1 &= dt\mathbf{F}(\mathbf{y},t) \ , \\ \mathbf{k}_2 &= dt\mathbf{F}(\mathbf{y} + \frac{1}{2}\mathbf{k}_1, t + \frac{1}{2}dt) \ , \\ \mathbf{k}_3 &= dt\mathbf{F}(\mathbf{y} + \frac{1}{2}\mathbf{k}_2, t + \frac{1}{2}dt) \ , \\ \mathbf{k}_4 &= dt\mathbf{F}(\mathbf{y} + \mathbf{k}_3, t + dt) \ , \\ \mathbf{y}(t+dt) &\approx \mathbf{y}(t) + \frac{1}{6}\left(\mathbf{k}_1 + 2\mathbf{k}_2 + 2\mathbf{k}_3 + \mathbf{k}_4\right) \ . \end{aligned}$$

The derivation of Runge-Kutta 4 is given in Appendix. (C.1)

3.4.4 Runge-Kutta 5 Cash-Karp

The Cash-Karp method incorporates both Runge-Kutta 4 and 5 solutions and makes a comparison of the two as a measure of the error incurred in each step of the numerical evaluation of the solution. This allows the Cash-Karp method to make adjustments to the integration step size dt during evaluation in order to minimise the numerical error. The ability both to change dynamically the step-size and to estimate the numerical error makes the Cash-Karp method an attractive choice of integrator.

The Cash-Karp method is given by the algorithm [62]:

$$\begin{aligned} k_1 &= dtF(y,t) \ , \\ k_2 &= dtF(y + b_{21}k_1, t + a_2 dt) \ , \\ k_3 &= dtF(y + b_{31}k_1 + b_{32}k_2, t + a_3 dt) \ , \\ k_4 &= dtF(y + b_{41}k_1 + b_{42}k_2 + b_{43}k_3, t + a_4 dt) \ , \\ k_5 &= dtF(y + b_{51}k_1 + b_{52}k_2 + b_{53}k_3 + b_{54}k_4, t + a_5 dt) \ , \\ k_6 &= dtF(y + b_{61}k_1 + b_{62}k_2 + b_{63}k_3 + b_{64}k_4 + b_{65}k_5, t + a_6 dt) \ , \\ y(t+dt) &= y(t) + c_1k_1 + c_2k_2 + c_3k_3 + c_4k_4 + c_5k_5 + c_6k_6 \ . \end{aligned} \tag{3.8}$$

Here the coefficients c_i, b_{ij} and a_i are defined in Table 3.1 [78] These generalised equations will be specialised to the appropriate equations of motion in the following Chapter.

The error estimate is of the form [62]

$$\Delta = \sum_{i=1}^{6} \left(c_i - d_i\right) k_i \ . \tag{3.9}$$

The t step-size correction method comes from considering the error incurred when using two different step sizes, dt_0 and dt_1:

$$\begin{aligned} \Delta_0 &= \beta dt_0^5 \ , \\ \Delta_1 &= \beta dt_1^5 \ , \end{aligned}$$

Table 3.1: Runge-Kutta 5 Cash-Karp Coefficients

i	a_i	b_{i1}	b_{i2}	b_{i3}	b_{i4}	b_{i5}	c_i	d_i
1							$\frac{37}{378}$	$\frac{2825}{27648}$
2	$\frac{1}{5}$	$\frac{1}{5}$					0	
3	$\frac{3}{10}$	$\frac{3}{40}$	$\frac{9}{40}$				$\frac{250}{621}$	$\frac{18575}{48384}$
4	$\frac{3}{5}$	$\frac{3}{10}$	$-\frac{9}{10}$	$\frac{6}{5}$			$\frac{125}{594}$	$\frac{13525}{55296}$
5	1	$-\frac{11}{54}$	$\frac{5}{2}$	$-\frac{70}{27}$	$\frac{35}{27}$		0	$\frac{277}{14336}$
6	$\frac{7}{8}$	$\frac{1631}{55296}$	$\frac{175}{512}$	$\frac{575}{13824}$	$\frac{44275}{110592}$	$\frac{253}{4096}$	$\frac{512}{1771}$	$\frac{1}{4}$

where β is some constant of proportionality. Then the ratio between these two errors is given by

$$\frac{\Delta_0}{\Delta_1} = \left(\frac{dt_0}{dt_1}\right)^5 .$$

This can be rearranged to yield the new form [62]

$$dt_1 = dt_0 \left(\frac{\Delta_1}{\Delta_0}\right)^{0.2} .$$

Therefore, let Δ_1 be the desired error tolerance and Δ_0 the error resulting from using the step size dt_0. This means that if the step size is adjusted to dt_1 and the computation is performed again, then the error will be Δ_1 as desired. If the problem being solved is a system of equations then there exists an error estimate Δ_k for each equation individually, the overall error can then be estimated:

$$\Delta = \sqrt{\sum_{i=1}^{N} \Delta_i^2} .$$

In the actual simulations error is controlled by this Cash-Karp error correction and the error in the results is monitored by observation of the conservation of the Hamiltonian and the trace of the density operator.

3.5 Phase-Space Averages

As seen in the chapter on the Wigner picture, calculation average properties in the partial Wigner picture involves integration over all phase space. In this work, such integrations will be performed via Simpson's rule, a proof of which is found in Appendix. (C.2). Simpson's rule can expressed, as shown in Eq. (C.4), as

$$\int_{R_0}^{R_2} dr\ f(r) = \frac{\Delta R}{3}\left(f(R_0) + 4f(R_1) + f(R_2)\right) ,$$

where $R_1 = \frac{R_2+R_0}{2}$ and $\Delta R = \frac{R_2-R_0}{2}$..

Therefore, an integration of the sort

$$\text{Int} = \frac{1}{h}\int_{R_0}^{R_n}\int_{P_0}^{P_m} dR\, dP\ \hat{A}_w(R,P)\hat{\rho}_w(R,P) ,$$

necessary to calculate a partial Wigner picture average as in Eq. (2.9), is approximated by

$$\text{Int} \approx \sum_{i=0}^{n}\sum_{j=0}^{m} \Delta R \Delta P w_R(i) w_P(j) \hat{A}_w(R_0 + i\Delta R, P_0 + j\Delta P)\hat{\rho}_w(R_0 + i\Delta R, P_0 + j\Delta P) .$$

Here $\Delta R = \frac{R_n - R_0}{n}$, $\Delta P = \frac{P_m - P_0}{m}$ and

$$w_R(i) = \begin{cases} \frac{1}{3} & i = 0, \text{or } i = n \\ \frac{4}{3} & i \bmod 2 \neq 0 \\ \frac{2}{3} & i \bmod 2 = 0 \end{cases} ,$$

$w_P(j)$ is similarly defined. This approximation also depends upon the requirement that $\hat{\rho}_w(R, P) = 0$ if $R \notin [R_0 : R_n]$ or $P \notin [P_0 : P_m]$

Chapter 4

Numerical Calculations

4.1 The Diabatic Basis

In much of the literature on the quantum-classical equation, presented in Eq. (2.17), the equations of motion are expressed in the adiabatic basis [20]. This basis is given by the eigenstates of the momentum-independent components of the Hamiltonian and thus, in the partial Wigner picture, the eigenstates are parameterised by the position $\mathbf{R}$. If, instead, one wishes to work with eigenstates that are independent of position, the basis of the eigenstates of the subsystem that is not Wigner transformed (s-subsystem) might be used instead. This basis is known as the diabatic or subsystem basis [20]. To properly define the diabatic basis, consider the Hamiltonian

$$\hat{H} = \hat{H}_s(\hat{s}) + \hat{H}_x(\hat{\mathbf{X}}) + \hat{H}_c(\hat{s}, \hat{\mathbf{X}}) \ ,$$

and its Wigner-transformed counterpart

$$\hat{H}_w(\mathbf{X}) = \hat{H}_s(\hat{s}) + H_{x,w}(\mathbf{X}) + \hat{H}_c(\hat{s}, \mathbf{X}) \ , \tag{4.1}$$

where $\mathbf{X} = (\mathbf{R}, \mathbf{P})$ and all symbols retain their previously defined meanings. Now let the eigenstates of the operator $\hat{H}_s$ be defined by

$$\hat{H}_s \left|\alpha\right\rangle = \epsilon_\alpha \left|\alpha\right\rangle \ , \tag{4.2}$$

additionally, $\hat{H}_x$ does not operate on the states $\left|\alpha\right\rangle$.

This definition can be used to evaluate the matrix element of Eq. (2.17), which is found to take the form

$$\frac{\partial}{\partial t}\rho_w^{\alpha\alpha'}(\mathbf{X}, t) = -\frac{i}{\hbar}\left\langle\alpha\right| \left[\hat{H}_w, \hat{\rho}_w\right] \left|\alpha'\right\rangle + \frac{1}{2}\left\langle\alpha\right| \Big(\{\hat{H}_w, \hat{\rho}_w\} - \{\hat{\rho}_w, \hat{H}_w\}\Big) \left|\alpha'\right\rangle \ .$$

The completeness of the eigenstates $\left|\alpha\right\rangle$ can be used to rewrite the first term as follows

$$\left\langle\alpha\right| \left[\hat{H}_w, \hat{\rho}_w\right] \left|\alpha'\right\rangle = \sum_{\alpha''} \left(H_w^{\alpha\alpha''}\rho_w^{\alpha''\alpha'} - \rho_w^{\alpha\alpha''}H_w^{\alpha''\alpha'}\right) \ , \tag{4.3}$$

where

$$\begin{aligned} H_w^{\alpha\alpha'} &= \left\langle\alpha\right| \hat{H}_w \left|\alpha'\right\rangle \ , \\ \rho_w^{\alpha\alpha'} &= \left\langle\alpha\right| \hat{\rho}_w \left|\alpha'\right\rangle \ . \end{aligned}$$

The definition Eq. (4.2) can be used to simplify equation Eq. (4.3) through consideration of the matrix element

$$H_w^{\alpha\alpha''} = \left\langle\alpha\right| \hat{H}_s \left|\alpha''\right\rangle + 0 + \left\langle\alpha\right| \hat{H}_c \left|\alpha''\right\rangle = \epsilon_{\alpha''}\delta_{\alpha\alpha''} + H_c^{\alpha\alpha''} \ .$$

Therefore,

$$\left\langle\alpha\right| \left[\hat{H}_w, \hat{\rho}_w\right] \left|\alpha'\right\rangle = \hbar\tilde{\omega}^{\alpha\alpha'}\rho_w^{\alpha\alpha'} + \sum_{\alpha''} \left(H_c^{\alpha\alpha''}\rho_w^{\alpha''\alpha'} - \rho_w^{\alpha\alpha''}H_c^{\alpha''\alpha'}\right) \ , \tag{4.4}$$

where

$$\tilde{\omega}^{\alpha\alpha'} = \frac{\epsilon_\alpha - \epsilon_{\alpha'}}{\hbar} \,. \tag{4.5}$$

Similarly, one can take the matrix element of the Poisson bracket component of Eq. (2.17)

$$\begin{aligned}\frac{1}{2}\langle\alpha|\left(\{\hat{H}_w,\hat{\rho}_w\}-\{\hat{\rho}_w,\hat{H}_w\}\right)|\alpha'\rangle = & -L\rho_w^{\alpha\alpha'} + \sum_{\alpha''}\frac{1}{2}\left(\frac{\partial H_c^{\alpha\alpha''}}{\partial\mathbf{R}}\cdot\frac{\partial\rho_w^{\alpha''\alpha'}}{\partial\mathbf{P}} - \frac{\partial H_c^{\alpha\alpha''}}{\partial\mathbf{P}}\cdot\frac{\partial\rho_w^{\alpha''\alpha'}}{\partial\mathbf{R}}\right) \\ & - \sum_{\alpha''}\frac{1}{2}\left(\frac{\partial\rho_w^{\alpha\alpha''}}{\partial\mathbf{R}}\cdot\frac{\partial H_c^{\alpha''\alpha'}}{\partial\mathbf{P}} - \frac{\partial\rho_w^{\alpha\alpha''}}{\partial\mathbf{P}}\cdot\frac{\partial H_c^{\alpha''\alpha'}}{\partial\mathbf{R}}\right) \,,\end{aligned}$$

where the classical Liouville operator L is defined

$$L \equiv -\frac{\partial H_{x,w}}{\partial\mathbf{R}}\cdot\frac{\partial}{\partial\mathbf{P}} + \frac{\partial H_{x,w}}{\partial\mathbf{P}}\cdot\frac{\partial}{\partial\mathbf{R}} \,. \tag{4.6}$$

If the coupling Hamiltonian $\hat{H}_c$ is taken to be independent of $\mathbf{P}$, then the associated derivatives vanish and one is left with the simplified result,

$$\frac{1}{2}\langle\alpha|\left(\{\hat{H}_w,\hat{\rho}_w\}-\{\hat{\rho}_w,\hat{H}_w\}\right)|\alpha'\rangle = -L\rho_w^{\alpha\alpha'} + \sum_{\alpha''}\frac{1}{2}\left(\frac{\partial H_c^{\alpha\alpha''}}{\partial\mathbf{R}}\cdot\frac{\partial\rho_w^{\alpha''\alpha'}}{\partial\mathbf{P}} + \frac{\partial\rho_w^{\alpha\alpha''}}{\partial\mathbf{P}}\cdot\frac{\partial H_c^{\alpha''\alpha'}}{\partial\mathbf{R}}\right) \,. \tag{4.7}$$

Combining the results in Eq. (4.4) and Eq. (4.7) yields the matrix element of Eq. (2.17), which is then expressed as

$$\begin{aligned}\frac{\partial}{\partial t}\rho_w^{\alpha\alpha'} = & -i\tilde{\omega}^{\alpha\alpha'}\rho_w^{\alpha\alpha'} - \frac{i}{\hbar}\sum_{\alpha''}\left(H_c^{\alpha\alpha''}\rho_w^{\alpha''\alpha'} - \rho_w^{\alpha\alpha''}H_c^{\alpha''\alpha'}\right) - L\rho_w^{\alpha\alpha'} \\ & + \sum_{\alpha''}\frac{1}{2}\left(\frac{\partial H_c^{\alpha\alpha''}}{\partial\mathbf{R}}\cdot\frac{\partial\rho_w^{\alpha''\alpha'}}{\partial\mathbf{P}} + \frac{\partial\rho_w^{\alpha\alpha''}}{\partial\mathbf{P}}\cdot\frac{\partial H_c^{\alpha''\alpha'}}{\partial\mathbf{R}}\right) \,.\end{aligned} \tag{4.8}$$

If the coupling is removed, each matrix element $\rho_w^{\alpha\alpha'}$ evolves independently with an equation of motion that consists of a classical Liouville operator L and a frequency $\tilde{\omega}^{\alpha\alpha'}$. Then, in this uncoupled case, the diagonal components of the density matrix evolve under purely classical dynamics, as the frequency $\tilde{\omega}^{\alpha\alpha}$ is zero; while the coherence elements will oscillate with a frequency dependent on the energy spacing of the eigenstates. This implies that the Wigner-transformed subsystem is evolving purely classically, as expected, as its dynamics are influenced only by the diagonal elements of the density matrix. However, the dynamics of the untransformed subsystem will be influenced by the oscillating coherence terms, as these will contribute to the calculation of eigenstate populations.

Returning to the case of non-zero coupling, one must now consider the projection of the quantum corrections onto the diabatic basis, to wit, the corrections stemming from the x-subsystem Hamiltonian:

$$\langle\alpha|\sum_{n=3,5,\ldots}\left(\frac{\hbar}{2i}\right)^{n-1}\frac{1}{n!}\frac{\partial^n H_{x,w}}{\partial\mathbf{R}^n}\cdot\frac{\partial^n\hat{\rho}_w}{\partial\mathbf{P}^n}|\alpha'\rangle = \sum_{n=3,5,\ldots}\left(\frac{\hbar}{2i}\right)^{n-1}\frac{1}{n!}\frac{\partial^n H_{x,w}}{\partial\mathbf{R}^n}\cdot\frac{\partial^n\rho_w^{\alpha\alpha'}}{\partial\mathbf{P}^n} \,.$$

Additionally, the corrections due to the coupling Hamiltonian (assuming it independent of $\mathbf{P}$) should be considered:

$$\begin{aligned}&\langle\alpha|\sum_{n=2,3,\ldots}\frac{1}{2^n n!}\left(\frac{i}{\hbar}\right)^{n-1}\left(\frac{\partial^n\hat{H}_c}{\partial\mathbf{R}^n}\cdot\frac{\partial^n\hat{\rho}_w}{\partial\mathbf{P}^n} + (-1)^{n-1}\frac{\partial^n\hat{\rho}_w}{\partial\mathbf{P}^n}\cdot\frac{\partial^n\hat{H}_c}{\partial\mathbf{R}^n}\right)|\alpha'\rangle \\ &= \sum_{n=2,3,\ldots}\sum_{\alpha''}\frac{1}{2^n n!}\left(\frac{i}{\hbar}\right)^{n-1}\left(\frac{\partial^n H_c^{\alpha\alpha''}}{\partial\mathbf{R}^n}\cdot\frac{\partial^n\rho_w^{\alpha''\alpha'}}{\partial\mathbf{P}^n} + (-1)^{n-1}\frac{\partial^n\rho_w^{\alpha\alpha''}}{\partial\mathbf{P}^n}\cdot\frac{\partial^n H_c^{\alpha''\alpha'}}{\partial\mathbf{R}^n}\right) \,.\end{aligned}$$

The exact partial-Wigner equations of motion in the diabatic basis are then given by

$$\begin{aligned}\frac{\partial}{\partial t}\rho_w^{\alpha\alpha'} =& -i\tilde{\omega}^{\alpha\alpha'}\rho_w^{\alpha\alpha'} - \frac{i}{\hbar}\sum_{\alpha''}\left(H_c^{\alpha\alpha''}\rho_w^{\alpha''\alpha'} - \rho_w^{\alpha\alpha''}H_c^{\alpha''\alpha'}\right) - L\rho_w^{\alpha\alpha'} \\ &+ \sum_{\alpha''}\frac{1}{2}\left(\frac{\partial H_c^{\alpha\alpha''}}{\partial\mathbf{R}}\cdot\frac{\partial\rho_w^{\alpha''\alpha'}}{\partial\mathbf{P}} + \frac{\partial\rho_w^{\alpha\alpha''}}{\partial\mathbf{P}}\cdot\frac{\partial H_c^{\alpha''\alpha'}}{\partial\mathbf{R}}\right) \\ &+ \sum_{n=2,3,\ldots}\sum_{\alpha''}\frac{1}{2^n n!}\left(\frac{i}{\hbar}\right)^{n-1}\left(\frac{\partial^n H_c^{\alpha\alpha''}}{\partial\mathbf{R}^n}\cdot\frac{\partial^n\rho_w^{\alpha''\alpha'}}{\partial\mathbf{P}^n} + (-1)^{n-1}\frac{\partial^n\rho_w^{\alpha\alpha''}}{\partial\mathbf{P}^n}\cdot\frac{\partial^n H_c^{\alpha''\alpha'}}{\partial\mathbf{R}^n}\right) \\ &+ \sum_{n=3,5,\ldots}\left(\frac{\hbar}{2i}\right)^{n-1}\frac{1}{n!}\frac{\partial^n H_{x,w}}{\partial\mathbf{R}^n}\cdot\frac{\partial^n\rho_w^{\alpha\alpha'}}{\partial\mathbf{P}^n}\,.\end{aligned} \tag{4.9}$$

In order to eliminate the explicit frequency term from the equations of motion, consider the change of variable

$$\rho_w^{\alpha\alpha'}(\mathbf{X},t) = \eta_w^{\alpha\alpha'}(\mathbf{X},t)\mathrm{e}^{-i\tilde{\omega}^{\alpha\alpha'}t}\,.$$

This substitution can then be applied to Eq. (4.9) to yield

$$\begin{aligned}\frac{\partial}{\partial t}\eta_w^{\alpha\alpha'} =& -\frac{i}{\hbar}\sum_{\alpha''}\left(H_c^{\alpha\alpha''}\eta_w^{\alpha''\alpha'}\mathrm{e}^{-i\tilde{\omega}^{\alpha''\alpha'}t} - \eta_w^{\alpha\alpha''}\mathrm{e}^{-i\tilde{\omega}^{\alpha\alpha''}t}H_c^{\alpha''\alpha'}\right)\mathrm{e}^{i\tilde{\omega}^{\alpha\alpha'}t} - L\eta_w^{\alpha\alpha'} \\ &+ \sum_{\alpha''}\frac{1}{2}\left(\frac{\partial H_c^{\alpha\alpha''}}{\partial\mathbf{R}}\cdot\frac{\partial\eta_w^{\alpha''\alpha'}}{\partial\mathbf{P}}\mathrm{e}^{-i\tilde{\omega}^{\alpha''\alpha'}t} + \frac{\partial\eta_w^{\alpha\alpha''}}{\partial\mathbf{P}}\mathrm{e}^{-i\tilde{\omega}^{\alpha\alpha''}t}\cdot\frac{\partial H_c^{\alpha''\alpha'}}{\partial\mathbf{R}}\right)\mathrm{e}^{i\tilde{\omega}^{\alpha\alpha'}t} \\ &+ \sum_{n=2,3,\ldots}\sum_{\alpha''}\frac{1}{2^n n!}\left(\frac{i}{\hbar}\right)^{n-1}\left(\frac{\partial^n H_c^{\alpha\alpha''}}{\partial\mathbf{R}^n}\cdot\frac{\partial^n\eta_w^{\alpha''\alpha'}}{\partial\mathbf{P}^n}\mathrm{e}^{-i\tilde{\omega}^{\alpha''\alpha'}t}\right)\mathrm{e}^{i\tilde{\omega}^{\alpha\alpha'}t} \\ &+ \sum_{n=2,3,\ldots}\sum_{\alpha''}\frac{(-1)^{n-1}}{2^n n!}\left(\frac{i}{\hbar}\right)^{n-1}\left(\frac{\partial^n\eta_w^{\alpha\alpha''}}{\partial\mathbf{P}^n}\mathrm{e}^{-i\tilde{\omega}^{\alpha\alpha''}t}\cdot\frac{\partial^n H_c^{\alpha''\alpha'}}{\partial\mathbf{R}^n}\right)\mathrm{e}^{i\tilde{\omega}^{\alpha\alpha'}t} \\ &+ \sum_{n=3,5,\ldots}\left(\frac{\hbar}{2i}\right)^{n-1}\frac{1}{n!}\frac{\partial^n H_{x,w}}{\partial\mathbf{R}^n}\cdot\frac{\partial^n\eta_w^{\alpha\alpha'}}{\partial\mathbf{P}^n}\,.\end{aligned} \tag{4.10}$$

This result is the system of equations that was used in the numerical simulation work undertaken in this study.

It is evident, from this analysis, that the inclusion of a non-zero coupling Hamiltonian also couples the evolution equations of the density matrix components. It is through this coupling that the coherence elements of the density matrix come to influence the dynamics of the phase-space subsystem. Similarly, the coherences can also then be influenced by the eigenstate occupation probabilities. In the quantum-classical equation, it is this coupling that results in the hybrid dynamics in a classical-like phase space. However, when the corrections are introduced the dynamics are reduced to those of two coupled quantum subsystems, one of which is represented in phase space.

4.2 Equations of Motion with Runge-Kutta 5

The numerical simulations conducted in this work aimed to evaluate the time evolution of the partial Wigner-transformed density operator $\eta_w^{\alpha\alpha'}(R,P,t)$, in the same notation as previously employed. There exists then an equation of motion for each density matrix element, given by the

quantum-state indices, so that the Runge-Kutta 5 method takes the form:

$$
\begin{aligned}
k_1^{\alpha\alpha'} &= dtF^{\alpha\alpha'}(\{\eta_w^{\beta\beta'}\}_{\beta\beta'}, R, P, t) \;, \\
k_2^{\alpha\alpha'} &= dtF^{\alpha\alpha'}(\{\eta_w^{\beta\beta'} + b_{21}k_1^{\beta\beta'}\}_{\beta\beta'}, R, P, t + a_2dt) \;, \\
k_3^{\alpha\alpha'} &= dtF^{\alpha\alpha'}(\{\eta_w^{\beta\beta'} + b_{31}k_1^{\beta\beta'} + b_{32}k_2^{\beta\beta'}\}_{\beta\beta'}, R, P, t + a_3dt) \;, \\
k_4^{\alpha\alpha'} &= dtF^{\alpha\alpha'}(\{\eta_w^{\beta\beta'} + b_{41}k_1^{\beta\beta'} + b_{42}k_2^{\beta\beta'} + b_{43}k_3^{\beta\beta'}\}_{\beta\beta'}, R, P, t + a_4dt) \;, \\
k_5^{\alpha\alpha'} &= dtF^{\alpha\alpha'}(\{\eta_w^{\beta\beta'} + b_{51}k_1^{\beta\beta'} + b_{52}k_2^{\beta\beta'} + b_{53}k_3^{\beta\beta'} + b_{54}k_4^{\beta\beta'}\}_{\beta\beta'}, R, P, t + a_5dt) \;, \\
k_6^{\alpha\alpha'} &= dtF^{\alpha\alpha'}(\{\eta_w^{\beta\beta'} + b_{61}k_1^{\beta\beta'} + b_{62}k_2^{\beta\beta'} + b_{63}k_3^{\beta\beta'} + b_{64}k_4^{\beta\beta'} + b_{65}k_5^{\beta\beta'}\}_{\beta\beta'}, R, P, t + a_6dt) \;, \\
\eta_w^{\alpha\alpha'}(R, P, t + dt) &= \eta_w^{\alpha\alpha'}(R, P, t) + c_1k_1^{\alpha\alpha'} + c_2k_2^{\alpha\alpha'} + c_3k_3^{\alpha\alpha'} + c_4k_4^{\alpha\alpha'} + c_5k_5^{\alpha\alpha'} + c_6k_6^{\alpha\alpha'} \;. \quad (4.11)
\end{aligned}
$$

In this notation $\{\eta_w^{\beta\beta'}\}_{\beta\beta'}$ represents a set density matrix elements, over all the combinations indices β and β'. The function $F^{\alpha\alpha'}(\{\eta_w^{\beta\beta'}\}_{\beta\beta'}, R, P, t)$ is defined by the equations of motion, from the earlier definition it must be given by

$$
F^{\alpha\alpha'}(\{\eta_w^{\beta\beta'}\}_{\beta\beta'}, R, P, t) = \frac{\partial}{\partial t}\eta_w^{\alpha\alpha'} \;.
$$

The equations of motion, including correction terms, are represented in the diabatic basis, shown in Eq. (4.10).

In these calculations the total error, for the complete system of evolution equations, in the Cash-Karp method is calculated via a weighted average over the phase space:

$$
E = \int\int dR\, dP\, \mathrm{Tr}\left(\hat{\rho}_w^{\alpha\alpha'}(R, P, t)\Delta^{\alpha\alpha'}(R, P)\right) \;,
$$

where there is an error function $\Delta^{\alpha\alpha'}(R, P)$ defined for the evolution equation of each density matrix element in the same manner as in Eq. (3.9).

4.3 Models

4.3.1 Pseudo-Spin Coupled to a Harmonic Oscillator

This is a special case of the well known Spin-Boson Hamiltonian, where the bath of oscillators consists of only a single oscillator. The Hamiltonian has the form:

$$
\hat{H} = -\hbar\Omega\hat{\sigma_x} + \frac{\hat{P}^2}{2M} + \frac{1}{2}\omega^2 M\hat{R}^2 - c\hat{R}\hat{\sigma_z} \;. \quad (4.12)
$$

where $\hat{\sigma}_x$ and $\hat{\sigma}_z$ are Pauli spin operators, Ω is the frequency proportional to the energy spacing between the spin eigenstates, ω is the frequency of the harmonic oscillator, with mass M, and c is the coupling constant. The correspondence with the previous general analysis can be found by making the identifications:

$$
\begin{aligned}
\hat{H}_s &= -\hbar\Omega\hat{\sigma_x} \;, \\
\hat{H}_c &= -c\hat{R}\hat{\sigma_z} \;, \\
\hat{H}_x &= \frac{\hat{P}^2}{2M} + \frac{1}{2}\omega^2 M\hat{R}^2 \;,
\end{aligned}
$$

which also allow for the identification of the diabatic eigenstates for this system. To this end, let the eigenstates of $\hat{\sigma}_x$ be $|0\rangle$ and $|1\rangle$. Then the properties of the spin operators yield

$$
\begin{aligned}
&\hat{H}_s|0\rangle = \hbar\Omega|0\rangle \;,\; \hat{H}_s|1\rangle = -\hbar\Omega|1\rangle \;, \\
&\hat{H}_c|0\rangle = -c\hat{R}|1\rangle \;,\; \hat{H}_c|1\rangle = -c\hat{R}|0\rangle \;.
\end{aligned} \quad (4.13)
$$

Furthermore, one can define the frequencies $\tilde{\omega}^{\alpha\alpha'}$ using the diabatic eigenstates

$$
\begin{aligned}
&\tilde{\omega}^{00} = 0 \;,\; \tilde{\omega}^{11} = 0 \;, \\
&\tilde{\omega}^{01} = 2\Omega \;,\; \tilde{\omega}^{10} = -2\Omega \;.
\end{aligned}
$$

The Hamiltonian from Eq. (4.12) can then be partially Wigner-transformed to yield

$$\hat{H}_w = -\hbar\Omega\hat{\sigma_x} + \frac{P^2}{2M} + \frac{1}{2}\omega^2 MR^2 - cR\hat{\sigma_z} \; . \tag{4.14}$$

For computational convenience this Hamiltonian can be rewritten in dimensionless form. To this end, consider the definition of the dimensionless variables:

$$R' = \left(\frac{M\omega}{\hbar}\right)^{1/2} R \;\; , \;\; P' = (\hbar M\omega)^{-1/2} P \; . \tag{4.15}$$

The Hamiltonian can then be made dimensionless through division by $\hbar\omega$,

$$\hat{H}'_w = \frac{\hat{H}_w}{\hbar\omega} = -\frac{\Omega}{\hbar\omega}\hat{\sigma_x} + \frac{P^2}{2M\hbar\omega} + \frac{1}{2\hbar\omega}\omega^2 MR^2 - \frac{cR}{\hbar\omega}\hat{\sigma_z} \; .$$

Now one can define the dimensionless constants

$$\Omega' = \frac{\Omega}{\omega} \;\; , \;\; c' = \frac{c}{\omega\sqrt{M\omega\hbar}} \; .$$

Then, making use of the dimensionless variables and constants, one finds the final form of the dimensionless Hamiltonian

$$\hat{H}'_w = -\Omega'\hat{\sigma_x} + \frac{P'^2}{2} + \frac{R'^2}{2} - c'R'\hat{\sigma_z} \; .$$

In any further appearances this Hamiltonian will be assumed to be dimensionless and will be displayed without the primed notation.

With this Hamiltonian, the exact diabatic equations of motion, given by Eq. (4.10), now take the form

$$\begin{aligned}\frac{\partial}{\partial t}\eta_w^{\alpha\alpha'} = &-\frac{i}{\hbar}\sum_{\alpha''}\left(H_c^{\alpha\alpha''}\eta_w^{\alpha''\alpha'}\mathrm{e}^{-i\tilde{\omega}^{\alpha''\alpha'}} - \eta_w^{\alpha\alpha''}\mathrm{e}^{-i\tilde{\omega}^{\alpha\alpha''}}H_c^{\alpha''\alpha'}\right)\mathrm{e}^{i\tilde{\omega}^{\alpha\alpha'}} - \left(P\frac{\partial}{\partial R} - R\frac{\partial}{\partial P}\right)\eta_w^{\alpha\alpha'} \\ &+\sum_{\alpha''}\frac{1}{2}\left(\frac{\partial H_c^{\alpha\alpha''}}{\partial R}\frac{\partial\eta_w^{\alpha''\alpha'}}{\partial P}\mathrm{e}^{-i\tilde{\omega}^{\alpha''\alpha'}} + \frac{\partial\eta_w^{\alpha\alpha''}}{\partial P}\mathrm{e}^{-i\tilde{\omega}^{\alpha\alpha''}}\frac{\partial H_c^{\alpha''\alpha'}}{\partial R}\right)\mathrm{e}^{i\tilde{\omega}^{\alpha\alpha'}} \; .\end{aligned}$$

Here it is understood that the summation over α'' runs over the two eigenstates $|0\rangle$ and $|1\rangle$. The definition in Eq. (4.13) can now be used to express the equation of motion explicitly, yielding

$$\begin{aligned}\frac{\partial\eta_w^{00}}{\partial t} &= icR\left(\eta_w^{01}\mathrm{e}^{i2\Omega t} - \eta_w^{10}\mathrm{e}^{-i2\Omega t}\right) - L\eta_w^{00} + \frac{c}{2}\left(\frac{\partial\eta_w^{10}}{\partial P}\mathrm{e}^{-i2\Omega t} + \frac{\partial\eta_w^{01}}{\partial P}\mathrm{e}^{i2\Omega t}\right) \; , \\ \frac{\partial\eta_w^{10}}{\partial t} &= icR\left(\eta_w^{11} - \eta_w^{00}\right)\mathrm{e}^{i2\Omega t} - L\eta_w^{10} + \frac{c}{2}\left(\frac{\partial\eta_w^{00}}{\partial P} + \frac{\partial\eta_w^{11}}{\partial P}\right)\mathrm{e}^{i2\Omega t} \; , \\ \frac{\partial\eta_w^{11}}{\partial t} &= -icR\left(\eta_w^{01}\mathrm{e}^{i2\Omega t} - \eta_w^{10}\mathrm{e}^{-i2\Omega t}\right) - L\eta_w^{11} + \frac{c}{2}\left(\frac{\partial\eta_w^{10}}{\partial P}\mathrm{e}^{-i2\Omega t} + \frac{\partial\eta_w^{01}}{\partial P}\mathrm{e}^{i2\Omega t}\right) \; .\end{aligned}$$

The coherence term η_w^{10} and its conjugate term η_w^{01} are potentially complex-valued. Therefore, for computational reasons, one divides these terms into their real and imaginary parts:

$$\begin{aligned}\eta_w^{10} &= \mathrm{Re}[\eta_w^{10}] + i\mathrm{Im}[\eta_w^{10}] \; , \\ \eta_w^{01} &= \mathrm{Re}[\eta_w^{10}] - i\mathrm{Im}[\eta_w^{10}] \; .\end{aligned}$$

Using these in the equations of motion and separating the η_w^{10} equation into real and imaginary

parts yield

$$\frac{\partial}{\partial t}\eta_w^{00} = 2cR\left(\mathrm{Re}[\eta_w^{10}]\sin(2\Omega t) + \mathrm{Im}[\eta_w^{10}]\cos(2\Omega t)\right) - L\eta_w^{00} + c\left(\frac{\partial}{\partial P}\mathrm{Re}[\eta_w^{10}]\cos(2\Omega t) - \frac{\partial}{\partial P}\mathrm{Im}[\eta_w^{10}]\sin(2\Omega t)\right) , \tag{4.16}$$

$$\frac{\partial}{\partial t}\mathrm{Re}[\eta_w^{10}] = -cR\left(\eta_w^{11} - \eta_w^{00}\right)\sin(2\Omega t) - L\mathrm{Re}[\eta_w^{10}] + \frac{c}{2}\left(\frac{\partial}{\partial P}\eta_w^{00} + \frac{\partial}{\partial P}\eta_w^{11}\right)\cos(2\Omega t) , \tag{4.17}$$

$$\frac{\partial}{\partial t}\mathrm{Im}[\eta_w^{10}] = cR\left(\eta_w^{11} - \eta_w^{00}\right)\cos(2\Omega t) - L\mathrm{Im}[\eta_w^{10}] - \frac{c}{2}\left(\frac{\partial}{\partial P}\eta_w^{00} + \frac{\partial}{\partial P}\eta_w^{11}\right)\sin(2\Omega t) , \tag{4.18}$$

$$\frac{\partial}{\partial t}\eta_w^{11} = -2cR\left(\mathrm{Re}[\eta_w^{10}]\sin(2\Omega t) + \mathrm{Im}[\eta_w^{10}]\cos(2\Omega t)\right) - L\eta_w^{11} + c\left(\frac{\partial}{\partial P}\mathrm{Re}[\eta_w^{10}]\cos(2\Omega t) - \frac{\partial}{\partial P}\mathrm{Im}[\eta_w^{10}]\sin(2\Omega t)\right) . \tag{4.19}$$

These four equations are a complete set of evolution equations for the density matrix of this system, as both coherences η_w^{01} and η_w^{10} can be constructed from the $\mathrm{Re}[\eta_w^{10}]$ and $\mathrm{Im}[\eta_w^{10}]$ equations. It might be noted at this point that there are no correction terms in the equation of motion. This is because an examination of Eq. (4.10) reveals that a Hamiltonian with linear coupling and a quadratic dependence on R and P will have no non-zero correction terms.

4.3.2 Pseudo-Spin Coupled to a Quartic Oscillator

This model is constructed through the modification of the previous model by the addition of a constant term and a term quartic in the position operator $\hat{R}$,

$$\hat{H} = -\hbar\Omega\hat{\sigma_x} + \frac{\hat{P}^2}{2M} + \frac{1}{4}b_4\hat{R}^4 + \frac{1}{2}b_2\hat{R}^2 + \frac{b_2^2}{4b_4} - c\hat{R}\hat{\sigma_z} , \tag{4.20}$$

where $b_2 = -M\omega^2$ and b_4 is a constant controlling the strength of the non-linearity of the oscillator. This Hamiltonian can be Wigner transformed to yield

$$\hat{H}_w = -\hbar\Omega\hat{\sigma_x} + \frac{P^2}{2M} + \frac{1}{4}b_4R^4 + \frac{1}{2}b_2R^2 + \frac{b_2^2}{4b_4} - cR\hat{\sigma_z} . \tag{4.21}$$

Introducing the dimensionless variables given by Eq. (4.15), so that $b_2' = -1$ and making the definition

$$b_4' = \frac{b_4\hbar}{M^2\omega^3} ,$$

one can produce the dimensionless form of the Hamiltonian:

$$\hat{H}_w = -\Omega\hat{\sigma_x} + \frac{P^2}{2} + b_2\frac{R^2}{2} + \frac{1}{4}b_4R^4 + \frac{1}{4b_4} - cR\hat{\sigma_z} .$$

The classical Liouville operator for this Hamiltonian is given by

$$L = P\frac{\partial}{\partial R} - \frac{\partial H_{x,w}}{\partial R}\frac{\partial}{\partial P} = P\frac{\partial}{\partial R} - (b_2R + b_4R^3)\frac{\partial}{\partial P} .$$

Therefore, with the above definition of L, the equations of motion are given, once more, by Eqs. (4.16 - 4.19). However, one must now consider whether there are any quantum correction terms stemming from the quartic addition to the Hamiltonian. Since the coupling is linearly dependent on R, the only possibly non-zero correction terms from Eq. (4.10) have the dimensionless form

$$\sum_{n=3,5,\cdots}^{N}\left(\frac{1}{2i}\right)^{n-1}\frac{1}{n!}\frac{\partial^n H_{x,w}}{\partial R^n}\frac{\partial^n \eta_w^{\alpha\alpha'}}{\partial P^n} .$$

As previously seen, the R^2 and P^2 terms in $H_{x,w}$ do not contribute any corrections; however, the R^4 term has a non-zero 3rd derivative in R. Therefore,

$$\sum_{n=3,5,\cdots}^{N}\left(\frac{1}{2i}\right)^{n-1}\frac{1}{n!}\frac{\partial^n H_{x,w}}{\partial R^n}\frac{\partial^n \eta_w^{\alpha\alpha'}}{\partial P^n}=-\frac{1}{24}\left(6b_4R\right)\frac{\partial^3\eta_w^{\alpha\alpha'}}{\partial P^3}=-\frac{1}{4}b_4R\frac{\partial^3\eta_w^{\alpha\alpha'}}{\partial P^3}\ .$$

This means the exact equations of motion for this Hamiltonian become

$$\begin{aligned}
\frac{\partial}{\partial t}\eta_w^{00}=&\,2cR\left(\mathrm{Re}[\eta_w^{10}]\sin\left(2\Omega t\right)+\mathrm{Im}[\eta_w^{10}]\cos\left(2\Omega t\right)\right)-L\eta_w^{00}\\
&+c\left(\frac{\partial}{\partial P}\mathrm{Re}[\eta_w^{10}]\cos\left(2\Omega t\right)-\frac{\partial}{\partial P}\mathrm{Im}[\eta_w^{10}]\sin\left(2\Omega t\right)\right)-\frac{b_4R}{4}\frac{\partial^3\eta_w^{00}}{\partial P^3}\ ,\\
\frac{\partial}{\partial t}\mathrm{Re}[\eta_w^{10}]=&-cR\left(\eta_w^{11}-\eta_w^{00}\right)\sin\left(2\Omega t\right)-L\mathrm{Re}[\eta_w^{10}]\\
&+\frac{c}{2}\left(\frac{\partial}{\partial P}\eta_w^{00}+\frac{\partial}{\partial P}\eta_w^{11}\right)\cos\left(2\Omega t\right)-\frac{b_4R}{4}\frac{\partial^3\mathrm{Re}[\eta_w^{10}]}{\partial P^3}\ ,\\
\frac{\partial}{\partial t}\mathrm{Im}[\eta_w^{10}]=&\,cR\left(\eta_w^{11}-\eta_w^{00}\right)\cos\left(2\Omega t\right)-L\mathrm{Im}[\eta_w^{10}]\\
&-\frac{c}{2}\left(\frac{\partial}{\partial P}\eta_w^{00}+\frac{\partial}{\partial P}\eta_w^{11}\right)\sin\left(2\Omega t\right)-\frac{b_4R}{4}\frac{\partial^3\mathrm{Im}[\eta_w^{10}]}{\partial P^3}\ ,\\
\frac{\partial}{\partial t}\eta_w^{11}=&-2cR\left(\mathrm{Re}[\eta_w^{10}]\sin\left(2\Omega t\right)+\mathrm{Im}[\eta_w^{10}]\cos\left(2\Omega t\right)\right)-L\eta_w^{11}\\
&+c\left(\frac{\partial}{\partial P}\mathrm{Re}[\eta_w^{10}]\cos\left(2\Omega t\right)-\frac{\partial}{\partial P}\mathrm{Im}[\eta_w^{10}]\sin\left(2\Omega t\right)\right)-\frac{b_4R}{4}\frac{\partial^3\eta_w^{11}}{\partial P^3}\ .
\end{aligned}$$

It is also worthwhile to examine the nature of the phase-space potential $V_x(R)=\frac{1}{4}b_4R^4+\frac{1}{2}b_2R^2+\frac{b_2^2}{4b_4}$. This has turning points at $R=0$ and $R=\pm i\sqrt{\frac{b_2}{b_4}}$. Therefore, if b_2 is positive there is only a single turning point at $R=0$ and the shape of the potential is vaguely similar to that in the quadratic case. However, if b_2 is negative, one has the well-known 'double well' potential. The significance in the choice of this potential comes down to the possibility of observing uniquely quantum dynamical behaviour in the phase-space system [79]. Moreover, because such quantum behaviour might be expected to affect the coherences of the total system density operator, the population statistics of the pseudo-spin system could provide a dynamical quantity that can be used to observe directly the effects of the quantum correction terms; one might expect a phase-space system evolving under quantum-classical dynamics either to lack completely such uniquely quantum behaviour or to show a large reduction in the magnitude of such effects.

The purpose of the constant term $\frac{b_2^2}{4b_4}$ now becomes apparent: it is the barrier height in the double-well configuration, this is evident through setting $R=0$, $V_x(0)=\frac{b_2^2}{4b_4}$. This elevates the minima of the double well exactly to zero, leaving the rest of the values of V_x positive. Therefore it is useful to introduce the notation

$$\begin{aligned}
d&=\frac{b_2^2}{4b_4}\ ,\\
w&=\sqrt{-\frac{b_2}{b_4}}\ .
\end{aligned}\tag{4.22}$$

Here w signifies the 'width' of one of the wells in the potential, or the distance to a minimum point from the origin; while d is well depth. Altering the constants b_2 and b_4 therefore influences both the depth and width of the wells, which have great impact on the potential for tunnelling [79].

4.3.3 Adiabatic Analysis

The Hamiltonians for both the models, outlined previously, can be written in the form

$$\hat{H}_w=-\Omega\hat{\sigma}_x+\gamma(R)\hat{\sigma}_z+\frac{P^2}{2}+V_x(R)\ ,$$

where γ and V_x are some functions of R. The adiabatic basis for such a system is defined as being composed of the eigenstates of the operator [3]

$$\hat{H}_{A,w} = -\Omega\hat{\sigma}_x + \gamma(R)\hat{\sigma}_z + V_x(R) \; .$$

In the basis of the eigenstates of $\hat{\sigma}_x$, this equation can be expressed in matrix form, which yields

$$H_{A,w} = \Omega \begin{pmatrix} 1 & 0 \\ 0 & -1 \end{pmatrix} + \gamma(R) \begin{pmatrix} 0 & 1 \\ 1 & 0 \end{pmatrix} + V_x(R) \begin{pmatrix} 1 & 0 \\ 0 & 1 \end{pmatrix} \; .$$

In order to find the eigenvalues of this Hamiltonian one must solve the characteristic equation

$$det \left[\begin{pmatrix} V_x + \Omega - \epsilon & \gamma \\ \gamma & V_x - \Omega - \epsilon \end{pmatrix} \right] = 0 \; ,$$

which results in the solutions [3]

$$\epsilon_{\pm}(R) = V_x(R) \pm \sqrt{\Omega^2 + \gamma^2(R)} \; .$$

These adiabatic eigenvalues are the potential energy surfaces along which the system moves [30, 61]. One therefore labels ϵ_+ as the adiabatic excited state of the system while ϵ_- is the adiabatic ground state. The adiabatic eigenvector problem can now be expressed in the basis of the eigenstates of σ_z:

$$\begin{pmatrix} \theta_1 \\ \theta_2 \end{pmatrix} \begin{pmatrix} -\Omega + V_x & \gamma \\ \gamma & \Omega + V_x \end{pmatrix} = \epsilon_{\pm} \begin{pmatrix} \theta_1 \\ \theta_2 \end{pmatrix} \; .$$

This has the solutions [3]

$$\frac{1}{\sqrt{2(1+G^2)}} \begin{pmatrix} 1+G \\ 1-G \end{pmatrix} \; , \quad \frac{1}{\sqrt{2(1+G^2)}} \begin{pmatrix} G-1 \\ 1+G \end{pmatrix} \; ,$$

where

$$G(R) = \frac{1}{\gamma(R)}(-\Omega + \sqrt{\Omega^2 + \gamma(R)^2}) \; .$$

The properties of this function $G(R)$ will reveal symmetries within the adiabatic composition of the initial state of the system. If the limit $\gamma(R) \to 0$ is taken, then

$$\lim_{\gamma(R)\to 0} G = 0 \; ,$$

by l'Hospital's rule. Now considering the extremes $\gamma(R) \to \infty$ and $\gamma(R) \to -\infty$, one finds:

$$\lim_{\gamma(R)\to \infty} G = 1 \; ,$$
$$\lim_{\gamma(R)\to -\infty} G = -1 \; .$$

One can apply these properties to the study of the initial spin-states, which can be represented in terms of the adiabatic eigenvalues by:

$$\begin{aligned} \begin{pmatrix} 1 \\ 0 \end{pmatrix} &= \frac{1}{2(1+G^2)}(1+G)^2 \left|\epsilon_-(R)\right\rangle + \frac{1}{2(1+G^2)}(1-G)^2 \left|\epsilon_+(R)\right\rangle \; , \\ \begin{pmatrix} 0 \\ 1 \end{pmatrix} &= \frac{1}{2(1+G^2)}(1-G)^2 \left|\epsilon_-(R)\right\rangle + \frac{1}{2(1+G^2)}(1+G)^2 \left|\epsilon_+(R)\right\rangle \; . \end{aligned} \tag{4.23}$$

Therefore, when $\gamma(R) = 0$ both of these states are perfect mixtures of the adiabatic eigenstates. While when $\gamma(R) \to \infty$ or $\gamma(R) \to -\infty$ the spin-up state is completely specified by the adiabatic ground state or excited state respectively. For the spin-down case the reverse is true.

The initial state of a hybrid system, like those presented previously in Section (4.3), is composed of both an initial direction for the spin system and a Wigner function for the phase-space system, see Section (4.4). The initial Wigner function supplies one with knowledge of the initial

average position $\langle R \rangle\big|_{t=0} = R_0$, this can be used with the assumption of a central limit approximation to determine the composition of the initial state in terms of the adiabatic eigenstates. Consider, for instance, a system where the coupling is an odd function, or $\gamma(-R) = -\gamma(R)$ and that $\lim_{R\to\infty} \gamma(R) = \infty$. Then, using the previous analysis, one finds:

$$\lim_{R_0\to\infty} G = 1 \, ,$$
$$\lim_{R_0\to-\infty} G = -1 \, .$$

More generally,

$$G(R_0) = -G(-R_0) \, .$$

This implies, considering Eq. (4.23), that the initial state with the excited-state spin and $R_0 < 0$ has the same adiabatic composition as the initial state with the ground-state spin and $R_0 > 0$, provided R_0 has the same magnitude in both cases.

The adiabatic symmetry of differing spin-states and initial average phase-space position combinations might be viewed as 'complete inversion antisymmetry', as the phase-space position must be reflected across the axis of symmetry and the alignment of the spin must be flipped to leave the initial state adiabatic composition of the system invariant. Given the similarity of the initial states, one might then expect the behaviour of the spin systems to be similar. However, the symmetry was dependent upon the flipping of the initial spin direction and therefore the properties of the spin, for the two adiabatically equivalent initial states, can only be expected to behave as mirror images, reflected through some axis of symmetry. The behaviour of the phase-space system might also be expected to exhibit a similar reflection symmetry.

The existence of this symmetry in the numerical results will provide an important verification of the effectiveness of the numerical method used to solve of the equations of motion. Therefore, numerical evidence of this symmetry will be given as part of this study and can be found in the Results chapter.

The case of $\gamma(R)$ being even or having no definite symmetry both yield

$$\lim_{R_0\to\infty} G = \lim_{R_0\to-\infty} G = \pm 1 \, ,$$

provided $\gamma(R)$ is not bounded. This suggests that, in the absence of reflection antisymmetry in $\gamma(R)$, a particular adiabatic eigenstate will be favoured by large initial displacements of the environment system, though there will be no guarantee of symmetry in the neighbourhood of the roots of coupling function unless *gamma* is even.

4.4 Initial State

In the computational work done in this study, the initial state of the system, when either model was in use, was taken to be either:

$$\rho_w^{\gamma\gamma'} = \begin{pmatrix} 0 & 0 \\ 0 & 1 \end{pmatrix} \otimes \rho_w(R,P) \, ,$$

or

$$\rho_w^{\gamma\gamma'} = \begin{pmatrix} 1 & 0 \\ 0 & 0 \end{pmatrix} \otimes \rho_w(R,P) \, ,$$

where $\rho_w^{\gamma\gamma'} = \langle\gamma|\,\hat{\rho}_w\,|\gamma'\rangle$ with $|\gamma\rangle$ and $|\gamma'\rangle$ being the eigenstates of the operator $\hat{\sigma}_z$.

This initial state is chosen to place the state of the spin in an eigenstate of the spin population operator. Additionally, the choice of both the excited and ground states of the spin system proves important, as suitable comparison can be used to demonstrate the complete inversion antisymmetry identified in Section. (4.3.3), which would act as verification of the effectiveness of the equations of motion.

In order to determine the initial state of the spin in the basis of $\hat{\sigma}_x$ (the diabatic basis) one must first perform an eigenvector rotation. The phase-space initial state $\rho_w(R,P)$ is taken to be a coherent state in position space, the Wigner transform of which must be performed to find the form

of $\rho_w(R,P)$. The coherent state is chosen due ot its similarity to the state of the classical harmonic oscillator [80, 81], this is because one wishes to compare the quantum-classical and quantum-corrected results using the same initial state. In this regard the coherent state is eminently useful, as it is suitable to represent both the classical and quantum-corrected environmental systems. Moreover, if one wishes to consider the quantum-to-classical transition of a nano-mechanical system then a coherent state seems an ideal starting point for an oscillator close to the transition.

The coherent state is still employed in the case of the quartic oscillator under the assumption that the quartic term is 'turned on' at time $t = 0$. .

The Wigner-transformed initial states, expressed in the diabatic basis are given by

$$\eta_w^{\alpha\alpha'}(R,P) = \frac{1}{\pi}\begin{pmatrix} \frac{1}{2} & \frac{1}{2} \\ \frac{1}{2} & \frac{1}{2} \end{pmatrix} \otimes \mathrm{e}^{-\frac{(R-R_0)^2}{2a^2}} \mathrm{e}^{-\frac{2a^2}{\hbar^2}(P-P_0)^2} ,$$

or

$$\eta_w^{\alpha\alpha'}(R,P) = \frac{1}{\pi}\begin{pmatrix} \frac{1}{2} & -\frac{1}{2} \\ -\frac{1}{2} & \frac{1}{2} \end{pmatrix} \otimes \mathrm{e}^{-\frac{(R-R_0)^2}{2a^2}} \mathrm{e}^{-\frac{2a^2}{\hbar^2}(P-P_0)^2} ,$$

with $\eta_w^{\alpha\alpha'} = \langle\alpha|\,\hat{\rho}_w\,|\alpha'\rangle\,\mathrm{e}^{-i\tilde{\omega}^{\alpha\alpha'}t}$ and where $|\alpha\rangle$ and $|\alpha'\rangle$ are eigenstates of the operator $\hat{\sigma}_x$. The Wigner transform of the coherent state and the eigenvector rotations needed to find the initial spin state in the diabatic basis are found in Appendix D.

4.4.1 Quantum Canonical Distribution

In some of the numerical calculations the initial state of the phase-space system will instead be taken to be the quantum canonical distribution for a harmonic oscillator, which is given by [3, 18]

$$\rho_x(R,P) = \tanh(0.5\beta\omega)\mathrm{e}^{-\frac{2}{\omega}\tanh(0.5\beta\omega)H_x(R,P)} , \tag{4.24}$$

where $H_x = \frac{P^2}{2M} + \frac{1}{2}M\omega^2R^2$ is the Hamiltonian of the phase-space system at time $t = 0$ and

$$\beta = \frac{1}{k_BT} .$$

Here T is the absolute temperature and k_B is the Boltzmann constant. In the scaled units, previously defined in Section 4.3, this distribution takes the form

$$\rho_x(R,P) = \tanh(0.5\beta')\mathrm{e}^{-2\tanh(0.5\beta')H'_x(R,P)} ,$$

where $H'_x = \frac{P^2}{2} + \frac{1}{2}R^2$, R and P are also the rescaled position and momentum and

$$\beta' = \beta\hbar\omega .$$

4.5 Computational Simulations

Computational calculations were performed for this study using the techniques outlined in Chapter (3) with the equations of motion and initial conditions established in this chapter. Initial simulations were carried out to determine if the partial differential equation method was both a stable integration technique for this problem and if it reproduced the results of established techniques for simulating the quantum-classical equation. The second set of simulation objectives was to establish numerically the effect of neglecting the quantum correction terms on the dynamics of a system whose evolution was modelled by the quantum-classical equation.

4.5.1 Selection of Parameters

The set of parameters that must be chosen for a given simulation are, using previously defined notation, Ω, R_0, P_0, a, b_2, b_4 and c. The most significant of these parameters is the coupling constant c, as a hypothesis of this study is that the effect of the quantum corrections will be

sensitive to the strength of the coupling. The selection of coupling parameter values is dictated by the bare coupling parameter λ, here defined in the dimensionless variables, Eq. (4.15), by

$$\lambda = \frac{c^2}{\Omega} \, .$$

The value of Ω is kept fixed and then c is varied to observe a variety of coupling strengths, taking values from 0.2 to 1.0. Given this range of c, λ then varies from 0.06 to 1.4, representing a variation from weak ($\lambda \ll 1$) to strong ($\lambda \geq 1$) couplings.

The diabatic level-spacing Ω was chosen to take a value of 0.6, which would ensure that a sufficient number of population cycles were observed to make meaningful comparison of observables such as the spin populations. The value of Ω represents the ratio between the pseudo-spin tunnelling frequency and the oscillator frequency due to the rescaling used in Eq. (4.15). Therefore Ω also dictates whether the dynamics take place in the adiabatic regime ($\Omega > 1$), where the pseudo-spin system has a shorter dynamical time-scale than the oscillator, or in the non-adiabatic regime ($\Omega < 1$), where the reverse is true.

The initial momentum P_0 is chosen to be 0 for all simulations. The remaining parameters are dealt with separately for each model under investigation.

Pseudo-Spin Coupled to Harmonic Oscillator

The initial position R_0 was chosen in the harmonic oscillator case to take the values 0 and 1 in separate simulations, as both these cases prove to be important tests of the dynamics. If for $R_0 = 0$, the coupling is set such that $c = 0$, the phase-space system is at equilibrium, meaning that the state of the system should be stationary in time. If $R_0 = 1$ and $c = 0$, then the phase-space evolution should exactly reproduce a classical harmonic oscillator, while the spin should execute simple population cycles. The case of $R_0 = 0$ and with non-zero c will be compared to the established 'surface-hopping' simulation technique [3, 60, 61], in order to verify the accuracy of the method-of-lines algorithm. In the case of this system $\Omega = 0.3$ is used to match the conditions used in testing the surface-hopping method in [3]. The surface-hopping algorithm for hybrid quantum-classical systems evaluates the dynamics in terms of phase-space trajectories on the adiabatic potential surfaces, incorporating non-adiabatic transitions between the potential surfaces by means of stochastic momentum jumps; the algorithm employs a hybrid molecular dynamics/Montecarlo method to sample and evolve trajectories [60, 61]. This method is chosen for comparison to the method of lines technique as its accuracy in hybrid problems has already been established in the literature [60].

The uncertainty parameter a is taken to be the minimum value for this model.

Pseudo-Spin Coupled to Quartic Oscillator

The parameters b_2 and b_4 are chosen such that the potential takes on a double-well configuration. This means that b_2 is negative while b_4 is positive. This configuration was chosen to produce a situation in which the non-linear oscillatory behaviour can be used to gauge the effects of the quantum corrections and which might encourage uniquely quantum-dynamical effects, such as tunnelling. The choice of parameter $b_2 = -1$ is made to be consistent with the rescaling procedure detailed in Eq. (4.15). The value of b_4 can then be varied to locate conditions under which the quantum corrections become significant.

The initial position R_0 is chosen both to aid the ground-state localisation of the initial distribution in one of the wells and to minimise the initial energy. So with previous well geometry specifications in mind, R_0 is set to be close to the potential energy minimum at a distance w from the origin. In order to aid the confinement of the initial state to one well of the potential function, a is chosen to take a non-minimal value, in this case $a = 0.6071$ is chosen to reduce position-based uncertainty.

Importantly, to ensure the accuracy of the computational method in the quartic case, the complete inversion antisymmetry identified in Section. (4.3.3) will be tested by comparing the cases of the excited-state spin and $R_0 < 0$ to the ground-state spin with $R_0 > 0$. Additionally, results will be presented for the excited-state spin with $R_0 < 0$ and $R_0 = 0$ for a variety of coupling

strengths, these results will form the basis for the conclusions drawn from this work and will be shown to have important consequences in the witnessing of quantum behaviours in nano-mechanical systems.

Chapter 5

Results

5.1 Harmonic Model

The Harmonic results demonstrate good agreement between the surface-hopping technique [3] and the method of lines approach. This agreement is clearly evident for shorter times in Figs. 5.1(a) and 5.1(b) but is present for long times as well in Fig. 5.1(c). Disagreement between the methods occurs only when the errors in the surface-hopping method become large, typically for the larger couplings and at longer times, as shown in Figs. 5.1(a) and 5.1(b). Furthermore, Figs. 5.2(a), 5.2(b) and 5.3 show that the method of lines technique is stable, trace preserving and obeys Hamiltonian energy conservation. Finally, Figs. 5.4(a) and 5.4(b) show that, when the coupling is removed, the oscillator and pseudo-spin systems evolve correctly in isolation, in that, the average oscillator behaviour corresponds to that of a classical oscillator and the pseudo-spin executes simple Rabi oscillations.

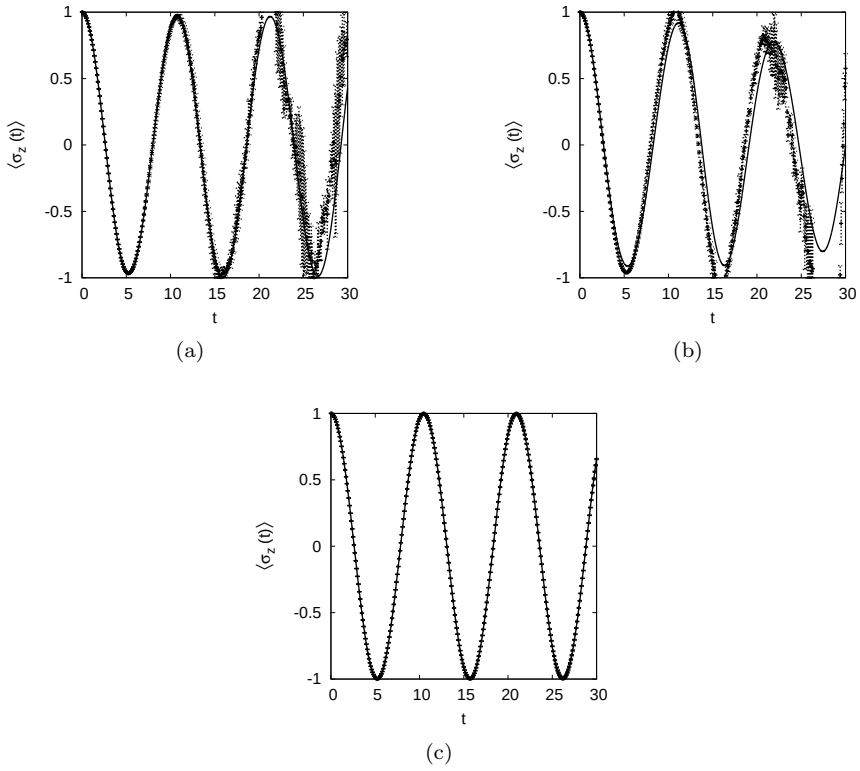

Figure 5.1: Comparison of the time dependence of $\langle \sigma_z \rangle$ between the method lines approach (solid line) and the surface-hopping technique (dashed line with error bars). Here $\Omega = 0.3$ $b_2 = 1$. In (a) $c = 0.1$ and the initial distribution is a coherent state with $R_0 = 0$, in (b) $c = 0.1$ and the initial distribution takes the form of the quantum canonical distribution with inverse temperature $\beta = 0.6$ (See Section 4.4.1) and in (c) $c = 0.01$ and the initial distribution is a coherent state with $R_0 = 0$

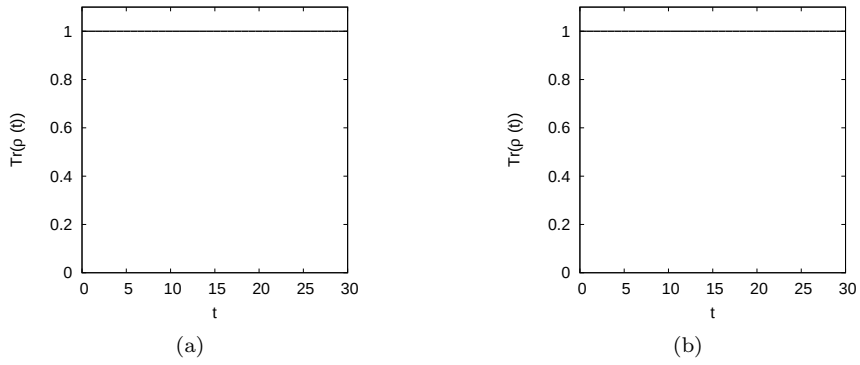

Figure 5.2: Time dependence of $\mathrm{Tr}(\hat{\rho})$ to demonstrate the stability of the method lines technique. Here $\Omega = 0.3$, $b_2 = 1$ and $R_0 = 0$. In (a) the two curves have $c = 0.1$ (solid line) and $c = 0.01$ (dashed line) and in (b) $c = 1.0$.

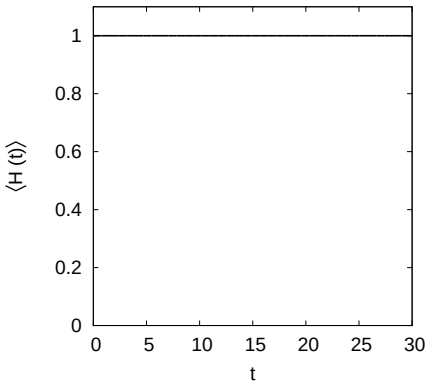

Figure 5.3: Time dependence of $\langle \hat{H} \rangle$ in order to demonstrate the stability of the method of lines approach. Here $\Omega = 0.6$, $c = 1.0$, $R_0 = 0.0$ (solid line) and $\Omega = 0.3$, $c = 1.0$, $R_0 = 0.0$ (dashed line). Values of $\langle \hat{H} \rangle$ have been normalised in this plot.

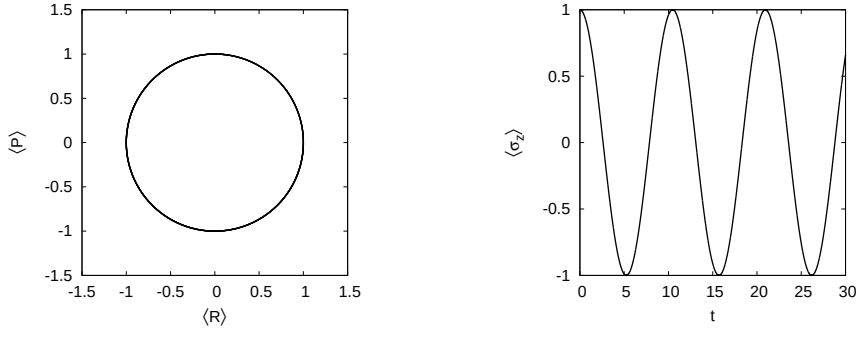

Figure 5.4: Demonstration of the isolated system behaviour at $c = 0$ for the method of lines technique. Here $\Omega = 0.3$, $b_2 = 1$ and $R_0 = 1$. Sub-figure (a) is a phase space plot for the oscillator system and (b) shows the time dependence of $\langle \sigma_z \rangle$ for the pseudo-spin system.

5.2 Quartic Model

5.2.1 Complete Inversion anti-Symmetry

The generic symmetry of pseudo-spin polynomial-potential Hamiltonians, as highlighted in Section 4.3.3, is evident in all Figs. 5.5(a) through 5.6(b). The population difference plots, in Figs. 5.5(a) through 5.5(c) all display inversion around the symmetry axis through the origin. The phase-space position distributions, Figs. 5.6(a) and 5.6(b) also exhibit the total inversion antisymmetry. Such results illustrate the fact that a coupling function with odd symmetry results in inverted behaviour at opposite extrema of the coupling. These particular plots were produced using the full quantum evolution but the quantum-classical evolution demonstrates the same results. Notably the critical point result in Fig. 5.5(c) displays the inversion but its phase-space distribution will not exhibit any reflection, simply because its initial position is identical in both cases; this illustrates that, at the roots of the coupling function, the state of the spin exclusively controls the adiabatic mixing of initial states.

The existence of this symmetry within the results provides a useful check that the method of lines algorithm conforms to theoretical expectations when used to analyse the quartic model system.

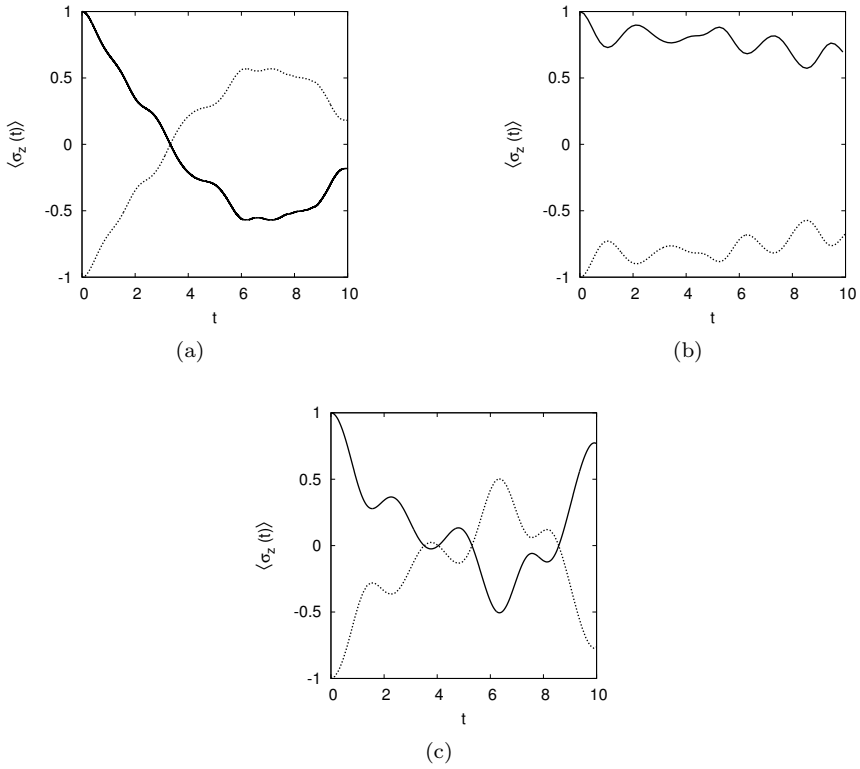

Figure 5.5: Comparison of the time dependence of $\langle \sigma_z \rangle$ for differing initial states: one with the spin initially excited (solid line) and the other initially in the ground state (dashed line). Here $\Omega = 0.6$, $c = 1.0$, $b_2 = -1$ and $b_4 = 0.5$. In (a) the excited-state spin has $R_0 = -1.6$ and the ground-state spin has $R_0 = 1.6$, in (b) the excited-state spin has $R_0 = 1.6$ and the ground-state spin has $R_0 = -1.6$ and in (c) both systems have $R_0 = 0.0$.

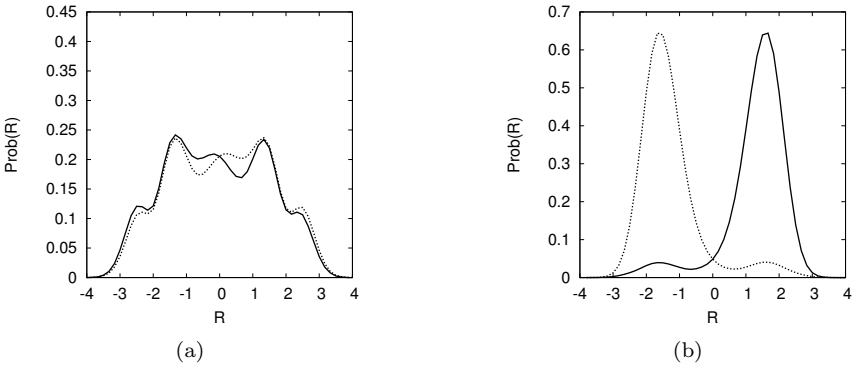

Figure 5.6: Comparison of the time-averaged position probability, Prob(R) for differing initial states: one with the spin initially excited (solid line) and the other initially in the ground state (dashed line). Here $\Omega = 0.6$, $c = 1.0$, $b_2 = -1$ and $b_4 = 0.5$. In (a) the excited-state spin has $R_0 = -1.6$ and the ground-state spin has $R_0 = 1.6$ and in (b) the excited-state spin has $R_0 = 1.6$ and the ground-state spin has $R_0 = -1.6$.

5.2.2 Critical point results

The central idea to be gleaned from the presented results is that the addition of quantum corrections can both increase and decrease the amplitude of Rabi oscillations in the pseudo-spin system. At short times ($t \leq 10$) there is a propensity for the quantum corrections to increase the damping experienced by the Rabi oscillations, however at longer times there exists the possibility of increased Rabi oscillation amplitude due to the addition of quantum effects to the dynamics. These dual possibilities arise because of quantum tunnelling effects that are introduced by the quantum corrections, thereby allowing the oscillator distribution to continuously fluctuate between a highly symmetric state (occupying both wells equally) and an asymmetric state (largely occupying a single well). In Fig. 5.7(a) the increased damping effects become visible after $t \geq 10$, with these

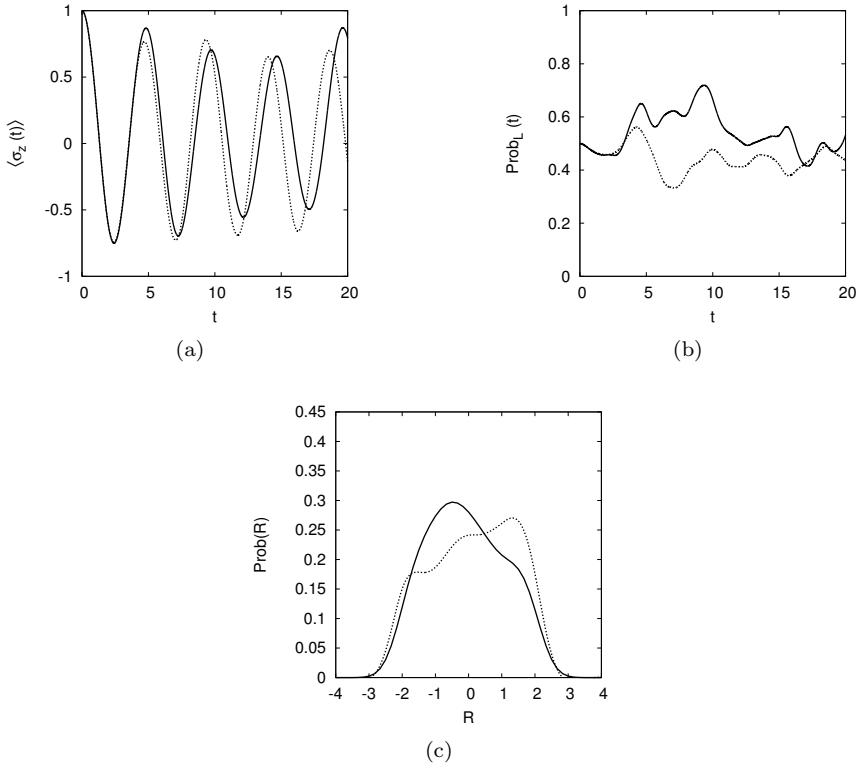

Figure 5.7: Comparison between the quantum-corrected (solid line) and quantum-classical (dashed line) dynamics. Here $R_0 = 0.0$, $\Omega = 0.6$, $c = 0.2$, $b_2 = -1$ and $b_4 = 0.5$. Sub-figure (a) shows the time dependence of $\langle \sigma_z \rangle$, (b) the time dependence of the probability of left well occupation, $\mathrm{Prob}_L(t)$ and (c) the time-averaged position probabilities $\mathrm{Prob}(R)$.

periods of increased damping correlating to the greater symmetry evident in the quantum phase-space distribution, as evinced by Fig. 5.7(b). Figure. 5.7(c) also indicates that both quantum and classical oscillators favour the right well initially, as this well is energetically favoured for the form of the coupling in use. However, the classical oscillator continues to reside largely in the right well at later times, while in the quantum case, the distribution favours the higher energy left well. This asymmetry between the quantum and classical cases is a strong indicator of the presence of quantum tunnelling effects in the dynamics of the quantum oscillator. However, due to the weak coupling, these quantum effects do not translate into large magnitude differences in the behaviour of the pseudo-spin. Further Figs. 5.8(a) and 5.9(a) demonstrate a more marked difference between the quantum and classical evolutions. However, much of the effect of the quantum dynamics here is to encourage, rather than damp, Rabi oscillation in the population difference. This is to be expected as both Fig. 5.8(b) and 5.9(b) show a trend towards increasing the asymmetry, favouring the left well in the quantum case, while the classical distribution remains largely static and

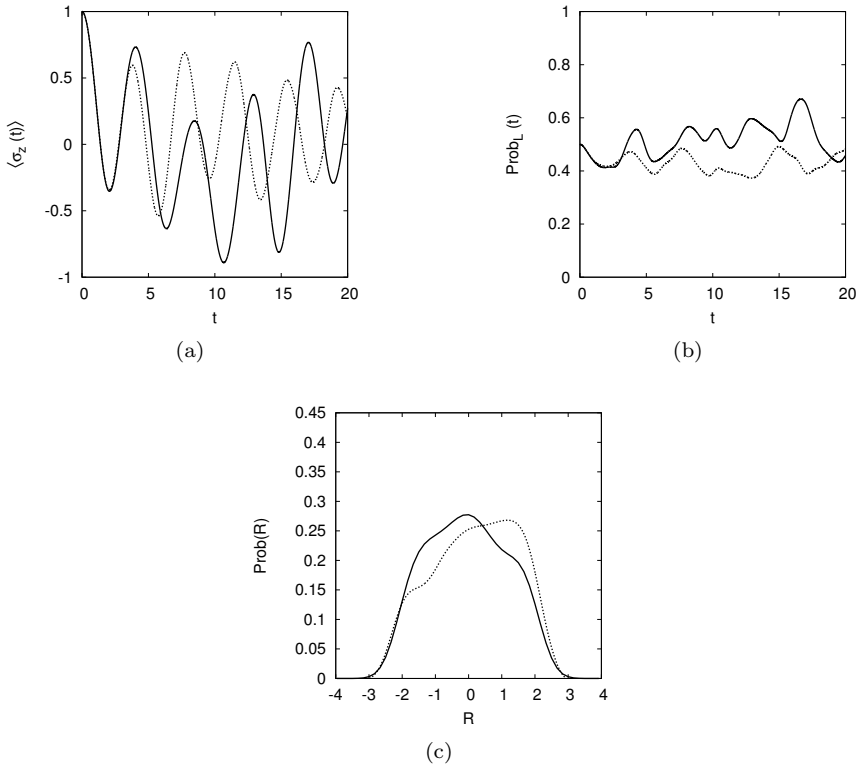

Figure 5.8: Comparison between the quantum-corrected (solid line) and quantum-classical (dashed line) dynamics. Here $R_0 = 0.0$, $\Omega = 0.6$, $c = 0.4$, $b_2 = -1$ and $b_4 = 0.5$. Sub-figure (a) shows the time dependence of $\langle \sigma_z \rangle$, (b) the time dependence of the probability of left well occupation, $\mathrm{Prob}_L(t)$ and (c) the time-averaged position probabilities $\mathrm{Prob}(R)$.

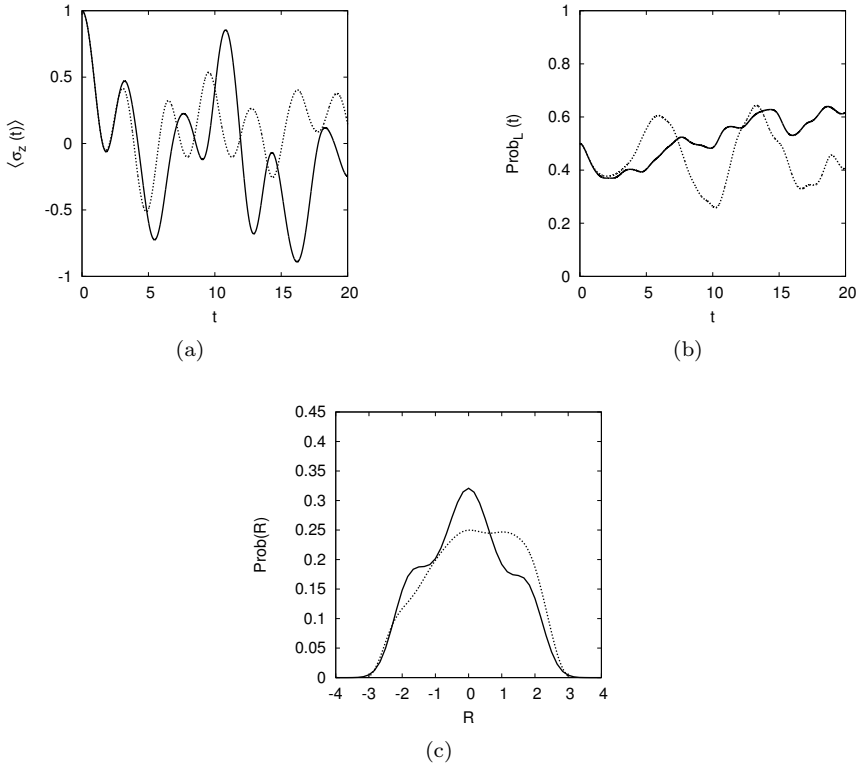

Figure 5.9: Comparison between the quantum-corrected (solid line) and quantum-classical (dashed line) dynamics. Here $R_0 = 0.0$, $\Omega = 0.6$, $c = 0.6$, $b_2 = -1$ and $b_4 = 0.5$. Sub-figure (a) shows the time dependence of $\langle \sigma_z \rangle$, (b) the time dependence of the probability of left well occupation, $\mathrm{Prob}_L(t)$ and (c) the time-averaged position probabilities $\mathrm{Prob}(R)$.

favouring the right well. Periods of increased symmetry around $T \approx 20$ allow the quantum case a brief period of damping more efficiently than the classical counterpart. As the coupling has increased, the time-averaged position probability, as seen in Figs. 5.7(c), 5.8(c) and 5.9(c), becomes more symmetric in both classical and quantum cases. The change, however, is more marked in the quantum case, where the peak of distribution shifts closer to the origin as the coupling increases. Moving to the higher coupling of $c = 0.8$ one can see that the differences induced by the quantum corrections are decreasing. The qualitative behaviour of the population differences in Fig. 5.10(a) has become more similar, although it is still possible to distinguish between cases. The increased similarity comes from the occupation probabilities in Fig. 5.10(b), where the classical case now displays greater oscillations about a more symmetric mean configuration. Quantum tunnelling effects still introduce some additional variation to the quantum case, which results in the distinctions in the population difference damping. This trend towards similarity is the result of non-adiabatic interactions with the pseudo-spin, which influence both the quantum and classical cases, as these effects become stronger, the differentiation caused by added tunnelling become less significant at short times. Figure. 5.10(c) illustrates the continued trend of time-averaged position probability towards symmetrisation, driven by the aforementioned non-adiabatic effects. Similarly the fact that tunnelling effects are not absent from the classical case is due to these non-adiabatic effects, though this becomes more directly apparent in the case where the oscillator is confined initially to one well of the potential profile.

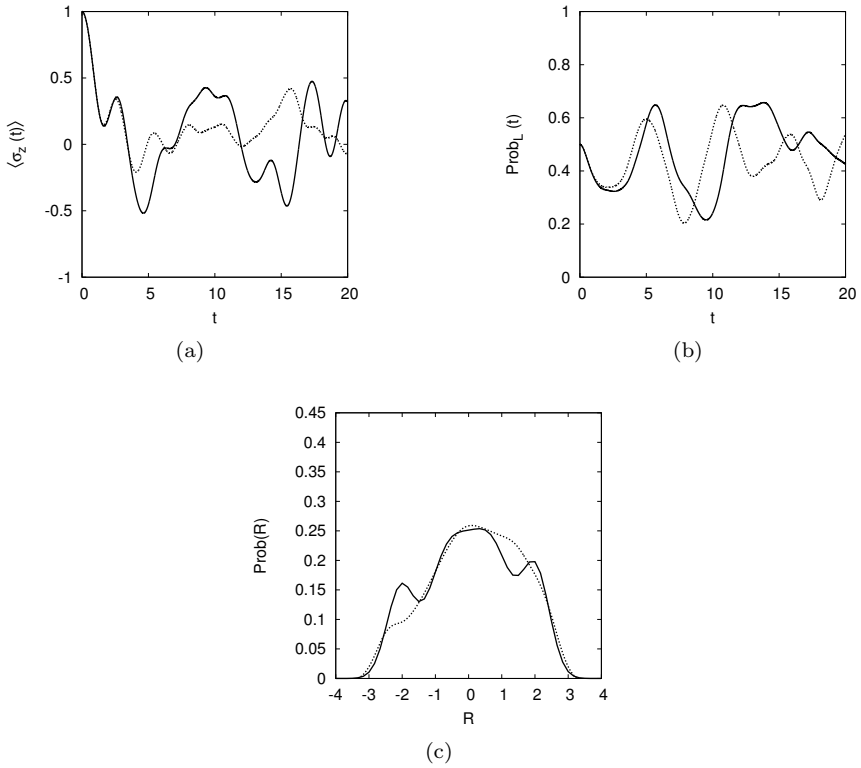

Figure 5.10: Comparison between the quantum-corrected (solid line) and quantum-classical (dashed line) dynamics. Here $R_0 = 0.0$, $\Omega = 0.6$, $c = 0.8$, $b_2 = -1$ and $b_4 = 0.5$. Sub-figure (a) shows the time dependence of $\langle \sigma_z \rangle$, (b) the time dependence of the probability of left well occupation, $\mathrm{Prob}_L(t)$ and (c) the time-averaged position probabilities $\mathrm{Prob}(R)$.

5.2.3 Left well results

The results when starting in the left well are similar in nature to those of the critical point. However, tunnelling is more explicitly evident, since the distribution is initially confined in one well. Increased damping effects due to the quantum evolution, though evident in Fig. 5.11(a), are

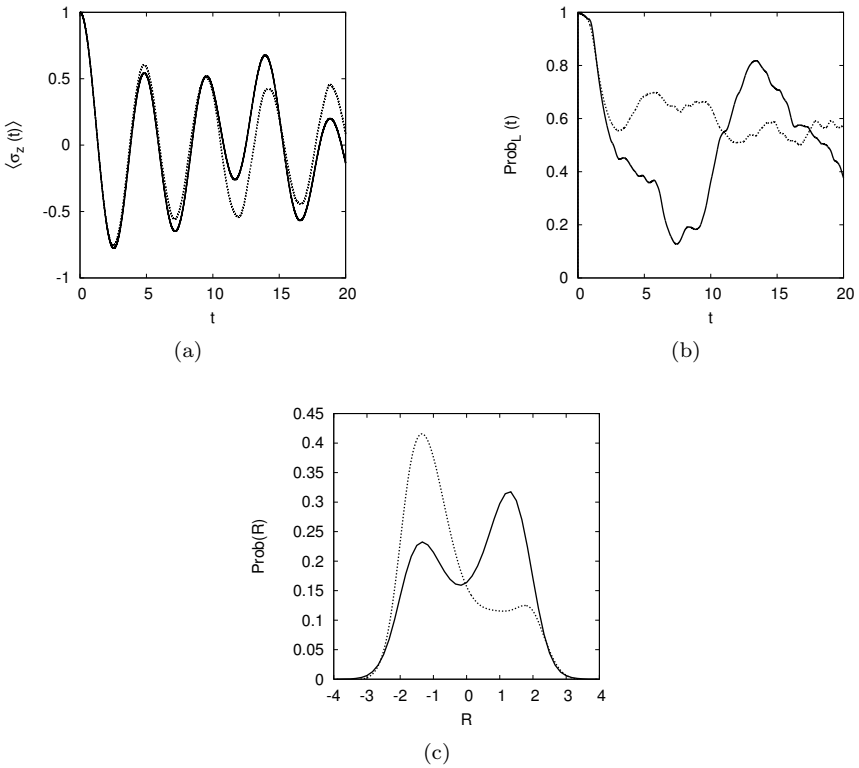

Figure 5.11: Comparison between the quantum-corrected (solid line) and quantum-classical (dashed line) dynamics. Here $R_0 = -1.6$, $\Omega = 0.6$, $c = 0.2$, $b_2 = -1$ and $b_4 = 0.5$. Subfigure (a) shows the time dependence of $\langle \sigma_z \rangle$, (b) the time dependence of the probability of left well occupation, $\mathrm{Prob}_L(t)$ and (c) the time-averaged position probabilities $\mathrm{Prob}(R)$.

not consistent. This is due to the fact that the quantum case demonstrates far larger oscillations in well occupation, visible in Fig. 5.11(b). It is also evident, from the aforementioned Figure, that the classical distribution still displays a tendency to subside to a quasi steady state after some initial transient behaviour. The oscillations in well occupation from Fig. 5.11(b) and the great differences evident in Fig. 5.11(c) evince that the quantum corrections contribute extensive tunnelling effects to the dynamics of the oscillator. However, the weak coupling in this case means that these effects do not greatly impact the population difference damping. As the coupling is increased to the cases of $c = 0.4$ and $c = 0.6$, a period of enhanced damping is observed for the quantum evolution at around $t \approx 10$, as seen in Figs. 5.12(a) and 5.13(a). These enhanced damping periods correspond to time intervals where the quantum oscillator distribution is more symmetric than the classical counterpart, readily seen in Figs. 5.12(b) and 5.13(b). Similarly, periods where the quantum oscillator encourages larger fluctuations in the population difference correspond well to intervals where the quantum distribution in phase space is more asymmetric than the classical case. These fluctuations in the quantum results are evidence of quantum tunnelling effects contributing to the dynamics of the oscillator, an assertion supported by the enhanced symmetry of the time-averaged position probabilities in Figs. 5.12(c) and 5.13(c). Further increase in the coupling enters the regime of strong coupling ($\lambda \geq 1$). Here one observes that the population difference fluctuations differ mainly in magnitude, the time interval shown in Fig. 5.14(a) does not display significant qualitative differences between quantum and classical evolutions. Indeed, in Fig. 5.14(b), it is

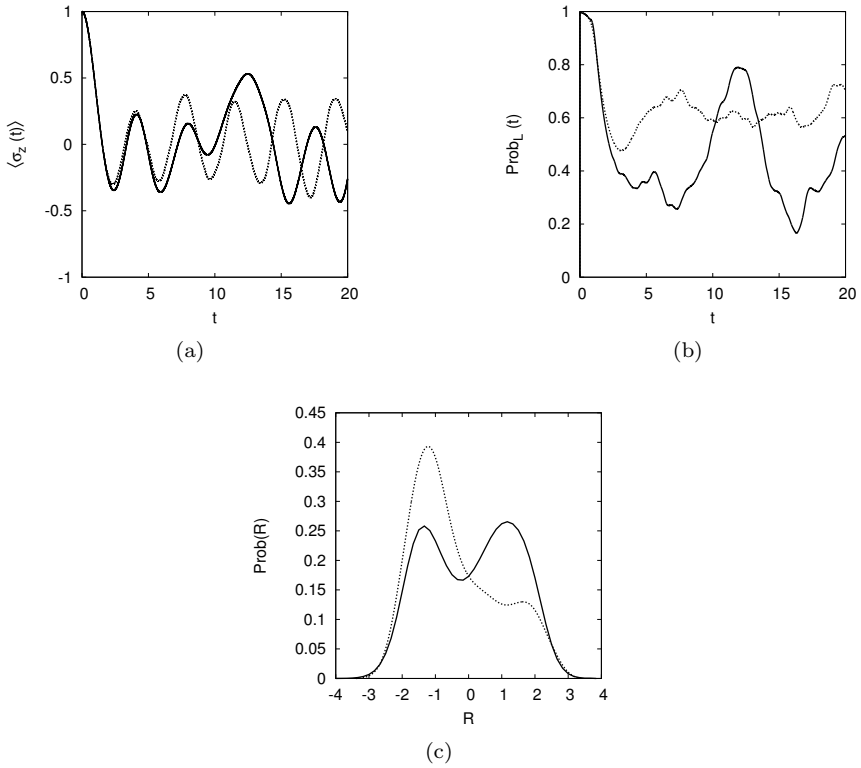

Figure 5.12: Comparison between the quantum-corrected (solid line) and quantum-classical (dashed line) dynamics. Here $R_0 = -1.6$, $\Omega = 0.6$, $c = 0.4$, $b_2 = -1$ and $b_4 = 0.5$. Subfigure (a) shows the time dependence of $\langle \sigma_z \rangle$, (b) the time dependence of the probability of left well occupation, $\mathrm{Prob}_L(t)$ and (c) the time-averaged position probabilities $\mathrm{Prob}(R)$.

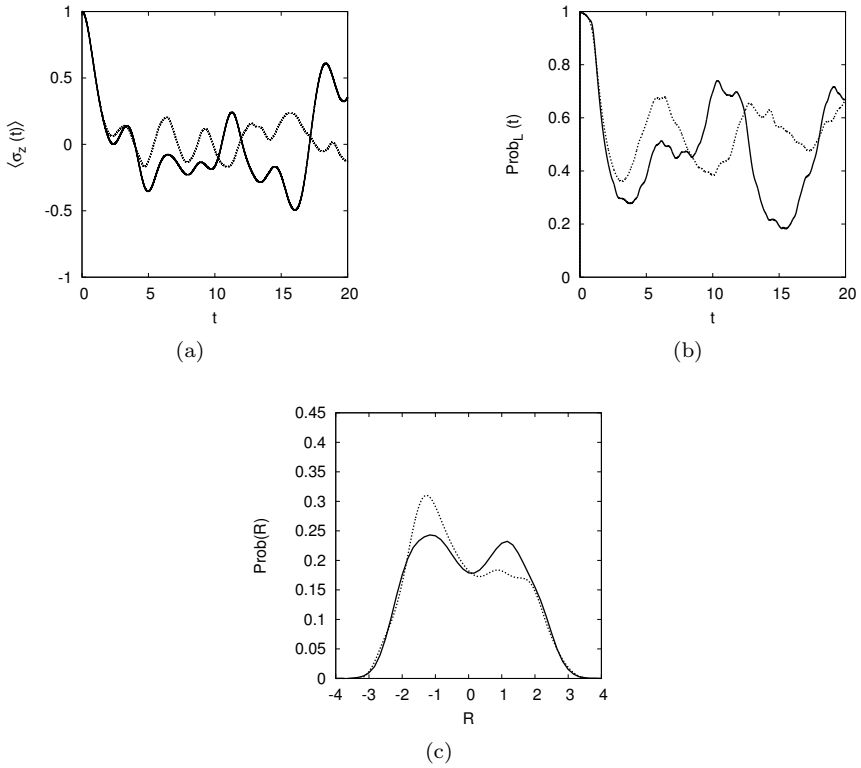

Figure 5.13: Comparison between the quantum-corrected (solid line) and quantum-classical (dashed line) dynamics. Here $R_0 = -1.6$, $\Omega = 0.6$, $c = 0.6$, $b_2 = -1$ and $b_4 = 0.5$. Subfigure (a) shows the time dependence of $\langle \sigma_z \rangle$, (b) the time dependence of the probability of left well occupation, $\mathrm{Prob}_L(t)$ and (c) the time-averaged position probabilities $\mathrm{Prob}(R)$.

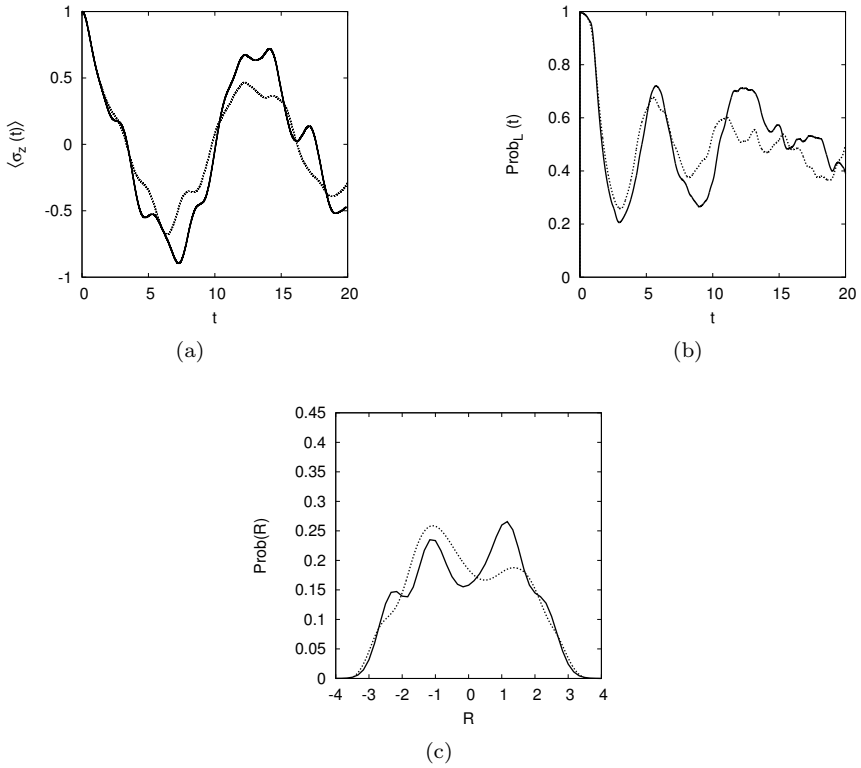

Figure 5.14: Comparison between the quantum-corrected (solid line) and quantum-classical (dashed line) dynamics. Here $R_0 = -1.6$, $\Omega = 0.6$, $c = 0.8$, $b_2 = -1$ and $b_4 = 0.5$. Subfigure (a) shows the time dependence of $\langle \sigma_z \rangle$, (b) the time dependence of the probability of left well occupation, $\mathrm{Prob}_L(t)$ and (c) the time-averaged position probabilities $\mathrm{Prob}(R)$.

evident that the occupation probabilities vary according to a very similar pattern and that the initial transient behaviour lasts far longer than at previous coupling values. Figure. 5.14(c) also shows a convergence of the quantum and classical time-averaged position probabilities, one that has become more evident as the coupling has increased. This drive towards similarity and towards a symmetric distribution at short times is a manifestation of strong non-adiabatic interactions with the pseudo-spin. In the region of strong couplings, such interactions dominate the short-time behaviour of the oscillator and, as such, the quantum dynamical effects are less visible at short times, appearing only in the slight magnitude differences in the Rabi oscillations of $\langle\sigma_z\rangle$ and in minor well occupation differences at $t \geq 10$. Drawing inference from the pattern of behaviour of previous couplings, one might conclude that the quantum effects will simply manifest more strongly at later times, as the strength of the coupling is merely prolonging the dominance of the non-adiabatic dynamical effects.

5.3 Application to Quantum Dynamics of a Buckled Nano-rod

The chosen system for this application consists of a nano-rod coupled capacitively to a Cooper-pair box through its buckled displacement. The nano-rod consists of a tiny bar of silicon that, when placed under compression, undergoes elastic, oscillatory buckling [56, 57]. A Cooper-pair box (CPB) consists of a small Josephson junction which has a Josephson energy much smaller than its charging energy and is voltage biased so that it behaves as a two-level system or pseudo-spin, having only two experimentally accessible energy levels as a result of the biasing [44, 53].

The Hamiltonian for a Cooper-pair box can be expressed as [53]:

$$\hat{H}_{CPB} = 4E_C(n_g - n - \frac{1}{2})\hat{\sigma}_z - \frac{1}{2}E_J\hat{\sigma}_x \ ,$$

where E_C is the charging energy, E_J is the Josephson energy, $n_g = \frac{(C_bV_b+C_gV_g)}{2e}$, here C_b and C_g are the bias capacitance of the CPB and capacitance between the nano-rod and CPB; while V_b and V_g are the bias voltage of the CPB and voltage between the nano-rod and CPB; lastly n is an integer giving the charge state of the CPB. The operators $\hat{\sigma}_z$ and $\hat{\sigma}_x$ are the Pauli spin operators for the pseudo-spin representation of the CPB.

The Hamiltonian of the nano-rod is chosen, in accordance with continuum elastic theory [56], to be

$$H_{NR} = \frac{P^2}{2M} + \frac{1}{2}\alpha R^2 + \frac{1}{4}\beta R^4 \ ,$$

where $\alpha = M\omega_0^2\frac{Y_c-Y}{Y_c}$, here Y is the compressive strain on the nano-rod, Y_c is the critical strain value, M is the mass of the nano-rod, ω_0 is the fundamental frequency of the nano-rod and $\beta = \frac{M\omega_0^2}{d^2}$ where d is the thickness of the nano-rod [56]. The fundamental frequency ω_0 is given by [56]

$$\omega_0 = \sqrt{\frac{Q}{12\rho}}d\left(\frac{\pi}{l}\right)^2 \ ,$$

where l is the length, Q is the quality factor and ρ the density of the nano-rod. In the notation used here, R represents the fundamental mode displacement of the nano-rod [56, 57] and P is the conjugate momentum to R.

The interaction Hamiltonian is chosen to represent the capacitive coupling through the displacement of the nano-rod and is therefore given by

$$\hat{H}_I = -cR\hat{\sigma}_z \ ,$$

where c is the coupling constant.

The total Hamiltonian then consists of the sum of these three parts, however, in H_{CPB} the term corresponding to a constant shift on $\hat{\sigma}_z$ is neglected to allow the Hamiltonian to match that

Table 5.1: Continuum Elastic Theory Nanorod Properties

Quantity	S. I. Value
l	200×10^{-9} m
w	5×10^{-9} m
d	1×10^{-9} m
ρ	2330 kg. m^{-3}
Q	130×10^{9} Pa
ω_0	5.0×10^{8} Hz
M	2.3×10^{-21} Kg
β	$\approx 1.0 \times 10^{15}$ kg. m^{-2}. s^{-2}

Table 5.2: Simulation Properties

Quantity	Simulation Value	S. I. Value
$E_J = 2\hbar\Omega$	0.6	0.4 μeV
R_0	1.6	1.4×10^{-11} m
t (time units)	1	2 ns
Y_1	$2Y_c$	-
β_1	0.5	$\approx 1.0 \times 10^{18}$ kg. m^{-2}. s^{-2}
Y_2	$1.1Y_c$	-
β_2	0.03	$\approx 1.0 \times 10^{17}$ kg. m^{-2}. s^{-2}
Y_3	$1.25Y_c$	-
β_3	0.03	$\approx 1.0 \times 10^{17}$ kg. m^{-2}. s^{-2}

displayed in Chapter 3 of this work. In order to compare this Hamiltonian to that presented previously, the following identifications must be made

$$\begin{aligned} 2\hbar\Omega &\to E_J \ , \\ b_2 &\to \alpha \ , \\ b_4 &\to \beta \ , \\ n_g - n - \frac{1}{2} &= 0 \ . \end{aligned}$$

Given this identification it is now possible to interpret the results displayed in the previous Chapter in terms of this model. Firstly, though, it is important to determine the S.I. values of the constants used in the simulation work, in order to compare these to the experimentally realisable values.

Table. (5.1) displays the properties of the nano-rod, the quality factor Q and density ρ are taken as those of silicon nano-rods [56]. Here l, w and d are the length, width an thickness of the nano-rod respectively; M and ω_0 are the mass and fundamental frequency.

Table. (5.2) displays the properties of the coupled system used in the simulation, along with their S. I. values. Clearly there is a discrepancy in the β values between the simulation properties and those calculated from the continuum elastic theory, however, adjustment of the quality factor could potentially bring the nano-rod into the regime of significant non-linear oscillatory effects. The initial state of the oscillator, used to obtain the numerical results in this study, was taken to be a coherent state, with the non-linear terms being 'switched on' at time $t = 0$. This is still consistent with the buckled nano-rod if one assumes the nano-rod was subjected to compression below the critical strain at $t < 0$ and at $t = 0$ the strain is increased beyond the critical value. The additional results presented in this chapter will include simulations where $b_2 \neq -1$, this is not inconsistent with the rescaling procedures, as the constant b_2 is redefined for this application.

Figure 5.15 presents the results for the simulation using β_2 and Y_2, despite the previous concerns these plots using the lower value of β also display clear differences between the quantum and classical results, in both the occupation probabilities, indicating quantum tunnelling effects, and in the Rabi oscillations of the CPB population difference. However these differences emerge only at longer times, it might therefore be necessary to find a system that exhibits stronger non-linearities

than a buckled nano-rod to experimentally observe the effects of the quantum corrections in this way, unless further adjustments can be made to the non-linearity to produce non-linear effects earlier in the evolution. The timing of the non-linear effects is of concern, not because of the decoherence time for the CPB, which is of the order of 500 ns [44] and $t = 20$ in the scaled units corresponds to 40 ns, but because of the more general problem of the long time integration of quantum dynamics. In terms of the other parameters: the Josephson energy is within an order of magnitude of lab realisable values [44] and the dimensions of the nano-rod are chosen to be close to those suggested in [56]. Finally, control of the compressive forces on the rod should not present great difficulty, despite requiring that the strain be held at one tenth above the critical strain, this is possible provided the ends are fixed [56].

Figure 5.16 displays a set of results, for similar simulation parameters β_3 and Y_3, where the dynamical differences emerge more rapidly. In this case Fig. 5.16(a) the quantum corrections show a propensity to increase the magnitude of the Rabi oscillations, this corresponds to the fact that the probability distribution is less symmetric than the classical case during these periods, as born out in Fig. 5.16(b). The extensive transfer from the left well to the right is clearly evident in Fig. 5.16(c), where the average position-probability appears to be extremely symmetric in the quantum case. This shows clear evidence of quantum tunnelling effects in the dynamics of the oscillator which are again witnessed by changes in the population difference of the pseudo-spin. This suggests that, even for much smaller non-linearity parameters, the CPB might still witness the quantum features of the nano-rod dynamics, provided the strain and the coupling are chosen correctly.

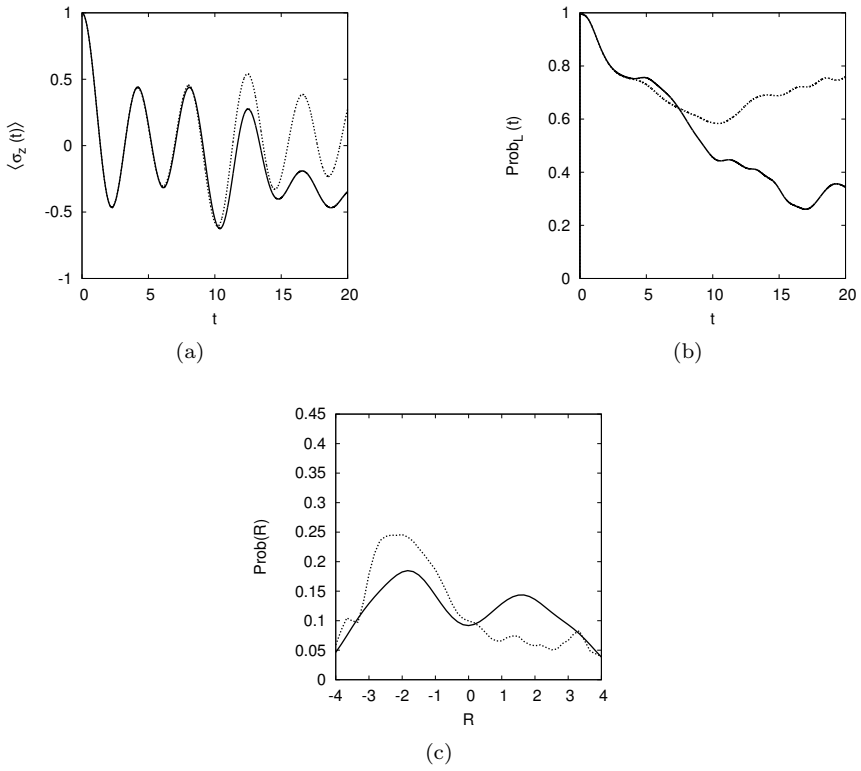

Figure 5.15: Comparison of the classical evolution (dashed line) with the quantum evolution (solid line), here $\Omega = 0.6$, $R_0 = -1.6$, $c = 0.2$, $b_2 = -0.1$ and $b_4 = 0.03$. Sub-figure (a) shows the time dependence of $\langle \sigma_z \rangle$, (b) the time dependence of the probability of left well occupation, $\mathrm{Prob}_L(t)$ and (c) the time-averaged position probabilities $\mathrm{Prob}(R)$.

The results of particular interest are those associated with the population operator $\hat{\sigma}_z$ [53]; as these results display distinct differences between the quantum-classical and quantum-corrected cases. Such differences indicate that, for a highly non-linear oscillation potential, where the quar-

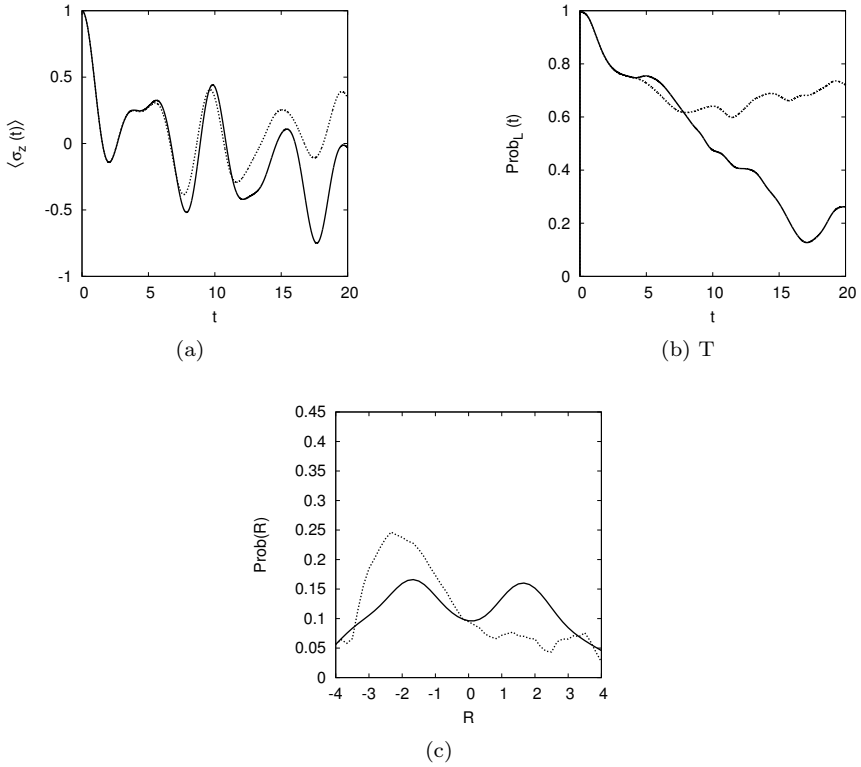

Figure 5.16: Comparison of the classical evolution (dashed line) with the quantum evolution (solid line), here $\Omega = 0.6$, $R_0 = -1.6$, $c = 0.3$, $b_2 = -0.25$ and $b_4 = 0.03$. Sub-figure (a) shows the time dependence of $\langle \sigma_z \rangle$, (b) the time dependence of the probability of left well occupation, $\mathrm{Prob}_L(t)$ and (c) the time-averaged position probabilities $\mathrm{Prob}(R)$.

tic coefficient is somewhat comparable to quadratic coefficient, measurement of the Cooper-pair number difference in the CPB would allow one to distinguish between classical and quantum mechanical behaviour in the coupled nano-rod; as the quantum-classical case represents a situation where the corrections are small and quantum dynamical effects are weak, whereas in the quantum-corrected case, such quantum effects are present in the dynamics. The strength of these corrections is controlled by the coefficient β, as can be seen in the analysis presented in Chapter 2, and for this reason the oscillator must exhibit significant non-linear behaviour in order for the corrections to make significant contributions to the dynamics. The presence of differences due to the quantum correction effects in a relatively large range of couplings, as displayed in Chapter 5, and even when the properties of the nano-rod are significantly adjusted, as in Figure 5.15, suggests that, in principle, it should be possible to experimentally detect quantum features of a buckled nano-rod, or similar non-linear nano-oscillator, through observation of the population difference of a coupled CPB. The apparent dynamical differences produced by significant non-linear oscillatory behaviour might therefore provide a method for witnessing the transition of a nano-mechanical from the regime of classical dynamics into the quantum realm. The differing behaviour of the pseudo-spin population difference under quantum and classical oscillator dynamics also provide a means of indirectly witnessing quantum tunnelling effects in the oscillator system, which are seen to be directly correlated to the apparent dynamical differences. The fact that such differences would become apparent before the decoherence time of the CPB is promising in regards to the possibility of detecting these dynamical features in suitably prepared experimental set-up.

Chapter 6

Conclusions and Perspectives

The quantum Liouville equation in the Wigner picture appears as the classical Poisson bracket equation with the addition of a series of non-local correction terms. This particular structure reveals that the correction terms hold the 'quantumness' that is present in the dynamics. Therefore, the study of such correction terms allows one to identify the peculiarly quantum features of a chosen system's dynamics; such a method of identification might allow for the witnessing of classical-to-quantum transitions in suitably chosen systems through observation of the dynamical signature of the quantum correction effects. The Wigner picture can also be employed in the case where two systems are coupled together, where one wishes only to express one of the systems in phase space. Such an approach is termed the partial Wigner picture, this approach can be effectively used to study the dynamical contribution of the quantum corrections by addressing both the cases where the correction terms are neglected, yielding a quasi-classical limit of the phase-space system, and the case where the correction terms are maintained, representing the case where both systems evolve under fully quantum dynamics. In this work, the form of the corrections was derived for the case of arbitrary polynomial potentials and couplings; the corrections were found to stem only from the forms of the coupling function and the phase-space potential. Additionally, the general form of the Wigner-Liouville propagator, including correction terms, can be conveniently realised in a bracket notation, providing an explicit form for the equation of motion that expresses the phase-space evolution in a manner similar to the full Wigner representation. It was also shown that the quantum corrections have a special form, identical to the form in the complete Wigner case, when the coupling was chosen to be a linear function of the phase-space position coordinate.

The hybrid dynamical formalism that can be reached through this partial Wigner picture has the significant advantage of allowing one to focus upon a few degrees of freedom of interest, those which determine the relevant physics within a condensed matter system that potentially contains many more degrees of freedom. The remaining degrees of freedom can then be treated as a semi-classical bath, allowing for the construction of more efficient computational methods without affecting the physics of the processes being studied. There are many systems in both chemical and biological physics that might benefit from examination under hybrid and non-Hamiltonian formalisms, particularly transport type processes taking place in environments composed of heavy molecules. Such systems exhibit little in the way of Hamiltonian symmetry and are therefore prime candidates for hybrid treatment, as they do not suffer from the hybrid theory's conditional violation of the Jacobi identity and the efficient simulation of such problems remains something of an open problem.

Furthermore, the algebraic structure of the quantum-classical formalism was examined, demonstrating the conditions under which it constitutes a Lie algebra. This analysis was accompanied by a study of how the quantum-corrections contributed to the preservation of Hamiltonian symmetries and to maintaining the Lie algebra structure, so important in physical theories. This analysis determined that each correction term added linearly increases the degree to which Hamiltonian symmetries are preserved. This means that the hybrid formalism can be employed as an approximation of full quantum dynamics, while preserving all symmetries up to a given order, by introducing a finite number of correction terms. This allows one to leverage the considerable computational advantages of the hybrid formalism even in situations that demand the preservation of particular

symmetries. This analysis also revealed that, despite the existence of seemingly consistent methods of obtaining the quantum-classical limit, the resulting quantum-classical bracket does not generally constitute a Lie bracket, thus compromising the Lie algebra properties of the hybrid theory. The loss of this property suggests, in this author's opinion, that this hybrid formalism cannot constitute a general prescription for treating interacting quantum and classical systems, although further study may be needed in this regard, as it is unclear as to whether preservation of general hybrid symmetries should be expected in physical systems. Never the less, this hybrid formalism does yield a powerful computational approximation and a method of studying the essential features of quantum dynamics in otherwise prohibitively complicated systems.

The observations presented here, pertaining to the coupled pseudo-spin, or two-level system, and quartic oscillator system, demonstrate that the effects of the quantum corrections can be observed within a balance of parameters. If the coupling was chosen to be too strong, then the differences in the pseudo-spin Rabi oscillation damping, between the uncorrected and quantum-corrected oscillator cases, do not become apparent at short times. In the case of weak couplings, the differences might also be too minor to be observed, even at longer times. However, when the bare coupling parameter λ is in the range $0.1 < \lambda < 1.0$ and the quartic coefficient is not too small in comparison to its quadratic counterpart, the addition of correction terms produce differences in both the magnitude of Rabi oscillations and in their qualitative behaviour. At shorter times the quantum corrections can, dependent on the geometry of the oscillator potential and thus the actual significance of the corrections, introduce more significant damping effects. However, at longer times the corrections are capable of inducing larger fluctuations in the pseudo-spin population difference than those produced in the uncorrected case. The variation in the behaviour of the population difference is induced by additional quantum tunnelling effects that are introduced into the dynamical behaviour of the oscillator via the correction terms. These tunnelling effects allow the quantum oscillator distribution to fluctuate continuously between the wells of the potential profile, shifting between symmetric configurations, where both wells are equally occupied, and asymmetric configurations, where largely one well is occupied. These shifts switch the influence on the Rabi oscillations from inducing greater damping than the uncorrected case, when the quantum oscillator distribution is more symmetric, or making the damping effects caused by the quantum oscillator less significant in the case where the quantum oscillator distribution is more asymmetric than the classical case. Throughout the results presented here, classical oscillator distribution was observed to settle into a quasi steady-state configuration after some short time transient behaviour. This behaviour is induced by non-adiabatic effects which were dependent on the strength of the coupling, such effects also cause the classical evolution to seemingly exhibit some lesser tunnelling effects by allowing non-adiabatic transitions between wells of the potential profile. The stronger the coupling chosen, the longer the period of transient behaviour was observed to be; during this transient period the non-adiabatic effects dominate and the quantum corrections provide little differentiation between the quantum and classical oscillator evolutions. However, after the transient behaviour dies down, the quantum corrections quickly assert themselves and differentiate the two cases.

The results demonstrated in this work can also be applied to the study of the classical-to-quantum transition of nano-mechanical systems. To this end, the coupled quartic oscillator and pseudo-spin model was applied to the study of a nano-rod under compression, capacitively coupled to a Cooper-pair box. In this model, the Cooper-pair box and nano-rod correspond to the pseudo-spin and quartic oscillator respectively. It was found that the effects of the quantum corrections could be potentially used to identify uniquely quantum features in the dynamics of the non-linear nano-oscillator by observing the damping of the Rabi oscillations in the Cooper-pair number. Importantly, differences between the quantum and classical evolutions of the nano-rod oscillations emerge for times shorter than the decoherence time of the Cooper-pair box, meaning that, provided a suitably non-linear oscillator can be prepared, the dynamical differences are, in principle, observable under conditions close to those which are currently lab realisable. This work also suggests that differences in the Cooper-pair number Rabi oscillation damping between the cases of coupling to either a classical or a quantum nano-oscillator are due to quantum tunnelling effects introduced by the quantum corrections. As such, observation of the Rabi oscillation damping in the Cooper-pair number allows for the detection of quantum or classical features of the oscillator dynamics, including the ability to indirectly witness quantum tunnelling, which was determined

to be at the heart of these dynamical differences. These results also formed the basis of a paper submitted recently for publication.

Appendix A

Review of Elementary Quantum Statistical Physics

A.1 Statistical Mechanics with Quantum Pure States

A.1.1 Definition of a Pure State

In quantum mechanics, any state of a physical system can be completely described [63] by some abstract vector $|i\rangle$, in Dirac notation [15], which is a member of some Hilbert space. This state vector forms a ray in the Hilbert space, rather than a point, since it is unique only to within a multiplicative, complex constant. The state is termed a 'pure' state if the physical configuration it represents is described by the measurement of a complete set of commuting observables on the state [15, 16, 63]. An observable of a quantum mechanical system is a physically measurable quantity represented by a linear, Hermitian operator on the Hilbert space of the system [70]. A set of commuting observables, given by the operators $\{\hat{A}_i\}$ where $[\hat{A}_i, \hat{A}_j] = 0 \ \forall\, i, j$, is defined as complete if for an observable operator $\hat{B}$,

$$[\hat{B}, \hat{A}_i] = 0 \ ,$$

iff $\hat{B} = f(\{\hat{A}_k\})$, where $\{\hat{A}_k\}$ is one or more of the operators $\hat{A}_i$ and $f(\hat{A})$ is a function of the operator $\hat{A}$.

These pure states form the quantum analogue of the classical systems which exhibit deterministic certainty, not of classical systems whose behaviour is described in statistical terms [15]. This analogy arises because the pure state accounts for a complete description of the system and so cannot give rise to probabilistic scenarios based on a lack of information, which is the reason for statistical treatments in classical mechanics [17]. Despite the fact that pure states represent a complete description of the system, they still exhibit probabilistic behaviour under measurement, as will be demonstrated. It must be made clear, however, that the probabilistic behaviour of a pure quantum state is of a different sort from the ensemble-based probabilities of classical statistics, this difference will also be illustrated in the following pages.

A.1.2 Statistical Behaviour of Pure States

The existence of this probabilistic behaviour under measurement, for a system in a pure state, will be demonstrated by the fact that it is possible to construct a probability distribution, $P_{Q,\psi}(a)$, for the results of measurement of the observable Q on the pure state $|\psi\rangle$. This probability distribution returns the probability of the result of the measurement of Q, such that it has a value less then a. To show that this P forms a valid probability distribution it must first satisfy the conditions of

probability theory, namely [15, 82]

$$\begin{aligned} P_{Q,\psi}(a) \leq P_{Q,\psi}(b) \text{ iff } a \leq b \ , \\ P(+\infty) = 1 \ , \\ P(-\infty) = 0 \ , \\ \lim_{\delta \to 0^+} P(a+\delta) = P(a) \ . \end{aligned} \tag{A.1}$$

Consider the pure state $|\psi\rangle$, which can be expressed in the orthonormal basis $\{|e_i\rangle \, , i \in n\}$:

$$|\psi\rangle = \sum_i c_i \, |e_i\rangle \ ,$$

where $c_i \in \mathbb{C}$, the set of complex numbers. By definition of an observable operator, its eigenstates form an orthonormal basis. Therefore, the orthonormal basis used previously can to be taken as the set of the eigenstates of the observable Q, such that Q has a value q_i in state $|e_i\rangle$. It makes sense then to relabel these eigenstates $|q_i\rangle$. The observable Q can then be represented by a family of projectors

$$\hat{Q} = \sum_i q_i \hat{\mathbb{P}}_i \ ,$$

where $\hat{\mathbb{P}}_i = |q_i\rangle \langle q_i|$. This representation assumes there is some countable, discrete set of possible measurement results for the observable Q on the given system. To guarantee this eigenvalue decomposition of $\hat{Q}$ is possible it must be assumed that $\hat{Q}$ is a compact Hermitian operator [15]. For a definition of compactness, in regards to linear operators, the reader is invited to consult the referenced works: [15, 72, 83].

Since the probability of measuring a particular eigenvalue q_i of the observable $\hat{Q}$ is given by the expectation value of the projector $|q_i\rangle \langle q_i|$ [17], the probability distribution, $P_{Q,\psi}(a)$, is now defined in terms of the action of the family of projectors associated with observable $\hat{Q}$, on the pure state $|\psi\rangle$:

$$P_{Q,\psi}(a) = \Big|\Big| \sum_{i, q_i < a} \hat{\mathbb{P}}_i \, |\psi\rangle \Big|\Big|^2 \ ,$$

where the summation, $\sum_{i,q_i \leq a}$, is performed over all the states $|q_i\rangle$ that have $\hat{Q} \, |q_i\rangle = q_i \, |q_i\rangle$, such that $q_i \leq a$. The more rigorous motivation for this definition is given by the fact that the set of projectors $\{\hat{\mathbb{P}}_i\}$ forms the spectral family of the operator $\hat{Q}$ and thus can be used to formulate Stieltjes integrals [15, 83].

Evaluation of this prospective probability distribution yields

$$\begin{aligned} P_{Q,\psi}(a) &= \sum_{j, q_j \leq a} \langle \psi | \, \hat{\mathbb{P}}_j \sum_{i, q_i \leq a} \hat{\mathbb{P}}_i \, |\psi\rangle \ , \\ &= \sum_{j, q_j \leq a} \sum_{i, q_i < a} \langle \psi | \, q_j \rangle \langle q_j | \, q_i \rangle \langle q_i | \, \psi \rangle \ , \\ &= \sum_{i, q_i \leq a} |c_i|^2 \ . \end{aligned}$$

To prove that this is a valid distribution, it must be first shown that it satisfies normalisation, to this end, consider the normalisation condition of the pure state $|\psi\rangle$ combined with the basis completeness:

$$\langle \psi | \, \psi \rangle = \sum_i \sum_j c_i c_j^* \langle q_j | \, q_i \rangle = \sum_i |c_i|^2 = 1 \ ,$$

where the summation over i is made over all the eigenstates indexed by i. Furthermore, it is trivial

to show that this satisfies the probability theory requirements outlined previously in Eq. (A.1):

$$P(+\infty) = \sum_{q_i \leq +\infty} |c_i|^2 = 1 \ ,$$
$$P(-\infty) = \sum_{q_i \leq -\infty} |c_i|^2 = 0 \ ,$$
$$\lim_{\delta \to 0^+} P(a+\delta) = \lim_{\delta \to 0^+} \sum_{i, q_i \leq a+\delta} |c_i|^2 = P(a) \ .$$

Finally, P is monotonic, non-decreasing because the terms $|c_i|^2$ are necessarily real and positive-definite. Therefore, under measurement of the observable Q, the pure state $|\psi\rangle$ exhibits probabilistic behaviour governed by the distribution $P_{Q,\psi}(a)$, with the coefficients $|c_i|^2$ giving the probability of measuring the observable value q_i corresponding to the eigenstate $|q_i\rangle$.

In general then, it is true that a family of projectors $\{\hat{\mathbb{P}}_i\}$, which forms a complete, orthonormal basis for the Hilbert space $\mathcal{H}$, also defines a probability distribution on any pure state $|\psi\rangle \in \mathcal{H}$. This can also be shown to be true in the case of an observable with a continuous range of measurement results, though it is considerably more involved [15].

A.1.3 Pure State Averages

Given the representation of the observable Q in terms of the projectors $\hat{\mathbb{P}}_i = |q_i\rangle \langle q_i|$, the expectation value of the observable is defined to be:

$$\langle\psi| \hat{Q} |\psi\rangle = \sum_i q_i \langle\psi| q_i\rangle \langle q_i| \psi\rangle = \sum_i q_i |c_i|^2 \ ,$$

which can be rewritten

$$\langle\psi| \hat{Q} |\psi\rangle = \sum_i q_i p_i \ ,$$

where $p_i = |c_i|^2$ is the probability of the system being measured in state $|q_i\rangle$. This result is equivalent to taking an average over the possible measurement results; therefore

$$\langle\psi| \hat{Q} |\psi\rangle = \langle\hat{Q}\rangle \ ,$$

where $\langle\hat{Q}\rangle$ is the average of the observable Q. This average can then be expressed in the basis of the eigenstates of $\hat{Q}$,

$$\langle\hat{Q}\rangle = \langle\psi| \hat{Q} |\psi\rangle = \sum_i \sum_j \langle\psi| q_j\rangle \langle q_j| \hat{Q} |q_i\rangle \langle q_i| \psi\rangle = \sum_i \sum_j c_j^* c_i Q_{ji} \ ,$$

where $Q_{ji} = \langle q_j| \hat{Q} |q_i\rangle$. These coefficients $c_j^* c_i$ might be used to define a matrix ρ with elements given by

$$\rho_{ij} = c_j^* c_i \ ,$$

from which, an operator can then be defined, such that its matrix elements are similar to Q_{ji}. Therefore, let $\rho_{ij} = \langle q_i| \hat{\rho} |q_j\rangle$. The form of this operator can then be deduced to be

$$\hat{\rho} = |\psi\rangle \langle\psi| = \hat{\mathbb{P}}_\psi \ ,$$

which can be proved by considering that

$$\rho_{ij} = \langle q_i| \psi\rangle \langle\psi| q_j\rangle = c_i c_j^* \ ,$$

as required. This operator $\hat{\rho}$ is known as the density operator and is vital to quantum statistical mechanics. Therefore it is worthwhile examining some of the properties of this operator.

The first property of this density operator under consideration is the nature of $\hat{\rho}^2$,

$$\hat{\rho}\hat{\rho} = |\psi\rangle \langle\psi| \psi\rangle \langle\psi| = \hat{\rho} \ .$$

If this equality holds the density operator can be shown to describe a pure state [15]. It can also be shown that $\hat{\rho}$ is self-adjoint. To accomplish this, consider the expectation value product of operators $\hat{A}\hat{B}$:

$$\begin{aligned} \langle\psi|\,\hat{A}\hat{B}\,|\psi\rangle = \langle\phi|\,\chi\rangle \ , \\ \langle\phi| = \langle\psi|\,\hat{A}\ , \\ |\chi\rangle = \hat{B}\,|\psi\rangle \ . \end{aligned}$$

Then the adjoint of this expectation value is given by

$$\Big(\langle\psi|\,\hat{A}\hat{B}\,|\psi\rangle\Big)^\dagger = \langle\chi|\,\phi\rangle = \langle\psi|\,\hat{B}^\dagger\hat{A}^\dagger\,|\psi\rangle \ .$$

But this implies that

$$\langle\psi|\,\Big(\hat{A}\hat{B}\Big)^\dagger\,|\psi\rangle = \langle\psi|\,\hat{B}^\dagger\hat{A}^\dagger\,|\psi\rangle \ ,$$

or, equivalently, that the adjoint of the product is given by product of the adjoints with operator order reversed. This can be stated mathematically as:

$$\Big(\hat{A}\hat{B}\Big)^\dagger = \hat{B}^\dagger\hat{A}^\dagger \ .$$

Considering the operator $\hat{\rho}$, the adjoint is therefore given by

$$\hat{\rho}^\dagger = (|\psi\rangle\,\langle\psi|)^\dagger = |\psi\rangle\,\langle\psi| = \hat{\rho} \ .$$

Which means that $\hat{\rho}$ is self-adjoint or Hermitian.

The density operator is also bounded, this can be proven directly from the definition of a bounded operator: An operator $\hat{A}$, acting on the Hilbert space $\mathcal{H}$, is bounded if it satisfies the inequality [72]

$$\big|\big|\hat{A}\,|v\rangle\,\big|\big| \leq M\big|\big|\,|v\rangle\,\big|\big| \ ,$$

where $\big|\big|\cdot\big|\big|$ is the norm on the Hilbert space $\mathcal{H}$ and M is a finite constant. Rewriting this inequality in Dirac notation and squaring it results in

$$\langle v|\,\hat{A}^\dagger\hat{A}\,|v\rangle \leq M^2\,\langle v|\,v\rangle \ , \tag{A.2}$$

where $|v\rangle$ is a member of the Hilbert space $\mathcal{H}$. Substituting $\hat{\rho}$ into the left-hand side of the inequality yields

$$\langle v|\,\hat{\rho}^\dagger\hat{\rho}\,|v\rangle = \langle v|\,\psi\rangle\,\langle\psi|\,v\rangle \ .$$

If the vectors are normalised it is clear that

$$\big|\,\langle v|\,\psi\rangle\,\big| \leq 1 \ .$$

Therefore,

$$\langle v|\,\hat{\rho}^\dagger\hat{\rho}\,|v\rangle \leq 1 \ ,$$

which proves that $\hat{\rho}$ is bounded. The importance of an operator being bounded can be illustrated by considering

$$\big|\big|\hat{A}(|v\rangle + |h\rangle) - \hat{A}\,|v\rangle\,\big|\big| = \big|\big|\hat{A}\,|h\rangle\,\big|\big| \ ,$$

if $\hat{A}$ is bounded Eq. (A.2) implies that

$$\big|\big|\hat{A}\,|h\rangle\,\big|\big| \leq M\big|\,|h\rangle\,\big| \ .$$

Therefore in the limit that $|h\rangle \to |0\rangle$:

$$\lim_{|h\rangle\to|0\rangle}\big|\big|\hat{A}(|v\rangle + |h\rangle) - \hat{A}\,|v\rangle\,\big|\big| = 0 \ ,$$

which means that $\hat{A}$ is continuous at $|v\rangle$. Therefore, one can see that boundedness of operators has important implications for defining continuity of operator action on the Hilbert space. Additionally, one can prove that the density operator is trace-class: An operator $\hat{A}$ is trace-class if

$$\mathrm{Tr}\left(\hat{A}^{\dagger}\hat{A}\right) \leq +\infty \ ,$$

which is clearly true for the density operator, since it is self-adjoint and has unit trace. Finally it is possible to show that the density operator is compact: A linear operator $\hat{A}$, acting on the Hilbert space $\mathcal{H}$, is compact if $\hat{A}$ is trace-class [15]. It is evident from the preceding discussion that $\hat{\rho}$ satisfies this requirement and is thus a compact operator. The fact that $\hat{\rho}$ is compact and trace-class is vital in guaranteeing that the trace $\mathrm{Tr}\left(\hat{\rho}\hat{Q}\right)$ is valid and finite for an arbitrary bounded operator $\hat{Q}$ [83, 84]. All of these properties have been proven here for the density operator of a pure state, however, it will seen later that these properties can be easily generalised to the density operators of mixed states.

Having established the properties of $\hat{\rho}$, we now consider the trace over $\hat{\rho}\hat{Q}$. As has been stated, this quantity is valid and finite provided the operator $\hat{Q}$ is bounded. The trace itself can then be evaluated

$$\mathrm{Tr}(\hat{\rho}\hat{Q}) = \langle\psi|\,\hat{Q}\,|\psi\rangle = \langle\hat{Q}\rangle \ .$$

Furthermore, if we take the trace of the density operator with some projector $\hat{\mathbb{P}}_i$, that is

$$\mathrm{Tr}(\hat{\rho}\hat{\mathbb{P}}_i) = \langle q_i|\ \psi\rangle\,\langle\psi|\ q_i\rangle = |c_i|^2 \ ,$$

then an alternative means of obtaining the probability distribution, $P_{Q,\psi}(a)$ can be found via this density operator

$$\mathrm{Tr}(\hat{\rho}\sum_{i,q_i\leq a}\hat{\mathbb{P}}_i) = \sum_{i,q_i\leq a}\langle q_i|\ \psi\rangle\,\langle\psi|\ q_i\rangle = \sum_{i,q_i\leq a}|c_i|^2 = P_{Q,\psi}(a) \ .$$

The structure of the density operator can be further analysed by employing the representation of the pure state $|\psi\rangle$ in the basis of the eigenstates $|q_i\rangle$

$$\hat{\rho} = \sum_i\sum_j c_i^* c_j\,|q_i\rangle\,\langle q_j| \ \ ,$$

which can be rewritten

$$\hat{\rho} = \sum_i |c_i|^2\,|q_i\rangle\,\langle q_i| + \sum_i\sum_{j,j\neq i} c_i c_j^*\,|q_i\rangle\,\langle q_j| \ \ .$$

In this the coefficients $|c_i|^2$ have already been shown to represent the probability of finding the system in the state indexed by i. However, the remaining terms of the density operator take the form of mixed projection operators $|q_i\rangle\,\langle q_j|$, with $i \neq j$. The operator $\hat{\rho}$ may then be represented as a matrix, with the rows and columns indexed by the vectors $|q_i\rangle$, such that the matrix element ρ_{ij} is given by

$$\rho_{ij} = \langle q_i|\,\hat{\rho}\,|q_j\rangle \ \ .$$

Then $|c_i|^2$ are the diagonal elements and $c_i c_j^*$ are the off-diagonal elements, often called *coherences*. Since the coefficients c_i are potentially complex, $c_i c_j^*$ are not guaranteed to be real and thus cannot constitute probabilities. Instead, they are representative of the correlations between the states labelled i and j [65]. These coherence terms demonstrate a difference between the pure state statistics and ensemble statistics of classical mechanics: such fundamental correlations between states do not occur in ensemble statistics, meaning that the pure state exhibits *quantum probabilities* rather than the classical variety [65]. This density operator constitutes a vehicle for calculating any quantum averages, or experimental observables, associated with a pure state system and is thus capable of describing a pure state completely [16, 17]. It will become evident, in the following section, that the density operator description can be extended even to systems whose state cannot be expressed as a pure state in some Hilbert space.

A.2 Mixed States and Density Operators

In quantum mechanics, a mixed state is defined to be one which cannot be described in terms of a single ray within a Hilbert space [15] or a state that cannot be described by a coherent superposition of pure states[16]. Systems for which this is true are the quantum analogy of classical systems that must be described in statistical terms, as it will turn out that their description is possible only in terms of an ensemble density operator [16, 17, 63, 65]. Such mixed state systems, since they cannot be expressed as a single vector pure state, can be described in terms of an ensemble of systems which can be measured to be in any one of a set of pure states $|i\rangle$ [16, 65]. Thus the density operator for such a system is the average of the density operators for each ensemble element. The summation in this average runs over all the ensemble elements $k \in [1, N]$, where there are N ensemble elements

$$\hat{\rho} = \frac{1}{N} \sum_{k}^{N} \hat{\rho}_k \ .$$

This can be converted to a sum over the set of pure states, $|i\rangle$, by including a factor d_i, the number of times each pure state, i, is measured in the ensemble. Thus

$$\hat{\rho} = \frac{1}{N} \sum_{i} d_i \hat{\mathbb{P}}_i \ .$$

From here on, the projectors $\hat{\mathbb{P}}_i$ are formulated in terms of the set of available pure states $\{|i\rangle\}$, such that $\hat{\mathbb{P}}_i = |i\rangle \langle i|$. Projectors onto other states will be written explicitly. The factor $\frac{d_i}{N}$ can be re-written as $p_i = \frac{d_i}{N}$, the classical probability of finding any system in the ensemble in the state $|i\rangle$. This allows the density operator to expressed in the form [15, 17]

$$\hat{\rho} = \sum_{i} p_i \hat{\mathbb{P}}_i \ ,$$

which is a weighted sum of the pure state density operators.

This density operator satisfies all the previously specified requirements, namely it is trace-class and compact, as it is the sum of trace-class, compact projectors. This follows from the fact that the proof of the pure state density operator being trace-class (and therefore compact) is clearly equivalent to proving a single projection operator is trace-class and compact. Additionally the mixed state density operator has unit trace

$$\mathrm{Tr}(\hat{\rho}) = \sum_{i} p_i \mathrm{Tr}(\hat{\mathbb{P}}_i) = \sum_{i} p_i = 1 \ .$$

It is also true that $\hat{\rho}$ is bounded as it is expressed as a linear combination of bounded projectors $\hat{\mathbb{P}}$, each with a real, finite coefficient p_i. It remains to demonstrate that a probability distribution for measurements on a mixed state can be derived from this density operator. First consider the average of an observable operator Q in the pure state case

$$\mathrm{Tr}(\hat{\rho}_p \hat{Q}) = \langle \hat{Q} \rangle \ ,$$

where $\hat{\rho}_p$ is the density operator of the pure case. So following the same pattern as the earlier derivation, consider

$$\mathrm{Tr}\left(\hat{\rho} \sum_{i, q_i \leq a} |q_i\rangle \langle q_i| \right) = \sum_{i, q_i \leq a} \langle q_i| \hat{\rho} |q_i\rangle \ ,$$

which is valid as $\hat{\rho}$ is trace-class. Including the form of $\hat{\rho}$ results in

$$\mathrm{Tr}\left(\hat{\rho} \sum_{i, q_i \leq a} |q_i\rangle \langle q_i| \right) = \sum_{j} \sum_{i, q_i \leq a} p_j \langle q_i| j\rangle \langle j| \hat{\rho} |j\rangle \langle j| q_i\rangle \ ,$$

and since

$$|j\rangle = \sum_{k} c_k^j |q_k\rangle \ ,$$

one obtains

$$\mathrm{Tr}\left(\hat{\rho}\sum_{i,q_i\leq a}|q_i\rangle\langle q_i|\right)=\sum_j\sum_{i,q_i\leq a}p_j|c_i^j|^2\ .$$

It is necessary now to show

$$\langle j|\ j\rangle=\sum_i\sum_k {c_k^j}^* c_i^j\langle q_i|\ q_k\rangle=\sum_i\sum_k {c_k^j}^* c_i^j\delta_{ik}=\sum_i {c_i^j}^* c_i^j=1\ ,$$

since the states $|q_i\rangle$ are orthonormal. Thus the probability distribution is given by

$$P_{Q,\psi}(a)=\mathrm{Tr}\left(\hat{\rho}\sum_{i,q_i\leq a}|q_i\rangle\langle q_i|\right)=\sum_j\sum_{i,q_i\leq a}p_j|c_i^j|^2\ ,$$

the validity of which is proven by first considering the normalisation

$$\sum_j\sum_i p_j|c_{ji}|^2=\sum_j p_j\sum_i|c_i^j|^2=\sum_j p_j=1\ .$$

With normalisation established it is simple to test the further requirements of probability theory

$$\begin{aligned}P_{Q,\psi}(+\infty)&=\sum_j p_j\sum_{i,q_i\leq+\infty}|c_i^j|^2=\sum_j p_j=1\ ,\\ P_{Q,\psi}(-\infty)&=\sum_j p_j\sum_{i,q_i\leq-\infty}|c_i^j|^2=0\ ,\\ \lim_{\delta\to0^+}P_{Q,\psi}(a+\delta)&=\lim_{\delta\to0^+}\sum_j p_j\sum_{i,q_i\leq a+\delta}|c_i^j|^2=P_{Q,\psi}(a)\ .\end{aligned}$$

Finally, P is monotonic non-decreasing because the terms $p_j|c_i^j|^2$ are necessarily real and positive-definite.

Therefore, the density operator still allows for the definition of a probability distribution for the measurement statistics of the observable $\hat{Q}$ on some mixed state system. This property preserves the equivalence of the trace over the product $\hat{\rho}\hat{Q}$ with the average of the observable Q, or

$$\mathrm{Tr}(\hat{\rho}\hat{Q})=\langle\hat{Q}\rangle\ .$$

Moreover, the density matrix for this system can be defined such that its elements ρ_{ij} are given by

$$\begin{aligned}\rho_{ij}&=\langle q_i|\,\hat{\rho}\,|q_j\rangle\ ,\\ &=\sum_k p_k\langle q_i|\ k\rangle\langle k|\ q_j\rangle\ ,\\ &=\sum_k p_k c_i^k {c_j^k}^*\ ,\\ &=\overline{c_i c_j^*}\ ,\end{aligned}$$

where $\overline{c_i c_j^*}=\sum_k p_k c_i^k {c_j^k}^*$, which is the ensemble average over the ij terms of all the pure state density matrices. Thus the density matrix still has the same form for a mixed state system and is functionally identical in terms of determining average properties. However, the terms of the matrix are dependent on classical ensemble probabilities. This means, that, unlike the pure case, the description of the system is not complete, the density operator can constitute, in classical terms, only a statistical description of the system.

In this case, there are two kinds of probability, the ensemble variety found in classical statistics, and the quantum variety, as exhibited in the case of the pure state system. These two kinds of probability are clearly distinct [65], as the quantum type possesses the correlations or coherences, while the classical type behaves as a simple ensemble frequency probability.

A.3 Time Evolution of the Density Operator

To determine the time evolution of the density operator an axiom of quantum mechanics must be considered first: if the system is described by a state vector $|\psi(t_0)\rangle$ at some time t_0, and is left to evolve without perturbation, then the state of the system at some time t, given by $|\psi(t)\rangle$, is entirely determined by the initial state [15]. Furthermore, it is required that the time evolution of the state is subject to a condition of strong continuity [15]

$$\lim_{dt\to 0} \big|\big|\, |\psi(t_0+dt)\rangle - |\psi(t_0)\rangle \,\big|\big| = 0\,.$$

Consequently, it must be true that

$$\big|\big|\, |\psi(t)\rangle \,\big|\big| = \big|\big|\, |\psi(t_0)\rangle \,\big|\big|\,,$$

provided the system is unperturbed during time evolution, with $\big|\big|\cdot\big|\big|$ constituting a norm within the Hilbert space of the system. This means that,

$$\big|\, \langle\psi(t)|\, \psi(t)\rangle \,\big| = \big|\, \langle\psi(t_0)|\, \psi(t_0)\rangle \,\big|\,.$$

Now a theorem of Wigner's must be invoked: "*Any bijection of rays in a Hilbert space conserving the absolute value of the scalar product can be implemented either as a linear, unitary operator, or, as an anti-linear, anti-unitary operator*" [69]. It is a clear consequence of this theorem, then, that

$$|\psi(t)\rangle = U(t,t_0)\,|\psi(t_0)\rangle\ ,$$

In order to preserve the inner-product norm, during time evolution

$$\langle\psi(t_0)|\, U^\dagger(t,t_0)U(t,t_0)\,|\psi(t_0)\rangle = \langle\psi(t_0)|\, \psi(t_0)\rangle\ ,$$

implying that $U(t,t_0)$ must be unitary. Additionally, it must be required, that, for such a system, starting at a time t_0 and evolving to a time t_1 is treated identically to evolving from t_1 to a later time t_2, or

$$\begin{aligned} |\psi(t_2)\rangle &= U(t_2,t_1)\,|\psi(t_1)\rangle\ ,\\ |\psi(t_2)\rangle &= U(t_2,t_1)U(t_1,t_0)\,|\psi(t_0)\rangle\ . \end{aligned}$$

This can be summarised by the general requirement that

$$U(t_2,t_0) = U(t_2,t_1)U(t_1,t_0)\,,$$

where $t_2 > t_1 > t_0$.

Consider now an isolated quantum system. The state of this system must be invariant under time translations, implying that the unitary operator $U(t,t_0)$ is identical to the time translation operator $U(t-t_0)$. Therefore, the time evolution of an isolated quantum system is generated by a set of strongly continuous, unitary operators $U(t)$, such that

$$|\psi(t)\rangle = U(t-t_0)\,|\psi(t_0)\rangle\ ,$$

where $t > t_0$.

Application of the Stone-von Neumann theorem [15, 85] would indicate that

$$U(t-t_0) = \mathrm{e}^{-\frac{i}{\hbar}(t-t_0)\hat{H}}\,,$$

where $\hat{H}$ is the Hamiltonian operator of the system. Then, taking the time derivative of

$$|\psi(t)\rangle = U(t-t_0)\,|\psi(t_0)\rangle\ ,$$

results in

$$\frac{d}{dt}\,|\psi(t)\rangle = -\frac{i}{\hbar}\hat{H}U(t-t_0)\,|\psi(t_0)\rangle\ .$$

This yields the Schrödinger equation

$$\frac{d}{dt}\left|\psi(t)\right\rangle = -\frac{i}{\hbar}\hat{H}\left|\psi(t)\right\rangle \ .$$

Now, consider the density operator $\hat{\rho}$

$$\begin{aligned}\hat{\rho}(t) &= \left|\psi(t)\right\rangle\left\langle\psi(t)\right| \\ &= U(t-t_0)\left|\psi(t_0)\right\rangle\left\langle\psi(t_0)\right|U^{\dagger}(t-t_0) \\ &= U(t-t_0)\hat{\rho}(t_0)U^{\dagger}(t-t_0)\,,\end{aligned}$$

where $\hat{\rho}(t_0) = \left|\psi(t_0)\right\rangle\left\langle\psi(t_0)\right|$. Then the average of some observable operator $\hat{A}$ is given by,

$$\langle\hat{A}\rangle = \mathrm{Tr}(\hat{\rho}(t)\hat{A})\,,$$

which is a feature of the Schrödinger picture, where operators are static in time and the state vector evolves. The time evolution of the density operator can be found by considering its definition

$$\begin{aligned}\frac{d}{dt}\hat{\rho}(t) &= \left(\frac{d}{dt}U(t-t_0)\right)\hat{\rho}(t_0)U^{\dagger}(t-t_0) + U(t-t_0)\hat{\rho}(t_0)\left(\frac{d}{dt}U^{\dagger}(t-t_0)\right) \\ &= -\frac{i}{\hbar}\hat{H}\hat{\rho}(t) + \frac{i}{\hbar}\hat{\rho}(t)\hat{H}\,,\end{aligned}$$

can be rewritten in terms of a quantum commutator

$$\frac{d}{dt}\hat{\rho}(t) = -\frac{i}{\hbar}[\hat{H},\hat{\rho}(t)]\,.$$

This result is known as the von Neumann equation or the quantum Liouville equation.

A.4 Derivations

A.4.1 Cyclic Invariance of the Trace

The trace of a bounded operator $\hat{A}$, as previously defined on the Hilbert space H, with basis $\left|e_i\right\rangle, i \in n$, is given by

$$\mathrm{Tr}(\hat{A}) = \sum_i \left\langle e_i\right|\hat{A}\left|e_i\right\rangle \ .$$

Therefore

$$\mathrm{Tr}(\hat{A}\hat{B}) = \sum_i \left\langle e_i\right|\hat{A}\hat{B}\left|e_i\right\rangle = \sum_i\sum_j \left\langle e_i\right|\hat{A}\left|e_j\right\rangle\left\langle e_j\right|\hat{B}\left|e_i\right\rangle \ ,$$

which can be re-arranged

$$\sum_i\sum_j \left\langle e_i\right|\hat{A}\left|e_j\right\rangle\left\langle e_j\right|\hat{B}\left|e_i\right\rangle = \sum_j\sum_i \left\langle e_j\right|\hat{B}\left|e_i\right\rangle\left\langle e_i\right|\hat{A}\left|e_j\right\rangle \ ,$$

and making use of the basis completeness

$$\sum_i\sum_j \left\langle e_i\right|\hat{A}\left|e_j\right\rangle\left\langle e_j\right|\hat{B}\left|e_i\right\rangle = \sum_j \left\langle e_j\right|\hat{B}\hat{A}\left|e_j\right\rangle = \mathrm{Tr}(\hat{B}\hat{A})\ .$$

This property holds true of Hilbert space operators: $\hat{A},\hat{B}$; provided they are compact and at least one of the operators is trace-class[15].

Appendix B

Additional Wigner Picture Material and Derivations

B.1 Wigner-Picture Averages

The relation

$$\mathrm{Tr}(\hat{A}\hat{B}) = \frac{1}{h^N}\int d\mathbf{X}\; A_W(\mathbf{X})B_W(\mathbf{X})\;,$$

can be proved by considering the definition of the Wigner transforms of these operators, namely

$$A_W(\mathbf{X}) = \int_{-\infty}^{\infty} d\mathbf{q}\; \mathrm{e}^{i\frac{\mathbf{P}}{\hbar}\cdot\mathbf{q}} \left\langle \mathbf{R} - \frac{\mathbf{q}}{2}\right| \hat{A} \left|\mathbf{R} + \frac{\mathbf{q}}{2}\right\rangle \;.$$

Substituting this into the relation for the trace, yields

$$\int d\mathbf{X}\; A_W(\mathbf{X})B_W(\mathbf{X}) = \int\int\int d\mathbf{X}\; d\mathbf{q}\; d\mathbf{s}\; \mathrm{e}^{i\frac{\mathbf{P}}{\hbar}\cdot\mathbf{q}} \left\langle \mathbf{R} - \frac{\mathbf{q}}{2}\right| \hat{A} \left|\mathbf{R} + \frac{\mathbf{q}}{2}\right\rangle \mathrm{e}^{i\frac{\mathbf{P}}{\hbar}\cdot\mathbf{s}} \left\langle \mathbf{R} - \frac{\mathbf{s}}{2}\right| \hat{B} \left|\mathbf{R} + \frac{\mathbf{s}}{2}\right\rangle \;,$$

since [21]

$$\int d\mathbf{P}\; \mathrm{e}^{i\frac{\mathbf{s}\cdot\mathbf{P}}{\hbar}} = h^N\delta(\mathbf{s})\;.$$

This relation is used to evaluate the $\mathbf{P}$ integral, which yields a delta function allowing for the evaluation of the integral in $\mathbf{s}$:

$$\int d\mathbf{X}\; A_W(\mathbf{X})B_W(\mathbf{X}) = h^N\int\int d\mathbf{R}\; d\mathbf{q}\; \left\langle \mathbf{R} - \frac{\mathbf{q}}{2}\right| \hat{A} \left|\mathbf{R} + \frac{\mathbf{q}}{2}\right\rangle \left\langle \mathbf{R} + \frac{\mathbf{q}}{2}\right| \hat{B} \left|\mathbf{R} - \frac{\mathbf{q}}{2}\right\rangle \;.$$

Introduce the variables $\mathbf{m} = \mathbf{R} - \frac{\mathbf{q}}{2}$ and $\mathbf{k} = \mathbf{R} + \frac{\mathbf{q}}{2}$, to obtain

$$\int d\mathbf{X}\; A_W(\mathbf{X})B_W(\mathbf{X}) = h^N\int\int d\mathbf{m}\; d\mathbf{k}\; \langle\mathbf{m}|\,\hat{A}\,|\mathbf{k}\rangle\,\langle\mathbf{k}|\,\hat{B}\,|\mathbf{m}\rangle \;.$$

The definition of the trace, in some suitably chosen basis, is given by [21]

$$\mathrm{Tr}(\hat{A}\hat{B}) = \int\int d\mathbf{m}\; d\mathbf{k}\; \langle\mathbf{m}|\,\hat{A}\,|\mathbf{k}\rangle\,\langle\mathbf{k}|\,\hat{B}\,|\mathbf{m}\rangle \;,$$

which proves the required result.

B.2 Wigner-Liouville Equation

Consider the Liouville equation

$$\frac{\partial}{\partial t}\hat{\rho} = \frac{i}{\hbar}[\hat{\rho}, \hat{H}]\;.$$

For convenience, the time-dependence of the density operator will be suppressed for the remainder of this derivation. Consider a closed quantum system with position-like degrees of freedom $\hat{\mathbf{r}}$ and their conjugate degrees of freedom $\hat{\mathbf{p}}$. For a Hamiltonian assumed to be of the form

$$\hat{H} = \frac{\hat{\mathbf{p}}^2}{2m} + V(\hat{\mathbf{r}}) \, ,$$

the Liouville equation can be re-cast in the basis of the position eigenstates $|\mathbf{r}\rangle$

$$\frac{\partial}{\partial t} \langle \mathbf{r}| \, \hat{\rho} \, |\mathbf{r}'\rangle = \frac{i}{\hbar} \langle \mathbf{r}| \left(\hat{\rho}\hat{H} - \hat{H}\hat{\rho} \right) |\mathbf{r}'\rangle \ .$$

Invoking the completeness of the position eigenstates allows the right-hand side of the previous equation to be expanded into the form

$$\langle \mathbf{r}| \left(\hat{\rho}\hat{H} - \hat{H}\hat{\rho} \right) |\mathbf{r}'\rangle = \int_{-\infty}^{\infty} d\mathbf{r}'' \ \langle \mathbf{r}| \, \hat{\rho} \, |\mathbf{r}''\rangle \langle \mathbf{r}''| \, \hat{H} \, |\mathbf{r}'\rangle - \langle \mathbf{r}| \, \hat{H} \, |\mathbf{r}''\rangle \langle \mathbf{r}''| \, \hat{\rho} \, |\mathbf{r}'\rangle \ .$$

The position-represented Hamiltonian now appears as [63]

$$\begin{aligned} \langle \mathbf{r}''| \, \hat{H} \, |\mathbf{r}'\rangle &= \langle \mathbf{r}''| \, \frac{\hat{\mathbf{p}}^2}{2m} + \hat{V} \, |\mathbf{r}'\rangle \\ &= -\frac{\hbar^2}{2m} \frac{\partial^2}{\partial \mathbf{r}''^2} \delta(\mathbf{r}' - \mathbf{r}'') + V(\mathbf{r}'')\delta(\mathbf{r}' - \mathbf{r}'') \, , \end{aligned}$$

which can be used to simplify the position-represented form of the commutator

$$\langle \mathbf{r}| \, [\hat{\rho}, \hat{H}] \, |\mathbf{r}'\rangle = \int_{-\infty}^{\infty} d\mathbf{r}'' \ \left[\rho(\mathbf{r}, \mathbf{r}'') \left(-\frac{\hbar^2}{2m} \frac{\partial^2}{\partial \mathbf{r}''^2} + V(\mathbf{r}'') \right) \delta(\mathbf{r}' - \mathbf{r}'') - \left(-\frac{\hbar^2}{2m} \frac{\partial^2}{\partial \mathbf{r}''^2} + V(\mathbf{r}'') \right) \delta(\mathbf{r} - \mathbf{r}'')\rho(\mathbf{r}'', \mathbf{r}') \right] \ .$$

Performing integration by parts twice and employing the properties of the dirac delta function yield

$$\begin{aligned} \langle \mathbf{r}| \, [\hat{\rho}, \hat{H}] \, |\mathbf{r}'\rangle = \int_{-\infty}^{\infty} d\mathbf{r}'' \ & \left[\left(-\frac{\hbar^2}{2m} \frac{\partial^2}{\partial \mathbf{r}''^2} \rho(\mathbf{r}, \mathbf{r}'') + V(\mathbf{r}'')\rho(\mathbf{r}, \mathbf{r}'') \right) \delta(\mathbf{r}' - \mathbf{r}'') \right. \\ & \left. + \left(\frac{\hbar^2}{2m} \frac{\partial^2}{\partial \mathbf{r}''^2} \rho(\mathbf{r}'', \mathbf{r}') - V(\mathbf{r}'')\rho(\mathbf{r}'', \mathbf{r}') \right) \delta(\mathbf{r} - \mathbf{r}'') \right] \\ = & -\frac{\hbar^2}{2m} \frac{\partial^2}{\partial \mathbf{r}'^2} \rho(\mathbf{r}, \mathbf{r}') + V(\mathbf{r}')\rho(\mathbf{r}, \mathbf{r}') + \frac{\hbar^2}{2m} \frac{\partial^2}{\partial \mathbf{r}^2} \rho(\mathbf{r}, \mathbf{r}') - V(\mathbf{r})\rho(\mathbf{r}, \mathbf{r}') \\ = & \frac{\hbar^2}{2m} \left(\frac{\partial^2}{\partial \mathbf{r}^2} - \frac{\partial^2}{\partial \mathbf{r}'^2} \right) \rho(\mathbf{r}, \mathbf{r}') + \left(V(\mathbf{r}') - V(\mathbf{r}) \right) \rho(\mathbf{r}, \mathbf{r}') \, . \end{aligned}$$

Thus the position-represented Liouville equation has the form

$$\frac{\partial}{\partial t} \rho(\mathbf{r}, \mathbf{r}') = \frac{i\hbar}{2m} \left(\frac{\partial^2}{\partial \mathbf{r}^2} - \frac{\partial^2}{\partial \mathbf{r}'^2} \right) \rho(\mathbf{r}, \mathbf{r}') + \frac{i}{\hbar} \left(V(\mathbf{r}') - V(\mathbf{r}) \right) \rho(\mathbf{r}, \mathbf{r}') \, .$$

It becomes useful now to consider the change of coordinates

$$\begin{aligned} \mathbf{r} &= \mathbf{R} - \frac{\mathbf{q}}{2} \, , \\ \mathbf{r}' &= \mathbf{R} + \frac{\mathbf{q}}{2} \, , \end{aligned} \tag{B.1}$$

which results in the transformation of the differential operators

$$\begin{aligned} \frac{\partial}{\partial \mathbf{r}} &= -\frac{\partial}{\partial \mathbf{q}} + \frac{1}{2} \frac{\partial}{\partial \mathbf{R}} \ \text{ and } \ \frac{\partial^2}{\partial \mathbf{r}^2} = \frac{\partial^2}{\partial \mathbf{q}^2} - \frac{\partial^2}{\partial \mathbf{R} \partial \mathbf{q}} + \frac{1}{4} \frac{\partial^2}{\partial \mathbf{R}^2} \, , \\ \frac{\partial}{\partial \mathbf{r}'} &= \frac{\partial}{\partial \mathbf{q}} + \frac{1}{2} \frac{\partial}{\partial \mathbf{R}} \ \text{ and } \ \frac{\partial^2}{\partial \mathbf{r}'^2} = \frac{\partial^2}{\partial \mathbf{q}^2} + \frac{\partial^2}{\partial \mathbf{R} \partial \mathbf{q}} + \frac{1}{4} \frac{\partial^2}{\partial \mathbf{R}^2} \, . \end{aligned}$$

Applying this change of coordinates to the Liouville equation yields

$$\begin{aligned}\frac{\partial}{\partial t}\rho\left(\mathbf{R}-\frac{\mathbf{q}}{2},\mathbf{R}+\frac{\mathbf{q}}{2}\right) = &-\frac{i\hbar}{2m}\frac{\partial^2}{\partial\mathbf{R}\partial\mathbf{q}}\rho\left(\mathbf{R}-\frac{\mathbf{q}}{2},\mathbf{R}+\frac{\mathbf{q}}{2}\right)\\ &-\frac{i}{\hbar}\left(V\left(\mathbf{R}-\frac{\mathbf{q}}{2}\right)-V\left(\mathbf{R}+\frac{\mathbf{q}}{2}\right)\right)\rho\left(\mathbf{R}-\frac{\mathbf{q}}{2},\mathbf{R}+\frac{\mathbf{q}}{2}\right)\ .\end{aligned} \tag{B.2}$$

Now consider the Fourier transform of the first term in Eq. (B.2)

$$\mathcal{F}\left(-\frac{i\hbar}{2m}\frac{\partial^2}{\partial\mathbf{R}\partial\mathbf{q}}\rho\left(\mathbf{R}-\frac{\mathbf{q}}{2},\mathbf{R}+\frac{\mathbf{q}}{2}\right)\right) = -\frac{i\hbar}{2m}\int_{-\infty}^{\infty}d\mathbf{q}\ \mathrm{e}^{\frac{i}{\hbar}\mathbf{P}\cdot\mathbf{q}}\frac{\partial^2}{\partial\mathbf{R}\partial\mathbf{q}}\rho\left(\mathbf{R}-\frac{\mathbf{q}}{2},\mathbf{R}+\frac{\mathbf{q}}{2}\right)\ .$$

Here it is understood that $d\mathbf{q} = dq_1dq_2dq_3\ldots dq_N$. Integrating by parts, with the assumption that ρ vanishes on the bounds of the integral, results in

$$\begin{aligned}\mathcal{F}\left(-\frac{i\hbar}{2m}\frac{\partial^2}{\partial\mathbf{R}\partial\mathbf{q}}\rho\left(\mathbf{R}-\frac{\mathbf{q}}{2},\mathbf{R}+\frac{\mathbf{q}}{2}\right)\right) &= -\frac{i\hbar}{2m}\frac{\partial}{\partial\mathbf{R}}\int_{-\infty}^{\infty}d\mathbf{q}\ \mathrm{e}^{\frac{i}{\hbar}\mathbf{P}\cdot\mathbf{q}}\left(-\frac{i\mathbf{P}}{\hbar}\right)\rho\left(\mathbf{R}-\frac{\mathbf{q}}{2},\mathbf{R}+\frac{\mathbf{q}}{2}\right)\\ &= -\frac{\mathbf{P}}{m}\frac{\partial}{\partial\mathbf{R}}\mathcal{W}(\hat{\rho})\ ,\end{aligned}$$

where $\mathcal{W}(\hat{\rho})$ is called the Wigner transform of the operator $\hat{\rho}$ and is defined by [18, 21]

$$\begin{aligned}\mathcal{W}(\hat{\rho}) &= \int_{-\infty}^{\infty}d\mathbf{q}\ \mathrm{e}^{\frac{i}{\hbar}\mathbf{P}\cdot\mathbf{q}}\rho\left(\mathbf{R}-\frac{\mathbf{q}}{2},\mathbf{R}+\frac{\mathbf{q}}{2}\right)\\ &= \int_{-\infty}^{\infty}d\mathbf{q}\ \mathrm{e}^{\frac{i}{\hbar}\mathbf{P}\cdot\mathbf{q}}\left\langle\mathbf{R}-\frac{\mathbf{q}}{2}\right|\hat{\rho}\left|\mathbf{R}+\frac{\mathbf{q}}{2}\right\rangle\ .\end{aligned} \tag{B.3}$$

Here the states $|\mathbf{R}\rangle$ are evidently still states of definite position.

The remaining term in Eq. (B.2) can be simplified by first making Taylor expansions of the two potential functions

$$V\left(\mathbf{R}-\frac{\mathbf{q}}{2}\right)-V\left(\mathbf{R}+\frac{\mathbf{q}}{2}\right) = -2\sum_{n=1,3,5,\cdots}\frac{1}{n!}\left(\frac{\mathbf{q}}{2}\right)^n\frac{\partial^nV(\mathbf{R})}{\partial\mathbf{R}^n}\ ,$$

which requires that the potential be continuous, with this in mind, all analysis presented in this thesis was performed on systems with continuous potentials.

Then the Fourier transform of the second term in Eq. (B.2) can be evaluated

$$\begin{aligned}&-\frac{i}{\hbar}\mathcal{F}\left(V\left(\mathbf{R}-\frac{\mathbf{q}}{2}\right)-V\left(\mathbf{R}+\frac{\mathbf{q}}{2}\right)\rho\left(\mathbf{R}-\frac{\mathbf{q}}{2},\mathbf{R}+\frac{\mathbf{q}}{2}\right)\right)\\ &\quad= \frac{2i}{\hbar}\sum_{n=1,3,5,\cdots}\frac{1}{n!}\frac{\partial^nV(\mathbf{R})}{\partial\mathbf{R}^n}\int_{-\infty}^{\infty}d\mathbf{q}\ \left(\frac{\mathbf{q}}{2}\right)^n\mathrm{e}^{\frac{i}{\hbar}\mathbf{P}\cdot\mathbf{q}}\rho\left(\mathbf{R}-\frac{\mathbf{q}}{2},\mathbf{R}+\frac{\mathbf{q}}{2}\right)\ ,\end{aligned}$$

which can then be re-arranged so that

$$\begin{aligned}&\frac{2i}{\hbar}\sum_{n=1,3,5,\cdots}\frac{1}{n!}\frac{\partial^nV(\mathbf{R})}{\partial\mathbf{R}^n}\int_{-\infty}^{\infty}dq^N\ \left(\frac{\mathbf{q}}{2}\right)^n\mathrm{e}^{\frac{i}{\hbar}\mathbf{P}\cdot\mathbf{q}}\rho\left(\mathbf{R}-\frac{\mathbf{q}}{2},\mathbf{R}+\frac{\mathbf{q}}{2}\right)\\ &= \frac{2i}{\hbar}\sum_{n=1,3,5,\cdots}\frac{1}{n!}\frac{\partial^nV(\mathbf{R})}{\partial\mathbf{R}^n}\int_{-\infty}^{\infty}d\mathbf{q}\ \left(\frac{\hbar}{2i}\right)^n\frac{\partial^n}{\partial\mathbf{P}^n}\mathrm{e}^{\frac{i}{\hbar}\mathbf{P}\cdot\mathbf{q}}\rho\left(\mathbf{R}-\frac{\mathbf{q}}{2},\mathbf{R}+\frac{\mathbf{q}}{2}\right)\\ &= \sum_{n=1,3,5,\cdots}\frac{1}{n!}\left(\frac{\hbar}{2i}\right)^{n-1}\frac{\partial^nV(\mathbf{R})}{\partial\mathbf{R}^n}\frac{\partial^n\mathcal{W}(\hat{\rho})}{\partial\mathbf{P}^n}\ .\end{aligned}$$

Recombining the two Fourier transformed terms yields

$$\frac{\partial}{\partial t}\mathcal{W}(\hat{\rho}) = -\frac{\mathbf{P}}{m}\frac{\partial}{\partial\mathbf{R}}\mathcal{W}(\hat{\rho})+\sum_{n=1,3,5,\cdots}\frac{1}{n!}\left(\frac{\hbar}{2i}\right)^{n-1}\frac{\partial^nV(\mathbf{R})}{\partial\mathbf{R}^n}\frac{\partial^n\mathcal{W}(\hat{\rho})}{\partial\mathbf{P}^n}\ ,$$

which is the Wigner-Liouville equation for the case of a continuous potential $V(\mathbf{r})$

It might be noted that there is nothing in this derivation that uniquely employs the properties of the density operator $\hat{\rho}$. Thus an analogous evolution equation might be defined for any operator $\hat{A}$ in which it is transformed according to

$$\begin{aligned}\mathcal{W}(\hat{A}) &= \int_{-\infty}^{\infty} d\mathbf{q}\, \mathrm{e}^{\frac{i}{\hbar}\mathbf{P}\cdot\mathbf{q}} A\left(\mathbf{R}-\frac{\mathbf{q}}{2},\mathbf{R}+\frac{\mathbf{q}}{2}\right) \\ &= \int_{-\infty}^{\infty} d\mathbf{q}\, \mathrm{e}^{\frac{i}{\hbar}\mathbf{P}\cdot\mathbf{q}} \left\langle \mathbf{R}-\frac{\mathbf{q}}{2}\right| \hat{A} \left|\mathbf{R}+\frac{\mathbf{q}}{2}\right\rangle \ .\end{aligned}$$

This means that the Wigner-Liouville equation can be rewritten in the form

$$\frac{\partial}{\partial t}W(\mathbf{X},t) = -\frac{\mathbf{P}}{m}\frac{\partial}{\partial \mathbf{R}}W(\mathbf{X},t) + \sum_{n=1,3,5,\cdots}\frac{1}{n!}\left(\frac{\hbar}{2i}\right)^{n-1}\frac{\partial^n V(\mathbf{R})}{\partial \mathbf{R}^n}\frac{\partial^n W(\mathbf{X},t)}{\partial \mathbf{P}^n} \ ,$$

where $\mathbf{X} = (R_1, P_1, \ldots, R_N, P_N)$. Additionally, the symbol W is defined by

$$W(\mathbf{X},t) = \frac{1}{h^N}\mathcal{W}(\hat{\rho}(t)) \ , \tag{B.4}$$

which is the Wigner-transformed density operator and is known as the Wigner function.

B.3 Moyal Bracket

Consider the Wigner-Liouville equation:

$$\frac{\partial}{\partial t}W(\mathbf{X},t) = \frac{\partial H_W(\mathbf{X})}{\partial \mathbf{R}}\frac{\partial W(\mathbf{X},t)}{\partial \mathbf{P}} - \frac{\partial H_W(\mathbf{X})}{\partial \mathbf{P}}\frac{\partial W(\mathbf{X},t)}{\partial \mathbf{R}} + \sum_{n=3,5,\cdots}\frac{1}{n!}\left(\frac{\hbar}{2i}\right)^{n-1}\frac{\partial^n H_W(\mathbf{X})}{\partial \mathbf{R}^n}\frac{\partial^n W(\mathbf{X},t)}{\partial \mathbf{P}^n} \ . \tag{B.5}$$

Given that the Hamiltonian has the same form as used in Eq. (2.3), the right-hand side of Eq. (B.5) can be completely incorporated into the summation

$$\begin{aligned}&\{H_W(\mathbf{X}), W(\mathbf{X},t)\} + \sum_{n=3,5,\cdots}\frac{1}{n!}\left(\frac{\hbar}{2i}\right)^{n-1}\frac{\partial^n H_W(\mathbf{X})}{\partial \mathbf{R}^n}\frac{\partial^n W(\mathbf{X},t)}{\partial \mathbf{P}^n} \\ &= \sum_{n=1,3,5,\cdots}\frac{1}{n!}\left(\frac{\hbar}{2i}\right)^{n-1}\left(\frac{\partial^n H_W}{\partial \mathbf{R}^n}\frac{\partial^n W}{\partial \mathbf{P}^n} - \frac{\partial^n H_W}{\partial \mathbf{P}^n}\frac{\partial^n W}{\partial \mathbf{R}^n}\right) \\ &= \sum_{n=1,3,5,\cdots}\frac{1}{n!}\left(\frac{\hbar}{2i}\right)^{n-1} H_W\left(\frac{\overleftarrow{\partial^n}}{\partial \mathbf{R}^n}\frac{\overrightarrow{\partial^n}}{\partial \mathbf{P}^n} - \frac{\overleftarrow{\partial^n}}{\partial \mathbf{P}^n}\frac{\overrightarrow{\partial^n}}{\partial \mathbf{R}^n}\right) W \ ,\end{aligned}$$

where an arrows indicates the direction in which the derivative acts.

Consider, now, the terms

$$\begin{aligned}H_W\left(\frac{\overleftarrow{\partial}}{\partial \mathbf{R}}\frac{\overrightarrow{\partial}}{\partial \mathbf{P}} - \frac{\overleftarrow{\partial}}{\partial \mathbf{P}}\frac{\overrightarrow{\partial}}{\partial \mathbf{R}}\right) W &= H_W\left(\frac{\overleftarrow{\partial}}{\partial \mathbf{R}}\frac{\overrightarrow{\partial}}{\partial \mathbf{P}} - \frac{\overleftarrow{\partial}}{\partial \mathbf{P}}\frac{\overrightarrow{\partial}}{\partial \mathbf{R}}\right) W \ , \\ H_W\left(\frac{\overleftarrow{\partial}}{\partial \mathbf{R}}\frac{\overrightarrow{\partial}}{\partial \mathbf{P}} - \frac{\overleftarrow{\partial}}{\partial \mathbf{P}}\frac{\overrightarrow{\partial}}{\partial \mathbf{R}}\right)^2 W &= H_W\left(\frac{\overleftarrow{\partial^2}}{\partial \mathbf{R}^2}\frac{\overrightarrow{\partial^2}}{\partial \mathbf{P}^2} + \frac{\overleftarrow{\partial^2}}{\partial \mathbf{P}^2}\frac{\overrightarrow{\partial^2}}{\partial \mathbf{R}^2} - 2\frac{\overleftarrow{\partial}^2}{\partial \mathbf{R}\partial \mathbf{P}}\frac{\overrightarrow{\partial}^2}{\partial \mathbf{R}\partial \mathbf{P}}\right) W \ , \\ H_W\left(\frac{\overleftarrow{\partial}}{\partial \mathbf{R}}\frac{\overrightarrow{\partial}}{\partial \mathbf{P}} - \frac{\overleftarrow{\partial}}{\partial \mathbf{P}}\frac{\overrightarrow{\partial}}{\partial \mathbf{R}}\right)^3 W &= H_W\left(\frac{\overleftarrow{\partial^3}}{\partial \mathbf{R}^3}\frac{\overrightarrow{\partial^3}}{\partial \mathbf{P}^3} - \frac{\overleftarrow{\partial^3}}{\partial \mathbf{P}^3}\frac{\overrightarrow{\partial^3}}{\partial \mathbf{R}^3}\right) W \\ &\quad - 3H_W\left(\frac{\overleftarrow{\partial}^3}{\partial \mathbf{R}^2\partial \mathbf{P}}\frac{\overrightarrow{\partial}^3}{\partial \mathbf{R}\partial \mathbf{P}^2} + 3\frac{\overleftarrow{\partial}^3}{\partial \mathbf{R}\partial \mathbf{P}^2}\frac{\overrightarrow{\partial}^3}{\partial \mathbf{R}^2\partial \mathbf{P}}\right) W \ .\end{aligned}$$

The form of the Hamiltonian also allows for the following simplification

$$H_W\left(\frac{\overleftarrow{\partial}}{\partial\mathbf{R}}\frac{\overrightarrow{\partial}}{\partial\mathbf{P}}-\frac{\overleftarrow{\partial}}{\partial\mathbf{P}}\frac{\overrightarrow{\partial}}{\partial\mathbf{R}}\right)^n W = H_W\left(\frac{\overleftarrow{\partial^n}}{\partial\mathbf{R}^n}\frac{\overrightarrow{\partial^n}}{\partial\mathbf{P}^n}+(-1)^n\frac{\overleftarrow{\partial^n}}{\partial\mathbf{P}^n}\frac{\overrightarrow{\partial^n}}{\partial\mathbf{R}^n}\right)W\ , \tag{B.6}$$

since

$$\frac{\partial^n}{\partial\mathbf{R}^k\partial\mathbf{P}^{n-k}}H_W = 0\ \ \{k>0\ \ ,\forall\, n\}\ .$$

This simplification allows for the expression

$$\begin{aligned}\sum_{n=1,3,5,\cdots}H_W\left(\frac{\overleftarrow{\partial^n}}{\partial\mathbf{R}^n}\frac{\overrightarrow{\partial^n}}{\partial\mathbf{P}^n}-\frac{\overleftarrow{\partial^n}}{\partial\mathbf{P}^n}\frac{\overrightarrow{\partial^n}}{\partial\mathbf{R}^n}\right)W &= \sum_{n=1,3,5,\cdots}\frac{1}{n!}\left(\frac{\hbar}{2i}\right)^{n-1}H_W\left(\frac{\overleftarrow{\partial}}{\partial\mathbf{R}}\frac{\overrightarrow{\partial}}{\partial\mathbf{P}}-\frac{\overleftarrow{\partial}}{\partial\mathbf{P}}\frac{\overrightarrow{\partial}}{\partial\mathbf{R}}\right)^n W \\ &= \frac{2}{\hbar}H_W\sin\left(\frac{\hbar}{2}\Lambda\right)W\end{aligned}\ . \tag{B.7}$$

Here the symbol Λ is defined

$$\Lambda = \frac{\overleftarrow{\partial}}{\partial\mathbf{R}}\frac{\overrightarrow{\partial}}{\partial\mathbf{P}}-\frac{\overleftarrow{\partial}}{\partial\mathbf{P}}\frac{\overrightarrow{\partial}}{\partial\mathbf{R}}\ .$$

One can now make use of the fact that

$$2i\sin(x) = \mathrm{e}^{ix}-\mathrm{e}^{-ix}\ ,$$

to write

$$\frac{2}{\hbar}H_W\sin\left(\frac{\hbar}{2}\Lambda\right)W = \frac{1}{i\hbar}\left(H_W\mathrm{e}^{\frac{i\hbar}{2}\Lambda}W - H_W\mathrm{e}^{-\frac{i\hbar}{2}\Lambda}W\right)\ .$$

As H_W and W are functions of the Wigner phase space, they commute under simple multiplication, meaning that

$$H_W\mathrm{e}^{-\frac{i\hbar}{2}\Lambda}W = W\mathrm{e}^{\frac{i\hbar}{2}\Lambda}H_W\ .$$

Therefore, the Wigner Liouville equation can be expressed in the following form

$$\frac{\partial}{\partial t}W(\mathbf{X},t) = -\frac{i}{\hbar}\left(H_W\mathrm{e}^{\frac{i\hbar}{2}\Lambda}W(\mathbf{X},t) - W(\mathbf{X},t)\mathrm{e}^{\frac{i\hbar}{2}\Lambda}H_W\right)\ .$$

The Moyal Bracket is then defined by [68]

$$(A,B)_M = \frac{1}{i\hbar}\left(A\,\mathrm{e}^{\frac{i\hbar}{2}\Lambda}B - B\,\mathrm{e}^{\frac{i\hbar}{2}\Lambda}A\right)\ ,$$

where A and B are assumed to be functions of the phase space.

B.4 Partial Wigner Picture Averages

Let $\hat{A} = F(\hat{\mathbf{X}})\otimes G(\hat{s})$ and $\hat{B} = Q(\hat{\mathbf{X}})\otimes K(\hat{s})$,

$$\mathrm{Tr}(\hat{A}\hat{B}) = \mathrm{Tr}_s\mathrm{Tr}_x(F(\hat{\mathbf{X}})\otimes G(\hat{s})\cdot Q(\hat{\mathbf{X}})\otimes K(\hat{s}))\ .$$

Since the operators $\hat{\mathbf{X}}$ and $\hat{s}$ act only on their respective subsystems

$$\mathrm{Tr}_s\mathrm{Tr}_x(F(\hat{\mathbf{X}})\otimes G(\hat{s})\cdot Q(\hat{\mathbf{X}})\otimes K(\hat{s})) = \mathrm{Tr}_s\left(G(\hat{s})K(\hat{s})\otimes\mathrm{Tr}_x\left(F(\hat{\mathbf{X}})Q(\hat{\mathbf{X}})\right)\right)\ .$$

Making use of Eq. (2.2) yields the result

$$\mathrm{Tr}(\hat{A}\hat{B}) = \mathrm{Tr}_s\left(G(\hat{s})K(\hat{s})\otimes\frac{1}{h^N}\int d\mathbf{X}\ F_W(\mathbf{X})Q_W(\mathbf{X})\right)\ ,$$

because the $\hat{s}$ degrees of freedom are not affected by the Wigner transform,

$$\mathrm{Tr}_s\left(G(\hat{s})K(\hat{s})\otimes\frac{1}{h^N}\int d\mathbf{X}\;F_W(\mathbf{X})Q_W(\mathbf{X})\right)=\mathrm{Tr}_s\left(\frac{1}{h^N}\int d\mathbf{X}\;F_W(\mathbf{X})\otimes G(\hat{s})\cdot Q_W(\mathbf{X})\otimes K(\hat{s})\right)\;.$$

Here, $F_W(\mathbf{X})G(\hat{s})$ is just $\hat{A}_w(\mathbf{X})$, the partial Wigner transformed operator, which means

$$\mathrm{Tr}(\hat{A}\hat{B})=\mathrm{Tr}_s\left(\frac{1}{h^N}\int d\mathbf{X}\;\hat{A}_w(\mathbf{X})\hat{B}_w(\mathbf{X})\right)\;,$$

as required. In general, then, it is evident that the trace over a partial Wigner-transformed operator consists of an integral over the Wigner-transformed degrees of freedom that parameterise it, as well as a trace over the untransformed degrees of freedom.

This result for the trace of an operator product allows the average of an observable operator $\hat{A}$ in the partial Wigner picture, to be expressed in the form

$$\langle\hat{A}(t)\rangle=\mathrm{Tr}(\hat{\rho}(t)\hat{A})=\mathrm{Tr}_s\left(\frac{1}{h^N}\int d\mathbf{X}\;\hat{\rho}_w(\mathbf{X},t)\hat{A}_w(\mathbf{X})\right)\;.$$

Appendix C

Numerical Methods Derivations and Proofs

C.1 Runge-Kutta 4

Given the problem

$$\frac{d}{dt}y(t) = F(y(t), t) \ ,$$

the solution might be formally expressed as

$$y(t+dt) = y(t) + \int_t^{t+dt} d\tau \ F(y(\tau), \tau) \ .$$

Applying Simpson's rule, Eq. (C.4), to this expression yields

$$y(t+dt) = y(t) + \frac{dt}{6}\left(F(y(t),t) + 4F\left(y\left(t+\frac{dt}{2}\right), t+\frac{dt}{2}\right) + F(y(t+dt), t+dt)\right) + \mathcal{O}(dt^5) \ . \tag{C.1}$$

This new approximation has the clear disadvantage that one must know $y(t+dt/2)$ and $y(t+dt)$ to find $y(t+dt)$. In order to alleviate this difficulty, these two quantities can be replaced by further approximations. At this point there are many possible ways in which these approximations might be made. However, this choice must be informed by the objective of obtaining a final approximation with local error $\mathcal{O}(dt^5)$. In order to ensure this requirement is met, the final approximation must be equivalent to the Taylor expansion

$$y(t+dt) = y(t) + dtF(y(t),t) + \frac{dt^2}{2}\frac{d}{dt}F(y(t),t) + \frac{dt^3}{6}\frac{d^2}{dt^2}F(y(t),t) + \frac{dt^4}{24}\frac{d^3}{dt^3}F(y(t),t) + \mathcal{O}(dt^5) \ .$$

However, this Taylor expansion contains five terms and our Simpson's rule solution possesses only four terms, this difficulty can be surmounted if one replaces the term $F(y(t+\frac{dt}{2}), t+\frac{dt}{2})$ by a weighted combination of two approximations:

$$F\left(y\left(t+\frac{dt}{2}\right), t+\frac{dt}{2}\right) \approx ak_2 + bk_3 \ ,$$

where

$$\begin{aligned} a+b &= 1 \ , \\ k_2 &\approx F\left(y\left(t+\frac{dt}{2}\right), t+\frac{dt}{2}\right) \ , \\ k_3 &\approx F\left(y\left(t+\frac{dt}{2}\right), t+\frac{dt}{2}\right) \ . \end{aligned}$$

In order to match the form of the Taylor expansion, consider

$$k_2 = F\left(y(t) + \frac{dt}{2}F(y,t), t + \frac{dt}{2}\right) = F(y(t),t) + \frac{dt}{2}\frac{d}{dt}F(y(t),t) + \mathcal{O}(dt^2) \; .$$

This form of k_2 is promising: therefore consider

$$k_3 = F\left(y(t) + \frac{dt}{2}k_2, t + \frac{dt}{2}\right) = F(y(t),t) + \frac{dt}{2}\frac{d}{dt}F(y(t),t) + \frac{dt^2}{4}\frac{d^2}{dt^2}F(y(t),t) + \mathcal{O}(dt^3) \; .$$

All that remains then is to approximate $F(y(t+dt), t+dt)$ in a form that might account for the $\mathcal{O}(dt^4)$ term of the Taylor expansion. Following on from the previous two approximations one takes

$$F(y(t+dt),t+dt) \approx F(y(t)+dtk_3, t+dt) = F(y(t),t)+dt\frac{d}{dt}F(y(t),t)+\frac{dt^2}{2}\frac{d^2}{dt^2}F(y(t),t)+\frac{dt^3}{4}\frac{d^3}{dt^3}F(y(t),t)+\mathcal{O}(dt^4) \; .$$

This set of approximations allows Eq. (C.1) to be written as

$$y(t+dt) \approx y(t)+\frac{dt}{6}(2+4a+4b)F(y(t),t)+\frac{dt^2}{6}(1+2a+2b)\frac{d}{dt}F(y(t),t)+\frac{dt^3}{6}\left(\frac{1}{2}+b\right)\frac{d^2}{dt^2}F(y(t),t)+\frac{dt^4}{24}\frac{d^3}{dt^3}F(y(t),t) \; . \tag{C.2}$$

In order for this approximation to have a local error of $\mathcal{O}(dt^5)$, the following equations must then be satisfied

$$\begin{aligned} 2 + 4a + 4b &= 6 \; , \\ 1 + 2a + 2b &= 3 \; , \\ \frac{1}{2} + b &= 1 \; , \\ a + b &= 1 \; . \end{aligned}$$

These equations have the simple solution

$$a = b = \frac{1}{2} \; .$$

Therefore, the full approximation may be written as

$$y(t+dt) = y(t) + \frac{dt}{6}\left(k_1 + 2k_2 + 2k_3 + k_4\right) + \mathcal{O}(dt^5) \; , \tag{C.3}$$

where

$$\begin{aligned} k_1 &= dtF(y,t) \; , \\ k_2 &= dtF\left(y + \frac{1}{2}k_1, t + \frac{1}{2}dt\right) \; , \\ k_3 &= dtF\left(y + \frac{1}{2}k_2, t + \frac{1}{2}dt\right) \; , \\ k_4 &= dtF(y + k_3, t + dt) \; . \end{aligned}$$

If this method is repeated making N steps of size dt over some interval, then

$$N \propto \frac{1}{dt} \; .$$

However, the global error E_g is equal to NE, where E is the local error per step. Therefore,

$$E_g \propto \mathcal{O}(dt^4) \; .$$

C.2 Simpson's Rule

Consider an interval defined by the points t_0, t_1 and t_2, such that $t_1 = t_0 + dt$ and $t_2 = t_1 + dt$. The quantity dt is a finite real constant. A smooth, continuous, function $f(t)$ has the values $f_0 = f(t_0)$, $f_1 = f(t_1)$ and $f_2 = f(t_2)$ on this interval. The equation of an interpolating parabola, joining f_0, f_1 and f_2, is given by

$$at^2 + bt + c = 0 \ .$$

These coefficients may be determined from the system of equations

$$\begin{aligned} at_0^2 + bt_0 + c &= f_0 \ , \\ at_1^2 + bt_1 + c &= f_1 \ , \\ at_2^2 + bt_2 + c &= f_2 \ . \end{aligned}$$

Defining the origin of the t coordinate to be at t_1 results in $t_1 = 0$, $t_0 = -dt$ and $t_2 = dt$. So that,

$$\begin{aligned} adt^2 - bdt + c &= f_0 \ , \\ c &= f_1 \ , \\ adt^2 + bdt + c &= f_2 \ . \end{aligned}$$

Therefore,

$$adt^2 = f_0 + bdt - f_1 \ .$$

This allows for the determination of b

$$b = \frac{1}{2dt}(f_2 - f_0) \ ,$$

and, consequently, the determination of a

$$a = \frac{1}{dt^2}\left(f_0 + \frac{1}{2}(f_2 - f_0) - f_1\right) \ .$$

Integrating the parabolic equation over the interval results in

$$\int_{t_0}^{t_2} d\tau \ a\tau^2 + b\tau + c = \left(\frac{1}{3}a\tau^3 + \frac{1}{2}b\tau^2 + c\tau\right)\Bigg|_{t_0}^{t_2} \ ,$$

which can be simplified by completing the integral evaluation and using previously derived results for a, b and c:

$$\begin{aligned} \int_{t_0}^{t_2} d\tau \ a\tau^2 + b\tau + c &= \left(\frac{2}{3}adt^3 + 2cdt\right) \ , \\ &= \frac{dt}{3}\left(f_0 + 4f_1 + f_2\right) \ . \end{aligned} \tag{C.4}$$

Consequently, $\int d\tau \ f(\tau)$ can be approximated, on this interval, by

$$\int_{t_0}^{t_2} d\tau \ f(\tau) \approx \frac{dt}{3}\left(f_0 + 4f_1 + f_2\right) \ ,$$

with an accuracy corresponding to the validity of the interpolating parabola. This can be extended to a larger interval, sub-divided into N 3-point intervals, each approximated by Eq. (C.4):

$$\int_a^b dy \ f(y) \approx \frac{dt}{3}\left(f_0 + 4f_1 + 2f_2 + 4f_3 + 2f_4 + \cdots + 2f_{N-2} + 4f_{N-1} + f_N\right) \ ,$$

where $dt = \frac{b-a}{2N}$. The error per interval E of this interpolation can be determined as follows:

$$E = \int_{t_0}^{t_2} dy \ f(y) - \frac{dt}{3}\left(f_0 + 4f_1 + f_2\right) \ .$$

Then $f(t)$ can be expanded about t_0, yielding

$$f(t) = f_0 + (t-t_0)f'(t_0) + \frac{1}{2}(t-t_0)^2 f''(t_0) + \frac{1}{6}(t-t_0)^3 f'''(t_0) + \frac{1}{24}(t-t_0)^4 f''''(t_0) + \mathcal{O}((t-t_0)^5) \; .$$

Similarly, $f(t_1)$ and $f(t_2)$ can be expanded about t_0, resulting in

$$\begin{aligned} f(t_1) &= f_0 + dtf'(t_0) + \frac{1}{2}dt^2 f''(t_0) + \frac{1}{6}dt^3 f'''(t_0) + \frac{1}{24}dt^4 f''''(t_0) + \mathcal{O}(dt^5) \; , \\ f(t_2) &= f_0 + 2dtf'(t_0) + \frac{1}{2}4dt^2 f''(t_0) + \frac{1}{6}8dt^3 f'''(t_0) + \frac{1}{24}16dt^4 f''''(t_0) + \mathcal{O}(dt^5) \; . \end{aligned}$$

Then the integral

$$\int_{-dt}^{dt} d\tau \; f(\tau) \; ,$$

can be rewritten using a change of variable $z = \tau - t_0$ and subsequent Taylor expansion about t_0, yielding

$$\begin{aligned} \int_0^{2dt} dz \; f(z+t_0) &= \left(zf_0 + \frac{1}{2}z^2 f'(t_0) + \frac{1}{6}z^3 f''(t_0) + \frac{1}{24}z^4 f'''(t_0) + \frac{1}{120}z^5 f''''(t_0) + \mathcal{O}(z^6) \right) \Bigg|_0^{2dt} \; , \\ &= \left(2dtf_0 + \frac{4}{2}dt^2 f'(t_0) + \frac{8}{6}dt^3 f''(t_0) + \frac{16}{24}dt^4 f'''(t_0) + \frac{32}{120}dt^5 f''''(t_0) + \mathcal{O}(dt^6) \right) \; . \end{aligned}$$

This expansion can then be compared to the Taylor expansion of the approximation in Eq. (C.4):

$$\frac{dt}{3}\left(f_0 + 4f_1 + f_2\right) = \left(2dtf_0 + 2dt^2 f'(t_0) + \frac{4}{3}dt^3 f''(t_0) + \frac{2}{3}dt^4 f'''(t_0) + \frac{5}{18}dt^5 f'''' + \mathcal{O}(dt^6) \right) \; .$$

Thus the comparison yields an expression for error E:

$$E = \left(\frac{32}{120} - \frac{5}{18} \right) dt^5 f'''' + \mathcal{O}(dt^6) \; ,$$

which means that

$$E \; \alpha \; \mathcal{O}(dt^5) \; .$$

The global error for Simpson's rule E_g is given by $N \times E$, but $N \propto \frac{1}{dt}$, so

$$E_g \propto \mathcal{O}(dt^4) \; .$$

Appendix D

Initial State Calculations

D.1 Eigenvector Rotations

In the basis of the eigenstates of $\hat{\sigma}_z$, the operators $\hat{\sigma}_z$ and $\hat{\sigma}_x$ can be expressed as the matrices [73]

$$\sigma_z = \begin{pmatrix} 1 & 0 \\ 0 & -1 \end{pmatrix} ,$$
$$\sigma_x = \begin{pmatrix} 0 & 1 \\ 1 & 0 \end{pmatrix} .$$

In order to find the expressions of these operators in the basis of $\hat{\sigma}_x$ one must perform an eigenvector rotation. To this end the eigenvalues and eigenvectors of σ_x matrix must be found. Consider, therefore, the characteristic equation for σ_x,

$$det\left[\begin{pmatrix} 0 & 1 \\ 1 & 0 \end{pmatrix} - \lambda \begin{pmatrix} 1 & 0 \\ 0 & 1 \end{pmatrix}\right] = 0 .$$

This yields the solutions

$$\lambda^2 - 1 = 0 ,$$
$$\lambda = \pm 1 .$$

Therefore, the eigenvectors may be found via the equations

$$\begin{pmatrix} 0 & 1 \\ 1 & 0 \end{pmatrix} \begin{pmatrix} a_1 \\ a_2 \end{pmatrix} = \begin{pmatrix} a_1 \\ a_2 \end{pmatrix} ,$$
$$\begin{pmatrix} 0 & 1 \\ 1 & 0 \end{pmatrix} \begin{pmatrix} b_1 \\ b_2 \end{pmatrix} = - \begin{pmatrix} b_1 \\ b_2 \end{pmatrix} ,$$

having normalised solutions given by

$$\begin{pmatrix} a_1 \\ a_2 \end{pmatrix} = \frac{1}{\sqrt{2}} \begin{pmatrix} 1 \\ 1 \end{pmatrix} ,$$
$$\begin{pmatrix} b_1 \\ b_2 \end{pmatrix} = \frac{1}{\sqrt{2}} \begin{pmatrix} -1 \\ 1 \end{pmatrix} .$$

The rotation matrix U is then formed from the eigenvectors of the matrix σ_x:

$$U = \begin{pmatrix} a_1 & b_1 \\ a_2 & b_2 \end{pmatrix} = \frac{1}{\sqrt{2}} \begin{pmatrix} 1 & -1 \\ 1 & 1 \end{pmatrix} .$$

The matrix U is Hermitian, since its entries are real-valued and it satisfies the equation

$$U^\dagger = U^T = \frac{1}{\sqrt{2}} \begin{pmatrix} 1 & 1 \\ -1 & 1 \end{pmatrix} .$$

Additionally, U is unitary, as evinced by

$$U^\dagger U = \frac{1}{2}\begin{pmatrix} 1 & 1 \\ -1 & 1 \end{pmatrix}\begin{pmatrix} 1 & -1 \\ 1 & 1 \end{pmatrix} = \frac{1}{2}\begin{pmatrix} 2 & 0 \\ 0 & 2 \end{pmatrix} = \begin{pmatrix} 1 & 0 \\ 0 & 1 \end{pmatrix} .$$

Applying this rotation matrix to the σ_x and σ_z matrices yields

$$U\sigma_x U^\dagger = \frac{1}{2}\begin{pmatrix} 1 & -1 \\ 1 & 1 \end{pmatrix}\begin{pmatrix} 0 & 1 \\ 1 & 0 \end{pmatrix}\begin{pmatrix} 1 & 1 \\ -1 & 1 \end{pmatrix} = \frac{1}{2}\begin{pmatrix} 1 & -1 \\ 1 & 1 \end{pmatrix}\begin{pmatrix} -1 & 1 \\ 1 & 1 \end{pmatrix} = -\begin{pmatrix} 1 & 0 \\ 0 & -1 \end{pmatrix} ,$$

$$U\sigma_z U^\dagger = \frac{1}{2}\begin{pmatrix} 1 & -1 \\ 1 & 1 \end{pmatrix}\begin{pmatrix} 1 & 0 \\ 0 & -1 \end{pmatrix}\begin{pmatrix} 1 & 1 \\ -1 & 1 \end{pmatrix} = \frac{1}{2}\begin{pmatrix} 1 & -1 \\ 1 & 1 \end{pmatrix}\begin{pmatrix} 1 & 1 \\ 1 & -1 \end{pmatrix} = \begin{pmatrix} 0 & 1 \\ 1 & 0 \end{pmatrix} .$$

Thus the rotation U takes σ_x to a basis in which it is diagonal, that is, the basis of its own eigenvectors. This means that if we write the initial state of the spin system in the basis of the eigenstates of σ_z as

$$\rho_0 = \begin{pmatrix} 0 & 0 \\ 0 & 1 \end{pmatrix} ,$$

it can be transformed, via the rotation U, into the basis of the eigenstates of σ_x. When the rotation is applied to the given initial state, the result is:

$$U\rho_0 U^\dagger = \frac{1}{2}\begin{pmatrix} 1 & -1 \\ 1 & 1 \end{pmatrix}\begin{pmatrix} 0 & 0 \\ 0 & 1 \end{pmatrix}\begin{pmatrix} 1 & 1 \\ -1 & 1 \end{pmatrix} = \frac{1}{2}\begin{pmatrix} 1 & -1 \\ 1 & 1 \end{pmatrix}\begin{pmatrix} 0 & 0 \\ -1 & 1 \end{pmatrix} = \frac{1}{2}\begin{pmatrix} 1 & -1 \\ -1 & 1 \end{pmatrix} .$$

Alternatively, the initial spin-state could be chosen to be

$$\rho_0 = \begin{pmatrix} 1 & 0 \\ 0 & 0 \end{pmatrix} ,$$

corresponding to the excited state of the spin system. This state can also be rotated via U to yield:

$$U\rho_0 U^\dagger = \frac{1}{2}\begin{pmatrix} 1 & 1 \\ 1 & 1 \end{pmatrix} .$$

These two results are taken to be the available initial states of the spin and will be used in the simulation work performed in this study.

D.2 Wigner Transform of a Coherent State

The wavefunction for a coherent state, represented in position space, takes the form [63]

$$\psi(r) = \left(\frac{1}{2\pi a^2}\right)^{1/4} \mathrm{e}^{-\frac{(r-r_0)^2}{4a^2}} \mathrm{e}^{\frac{i}{\hbar}p_0 r} , \tag{D.1}$$

where a, r_0 and p_0 are constants and the wavefunction ψ is defined by

$$\psi(r) = \langle r|\ \psi\rangle \ ,$$

where $|\psi\rangle$ is the state of the system and $|r\rangle$ are states of definite position.

The Wigner function is found by Wigner transforming the density operator associated with ψ:

$$W(r,p) = \int dq\ \mathrm{e}^{\frac{i}{\hbar}pq} \left\langle r - \frac{q}{2}\right|\ \psi\right\rangle \left\langle \psi\right|\ r + \frac{q}{2}\right\rangle = \int dq\ \mathrm{e}^{\frac{i}{\hbar}pq} \psi(r - \frac{q}{2})\psi^*(r + \frac{q}{2}) ,$$

where the coordinate shifted probability density is expressed as

$$\psi(r - \frac{q}{2})\psi^*(r + \frac{q}{2}) = \frac{1}{\sqrt{2\pi a^2}} \mathrm{e}^{-\frac{(r-\frac{q}{2}-r_0)^2}{4a^2}} \mathrm{e}^{-\frac{(r+\frac{q}{2}-r_0)^2}{4a^2}} \mathrm{e}^{-\frac{i}{\hbar}p_0 q} .$$

In order to simplify this Wigner transform, consider first the expansions

$$\begin{aligned}(r-\frac{q}{2}-r_0)^2 &= r^2+\frac{q^2}{4}+r_0^2-rq-2rr_0+qr_0\ ,\\ (r+\frac{q}{2}-r_0)^2 &= r^2+\frac{q^2}{4}+r_0^2+rq-2rr_0-qr_0\ ,\\ (r+\frac{q}{2}-r_0)^2+(r-\frac{q}{2}-r_0)^2 &= 2(r^2+\frac{q^2}{4}+r_0^2)+2(-2rr_0)\ .\end{aligned} \tag{D.2}$$

These allow one to rewrite the above Wigner transform as

$$W(r,p)=\frac{1}{\sqrt{2\pi a^2}}\int dq\ \mathrm{e}^{\frac{i}{\hbar}(p-p_0)q}\mathrm{e}^{-\frac{1}{2a^2}(r^2+\frac{q^2}{4}+r_0^2-2rr_0)}=\frac{1}{\sqrt{2\pi a^2}}\int dq\ \mathrm{e}^{\frac{i}{\hbar}(p-p_0)q}\mathrm{e}^{-\frac{1}{2a^2}(r^2+r_0^2-2rr_0)}\mathrm{e}^{-\frac{1}{8a^2}q^2}\ ,$$

which can be further simplified to

$$W(r,p)=\frac{1}{\sqrt{2\pi a^2}}\mathrm{e}^{-\frac{(r-r_0)^2}{2a^2}}\int dq\ \mathrm{e}^{\frac{i}{\hbar}(p-p_0)q}\mathrm{e}^{-\frac{1}{8a^2}q^2}\ .$$

In order to evaluate the integral in q one must complete the square on the argument of the exponential:

$$\begin{aligned}-\frac{1}{8a^2}+\frac{i}{\hbar}(p-p_0)q &= -\frac{1}{2}\left(\frac{q^2}{4a^2}-\frac{2iq}{\hbar}(p-p_0)\right)\\ &= -\frac{1}{2}\left(\left(\frac{q}{2a}\right)^2-2\left(\frac{i}{\hbar}(p-p_0)2a\right)\frac{q}{2a}-\frac{4a^2}{\hbar^2}(p-p_0)^2+\frac{4a^2}{\hbar^2}(p-p_0)^2\right)\\ &= -\frac{2a^2}{\hbar^2}(p-p_0)^2-\frac{1}{2}\left(\frac{q}{2a}+\frac{2ia}{\hbar}(p-p_0)\right)^2\ .\end{aligned}$$

With the integral in q being taken over an exponential with a squared argument, the Wigner transform can now be expressed as

$$W(r,p)=\frac{1}{\sqrt{2\pi a^2}}\mathrm{e}^{-\frac{(r-r_0)^2}{2a^2}}\mathrm{e}^{-\frac{2a^2}{\hbar^2}(p-p_0)^2}\int dq\ \mathrm{e}^{-\frac{1}{2}(\frac{q}{2a}+\frac{12a}{\hbar}(p-p_0))^2}\ .$$

Performing some algebraic manipulations on the argument of the exponential allows one to express the integral as being over a Gaussian exponential:

$$\begin{aligned}\mathrm{e}^{-\frac{1}{2}(\frac{q}{2a}+\frac{12a}{\hbar}(p-p_0))^2} &= \mathrm{e}^{-\frac{1}{2}\left(\frac{1}{2a}\left(q+i\frac{4a^2}{\hbar}(p-p_0)\right)\right)^2}\\ &= \mathrm{e}^{-\frac{1}{8a^2}\left(q+i\frac{4a^2}{\hbar}(p-p_0)\right)^2}\ ,\end{aligned}$$

the evaluation of which is now trivial

$$\int dq\ \mathrm{e}^{-\frac{1}{8a^2}\left(q+i\frac{4a^2}{\hbar}(p-p_0)\right)^2}=\sqrt{8a^2\pi}\ .$$

Thus, the final expression for the Wigner-transformed coherent state is found to be:

$$W(r,p)=\frac{1}{\pi}\mathrm{e}^{-\frac{(r-r_0)^2}{2a^2}}\mathrm{e}^{-\frac{2a^2}{\hbar^2}(p-p_0)^2}\ ,$$

where the Wigner function was multiplied by $\frac{1}{2\pi}$ to ensure normalisation.

Despite being a function of both r and p, the uncertainty principle is still manifest through the constant a. If one were to minimise the width of the Gaussian in r by reducing a, the width of Gaussian in p expands correspondingly. The point of mutual minimum in these two Gaussians occurs at $a^2=\frac{\hbar}{2}$, giving a minimum uncertainty product of $\Delta r\Delta p=\hbar$ in manifest accordance with Heisenberg's uncertainty principle.

Appendix E

Bibliography

[1] R. Grunwald, H. Kim, and R. Kapral. Surface-hopping dynamics and decoherence with quantum equilibrium structure. *J. Chem. Phys.*, 128:164110, 2008.

[2] A. Sergi and P. V. Giaquinta. On computational strategies within molecular dynamics simulation. *Physics Essays*, 20(4):629–640, 2007.

[3] D. Mac Kernan, G. Ciccotti, and R. Kapral. Surface-hopping dyanmics of a spin-boson system. *J. Chem. Phys*, 116(6):2346–2352, February 2002.

[4] A. Kelly, R. van Zon, J. Schofield, and R. Kapral. Mapping quantum-classical liouville equation: projectors and trajectories. *arXiv:1201.1042*.

[5] F. Webster, P. J. Rossky, and P. A. Friesner. Nonadiabatic processes in condensed matter: semi-classical theory and implementation. *Comp. Phys. Comm.*, 63:494, 1991.

[6] L. Xiao and D. F. Coker. The influence of nonadiabatic rotational transitions on the line shapes of the rotational raman spectrum of h2 in liquid argon. *J. Chem. Phys.*, 100:8646, 1994.

[7] J. C. Tully. Molecular dynamics with electronic transitions. *J. Chem. Phys.*, 93:1061, 1990.

[8] P. Pechukas. Time-dependent semiclassical scattering theory. i. potential scattering. *Phys. Rev.*, 181:166174, 1969.

[9] M. Born and R. Oppenheimer. Zur quantentheorie der molekeln. *Annalen der Physik*, 389:457–484, 1962.

[10] W. Boucher and J. Traschen. *Phys. Rev. D.*, 37:3522, 1988.

[11] R. Kapral. Progress in the theory of mixed quantum-classical dynamics. *Ann. Rev. Phys. Chem.*, 57:129, 2006.

[12] J. Caro and L. L. Salcedo. Impediments to mixing classical and quantum dynamics. *Phys. Rev.*, 60(2):842–852, August 1999.

[13] A. Anderson. Quantum backreaction on "classical" variables. *Phys. Rev. Let.*, 74(5):621, January 1995.

[14] O. V. Prezhdo and V. V. Kisil. Mixing quantum and classical mechanics. *Phys. Rev. A*, 56(1):162, July 1997.

[15] G. Morandi, F. Napoli, and E. Ercolessi. *Statistical Mechanics*. World Scientific, Singapore, 2nd edition, 2001.

[16] U. Fano. Description of states in quantum mechanics by density matrix and operator techniques. *Rev. Mod. Phys.*, 29(1):74, 1957.

[17] E. T. Jaynes. Information theory and statistical mechanics. ii. *Phys. Rev.*, 108(2):171, 1957.

[18] E. Wigner. On the quantum correction for thermodynamic equilibrium. *Phys. Rev.*, 40:749, 1932.

[19] I. V. Bazarov. Synchrotron radiation representation in phase space. *Phys. Rev. ST Accel. Beams*, 15:050703, 2012.

[20] R. Kapral and G. Ciccotti. Mixed quantum-classical dynamics. *J. Chem. Phys*, 110(18):8919–8929, May 1999.

[21] W. B. Case. Wigner functions and weyl transforms for pedestrians. *Am. J. Phys.*, 76(10):937, October 2008.

[22] E. J. Heller. Wigner phase space method: Analysis for semi-classical applications. *J. Chem. Phys.*, 65:1289–1298, 1976.

[23] D. J. Tannor. *Introduction to Quantum Mechanics, A Time Dependent Perspective*. University Science Books, 2007.

[24] P. Rammond. *Group Theory, A Physicist's Survey*. Cambridge University Press, 2010.

[25] A. Sergi. Non-hamiltonian equilibrium statistical mechanics. *Phys. Rev. E.*, 67:021101, 2003.

[26] A. Sergi. Non-hamiltonian commutators in quantum mechanics. *Phys. Rev. E.*, 72:066125, 2005.

[27] K. Shiokawa and R. Kapral. Emergence of quantum-classical dynamics in an open quantum environment. *J. Chem. Phys.*, 117:7852, 2002.

[28] A. J. Leggett, S. Chakravarty, A. T. Dorsey, M. P. A. Fisher, A. Garg, and W. Zwerger. Dynamics of a dissipative two-state system. *Rev. Mod. Phys.*, 59(1), January 1987.

[29] S. D. Feyter F. D. Schryver and G. Schweitzer, editors. *Femtochemistry*. Wiley - VCH, Germany, 2001.

[30] A. Sergi and R. Kapral. Quantum-classical dynamics of nonadiabatic chemical reactions. *J. Chem. Phys*, 118(19):8566–8575, May 2003.

[31] G. S. Engel, T. R. Calhoun, E. L. Read, T.-K. Ahn, T. Mancal, T.-C. Cheng, R. E. Blankenship, and G. R. Fleming. Evidence for wavelike energy transfer through quantum coherence in photosynthetic systems. *Nature*, 446:782–786, 2007.

[32] T. L. Schmidt, K. Børkje, C. Bruder, and B. Trauzettel. Detection of qubit-oscillator entanglement in nanoelectromechanical systems. *Phys. Rev. Lett.*, 104:177205, 2010.

[33] Z. Li, S. Ouyang, C. Lam, and J. Q. You. Probing the quantum behaviour of a nanomechanical resonator coupled to a double quantum dot. *Phys. Rev. B*, 85:235420, 2012.

[34] A. Gaidarzhy, G. Zolfagharkhani, R. L. Badzey, and P. Mohanty. Evidence for quantized displacement in macroscopic nanomechanical oscillators. *Phys. Rev. Lett.*, 94:030402, 2005.

[35] R. L. Badzey and P. Mohanty. Coherent signal amplification in bistable nanomechanical oscillators by stochastic resonance. *Nature (London)*, 437:995, 2005.

[36] M. D. LaHaye, O. Buu, B. Camarota, K. C. Schwab, C. Monroe, and G. J. Milburn. Approaching the quantum limit of a nanomechanical resonator. *Science*, 304:74, 2004.

[37] I. Wilson-Rae, N. Nooshi, W. Zwerger, and T. J. Kippenberg. Theory of ground state cooling of a mechanical oscillator using dynamical backaction. *Phys. Rev. Lett.*, 99:093901, 2007.

[38] F. Marquardt, J. P. Chen, A. A. Clerk, and S. M. Girvin. Quantum theory of cavity-assisted sideband cooling of mechanical motion. *Phys. Rev. Lett.*, 99:093902, 2007.

[39] T. Rocheleau, T. Ndukum, C. Macklin, J. B. Hertzberg, A. A. Clerk, and K. C. Schwab, 2010.

[40] C. A. Regal and K. W. Lehnert. From cavity electromechanics to cavity optomechanics. *J. Phys.: Conf. Ser.*, 264:012025, 2011.

[41] M. P. Blencowe. Quantum electromechanical systems. *Phys. Rep.*, (395):159, 2004.

[42] K. C. Schwab and M. L. Roukes. Putting mechanics into quantum mechanics.

[43] S. L. Adler and A. Bassi. Is quantum theory exact? *Science*, 325:275, 2009.

[44] E. K. Irish and K. Schwab. Quantum measurement of a coupled nanomechanical resonator-cooper-pair box system. *Phys. Rev. B*, 68:155311, 2003.

[45] S. M. Carr, W. E. Lawrence, and M. N. Wybourne. Quantum effects in the mechanical properties of suspended nanomechanical systems. *Phys. Rev. B*, 64:220101, 2001.

[46] K. Schwab. Quantum measurement with nanomechanical systems. In R. G. Clark, editor, *Proceedings of the 1st International Conference on Experimental Implementation of Quantum Computing*, pages 189–194. Riton Press, Princeton, New Jersey, 2001.

[47] I. Katz, A. Retzker, R. Straub, and R. Lifshitz. Classical to quantum transition of a driven nonlinear nanomechanical resonator. *Phys. Rev. Lett.*, 99:040404, 2007.

[48] I. Katz, R. Lifshitz, A. Retzker, and R. Straub. Classical to quantum transition of a driven nonlinear nanomechanical resonator. *New J. Phys.*, 10:125023, 2008.

[49] J. Claudon, A. Zazunov, F. W. J. Hekking, and O. Buisson. Rabi-like oscillations of an anharmonic oscillator : Classical versus quantum interpretation. *Phys. Rev. B*, 78:184503, 2008.

[50] L.-Z. Guo, Z.-G. Zheng, , and X.-Qi Li. Quantum dynamics of mesoscopic driven duffing oscillators. *EPL*, 90:10011, 2010.

[51] S. Rips, M. Kiffner, I. Wilson-Rae, and M. J. Hartmann. Steady-state negative wigner functions of nonlinear nanomechanical oscillators. *New J. Phys.*, 14:023042, 2012.

[52] A. D. Armour, M. P. Blencowe, and K. C. Schwab. Entanglement and decoherence of a micromechanical resonator via coupling to a cooper-pair box. *Phys. Rev. Lett.*, 88:148301, 2002.

[53] R. P. Tiwari and D. Stroud. Numerical study of energy loss by a nanomechanical oscillator coupled to a cooper-pair box. *Phys. Rev. B*, 77:214520, 2008.

[54] S. Brouard, D. Alonso, and D. Sokolovski. Decoherence of a quantum harmonic oscillator monitored by a bose-einstein condensate. *Phys. Rev. A*, 84:012114, 2011.

[55] Y. Nakamura, Y. A. Pashkin, T. Yamamoto, and J. S. Tsai. Charge echo in a cooper-pair box. *Phys. Rev. Lett.*, 88:047901, 2002.

[56] S. M. Carr, W. E. Lawrence, and M. N. Wybourne. Accessibility of quantum effects in mesomechanical systems. *Phys. Rev. B*, 64:220101, 2001.

[57] A. Chakraborty. Buckled nano rod - a two state system: quantum effects on its dynamics. *Molecular Physics*, 107(17):1777–1786, 2009.

[58] R. P. Feynman and F. L. Vernon. *Ann. Phys. (N. Y.)*, 24:118, 1963.

[59] M. Schlosshauer, A. P. Hines, and G. J. Milburn. Decoherence and dissipation of a quantum harmonic oscillator coupled to two-level systems. *Phys. Rev. A.*, 77:022111, 2008.

[60] S. Nielsen, R. Kapral, and G. Ciccotti. Mixed quantum-classical surface hopping dynamics. *J. Chem. Phys.*, 112(15):6543, 2000.

[61] A. Sergi, D. Mac Kernan, G. Ciccotti, and R. Kapral. Simulating quantum dynamics in classical environments. *Theor. Chem. Acc.*, 110:49–58, 2003.

[62] J. R. Cash and A. H. Karp. A variable order runge-kutta method for initial value problems with rapidly varying right-hand sides. *ACM Transactions on Mathematical Software*, (16):201, 1990.

[63] L. D. Landau and E. M. Lifshitz. *Quantum Mechanics*. Butterworth-Heinemann, 3rd edition, 1977.

[64] R. Eisberg and R. Resnick. *Quantum Physics of Atoms, Molecules, Solids, Nuclei and Particles*. John Wiley and Sons, 2 edition, 1985.

[65] R. Jancel. *Foundations of Classical and Quantum Statistical Mechanics*. Pergamon Press, 1969.

[66] K. E. Cahill and R. J. Glauber. Density operators and quasiprobability distributions. *Phys. Rev.*, 177(5):1882, January 1969.

[67] A. Kenfack and K. Zyczkowski. Negativity of the wigner function as an indicator of nonclassicality. *J. Opt. B: Quantum Semiclass. Opt.*, 6:396–404, 2004.

[68] J. E. Moyal. Quantum mechanics as a statistical theory. *Proceedings of the Cambridge Philosophical Society*, 45:99–124, 1949.

[69] A. Messiah. *Quantum Mechanics*. North Holland, 1961.

[70] A. Bohm. *Quantum Mechanics, Foundations and Applications*. Springer-Verlag, 3rd edition, 1993.

[71] K. Imre, E. Ozizmir, M. Rosenbaum, and P. F. Zwiefel. *J. Math. Phys.*, 5:1097, 1967.

[72] V. Hutson and J. S. Pym. *Applications of Functional Analysis and Operator Theory*. Academic Press, 2nd edition, 1980.

[73] H. F. Jones. *Groups, representations and physics*. Hilger, 1990.

[74] V. I. Arnold. *Mathematical Methods of Classical Mechanics*. Springer New York, 1989.

[75] B. S. De Witt. Quantization of fields with infinite-dimensional invariance groups. ii. anticommuting fields. *J. Math. Phys*, 3:619, 1962.

[76] H. Breuer and F. Petruccione. *The Theory of Open Quantum Systems*. Oxford University Press, 2007.

[77] W. E. Schiesser. *The Numerical Method of Lines*. Academic Press, 1991.

[78] W. H. Press, S. A. Teukolsky, W. T. Vetterling, and B. P. Flannery. *Numerical Recipes*. Cambridge University Press, 1992.

[79] L. A. Veguilla-Berdecia. Tunnelling in a quartic, symmetric, double well potential. *Journal of Chemical Education*, 70(11):928–931, November 1993.

[80] V. P. Gutschick and M. M. Nieto. Coherent states for general potentials. v. time evolution. *Phys. Rev. D.*, 22:403, 1980.

[81] J. R. Klauder and B. S. Skagerstam. *Coherent States*. World Scientific, Singapore, 1985.

[82] E. T. Jaynes. *Probability Theory, The Logic of Science*. Cambridge University Press, 2003.

[83] R. D. Richtmeyer. *Principles of Advanced Mathematical Physics*. Springer, 1978.

[84] M. Hazewinkel, editor. *Encyclopedia of Mathematics*. Springer, 2001.

[85] M. Reed and B. Simon. *Functional Analysis*, volume 1 of *Methods of Modern Mathematical Physics*. Academic Press, 1972.

Appendix F

Computer Codes

```
program diabatic_basis_qc
    use data
    use observables
    use numerical
    implicit none
    !=============================================================
    !  qpij is the phase-space grid corresponding to density matrix indices
    !  i and j. qps grids are results after integrating a new step in time
    !=============================================================
    real*8 :: qp00(Mq,Mp),qps00(Mq,Mp)
    real*8 :: qp10(Mq,Mp),qps10(Mq,Mp)
    real*8 :: qpi10(Mq,Mp),qpsi10(Mq,Mp)
    real*8 :: qp11(Mq,Mp),qps11(Mq,Mp)
    !=============================================================
    !  t,q,p,tend -> time,position,momentum,ending time
    !  pr1,pr2,ex1,ex2 -> temporary variables
    !  tr_rho0 and tr_rho_sum track variation of trace(rho) over time evolution
    !  converge -> flags rk5 c-k convergence
    !  tsteps -> total no. of time steps
    !  countt -> no. of tsteps so far
    !  i,j,n,o -> loop counters
    !=============================================================
    real*8 :: t,q,p,tend
    real*8 :: pr1,pr2,ex1=1.0,ex2=2.0
    real*8 :: tr_rho0,tr_rho_sum
    logical :: converge
    integer :: n,o,tsteps,countt,i,j

    call inicon(qp00,qp10,qpi10,qp11,tsteps) !initial conditions + read data
    write(*,*) 'Grid Size q,p: ',Mq,Mp
    write(*,*) 'Coupling: ', cp
    write(*,*) 'Omega: ', omega

    !=============================================================
    !  Opening output files requested by input data
    !=============================================================
    if(spin_write == 1) then
        open(2,file='odata')
        open(17,file='rhodata')
    end if
    if(ham_write == 1) open(3,file='edata')
```

```
if(posp_write == 1)open(4,file='rpdata')
if(prob_write == 1)  open(15,file='probdata')
if(prof_write == 1)  open(16,file='rprofiledata')
if(rho_write == 1) then
    open(10,file='rho00')
    open(13,file='rho11')
end if
open(14,file='log')

if(qm /= 0.0) write(14,*) 'Full Quantum Dynamics'
write(14,*) 'b3 =', b3, 'c=',cp, 'b4=',b4,'b2=',b2
write(14,*) 'dt =', dt, 'tsteps=', tsteps
write(14,*) 'x_steps =', Mq, 'p_steps =', Mp

!=====================================================
!  Writing initial data
!=====================================================

if(rho_write == 1) then
    do n =1,Mq
        do o =1,Mp
            write(10,*) n,o,qp00(n,o)+qp11(n,o)
        end do
        write(10,*) ' '
    end do
    write(10,*) ' '
end if

t = 0.0

if(spin_write == 1) then
    write(2,*) t, rho(qp00,qp10,qpi10,qp11,.false.),&
    sigz(qp10,qpi10,t,0),sigx(qp00,qp11),rho(qp00,qp10,qpi10,qp11,.true.)
    write(17,*) t, rhoij(qp00,qp10,qpi10,qp11,1,t),&
    rhoij(qp00,qp10,qpi10,qp11,-1,t)
end if
if(ham_write == 1) then
    write(3,*) t, H(qp00,qp11,qp10,qpi10,t),&
    sigz(qp10,qpi10,t,1),omega*sigx(qp00,qp11),osc(qp00,qp11)
end if
if(posp_write == 1) then
    write(4,*) t, qavg(qp00,qp11,ex1,.true.),&
    qavg(qp00,qp11,ex1,.false.),qavg(qp00,qp11,ex2,.true.),&
    qavg(qp00,qp11,ex2,.false.)
end if

if(prof_write == 1) then
    do i = 1,Mq
        q = (i- Mq/2)*qgrid
        pr1 = qprob_part(i,qp00,qp10,qpi10,qp11,.false.,.true.,t)
        pr2 = qprob_part(i,qp00,qp10,qpi10,qp11,.true.,.true.,t)
        write(16,*) q,pr1,pr2,qcorrection(qp00,qp11,i)
    end do
    write(16,*) ' '
    write(16,*) ' '
end if
```

```
if(prob_write == 1) then
    pr1 = regionProb_part(Mq/2,Mq,qp00,qp10,qpi10,qp11,.false.,.true.,t)
    pr2 = regionProb_part(Mq/2,Mq,qp00,qp10,qpi10,qp11,.true.,.true.,t)
    write(15,*) t,pr1,pr2
end if
if(rho_write == 1) then
    do n =1,Mq
        do o =1,Mp
            write(10,*) n,o,qp00(n,o)+qp11(n,o)
        end do
        write(10,*) ' '
    end do
    write(10,*) ' '
end if


tr_rho_sum = rho(qp00,qp10,qpi10,qp11,.false.)
tr_rho0 = tr_rho_sum
write(14,*) 'H_0 = ', H(qp00,qp11,qp10,qpi10,t)
write(*,*) 'H_0 = ', H(qp00,qp11,qp10,qpi10,t)

countt  = 1;
tend = tsteps*dt
!=============================================================
!  Begin Main Loop, integration method selected by input data
!=============================================================
Do while(t <= tend)
    if(method == 1) then
        call eulerfullimplicit(qp00,qp10,qpi10,qp11,qps00,qps10,qpsi10,qps11,t)
    else if(method == 2) then
        call eulerimplicit(qp00,qp10,qpi10,qp11,qps00,qps10,qpsi10,qps11,t)
        print*, 'step:', countt
    else if(method == 3) then
        call rk2(qp00,qp10,qpi10,qp11,qps00,qps10,qpsi10,qps11,t)
    else if(method == 4) then
        call rk4(qp00,qp10,qpi10,qp11,qps00,qps10,qpsi10,qps11,t,dt)
    else
        call rk5ck(qp00,qp10,qpi10,qp11,qps00,qps10,qpsi10,qps11,t,converge)
        if(.not. converge) then
            write(14,*) 'FAILED AT:',t, &
            'WITH DEVIATION FROM INITIAL RHO:',abs(tr_rho0-tr_rho_sum/t)
            write(*,*) t,abs(tr_rho0-tr_rho_sum/t)
            stop
        end if
    end if
!=============================================================
!  Data for Prob(Q) and Wigner functions written 40 times
!=============================================================
    if(mod(countt,tsteps/40) == 0) then
        if(rho_write == 1) then
            do n =1,Mq
                do o =1,Mp
                    write(10,*) n,o,qp00(n,o)+qp11(n,o)
                end do
                write(10,*) ' '
```

```
            end do
            write(10,*) ' '
        end if
        if(prof_write == 1) then
            do i = 1,Mq
                q = (i- Mq/2)*qgrid
                pr1 = qprob_part(i,qp00,qp10,qpi10,qp11,.false.,.true.,t)
                pr2 = qprob_part(i,qp00,qp10,qpi10,qp11,.true.,.true.,t)
                write(16,*) q,pr1,pr2,qcorrection(qp00,qp11,i)
            end do
            write(16,*) ' '
            write(16,*) ' '
        end if
    end if
    do n = 1,Mq
        do o = 1,Mp
            if(n <= 5 .or. o <= 5 .or.n >= Mq-5 .or.o >= Mp-5) then
                !enforce boundary conditions
                qp00(n,o) = 0.0
                qp10(n,o) = 0.0
                qpi10(n,o) = 0.0
                qp11(n,o) = 0.0
            else
                qp00(n,o) = qps00(n,o)
                qp10(n,o) = qps10(n,o)
                qpi10(n,o) = qpsi10(n,o)
                qp11(n,o) = qps11(n,o)
            end if
        end do
    end do
    countt = countt + 1
!=============================================================
!  Data written for current time step
!=============================================================
    if(mod(countt,tsteps/5000) == 0) then
        if(spin_write == 1) then
            write(2,*) t, rho(qp00,qp10,qpi10,qp11,.false.),&
            sigz(qp10,qpi10,t,0),&
            sigx(qp00,qp11),rho(qp00,qp10,qpi10,qp11,.true.)
            write(17,*) t, rhoij(qp00,qp10,qpi10,qp11,1,t),&
            rhoij(qp00,qp10,qpi10,qp11,-1,t)
        end if
        if(ham_write == 1) then
            write(3,*) t, H(qp00,qp11,qp10,qpi10,t),sigz(qp10,qpi10,t,1),&
            omega*sigx(qp00,qp11),osc(qp00,qp11)
        end if
        if(posp_write == 1) then
            write(4,*) t, qavg(qp00,qp11,ex1,.true.),&
            qavg(qp00,qp11,ex1,.false.),&
            qavg(qp00,qp11,ex2,.true.), qavg(qp00,qp11,ex2,.false.)
        end if

        if(prob_write == 1) then
            pr1 = regionProb_part(1,Mq/2,qp00,qp10,qpi10,qp11,.false.,.true.,t)
            pr2 = regionProb_part(1,Mq/2,qp00,qp10,qpi10,qp11,.true.,.true.,t)
            write(15,*) t,pr1,pr2
```

```
            end if
        end if

        tr_rho_sum = tr_rho_sum+ rho(qp00,qp10,qpi10,qp11,.false.)

    end do

    print*, abs((tr_rho0-tr_rho_sum/(tsteps+1)))

    close(2)
    close(3)
    close(4)
    close(15)
    close(10)
    close(13)
    close(14)
    close(16)

end program

module data
    implicit none
    !=====================================================================
    ! Mq,Mp -> No. of phase-space grid points on one axis
    ! qgrid, pgrid -> phase-space grid spacings
    ! omega -> diabatic level spacing
    ! dt,cp -> time step, coupling constant
    ! qm -> turns quantum corrections on and off (values 1 or 0)
    ! method -> selects integrator
    ! w ->  oscillator frequency
    ! b2,b3,b4 -> potential coefficients
    !=====================================================================
    ! param.h contains data stored with parameter type
    !=====================================================================
    include 'param.h'
    real*8 :: qgrid,pgrid,dt,q_size,p_size
    real*8 :: w,omega,cp
    real*8 :: b2,b3,b4
    real*8 :: pi
    integer :: qm,method
    !=====================================================================
    !  These flags decide what output is written
    !=====================================================================
    integer :: rho_write,ham_write,prob_write,prof_write,spin_write,posp_write

contains

subroutine inicon(qp00,qp10,qpi10,qp11,tsteps)
    implicit none
    real*8,intent(out) :: qp00(Mq,Mp),qp10(Mq,Mp),qpi10(Mq,Mp),qp11(Mq,Mp)
    integer,intent(out) :: tsteps
    real*8 :: r0,p01,p02,s,q,p,wr,wp,exa
    real*8 :: spin00,spin10,spini10,spin11,beta,expo,zfac
    integer :: n,o,therm

    open(45,file='indata')
```

```
read(45,*)
read(45,*) q_size, p_size
read(45,*)
read(45,*) w, r0, p01, p02, s
read(45,*)
read(45,*) b2, b3, b4, omega
read(45,*)
read(45,*) dt, tsteps
read(45,*)
read(45,*) qm, cp
read(45,*)
read(45,*) method
read(45,*)
read(45,*) spin00, spin10, spini10, spin11
read(45,*)
read(45,*) rho_write, ham_write, prob_write, prof_write, spin_write, posp_write
read(45,*)
read(45,*) therm, beta
close(45)

zfac = 0.0

qgrid = 2*q_size/Mq
pgrid = 2*p_size/Mp

pi = 4.0*atan(1.0)

!=============================================================
!  This sets up the partition function for classical thermal states
!=============================================================
do n = 1,Mq
    if(n == 1 .or. n == Mq) then
        wr = 1.0/3.0
    else if(mod(n-1,2) == 0) then
        wr = 4.0/3.0
    else
        wr = 2.0/3.0
    end if

    q = (n-Mq/2)*qgrid
    do o = 1,Mp
        if(o == 1 .or. o == Mp) then
            wp = 1.0/3.0
        else if(mod(o-1,2) == 0) then
            wp = 4.0/3.0
        else
            wp = 2.0/3.0
        end if
        p = (o-Mp/2)*pgrid
        zfac = zfac + wp*wr*pgrid*qgrid*exp(-beta*(0.5*p**2+0.5*w**2*q**2))
    end do
end do

!=============================================================
!  Initial state chosen by therm parameter
!  Beta is inverse temperature
```

```
    !  0 -> coherent state
    !  1 -> quantum canonical
    !  2 -> classical canonical
    !  spinij values are initial reduced density matrix entries for spin
    !  r0,p0 are initial position and momentum averages
    !  s is the uncertainty parameter for the coherent state
    !=============================================================
    do n =1,Mq
        do o = 1,Mp
            q = (n-Mq/2)*qgrid
            p = (o-Mp/2)*pgrid
            if(therm == 0) then
                expo = exp(-(q-r0)**2/(2*s**2))*exp(-2*s**2*(p-p01)**2)/pi
                qp00(n,o) = spin00*expo
                qp10(n,o) = spin10*expo
                qpi10(n,o) = spini10*expo
                qp11(n,o) = spin11*expo
            else if(therm == 1) then
                exa = 0.5*p**2+0.5*w**2*abs(b2)*q**2
                expo = tanh(0.5*beta*w)*exp(-2/w*tanh(0.5*beta*w)*exa)/pi
                qp00(n,o) = spin00*expo
                qp10(n,o) = spin10*expo
                qpi10(n,o) = spini10*expo
                qp11(n,o) = spin11*expo
            else
                expo = exp(-beta*(0.5*p**2+0.5*w**2*abs(b2)*q**2))/zfac
                qp00(n,o) = spin00*expo
                qp10(n,o) = spin10*expo
                qpi10(n,o) = spini10*expo
                qp11(n,o) = spin11*expo
            end if
        end do
    end do

end subroutine

end module data


module numerical

contains
!=============================================================
!  Louiville Operator
!=============================================================
real*8 function Lr(qp,n,o)
    use data
    implicit none

    integer, intent(in) :: n,o
    real*8, intent(in) :: qp(Mq,Mp)
    real*8 :: q,p
    integer :: i,j

    p = (o-Mp/2)*pgrid
    q = (n-Mq/2)*qgrid
```

```
    Lr = -p*fdiff(qp,n,o,.true.) + (b4*q**3+b2*q+b3*q**2)*fdiff(qp,n,o,.false.)

end function

!=======================================================================
! n-point first derivative, n is dictated by param.h file
!=======================================================================
real*8 function fdiff(qp,i,j,r)
    use data
    implicit none

    real*8,intent(in) :: qp(Mq,Mp)
    integer,intent(in) :: i,j
    logical,intent(in) :: r
    integer :: n,o,k,l,q,p,u,v,vars,M
    real*8,allocatable :: wts(:)

    M = Mp
    if(r) M = Mq
    if(der_1_order == 2) then
        allocate(wts(1))
        vars = 1
        wts = (/-0.5/)
    else if(der_1_order == 4) then
        allocate(wts(2))
        wts = (/-2.0/3,1.0/12/)
        vars = 2
    else if (der_1_order == 6) then
        allocate(wts(3))
        vars = 3
        wts = (/-0.75,3.0/20,-1.0/60/)
    else if (der_1_order == 8) then
        allocate(wts(4))
        vars = 4
        wts = (/-0.8,0.2,-4.0/105,1.0/280/)
    end if
    fdiff = 0.0
    do n = 1,vars
        if (r) then
            if ((i-n >= 1) .and. (i+n <= M)) then
                fdiff = fdiff + &
                (qp(i-n,j)*wts(n) - qp(i+n,j)*wts(n))/qgrid
            else
                fdiff = 0.0
                exit
            end if
        else
            if((j-n >= 1) .and. (j+n <= M)) then
                fdiff = fdiff + &
                (qp(i,j-n)*wts(n) - qp(i,j+n)*wts(n))/pgrid
            else
                fdiff = 0.0
                exit
            end if
        end if
    end do
```

```
end function
!=======================================================================
!  2nd derivative
!=======================================================================
real*8 function fdiff2(qp,i,j,r)
    use data
    implicit none

    real*8,intent(in) :: qp(Mq,Mp)
    integer,intent(in) :: i,j
    logical,intent(in) :: r
    real*8 :: wts(3)
    integer :: n,M

    M = Mp
    if(r) M = Mq
    wts = (/-2.5,4.0/3,-1.0/12/)
    fdiff2 = 0.0
    do n = 1,3
        if (r) then
            if ((i-n >= 1) .and. (i+n <= M)) then
                if(n == 1) then
                    fdiff2 = fdiff2 + qp(i,j)*wts(n)/qgrid**3
                else
                    fdiff2 = fdiff2 + &
                    (qp(i-n,j)*wts(n) + qp(i+n,j)*wts(n))/qgrid**3
                end if
            else
                fdiff2 = 0.0
            end if
        else
            if((j-n >= 1) .and. (j+n <= M)) then
                if(n == 1) then
                    fdiff2 = fdiff2 + qp(i,j)*wts(n)/pgrid**3
                else
                    fdiff2 = fdiff2 + &
                    (qp(i,j-n)*wts(n) + qp(i,j+n)*wts(n))/pgrid**3
                end if
            else
                fdiff2 = 0.0
            end if
        end if
    end do
end function

!=======================================================================
!  3rd derivative
!=======================================================================
real*8 function fdiff3(qp,i,j,r)
    use data
    implicit none

    real*8,intent(in) :: qp(Mq,Mp)
    integer,intent(in) :: i,j
    logical,intent(in) :: r
```

```
    real*8 :: wts(4)
    integer :: n,M

    M = Mp
    if(r) M = Mq
    wts = (/61.0/30,-169.0/120,0.3,-7.0/240/)
    fdiff3 = 0.0
    do n = 1,4
        if (r) then
            if ((i-n >= 1) .and. (i+n <= M)) then
                fdiff3 = fdiff3 + &
                (qp(i-n,j)*wts(n) - qp(i+n,j)*wts(n))/qgrid**3
            else
                fdiff3 = 0.0
                exit
            end if
        else
            if((j-n >= 1) .and. (j+n <= M)) then
                fdiff3 = fdiff3 + &
                (qp(i,j-n)*wts(n) - qp(i,j+n)*wts(n))/pgrid**3
            else
                fdiff3 = 0.0
                exit
            end if
        end if
    end do

end function

!=============================================================
! Evaluates time derivatives of density matrix elements in diabatic basis
!=============================================================
subroutine deriv(qp00,qp10,qpi10,qp11,dqp00,dqp10,dqpi10,dqp11,t)
    use data
    implicit none

    real*8,intent(in) :: qp00(Mq,Mp),qp10(Mq,Mp),qpi10(Mq,Mp),qp11(Mq,Mp),t
    real*8,intent(out) :: dqp00(Mq,Mp),dqp10(Mq,Mp),dqpi10(Mq,Mp),dqp11(Mq,Mp)
    real*8 :: q
    integer :: n,o,lax
    lax = 0
    do n = 1,Mq
        do o = 1,Mp
            !first derivatives on whole grid
            q = (n-Mq/2)*qgrid
            !=============================================================
            ! Liouville term
            !=============================================================
            dqp00(n,o) = Lr(qp00,n,o)
            dqp10(n,o) = Lr(qp10,n,o)
            dqpi10(n,o) = Lr(qpi10,n,o)
            dqp11(n,o) = Lr(qp11,n,o)

            !=============================================================
            ! Coupling terms
            !=============================================================
```

```
                dqp00(n,o) = dqp00(n,o) - &
                2*cp*q*(qp10(n,o)*sin(2*omega*t)+&
                qpi10(n,o)*cos(2*omega*t))
                dqp10(n,o) = dqp10(n,o) - &
                cp*q*(qp11(n,o)-qp00(n,o))*sin(2*omega*t)
                dqpi10(n,o) = dqpi10(n,o) - &
                cp*q*(qp11(n,o)-qp00(n,o))*cos(2*omega*t)
                dqp11(n,o) = dqp11(n,o) + &
                2*cp*q*(qp10(n,o)*sin(2*omega*t)+&
                qpi10(n,o)*cos(2*omega*t))

                dqp00(n,o) = dqp00(n,o)-&
                cp*(fdiff(qp10,n,o,.false.)*cos(2*omega*t))
                dqp00(n,o) = dqp00(n,o)+&
                cp*(fdiff(qpi10,n,o,.false.)*sin(2*omega*t))
                dqp10(n,o) = dqp10(n,o)- &
                0.5*cp*(fdiff(qp00,n,o,.false.)*cos(2*omega*t))
                dqp10(n,o) = dqp10(n,o)- &
                0.5*cp*(fdiff(qp11,n,o,.false.)*cos(2*omega*t))
                dqpi10(n,o) = dqpi10(n,o)+ &
                0.5*cp*(fdiff(qp00,n,o,.false.)*sin(2*omega*t))
                dqpi10(n,o) = dqpi10(n,o)+ &
                0.5*cp*(fdiff(qp11,n,o,.false.)*sin(2*omega*t))
                dqp11(n,o) = dqp11(n,o)-&
                cp*(fdiff(qp10,n,o,.false.)*cos(2*omega*t))
                dqp11(n,o) = dqp11(n,o)+&
                cp*(fdiff(qpi10,n,o,.false.)*sin(2*omega*t))

                !=============================================================
                ! Quantum Corrections
                !=============================================================
                dqp00(n,o) = dqp00(n,o) -&
                (6*b4*q + 2*b3)*qm*fdiff3(qp00,n,o,.false.)/24.0
                dqp10(n,o) = dqp10(n,o) -&
                (6*b4*q +2*b3)*qm*fdiff3(qp10,n,o,.false.)/24.0
                dqpi10(n,o) = dqpi10(n,o)-&
                (6*b4*q + 2*b3)*qm*fdiff3(qpi10,n,o,.false.)/24.0
                dqp11(n,o) = dqp11(n,o) -&
                (6*b4*q+2*b3)*qm*fdiff3(qp11,n,o,.false.)/24.0

            end do
        end do

end subroutine

!=============================================================
!  Runge-Kutta 4 double-step corrector method
!=============================================================
subroutine rk4ds(qp00,qp10,qpi10,qp11,qps00,qps10,qpsi10,qps11,t,h)
    use data
    implicit none

    real*8,intent(in) :: qp00(Mq,Mp),qp10(Mq,Mp),qpi10(Mq,Mp),qp11(Mq,Mp),h
    real*8,intent(inout) :: t
    real*8,intent(out) :: qps00(Mq,Mp),qps10(Mq,Mp),qpsi10(Mq,Mp),qps11(Mq,Mp)
    real*8 :: k00(Mq,Mp),k10(Mq,Mp),ki10(Mq,Mp),k11(Mq,Mp),h2,div
```

```
    integer :: i,j,nst
    logical :: err = .true.,maxit = .false.

    h2 = h/2.0;div = 1.0;nst = 0
    err = .true.; maxit = .false.

    do while(err .and. (.not.maxit))
        err = .false.
        call rk4(qp00,qp10,qpi10,qp11,qps00,qps10,qpsi10,qps11,t,h/div)
        call rk4(qp00,qp10,qpi10,qp11,k00,k10,ki10,k11,t,h2/div)
        t = t - h/div-h2/div
        do i = 1,Mq
            do j = 1,Mp
                if(abs(qps00(i,j) - k00(i,j)) > tol) err = .true.
                if(abs(qps10(i,j) - k10(i,j)) > tol) err = .true.
                if(abs(qpsi10(i,j) - ki10(i,j)) > tol) err = .true.
                if(abs(qps11(i,j) - k11(i,j)) > tol) err = .true.
            end do
        end do
        div = div*2.0
        nst = nst + 1
        if(nst > 50) then
            maxit = .true.
            print*, 'Accuracy Warning: Max Step Size Reductions Exceeded!'
        end if
    end do
    t = t + h/div

end subroutine

!=============================================================
! Runge-Kutta 4
!=============================================================
subroutine rk4(qp00,qp10,qpi10,qp11,qps00,qps10,qpsi10,qps11,t,h)
    use data
    implicit none

    real*8,intent(in) :: qp00(Mq,Mp),qp10(Mq,Mp),qpi10(Mq,Mp),qp11(Mq,Mp),h
    real*8,intent(inout) :: t
    real*8,intent(out) :: qps00(Mq,Mp),qps10(Mq,Mp),qpsi10(Mq,Mp),qps11(Mq,Mp)
    real*8 :: k00(Mq,Mp),k10(Mq,Mp),ki10(Mq,Mp),k11(Mq,Mp)
    real*8 :: t00(Mq,Mp),t10(Mq,Mp),ti10(Mq,Mp),t11(Mq,Mp)
    integer :: i,j

    call deriv(qp00,qp10,qpi10,qp11,k00,k10,ki10,k11,t)
    qps00 = k00;qps10=k10;qpsi10=ki10;qps11=k11
    t00 = qp00+0.5*h*k00
    t10 = qp10+0.5*h*k10
    ti10 = qpi10+0.5*h*ki10
    t11 = qp11+0.5*h*k11
    call deriv(t00,t10,ti10,t11,k00,k10,ki10,k11,t+0.5*h)
    qps00 = qps00+2*k00;qps10=qps10+2*k10;qpsi10=qpsi10+2*ki10;qps11=qps11+2*k11
    t00 = qp00+0.5*h*k00
    t10 = qp10+0.5*h*k10
    ti10 = qpi10+0.5*h*ki10
    t11 = qp11+0.5*h*k11
```

```
      call deriv(t00,t10,ti10,t11,k00,k10,ki10,k11,t+0.5*h)
      qps00 = qps00+2*k00;qps10=qps10+2*k10
      qpsi10=qpsi10+2*ki10;qps11=qps11+2*k11
      t00 = qp00+h*k00
      t10 = qp10+h*k10
      ti10 = qpi10+h*ki10
      t11 = qp11+h*k11
      call deriv(t00,t10,ti10,t11,k00,k10,ki10,k11,t+h)
      qps00 = qps00+k00;qps10=qps10+k10
      qpsi10=qpsi10+ki10;qps11=qps11+k11
      qps00 = qps00*h/6.0;qps10 = qps10*h/6.0
      qpsi10 = qpsi10*h/6.0;qps11 = qps11*h/6.0
      qps00 = qps00+qp00;qps10=qps10+qp10
      qpsi10=qpsi10+qpi10;qps11=qps11+qp11

      t = t + h

end subroutine

!=======================================================================
! Runge-Kutta 5 Cash-Karp
! Features weighted phase-space averaged error
! (improvised by me and providing order of magnitude greater accuracy)
!=======================================================================
subroutine rk5ck(qp00,qp10,qpi10,qp11,qps00,qps10,qpsi10,qps11,t,converge)
      use data
      implicit none

      real*8,intent(in) :: qp00(Mq,Mp),qp10(Mq,Mp),qpi10(Mq,Mp),qp11(Mq,Mp)
      real*8,intent(inout) :: t
      real*8,intent(out) :: qps00(Mq,Mp),qps10(Mq,Mp),qpsi10(Mq,Mp),qps11(Mq,Mp)
      real*8 :: k100(Mq,Mp),k110(Mq,Mp),k1i10(Mq,Mp),k111(Mq,Mp)
      real*8 :: k200(Mq,Mp),k210(Mq,Mp),k2i10(Mq,Mp),k211(Mq,Mp)
      real*8 :: k300(Mq,Mp),k310(Mq,Mp),k3i10(Mq,Mp),k311(Mq,Mp)
      real*8 :: k400(Mq,Mp),k410(Mq,Mp),k4i10(Mq,Mp),k411(Mq,Mp)
      real*8 :: k500(Mq,Mp),k510(Mq,Mp),k5i10(Mq,Mp),k511(Mq,Mp)
      real*8 :: k600(Mq,Mp),k610(Mq,Mp),k6i10(Mq,Mp),k611(Mq,Mp)
      real*8 :: t00(Mq,Mp),t10(Mq,Mp),ti10(Mq,Mp),t11(Mq,Mp)
      real*8 :: delta00,delta10,deltai10,delta11
      real*8 :: a2,a3,a4,a5,a6
      real*8 :: c1,c2,c3,c4,c5,c6
      real*8 :: d1,d2,d3,d4,d5,d6
      real*8 :: b21,b31,b41,b51,b61
      real*8 :: b32,b42,b52,b62
      real*8 :: b43,b53,b63
      real*8 :: b54,b64
      real*8 :: b65,delta,h,wq,wp,del
      integer :: i,j,rk5count,count_max
      logical :: err
      logical,intent(out) :: converge

      a2=0.2;a3=0.3;a4=0.6;a5=1.0;a6=7.0/8
      c1=37.0/378;c2=0.0;c3=250.0/621;c4=125/594.0;c5=0;c6=512/1771.0
      d1=2825/27648.0;d2=0.0;d3=18575/48384.0;d4=13525/55296.0;d5=277/14336.0;d6=0.25
      b21=0.2;b31=3/40.0;b41=0.3;b51=-11/54.0;b61=1631/55296.0
      b32=9/40.0;b42=-0.9;b52=2.5;b62=175/512.0
```

```
b43=1.2;b53=-70/27.0;b63=575/13824.0
b54=35/27.0;b64=44275/110592.0
b65=253/4096.0
h = dt
err = .true.
converge = .true.
rk5count  = 0
count_max = 100

do while(err .and. converge)
    rk5count = rk5count + 1
    call deriv(qp00,qp10,qpi10,qp11,k100,k110,k1i10,k111,t)
    t00 = qp00+b21*h*k100
    t10 = qp10+b21*h*k110
    ti10 = qpi10+b21*h*k1i10
    t11 = qp11+b21*h*k111
    call deriv(t00,t10,ti10,t11,k200,k210,k2i10,k211,t+a2*h)
    t00 = qp00+b31*h*k100+b32*h*k200
    t10 = qp10+b31*h*k110+b32*h*k210
    ti10 = qpi10+b31*h*k1i10+b32*h*k2i10
    t11 = qp11+b31*h*k111+b32*h*k211
    call deriv(t00,t10,ti10,t11,k300,k310,k3i10,k311,t+a3*h)
    t00 = qp00+b41*h*k100+b42*h*k200 + b43*h*k300
    t10 = qp10+b41*h*k110+b42*h*k210+b43*h*k310
    ti10 = qpi10+b41*h*k1i10+b42*h*k2i10+b43*h*k3i10
    t11 = qp11+b41*h*k111+b42*h*k211+b43*h*k311
    call deriv(t00,t10,ti10,t11,k400,k410,k4i10,k411,t+a4*h)
    t00 = qp00+b51*h*k100+b52*h*k200 + b53*h*k300+b54*h*k400
    t10 = qp10+b51*h*k110+b52*h*k210+b53*h*k310+b54*h*k410
    ti10 = qpi10+b51*h*k1i10+b52*h*k2i10+b53*h*k3i10+b54*h*k4i10
    t11 = qp11+b51*h*k111+b52*h*k211+b53*h*k311+b54*h*k411
    call deriv(t00,t10,ti10,t11,k500,k510,k5i10,k511,t+a5*h)
    t00 = qp00+b61*h*k100+b62*h*k200 + b63*h*k300+b64*h*k400+b65*h*k500
    t10 = qp10+b61*h*k110+b62*h*k210+b63*h*k310+b64*h*k410+b65*h*k510
    ti10 = qpi10+b61*h*k1i10+b62*h*k2i10+b63*h*k3i10+b64*h*k4i10+b65*h*k5i10
    t11 = qp11+b61*h*k111+b62*h*k211+b63*h*k311+b64*h*k411+b65*h*k511
    call deriv(t00,t10,ti10,t11,k600,k610,k6i10,k611,t+a6*h)

    qps00 = qp00+c1*h*k100+c2*h*k200+c3*h*k300+c4*h*k400+&
    c5*h*k500+c6*h*k600
    qps10 = qp10+c1*h*k110+c2*h*k210+c3*h*k310+c4*h*k410+&
    c5*h*k510+c6*h*k610
    qpsi10 = qpi10+c1*h*k1i10+c2*h*k2i10+c3*h*k3i10+c4*h*k4i10+&
    c5*h*k5i10+c6*h*k6i10
    qps11 = qp11+c1*h*k111+c2*h*k211+c3*h*k311+c4*h*k411+&
    c5*h*k511+c6*h*k611

    err = .false.
    delta = 0.0
    do i = 1,Mq
        do j = 1,Mp
            delta00 =(c1-d1)*k100(i,j)+(c2-d2)*k200(i,j)+(c3-d3)*k300(i,j)+&
            (c4-d4)*k400(i,j)+(c5-d5)*k500(i,j)+(c6-d6)*k600(i,j)
            delta10 =(c1-d1)*k110(i,j)+(c2-d2)*k210(i,j)+(c3-d3)*k310(i,j)+&
            (c4-d4)*k410(i,j)+(c5-d5)*k510(i,j)+(c6-d6)*k610(i,j)
            deltai10 =(c1-d1)*k1i10(i,j)+(c2-d2)*k2i10(i,j)+(c3-d3)*k3i10(i,j)+&
```

```
                (c4-d4)*k4i10(i,j)+(c5-d5)*k5i10(i,j)+(c6-d6)*k6i10(i,j)
                delta11 =(c1-d1)*k111(i,j)+(c2-d2)*k211(i,j)+(c3-d3)*k311(i,j)+&
                (c4-d4)*k411(i,j)+(c5-d5)*k511(i,j)+(c6-d6)*k611(i,j)

                delta = delta + sqrt(delta00**2+delta10**2+deltai10**2+delta11**2)
            end do
        end do
        delta = delta/(Mq*Mp)
        delta = 0.0
        do i = 1,Mq
            if(i == 1 .or. i == Mq) then
                wq = 1.0/3.0
            else if(mod(i-1,2) == 0) then
                wq = 4.0/3.0
            else
                wq = 2.0/3.0
            end if
            do j = 1,Mp
                if(j == 1 .or. j == Mq) then
                    wp = 1.0/3.0
                else if(mod(j-1,2) == 0) then
                    wp = 4.0/3.0
                else
                    wp = 2.0/3.0
                end if
                delta00 =(c1-d1)*k100(i,j)+(c2-d2)*k200(i,j)+(c3-d3)*k300(i,j)+&
                (c4-d4)*k400(i,j)+(c5-d5)*k500(i,j)+(c6-d6)*k600(i,j)
                delta10 =(c1-d1)*k110(i,j)+(c2-d2)*k210(i,j)+(c3-d3)*k310(i,j)+&
                (c4-d4)*k410(i,j)+(c5-d5)*k510(i,j)+(c6-d6)*k610(i,j)
                deltai10 =(c1-d1)*k1i10(i,j)+(c2-d2)*k2i10(i,j)+(c3-d3)*k3i10(i,j)+&
                (c4-d4)*k4i10(i,j)+(c5-d5)*k5i10(i,j)+(c6-d6)*k6i10(i,j)
                delta11 =(c1-d1)*k111(i,j)+(c2-d2)*k211(i,j)+(c3-d3)*k311(i,j)+&
                (c4-d4)*k411(i,j)+(c5-d5)*k511(i,j)+(c6-d6)*k611(i,j)

                del = sqrt(delta00**2+delta10**2+deltai10**2+delta11**2)
                delta = delta + (qp00(i,j)+qp11(i,j))*wp*wq*qgrid*pgrid*del
            end do
        end do
        if((delta > tol) .and. (.not.err)) then
            err = .true.
            h = 0.7*h*(tol/delta)**0.2
            dt = h
            print*,delta/tol,rk5count,h
        end if
        if(rk5count > count_max) then
            print*, 'Accuracy Warning: Minimum Step Size Reached Without Convergence'
            converge = .false.
        end if
    end do
    t = t + h

end subroutine
!=======================================================================
!  Euler implicit method using forward Euler future step
!=======================================================================
subroutine eulerimplicit(qp00,qp10,qpi10,qp11,qps00,qps10,qpsi10,qps11,t)
```

```
    use data
    implicit none

    real*8,intent(in) :: qp00(Mq,Mp),qp10(Mq,Mp),qpi10(Mq,Mp),qp11(Mq,Mp),t
    real*8,intent(out) :: qps00(Mq,Mp),qps10(Mq,Mp),qpsi10(Mq,Mp),qps11(Mq,Mp)
    real*8 :: dqp00(Mq,Mp),dqp10(Mq,Mp),dqpi10(Mq,Mp),dqp11(Mq,Mp),u,v,y
    integer :: i,j

    call deriv(qp00,qp10,qpi10,qp11,dqp00,dqp10,dqpi10,dqp11,t)

    do i = 1,Mq
        u = cp*(i-Mq/2)*qgrid*sin(2*omega*t)*dt
        v = cp*(i-Mq/2)*qgrid*cos(2*omega*t)*dt
        y = 1 + 4*u**2 - 4*v**2
        do j = 1,Mp
            qps00(i,j) = qp00(i,j)+&
            dt/y*(dqp00(i,j)*(1+2*u**2-2*v**2)-2*u*dqp10(i,j))-&
            dt/y*(2*v*dqpi10(i,j)+dqp11(i,j)*(2*u**2-2*v**2))
            qps10(i,j) = qp10(i,j)+&
            dt/y*(u*dqp00(i,j)+dqp10(i,j)*(1-4*v**2)-&
            4*u*v*dqpi10(i,j)-u*dqp11(i,j))
            qpsi10(i,j) = qpi10(i,j)+&
            dt/y*(-v*dqp00(i,j)+dqpi10(i,j)*(1+4*u**2)+&
            4*u*v*dqp10(i,j)+v*dqp11(i,j))
            qps11(i,j) = qp11(i,j)+&
            dt/y*(dqp00(i,j)*(2*u**2-2*v**2)+2*u*dqp10(i,j))+&
            dt/y*(2*v*dqpi10(i,j)+dqp11(i,j)*(1+2*u**2-2*v**2))
        end do
    end do

end subroutine

!=======================================================================
! Euler implicit method by iteration
!=======================================================================
subroutine eulerfullimplicit(qp00,qp10,qpi10,qp11,qps00,qps10,qpsi10,qps11,t)
    use data
    implicit none

    real*8,intent(in) :: qp00(Mq,Mp),qp10(Mq,Mp),qpi10(Mq,Mp),qp11(Mq,Mp)
    real*8,intent(inout) :: t
    real*8,intent(out) :: qps00(Mq,Mp),qps10(Mq,Mp),qpsi10(Mq,Mp),qps11(Mq,Mp)
    real*8 :: dqp00(Mq,Mp),dqp10(Mq,Mp),dqpi10(Mq,Mp),dqp11(Mq,Mp)
    real*8 :: k00(Mq,Mp),k10(Mq,Mp),ki10(Mq,Mp),k11(Mq,Mp)
    integer :: i,j,k
    logical :: err

    err = .true.
    qps00 = qp00;qps10=qp10;qpsi10=qpi10;qps11=qp11;k=0

    do while(err .and. (k <= 150))
        err = .false.
        k00 = qps00;k10=qps10;ki10=qpsi10;k11=qps11
        call deriv(k00,k10,ki10,k11,dqp00,dqp10,dqpi10,dqp11,t+dt)
        do i = 1,Mq
            do j = 1,Mp
```

```
                qps00(i,j) = qp00(i,j) + dt*dqp00(i,j)
                qps10(i,j) = qp10(i,j) + dt*dqp10(i,j)
                qpsi10(i,j) = qpi10(i,j) + dt*dqpi10(i,j)
                qps11(i,j) = qp11(i,j) + dt*dqp11(i,j)
            end do
        end do
        do i = 1,Mq
            do j = 1,Mp
                if(abs(qps00(i,j)-k00(i,j)) > 1e-8) err = .true.
                if(abs(qps10(i,j)-k10(i,j)) > 1e-8) err = .true.
                if(abs(qpsi10(i,j)-ki10(i,j)) > 1e-8) err = .true.
                if(abs(qps11(i,j)-k11(i,j)) > 1e-8) err = .true.
            end do
        end do
        k = k + 1
    end do
    if(k > 150) print*, 'Accuracy Warning: Max Iterations Exceeded'
    call deriv(qps00,qps10,qpsi10,qps11,dqp00,dqp10,dqpi10,dqp11,t+dt)
    do i = 1,Mq
        do j = 1,Mp
            qps00(i,j) = qp00(i,j) + dt*dqp00(i,j)
            qps10(i,j) = qp10(i,j) + dt*dqp10(i,j)
            qpsi10(i,j) = qpi10(i,j) + dt*dqpi10(i,j)
            qps11(i,j) = qp11(i,j) + dt*dqp11(i,j)
        end do
    end do
    t = t + dt

end subroutine

!=======================================================
! Crank-Nicholson Scheme
!=======================================================
subroutine crank(qp00,qp10,qpi10,qp11,qps00,qps10,qpsi10,qps11,t)
    use data
    implicit none

    real*8,intent(in) :: qp00(Mq,Mp),qp10(Mq,Mp),qpi10(Mq,Mp),qp11(Mq,Mp)
    real*8,intent(inout) :: t
    real*8,intent(out) :: qps00(Mq,Mp),qps10(Mq,Mp),qpsi10(Mq,Mp),qps11(Mq,Mp)
    real*8 :: dqp00(Mq,Mp),dqp10(Mq,Mp),dqpi10(Mq,Mp),dqp11(Mq,Mp)
    real*8 :: k00(Mq,Mp),k10(Mq,Mp),ki10(Mq,Mp),k11(Mq,Mp)
    integer :: i,j,l,k
    logical :: err

    err = .true.
    k  = 0
    qps00 = qp00;qps10=qp10;qpsi10=qpi10;qps11=qp11

    do while(err .and. (k <= 150))
        err = .false.
        k00 = qps00;k10=qps10;ki10=qpsi10;k11=qps11
        call deriv(k00,k10,ki10,k11,dqp00,dqp10,dqpi10,dqp11,t)
        do i = 1,Mq
            do j = 1,Mp
                qps00(i,j) = qp00(i,j) + dt*dqp00(i,j)
```

```
                qps10(i,j) = qp10(i,j) + dt*dqp10(i,j)
                qpsi10(i,j) = qpi10(i,j) + dt*dqpi10(i,j)
                qps11(i,j) = qp11(i,j) + dt*dqp11(i,j)
            end do
        end do
        do i = 1,Mq
            do j = 1,Mp
                if(abs(qps00(i,j)-k00(i,j)) > 1e-8) err = .true.
                if(abs(qps10(i,j)-k10(i,j)) > 1e-8) err = .true.
                if(abs(qpsi10(i,j)-ki10(i,j)) > 1e-8) err = .true.
                if(abs(qps11(i,j)-k11(i,j)) > 1e-8) err = .true.
            end do
        end do
        k = k + 1
    end do
    if(k > 150) print*, 'Accuracy Warning: Max Iterations Exceeded'
    call deriv(qps00,qps10,qpsi10,qps11,dqp00,dqp10,dqpi10,dqp11,t+dt)
    do i = 1,Mq
        do j = 1,Mp
            qps00(i,j) = qp00(i,j) + 0.5*dt*dqp00(i,j)
            qps10(i,j) = qp10(i,j) + 0.5*dt*dqp10(i,j)
            qpsi10(i,j) = qpi10(i,j) + 0.5*dt*dqpi10(i,j)
            qps11(i,j) = qp11(i,j) + 0.5*dt*dqp11(i,j)
        end do
    end do
    call deriv(qp00,qp10,qpi10,qp11,dqp00,dqp10,dqpi10,dqp11,t)
    do i = 1,Mq
        do j = 1,Mp
            qps00(i,j) = qp00(i,j) + 0.5*dt*dqp00(i,j)
            qps10(i,j) = qp10(i,j) + 0.5*dt*dqp10(i,j)
            qpsi10(i,j) = qpi10(i,j) + 0.5*dt*dqpi10(i,j)
            qps11(i,j) = qp11(i,j) + 0.5*dt*dqp11(i,j)
        end do
    end do
    t = t + dt

end subroutine

!=======================================================================
! Runge-Kutta 2
!=======================================================================
subroutine rk2(qp00,qp10,qpi10,qp11,qps00,qps10,qpsi10,qps11,t)
    use data
    implicit none

    real*8,intent(in) :: qp00(Mq,Mp),qp10(Mq,Mp),qpi10(Mq,Mp),qp11(Mq,Mp)
    real*8,intent(inout) :: t
    real*8,intent(out) :: qps00(Mq,Mp),qps10(Mq,Mp),qpsi10(Mq,Mp),qps11(Mq,Mp)
    real*8 :: dqp00(Mq,Mp),dqp10(Mq,Mp),dqpi10(Mq,Mp),dqp11(Mq,Mp)
    real*8 :: k00(Mq,Mp),k10(Mq,Mp),ki10(Mq,Mp),k11(Mq,Mp)
    real*8 :: k200(Mq,Mp),k210(Mq,Mp),k2i10(Mq,Mp),k211(Mq,Mp)
    integer :: i,j,l,k
    logical :: err

    err = .true.
    k   = 0
```

```
do i = 1,Mq
    do j = 1,Mp
        qps00(i,j) = qp00(i,j)
        qps10(i,j) = qp10(i,j)
        qpsi10(i,j) = qpi10(i,j)
        qps11(i,j) = qp11(i,j)
    end do
end do

do while(err .and. (k <= 150))
    err = .false.
    do i = 1,Mq
        do j = 1,Mp
            k00(i,j) = qps00(i,j)
            k10(i,j) = qps10(i,j)
            ki10(i,j) = qpsi10(i,j)
            k11(i,j) = qps11(i,j)
        end do
    end do
    call deriv(k00,k10,ki10,k11,dqp00,dqp10,dqpi10,dqp11,t)
    do i = 1,Mq
        do j = 1,Mp
            qps00(i,j) = qp00(i,j) + dt*dqp00(i,j)
            qps10(i,j) = qp10(i,j) + dt*dqp10(i,j)
            qpsi10(i,j) = qpi10(i,j) + dt*dqpi10(i,j)
            qps11(i,j) = qp11(i,j) + dt*dqp11(i,j)
        end do
    end do
    do i = 1,Mq
        do j = 1,Mp
            if(abs(qps00(i,j)-k00(i,j)) > 1e-8) err = .true.
            if(abs(qps10(i,j)-k10(i,j)) > 1e-8) err = .true.
            if(abs(qpsi10(i,j)-ki10(i,j)) > 1e-8) err = .true.
            if(abs(qps11(i,j)-k11(i,j)) > 1e-8) err = .true.
        end do
    end do
    k = k + 1
end do
if(k > 150) print*, 'Accuracy Warning: Max Iterations Exceeded'

call deriv(qp00,qp10,qpi10,qp11,dqp00,dqp10,dqpi10,dqp11,t)
k00 = dt*dqp00;k10 = dt*dqp10;ki10 = dt*dqpi10;k11 = dt*dqp11
call deriv(qps00,qps10,qpsi10,qps11,dqp00,dqp10,dqpi10,dqp11,t+dt)
k200 = dt*dqp00;k210 = dt*dqp10;k2i10 = dt*dqpi10;k211 = dt*dqp11
call deriv(qp00+0.5*(k00+k200),qp10+0.5*k10+0.5*k210,qpi10+0.5*ki10+0.5*k2i10, &
qp11+0.5*k11+0.5*k211,dqp00,dqp10,dqpi10,dqp11,t+dt)
k200 = dt*dqp00;k210 = dt*dqp10;k2i10 = dt*dqpi10;k211 = dt*dqp11
do i = 1,Mq
    do j = 1,Mp
        qps00(i,j) = qp00(i,j) + 0.5*(k00(i,j)+k200(i,j))
        qps10(i,j) = qp10(i,j) + 0.5*(k10(i,j)+k210(i,j))
        qpsi10(i,j) = qpi10(i,j) + 0.5*(ki10(i,j)+k2i10(i,j))
        qps11(i,j) = qp11(i,j) + 0.5*(k11(i,j)+k211(i,j))
    end do
end do
t = t + dt
```

```
end subroutine

end module

module observables

contains

!=======================================================================
!  Simpson's rule weighting function
!=======================================================================
real*8 function weight(i,istart,iend)
    use data
    implicit none

    integer, intent(in) :: i,istart,iend

    if(i == istart .or. i == iend) then
        weight = 1.0/3.0
    else if(mod(i-istart,2) == 0) then
        weight = 4.0/3.0
    else
        weight = 2.0/3.0
    end if

end function

!=======================================================================
! <H> -> Hamiltonian average
!=======================================================================
real*8 function H(qp00,qp11,qp10,qpi10,t)
    use data
    implicit none
    real*8, intent(in) :: qp00(Mq,Mp),qp10(Mq,Mp),qp11(Mq,Mp),qpi10(Mq,Mp)
    real*8, intent(in) :: t
    real*8 :: q,p,wp,wq,jsum
    integer :: i,j

    H = 0.0

    do i = 1,Mq
        wq = weight(i,1,Mq)
        jsum = 0.0
        q = (i-Mq/2)*qgrid
        do j = 1,Mp
            wp = weight(j,1,Mp)
            p = (j-Mp/2)*pgrid
            !oscillator part
            if(.not.(b4 == 0)) then
                jsum = p**2/2 + b2*q**2/2 + &
                b4*q**4/4 + 1/3.0*b3*q**3 + 0.25*b2**2/b4
                jsum = wp*jsum*(qp00(i,j)+qp11(i,j))
            else
                jsum =  p**2/2 + b2*q**2/2 + b4*q**4/4 + 1/3.0*b3*q**3
                jsum = wp*jsum*(qp00(i,j)+qp11(i,j)))
```

```
            end if
            H = H + jsum
            !subsystem part
            H = H + wp*omega*(qp00(i,j)-qp11(i,j))
            !coupling part
            H = H - wp*2*cp*q*(qp10(i,j)*cos(2*omega*t)-qpi10(i,j)*sin(2*omega*t))
        end do
        H = wq*qgrid*pgrid*H
    end do

end function

!=============================================================
! Trace of density operator or purity (flagged by tr2)
!=============================================================
real*8 function rho(qp00,qp10,qpi10,qp11,tr2)
    use data
    implicit none
    real*8, intent(in) :: qp00(Mq,Mp),qp11(Mq,Mp),qpi10(Mq,Mp),qp10(Mq,Mp)
    logical,intent(in) :: tr2
    real*8 :: wr,wp,jsum
    integer :: i,j,wrc,wpc

    rho = 0.0;wrc = 0;wpc = 0

    do i = 1,Mq
        wq = weight(i,1,Mq)
        jsum = 0.0
        do j = 1,Mp
            wp = weight(j,1,Mp)
            if(.not. tr2) then
                jsum = jsum + wp*pgrid*(qp00(i,j)+qp11(i,j))
            else
                jsum = jsum +wp*pgrid*(qp00(i,j)**2+qp11(i,j)**2)+&
                2.0*(qp10(i,j)**2+qpi10(i,j)**2)*wp*pgrid
            end if

        end do
        rho = rho + jsum*wr*qgrid
    end do

end function

!=============================================================
! Average of density matrix element (sigz basis), either 00 or 11 decide by tr2
!=============================================================
real*8 function rhoij(qp00,qp10,qpi10,qp11,tr2,t)
    use data
    implicit none
    real*8, intent(in) :: qp00(Mq,Mp),qp11(Mq,Mp),qp10(Mq,Mp),qpi10(Mq,Mp)
    real*8, intent(in) :: t
    integer,intent(in) :: tr2
    real*8 :: wr,wp,jsum
    integer :: i,j,wrc,wpc

    rhoij = 0.0;wrc = 0;wpc = 0
```

```
    do i = 1,Mq
        wq = weight(i,1,Mq)
        do j = 1,Mp
            wp = weight(j,1,Mp)
            jsum = qp00(i,j)+qp11(i,j)
            jsum = jsum + 2*tr2*qp10(i,j)*cos(2*omega*t)
            jsum = jsum - 2*tr2*qpi10(i,j)*sin(2*omega*t)
            jsum = 0.5*wp*pgrid*wr*qgrid*jsum
            rhoij = rhoij + jsum
        end do
    end do

end function

!=======================================================================
! Trace of sigma_z
!=======================================================================
real*8 function sigz(qp10,qpi10,t,z)
    use data
    implicit none
    real*8, intent(in) :: qp10(Mq,Mp),qpi10(Mq,Mp),t
    real*8 :: wq,wp,jsum,q,coeff
    integer :: i,j
    integer, intent(in) :: z

    sigz = 0.0

    do i = 1,Mq
        wq = weight(i,1,Mq)
        jsum = 0.0
        do j = 1,Mp
            wp = weight(j,1,Mp)
            !calculated exponential form for off-diagonal parts of rho
            coeff = (1*(1-z) - cp*q*z)*2.0*wp*pgrid
            jsum = jsum + coeff*(qp10(i,j)*cos(2*omega*t)-qpi10(i,j)*sin(2*omega*t))

        end do
        sigz = sigz + jsum*wq*qgrid
    end do

end function

!=======================================================================
!  Trace of sigma_x
!=======================================================================
real*8 function sigx(qp00,qp11)
    use data
    implicit none
    real*8, intent(in) :: qp00(Mq,Mp),qp11(Mq,Mp)
    real*8 :: wr,wp,jsum
    integer :: i,j,wrc,wpc

    sigx = 0.0;wrc=0;wpc=0

    do i = 1,Mq
```

```
        wq = weight(i,1,Mq)
        jsum = 0.0
        do j = 1,Mp
            wp = weight(j,1,Mp)
            jsum = jsum + wp*pgrid*(qp11(i,j)-qp00(i,j))

        end do
        sigx = sigx + jsum*wr*qgrid
    end do

end function

!=======================================================================
!  oscillator hamiltonian component
!=======================================================================
real*8 function osc(qp00,qp11)
    use data
    implicit none
    real*8, intent(in) :: qp00(Mq,Mp),qp11(Mq,Mp)
    real*8 :: wr,wp,jsum,q,p
    integer :: i,j,wrc,wpc

    osc = 0.0;wrc=0;wpc=0

    do i = 1,Mq
        wq = weight(i,1,Mq)
        jsum = 0.0
        q = (i-Mq/2)*qgrid
        do j = 1,Mp
            wp = weight(j,1,Mp)
            p = (j-Mp/2)*pgrid
            jsum = jsum + p**2/2+0.5*b2*q**2+1/3.0*b3*q**3
            jsum = jsum + 0.25*b4*q**4+0.25*b2**2/b4
            jsum = jsum*wp*pgrid*(qp00(i,j)+qp11(i,j))
        end do
        osc = osc + jsum*wr*qgrid
    end do

end function

!=======================================================================
! Average of either q or p (decided by qflag) raised to exponent ex
!=======================================================================
real*8 function qavg(qp00,qp11,ex,qflag)
    use data
    implicit none

    real*8, intent(in) :: qp00(Mq,Mp),qp11(Mq,Mp),ex
    logical, intent(in) :: qflag
    real*8 :: wq,wp,jsum,q,p,kgrid
    integer :: i,j,wrc,wpc

    qavg = 0.0;wrc=0;wpc=0
    kgrid = pgrid
    if(qflag) kgrid = qgrid
```

```
    do i = 1,Mq
        wq = weight(i,1,Mq)
        jsum = 0.0
        q = (i-Mq/2)*qgrid
        do j = 1,Mp
            wp = weight(j,1,Mp)
            p = (j-Mp/2)*pgrid
            if(qflag) then
                jsum = jsum + kgrid*wp*q**ex*(qp00(i,j)+qp11(i,j))
            else
                jsum = jsum + kgrid*wp*p**ex*(qp00(i,j)+qp11(i,j))
            end if
        end do
        qavg = qavg + jsum*wq*qgrid
    end do
end function

!=============================================================
!  Prob(Q) or Prob(P) dependent on qflag
! i gives Q/P-position on phase-space
!=============================================================
real*8 function qprob(i,qp00,qp11,qflag)
    use data
    implicit none

    real*8, intent(in) :: qp00(Mq,Mp),qp11(Mq,Mp)
    logical, intent(in) :: qflag
    integer, intent(in) :: i
    real*8 :: wp,kgrid
    integer :: j,wpc,M

    qprob = 0.0;wpc=0
    kgrid = pgrid
    if(qflag) kgrid = qgrid
    M = Mp
    if(qflag) M = Mq

    do j = 1,M
        wp = weight(j,1,M)
        if(qflag) then
            qprob = qprob + kgrid*wp*(qp00(i,j)+qp11(i,j))
        else
            qprob = qprob + kgrid*wp*(qp00(j,i)+qp11(j,i))
        end if

    end do

end function

!=============================================================
! Contribution to Prob(Q) or Prob(P) from 00 or 11 component of density
!  matrix, decided by ex_flag
! i gives Q/P-position on phase-space
!=============================================================
real*8 function qprob_part(i,rp00,rp10,rpi10,rp11,ex_flag,qflag,t)
    use data
```

```
    implicit none

    real*8, intent(in) :: rp00(Mq,Mp)
    real*8, intent(in) :: rpi10(Mq,Mp)
    real*8, intent(in) :: rp10(Mq,Mp)
    real*8, intent(in) :: rp11(Mq,Mp)
    real*8, intent(in) :: t
    logical, intent(in) :: ex_flag,qflag
    integer, intent(in) :: i
    real*8 :: wp,kgrid,ex,real_rp
    integer :: j,wpc,M

    qprob_part = 0.0;wpc=0;real_rp = 0.0
    ex = -1.0
    if(ex_flag) ex = 1.0
    kgrid = qgrid
    if(qflag) kgrid = pgrid
    M = Mq
    if(qflag) M = Mp

    do j = 1,M
        wp = weight(j,1,M)
        if(qflag) then
            real_rp = rp10(i,j)*cos(2*omega*t) - rpi10(i,j)*sin(2*omega*t)
            qprob_part = qprob_part + &
            kgrid*wp*0.5*(rp00(i,j)+rp11(i,j)+2*ex*real_rp)
        else
            real_rp = rp10(j,i)*cos(2*omega*t) - rpi10(j,i)*sin(2*omega*t)
            qprob_part = qprob_part + &
            kgrid*wp*0.5*(rp00(j,i)+rp11(j,i)+2*ex*real_rp)
        end if
    end do

end function

!=====================================================================
! Sum over Prob(Q) or Prob(P) of occupying a region outlined by q_min:q_max
!=====================================================================
real*8 function regionProb_part(q_min,q_max,qp00,qp10,qpi10,qp11,exflag,qflag,t)
    use data
    implicit none

    real*8, intent(in) :: qp00(Mq,Mp),qp11(Mq,Mp),qp10(Mq,Mp),qpi10(Mq,Mp)
    real*8, intent(in) :: t
    integer, intent(in) :: q_min,q_max
    integer :: i
    logical, intent(in) :: qflag,exflag
    real*8 :: wq

    regionProb_part = 0.0
    do i = q_min,q_max
        wq = weight(i,q_min,q_max)
        regionProb_part = regionProb_part + &
        wq*qgrid*qprob_part(i,qp00,qp10,qpi10,qp11,exflag,qflag,t)

    end do
```

```
end function

!=======================================================================
! Quantum correction averaged over P as function of Q
! i gives Q-position on phase-space
!=======================================================================
real*8 function qcorrection(qp00,qp11,i)
    use data
    use numerical
    implicit none
    real*8,intent(in) :: qp00(Mq,Mp),qp11(Mq,Mp)
    integer, intent(in) :: i
    real*8 :: wp
    integer :: j

    qcorrection = 0.0

    do j = 1,Mp
        wp = weight(j,1,Mp)

        qcorrection = qcorrection -&
        0.25*b4*(i-Mq/2)*qgrid*pgrid*wp*fdiff3(qp00,i,j,.false.)+&
        0.25*b4*(i-Mq/2)*fdiff3(qp11,i,j,.false.)

    end do

end function

!=======================================================================
! Hamiltonian of oscillator averaged over P as function of Q
! i gives Q-position on phase-space
!=======================================================================
real*8 function hinq(qp00,qp11,i)
    use data
    use numerical
    implicit none
    real*8,intent(in) :: qp00(Mq,Mp),qp11(Mq,Mp)
    integer, intent(in) :: i
    real*8 :: wp,p,q,jsum
    integer :: j

    hinq = 0.0

    do j = 1,Mp
        wp = weight(j,1,Mp)
        p = (j-Mp/2)*pgrid
        q = (i-Mq/2)*qgrid
        jsum = p**2/2 + b2*q**2/2 + b4*q**4/4 + 1/3.0*b3*q**3
        jsum = jsum*wp*qgrid
        hinq = hinq + jsum*(qp00(i,j)+qp11(i,j))

    end do

end function
```

```
end module
```